

# **Cloud Radio Access Network in Constrained Fronthaul**

Rui Lei

Doctor of Philosophy

University of York

Electronic Engineering

January 2017

## Abstract

The Cloud Radio Access Network (C-RAN) has been proposed for the provision of advanced fourth and fifth generation wireless communication services. The C-RAN system have been shown to reduce costs, and can provide high spectral efficiency and energy efficiency. The fronthaul in such networks, defined as the transmission links between Remote Radio Units (RRUs) and a central Baseband Unit (BBU), usually has high fronthaul load and constrained capacity.

In this thesis, we explore and investigate the basic C-RAN system structure, based on which we propose two developed C-RAN systems. With each system we evaluate the Bit Error Ratio (BER) performance and transmission efficiency in multiple scenarios, and give advanced solutions to reduce the fronthaul load. We also analyse the effect of quantization on BPSK and QPSK modulation schemes, with different detection methods.

Error control in fronthaul transmission is considered as erroneous frames may be received at the BBU. Error Detection Coding and Error Correction Coding approaches can be applied to the fronthaul network. They may increase the fronthaul latency, but great improve the end-to-end BER performance.

Source compression techniques such as Slepian-Wolf (SW) coding can compress two correlated sources separately and de-compress them jointly. Since each RRU serves many user terminals, and some of them may also be served by another neighbour RRU, which results similarly in correlation of the received data between two RRUs. In this thesis, we applied the SW code to the C-RAN system and evaluate the compression rate achieved in fronthaul networks.

# Content

Abstract.....	II
Content.....	III
List of Figures.....	VI
List of Tables.....	IX
Acknowledgements.....	X
Declaration.....	XI
Chapter 1 Introduction.....	1
1.1. Background.....	1
1.2. Problems and Objectives.....	2
1.2.1. Problems.....	2
1.2.2. Objectives.....	2
1.3. Contributions.....	3
1.4. Thesis Outline.....	4
1.5. List of Publications.....	5
Chapter 2 Literature Review.....	6
2.1. Introduction.....	6
2.2. C-RAN.....	6
2.3. System and Channel Model.....	9
2.3.1. MIMO.....	9
2.3.2. MIMO Diversity.....	10
2.3.3. Channel Model.....	11
2.4. Detection Techniques.....	13
2.4.1. Zero-Forcing.....	13
2.4.2 Minimum Mean Square Error.....	14
2.4.3 Maximum Likelihood.....	14
2.5. Quantization.....	15
2.6. Combiner.....	16
2.6.1 Equal-gain Combining.....	17
2.6.2 Maximum-ratio Combining.....	18
2.7. OFDM.....	19
2.8. Information Theory.....	20
2.8.1. Entropy.....	20
2.8.2. Joint Entropy.....	21

---

2.8.3. Mutual Information .....	22
2.8.4. Mutual Information and Entropy .....	22
2.9. Slepian-Wolf Code .....	23
2.10. Chapter Summary .....	25
Chapter 3    Detection Techniques with Quantization at Receiver in Single Carrier Scheme .....	26
3.1. Introduction .....	26
3.2. System Model.....	27
3.3. Theory Analysis .....	29
3.3.1 Quantization with BPSK Modulation Scheme .....	29
3.3.2 Quantization with QPSK Modulation Scheme .....	45
3.4. Simulations with C-RAN .....	69
3.4.1. ZF Signal Detection .....	69
3.4.2. MMSE Signal Detection .....	70
3.4.3. Maximum Likelihood Signal Detection.....	71
3.4.4. Comparisons .....	72
3.4.5. Modulation Schemes.....	73
3.5. Chapter Summary .....	74
Chapter 4    Quantization Position Design with C-RAN Fronthaul in Multiple Carrier Scheme .....	76
4.1. Introduction .....	76
4.2. System Design.....	77
4.2.1. Quantization before FFT.....	77
4.2.2. Quantize after Beamformer.....	79
4.3. Performance on Rayleigh Channel.....	81
4.4. Performance on Rician and Frequency-selective Channels .....	94
4.5. Chapter Conclusion .....	100
Chapter 5    Physical Layer: Error Control in Fronthaul .....	103
5.1. Introduction .....	103
5.2. System Structure.....	104
5.2.1. Error Detection Coding Approach .....	105
5.2.2. Error Correction Coding Approach .....	107
5.3. Simulation Results.....	110
5.3.1. Simulation Results with CRC code.....	111
5.3.2. Simulation Results with RSC code .....	113

---

5.3.3. Simulation Results with Different Scenarios .....	116
5.4. Chapter Summary .....	120
Chapter 6 Compression Techniques .....	122
6.1. Introduction .....	122
6.2. Slepian-Wolf Overall Structure .....	123
6.3. Accumulate-Repeat-Accumulate Code .....	126
6.3.1. Accumulate-Repeat-Accumulate Encoder .....	126
6.3.2. Accumulate-Repeat-Accumulate Decoder .....	128
6.4. Simulation Results and Analysis .....	130
6.5. System Development .....	134
6.6. Chapter Summary .....	136
Chapter 7 Conclusions and Further Work .....	137
7.1 Summary of the Achievements .....	137
7.2 Future Work .....	138
Appendix .....	140
Definitions of Acronyms .....	180
List of Symbols .....	182
Bibliography .....	184

## List of Figures

Figure 2.1 C-RAN system structures .....	7
Figure 2.2 MIMO system model with $N_t$ transmit antennas and $N_r$ receive antennas....	9
Figure 2.3 Uniform quantization.....	16
Figure 2.4 Equal-gain combiner .....	17
Figure 2.5 Maximum-ratio combining structure.....	19
Figure 2.6 Block diagram of an OFDM system.....	20
Figure 2.7 Relationship between entropy and mutual information.....	23
Figure 2.8 Slepian-Wolf concept, $\hat{x}_1$ and $\hat{x}_2$ are the estimation of source $x_1$ and $x_2$ .....	24
Figure 2.9. Slepian-Wolf rate region .....	25
Figure 3.1 System model of a basic C-RAN system .....	27
Figure 3.2 Detection techniques after quantizer. ....	28
Figure 3.3 Extra quantization index bits need to be transmitted in fronthaul.....	28
Figure 3.4 Constellation of received points with $h_1 = 1, h_2 = 0.8$ .....	31
Figure 3.5 Constellation of received points with $h_1 = 1.6, h_2 = 0.2$ .....	32
Figure 3.6 Constellation of received points with two-domain quantizer.....	36
Figure 3.7 Outage case with ML detection without quantize the possible received symbol.....	38
Figure 3.8 Constellation of received points for QPSK .....	46
Figure 3.9 Define the region positions.....	49
Figure 3.10 Case with four points in region B.....	50
Figure 3.11 Case with four points in region A and D.....	51
Figure 3.12 Monte Carlo sampling range with $h_1$ and $h_2$ .....	53
Figure 3.13 Three points in outage in region B .....	56
Figure 3.14 Three points in outage in region A and D .....	58
Figure 3.15 Two points in outage in region B .....	63
Figure 3.16 Two points in outage in region B .....	64
Figure 3.17 BER performance comparison with Zero Forcing .....	69
Figure 3.18 BER performance comparison with MMSE.....	70
Figure 3.19 BER performance comparison with ML .....	71
Figure 3.20 BER performance comparison with multiple detection approaches .....	72
Figure 3.21 BER performance with Zero-Forcing detection in different modulation level.....	73
Figure 4.1 C-RAN system with quantize before FFT.....	78
Figure 4.2 C-RAN with quantize after beamformer .....	79

Figure 4.3 Quantize before FFT: $N_u = N_B = N_r = 2$ ; QPSK modulation with 6-10 extra bits.....	81
Figure 4.4 Quantize before FFT: $N_u = N_B = N_r = 2$ ; 16QAM modulation with 4-10 extra bits.....	82
Figure 4.5 Quantize before FFT: $N_u = N_B = N_r = 2$ ; 64QAM modulation with 4-8 extra bits.....	83
Figure 4.6 Comparison of quantizer before FFT and after separate beamformer, and of joint and separate beamformer without quantization; $N_u = N_B = N_r = 2$ ; QPSK with 16-level quantization (2 extra bits).....	84
Figure 4.7 Comparison of quantizer before FFT and after (separate) beamformer, and of joint and separate beamformer without quantization; $N_u = N_B = N_r = 2$ ; 16QAM with 64-level quantization (2 extra bits) .....	85
Figure 4.8 Comparison of quantizer before FFT and after beamformer, and of joint and separate beamformer without quantization; $N_u = N_B = N_r = 2$ ; 64QAM with 256-level quantization (2 extra bits) .....	86
Figure 4.9 Quantize-before-FFT (with joint beamformer): $N_u = 4, N_B = 2, N_r = 8$ ; QPSK modulation with 2-6 extra bits .....	87
Figure 4.10 Quantize-before-FFT: $N_u = 4, N_B = 2, N_r = 8$ ; 16QAM modulation with 2-6 extra bits.....	88
Figure 4.11 Quantize-before-FFT: $N_u = 4, N_B = 2, N_r = 8$ ; 64QAM modulation with 2-6 extra bits.....	89
Figure 4.12 Quantize after (separate) beamformer: $N_u = 4, N_B = 2, N_r = 8$ ; QPSK modulation with 2-4 extra bits .....	90
Figure 4.13 Quantize after beamformer: $N_u = 4, N_B = 2, N_r = 8$ ; 64QAM modulation with 0-4 extra bits .....	91
Figure 4.14 Quantize-after-beamformer: $N_u = 4, N_B = 2, N_r = 8$ ; 64QAM modulation with 0-4 extra bits .....	92
Figure 4.15 Location of RRUs and terminals in Rician channel .....	94
Figure 4.16 BER on Rician channel, random terminal positions, with different $K$ -factors .....	95
Figure 4.17 Noise enhancement factor in Gaussian channel <i>versus</i> distance between terminals.....	96
Figure 4.18 Quantize before FFT, Rician channel with various $K$ -factors, 16QAM modulation with 4 extra bits .....	97
Figure 4.19 Quantize after beamformer, Rician channel with various $K$ -factors, 16QAM modulation with 2 extra bits .....	97
Figure 4.20 Comparison of quantizer positions on frequency-selective channel, Rayleigh fading, $N_u = 2, N_B = 2, N_r = 2$ ; 16QAM modulation with 2 extra bits.....	98
Figure 4.21 Comparison of quantizer positions on frequency-selective channel, Rayleigh fading, $N_u = 4, N_B = 2, N_r = 8$ ; 16QAM modulation with 2 extra bits.....	99
Figure 4.22 Channel power-delay profile for frequency-selective channel.....	100
Figure 5.1 Fronthaul error handling.....	104

Figure 5.2 CRC generator and checker.....	105
Figure 5.3 System flowchart with CRC codes.....	106
Figure 5.4 Reed-Solomon code definitions .....	108
Figure 5.5 Main processes of a Reed-Solomon decoder.....	109
Figure 5.6 System flowchart applying RSC and CRC codes.....	110
Figure 5.7 Comparison with different BER level in fronthaul; Without error correction code; Quantize-after-beamformer; $N_u = 2, N_B = 2, N_r = 2$ .....	111
Figure 5.8 With and without erroneous packets discarded;.....	112
Figure 5.9 With error correction code; Quantize-after-beamformer; $N_u = 2, N_B = 2, N_r = 2$ .....	113
Figure 5.10 With error correction code; Quantize-after-beamformer; $N_u = 2, N_B = 2, N_r = 2$ .....	114
Figure 5.11 With error correction code; Quantize-after-beamformer; $N_u = 2, N_B = 2, N_r = 2$ .....	115
Figure 5.12 With and without erroneous packets discarded; With error correction code; Quantize-after-beamformer; $N_u = 2, N_B = 2, N_r = 2$ .....	116
Figure 5.13 Comparison with different length of transmitted data. With error correction code; Quantize-after-beamformer; $N_u = 2, N_B = 2, N_r = 2$ .....	117
Figure 5.14 Without error correction code; Quantize-after-beamformer; $N_u = 4, N_B=2, N_r = 8$ .....	119
Figure 5.15 With error correction code; Quantize-after-beamformer; $N_u = 4, N_B = 2, N_r = 8$ .....	120
Figure 6.1 System structure with Slepian-Wolf code applied .....	123
Figure 6.2 Slepian-Wolf encoder implementation.....	124
Figure 6.3 Slepian-Wolf decoder implementation;.....	124
Figure 6.4 Accumulate-Repeat-Accumulate encoder .....	127
Figure 6.5 Doped accumulator.....	128
Figure 6.6 Accumulate-Repeat-Accumulate decoder, $\pi$ , $\pi_1$ and $\pi_2$ are interleavers, and $\pi^{-1}$ , $\pi_1^{-1}$ and $\pi_2^{-1}$ are de-interleavers.....	129
Figure 6.7 Program design flowchart.....	131
Figure 6.8 Compression rate with Slepian-Wolf code.....	133
Figure 6.9 Compression failure rate with Slepian-Wolf code .....	133
Figure 6.10 Each symbol is quantized with 8 level quantizer and output 3 binary bits: MSB, SSB and LSB.....	134
Figure 6.11 Compression rate comparison between joint transmission ratio and separate transmission ratios .....	135
Figure 7.1 Wyner-Ziv compression approach .....	139

## List of Tables

Table 3.1 Quantization results of received signal with $h_1 = 1, h_2 = 0.8$ .....	31
Table 3.2 Quantization results of received signal with $h_1 = 1.6, h_2 = 0.2$ .....	32
Table 3.3 Comparison between the theoretical and simulation results for BPSK with real-only channel.....	34
Table 3.4 Comparison between the theoretical and simulation results for BPSK with complex channel .....	39
Table 3.5 Comparison between the theoretical and simulation results for BPSK with complex channel with two APs.....	40
Table 3.6 Integer quantization results of received signal with $h_1 = 1, h_2 = 0.8$ .....	41
Table 3.7 Integer quantization results of received signal with $ h_2  < \frac{ h_1 }{5}$ .....	41
Table 3.8 Integer quantization results and condition probability with sign of $h_1$ and $h_2$ .....	42
Table 3.9 Comparison between the theoretical and simulation results for the outage probability in different conditions .....	44
Table 3.10 Comparison between simulation and Monte Carlo results with four points in different region .....	54
Table 3.11 Number of erroneous bit table for desired bits and transmitted bits for $s_2$ with four points in outage .....	55
Table 3.12 Comparison between simulation and Monte Carlo results with three points in different region .....	60
Table 3.13 Number of erroneous bit table for desired bits and transmitted bits for $s_2$ with three points in outage .....	61
Table 3.14 Bit outage probability with each case for three points in outage.....	62
Table 3.15 Comparison between simulation and Monte Carlo results with two points in different region.....	66
Table 3.16 Number of erroneous bit table for desired bits and transmitted bits for $s_2$ with two points in outage.....	67
Table 3.17 Bit outage probability with each case for two points in outage.....	67
Table 3.18 BER comparison between theoretical and simulation results for QPSK modulation scheme and ML detection method.....	68
Table 3.19 Comparison the performance with multiple detection methods .....	73
Table 3.20 Transmission efficiency with various modulation schemes .....	74
Table 4.1: Comparison of Quantize-before-FFT (QbFFT) and Quantize-after-Beamformer (QaBF) for the two different scenarios and various modulation schemes .....	93
Table 5.1 Comparison of throughput efficiency with different data lengths and fronthaul error rate, giving minimum error correction capacity and minimum $E_b/N_0$ to meet the required BER .....	118

## Acknowledgements

This dissertation would not be possible without the contribution of several people. Firstly, I would like to give my sincere gratitude to my supervisor Prof. Alister G. Burr for the continuous support of my Ph.D study and related research, for his patience, motivation, and immense knowledge. His guidance helped me in all the time of research and writing of this dissertation. I could not have imagined having a better advisor and mentor for my Ph.D study.

Special thanks to Dr. Kanapathippillai Cumanan and Dr. Yury Zakharov, for their help and useful advice for my research. I would also thank Dr. Nian Xie, for his help and support on part of this work. Further I would like to thank all University of York Communication Group members for their help and support throughout my research.

Finally, I would like to thank my parents and my wife for the unconditional support and encouragement on my research.

## **Declaration**

I declare that this thesis is a presentation of original work and I am the sole author. This work has not previously been presented for an award at this, or any other, University. All sources are acknowledged as References.

---

# Chapter 1 Introduction

## 1.1. Background

The Cloud Radio Access Network (C-RAN) has been proposed for the provision of advanced fourth generation and fifth generation wireless communication services. The concept is that instead of full base station functionality being provided at each antenna site, the antenna should be equipped only with a Remote Radio Unit (RRU), which contains only Radio Frequency (RF) processing equipment which converts the radio signal to complex baseband (containing in phase and quadrature modulating signals) plus an analogue to digital converter (ADC) which quantizes the signals to convert them to digital form. They are then transmitted over the fronthaul network to a central Baseband Unit (BBU) which performs all processing of the complex baseband signals (modulation/demodulation, coding/decoding, higher layer protocols, etc) from antenna sites covering a wide area. This may provide economies of scale in performing the processing, and reduces the energy requirements at the antenna sites, potentially saving energy. It also allows joint processing of signals from multiple antenna sites, which has potential to greatly improve the performance of the radio access network. Note that this operates in both up and down-link: in both cases the fronthaul network carried quantized signals rather than user data.

The disadvantage of C-RAN is that the load on the fronthaul network is very large in comparison with what would be required for the more conventional backhaul network which is used in current radio access networks to connect base stations to the core network. In principle each RRU requires a data rate proportional to the bandwidth of

the signals and the number of antennas, regardless of how many users are being served. The load may easily be in the tens of Gbps per RRU, and is typically many times the total data rate of the users being served.

## **1.2. Problems and Objectives**

### **1.2.1. Problems**

The primary problem of C-RAN in general is the very large fronthaul load. This applies particularly to the uplink, where very fine quantization, and therefore very long sample word lengths, are required to accurately reproduce the signals received by the RRUs and the BBU. The problem is particularly severe when multiple antennas are provided on the RRUs.

Quantization is a non-linear process, and when applied to mixed signals it generates additional spurious components which interfere with the intended signals, and which therefore give rise to an “error floor” for the bit error ratio (BER), that is, an irreducible BER which remains significant however high the signal to noise ratio (SNR) on the radio access links. To bring this error floor down to an acceptable level requires much finer quantization, and hence a larger fronthaul load.

### **1.2.2. Objectives**

The overall objective of this thesis is to reduce the uplink fronthaul load in a C-RAN system using multiple antenna RRUs.

- Investigate the C-RAN model and its related techniques from the theoretical and practical point of view.
- Build up the C-RAN model in MATLAB and explore the potential ways to minimize the fronthaul load and achieve the expected end-to-end BER performance.

- Analyse the system performances and give the best solutions to reduce the fronthaul load and improve the transmission efficiency.

### 1.3. Contributions

- Detection techniques in C-RAN system
  - Build up a C-RAN simulation and investigate the impact of quantization levels and modulation schemes on the system BER performance. Conclude that at least 10 extra bits are needed to be transmitted in fronthaul network to reach the expected end-to-end BER level ( $10^{-4}$ ).
- Analysis of effects of quantization
  - Analyse the effect of quantization on BPSK and QPSK modulation schemes, with ML and ZF detection methods. Conclude that quantization of the combined symbols transmitted from multiple sources will cause outage in fading, and hence an error floor in the average BER performance.
- Evaluation of quantization positions in C-RAN system
  - Build up and develop the C-RAN system in a multiple carrier scheme with quantizer in different positions: before Fast Fourier transform (FFT) and after beamforming.
  - Evaluate the effect of quantization levels on multiple modulation schemes with different quantization positions. The results shows that with quantization after beamformer, the system needs much fewer extra bits to be transmitted, especially for low modulation level.
  - Develop the system with more antenna diversity at RRUs and evaluate the performance. We discover that a higher antenna diversity at RRU can reduce the fronthaul load.

- Analyse the simulation results for the two systems with different scenarios and provide advanced solutions to the system. Finally conclude that quantization after beamformer improves transmission efficiency in multiple scenarios.

➤ Design of error control in fronthaul

- Propose two error control systems in fronthaul network.

- Examine two error control systems at different error rates for transmission between RRUs and BBU, and evaluate their performance. Finally conclude that the first system (error detection approach) can be used with low fronthaul BER level (less than  $10^{-6}$ ) and the second system (error correction approach) can be used with high fronthaul BER level (more than  $10^{-6}$ ).

- Develop the system with more antenna diversity at each RRU.

➤ Compression techniques in fronthaul

- Apply Slepian-Wolf code to the C-RAN system.

- Evaluate the compression rate of SW code, showing that the similarity between two sources from RRUs affects the compression rate achieved.

- Show that compression rate can be improved by separate compression of the most significant bit (MSB), second significant bit (SSB) and least significant bit (LSB).

#### **1.4. Thesis Outline**

- Chapter 2 provides background information which introduces the basic concept of C-RAN system in Fronthaul Network, and then the background relates to the scenarios and techniques used to build up the C-RAN system, which include channels, carrier schemes, quantization, combiners and detection approaches. In the last part of this chapter we introduces the concept relates to source compression techniques.

- 
- In Chapter 3, a basic C-RAN system is set up, and several detection methods are applied and tested. The performance with transmitting quantized signals are given. The problems of the system are introduced.
  - In chapter 4, two C-RAN systems are proposed with multicarrier schemes, based on chapter 3. The solutions for the problems encountered in chapter 3 are explored and discovered. The BER performance of the systems in different scenarios are evaluated.
  - In chapter 5, two error control methods are introduced, and two fronthaul error control systems are built up. The end-to-end BER performance and throughput efficiency in fronthaul are evaluated and discussed.
  - In chapter 6, the Slepian-Wolf code is studied and designed. Then the compression rate in fronthaul is evaluated. Furthermore, a more efficient compression scheme is proposed, and the results are compared and discussed.
  - In chapter 7, we conclude the contributions and give suggestions for future work.

### **1.5. List of Publications**

R. Lei, A. Burr, T. Cai and K. Leppanen, " A network device and a baseband unit for a telecommunication system," European Patent Application, 4823197, 23 Nov 2016.

---

## Chapter 2 Literature Review

### 2.1. Introduction

The fronthaul in Radio Access Networks (RAN) requires high capacity, but is often constrained. This chapter presents literature reviews of C-RAN in fronthaul-constrained networks which includes system architectures and related key techniques. The structure of this chapter is given below.

First of all, the definition and architectures of C-RAN is given in section 2.2. Because this project is primarily focused on MIMO systems, the system will also be modelled in different types of channel, thus the basic structure of traditional MIMO and channel models are given in section 2.3. Then, the detection techniques normally used in MIMO systems are introduced in section 2.4. Quantization and combining are two main processes when modelling the system, and therefore their concepts are described in section 2.5 and 2.6. This project will examine C-RAN with different carrier schemes (especially OFDM); the background of such carrier schemes is given in section 2.7. Furthermore, as one of the key techniques to alleviate the impact of constrained fronthaul, source compression techniques are discussed in section 2.8.

### 2.2. C-RAN

Radio Access Networks (RAN) usually consist many BBUs. These BBUs cover a continuous area by covering a group of small regions with each base station (BS). Each BS processes and transmits the signal data from multiple mobile users and then forward the data to the core network via the backhaul. In each BBU area, system has its own backhaul transportation, cooling system, battery monitoring system. However, due to

the limitation of spectral resource, all of the base stations use the same frequency bandwidth which cause interference among neighbouring cells [2].

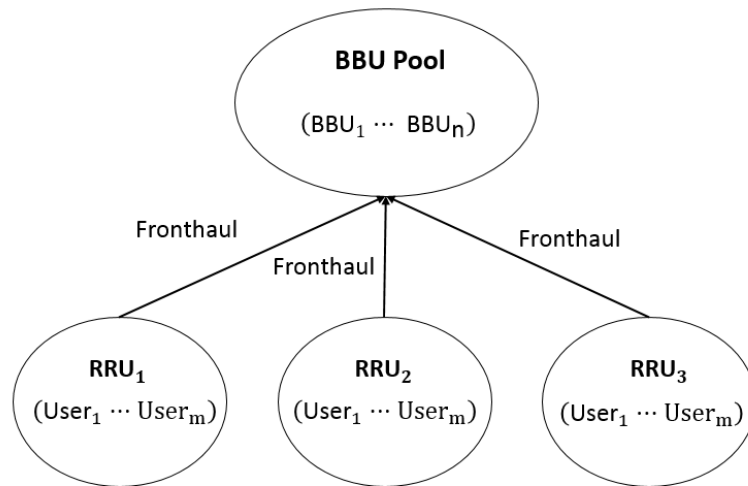


**Figure 2.1 C-RAN system structures**

C-RAN may be viewed as an evolution of the BS system and is introduced in [2, 3, 5, 6]. It takes advantage of many technological advances in wireless, optical and IT communications systems. For example, it is implemented by the Common public Radio Interface (CPRI) specification [3], low cost Coarse Wavelength Division Multiplexing (CWDM) and Dense Wavelength Division Multiplexing (DWDM) technology [8], and Millimetre Wave (mmWave), which achieve the large scale centralised BS can transmit the baseband signal over long distance. It applies Data Centre Network technology [9] to achieve high reliability, low cost, low latency and high bandwidth interconnect network in BBU pool [10].

The general architecture of a C-RAN consists of three components: a BBU pool which consists a group number of BBUs with centralized processors, RRUs with antennas located at remote sites, and fronthaul network between RRU and BBU with high capacity. The components are shown is figure 2.1. Note that the RRU also called a

Remoted Radio Head (RRH). To harmonize with the acronym, RRU will be used in this thesis.

A BBU pool usually consists of time-varying sets of software defined BBUs and the radio resources of different BBUs are fully shared with each other, and this forms a large-scale virtual multiple-input-multiple-output system from the BBU pool's perspective. The software defined BBUs process the received baseband signals and optimize radio resource allocation [1, 2].

RRUs can provide high data rate for user terminals with basic wireless signal coverage. In uplink, RRUs are used to forward the baseband signals from user terminals to the BBU pool for centralized processing. In downlink, RRUs transmit RF signals to user terminals. The functions of RRUs usually perform RF amplification, analog-to-digital conversion (ADC), digital-to-analog conversion (DAC) and interface adaptation. Because of the low complexity and expense, RRUs can be distributed in a large scale scenario [1, 2].

Fronthaul is defined as the link between BBUs and RRUs. The transmission methods of fronthaul network can be realized via several ways: optical fibre communication, cellular communication, and millimetre wave communication. Optical fibre communication [43] is considered to be the ideal fronthaul transmission without any constraints. It can provide high transmission efficiency and capacity with high expense and inflexible deployment. Cellular and millimetre wave communication technologies are considered to be non-ideal with capacity constraints in fronthaul network. Since wireless fronthaul is cheap and flexible to deploy, these technologies are anticipated to be prominent in practical C-RANs [2].

## 2.3. System and Channel Model

### 2.3.1. MIMO

A MIMO system uses multiple antennas to increase data rates through multiplexing or to improve performance through diversity. In MIMO systems, transmit and receive antennas can both be used for diversity gain. Multiplexing exploits the structure of the channel gain matrix to obtain independent signaling paths that can be used to send independent data. These spectral efficiency gains often require accurate knowledge of the channel at both the receiver and transmitter. In addition to spectral gains, ISI and interference from other users can be reduced using smart antenna techniques. The cost of the performance enhancements obtained through MIMO techniques is the added cost of deploying multiple antennas, the space and circuit power requirements of these extra antennas, and the added complexity required for multidimensional signal processing [14].

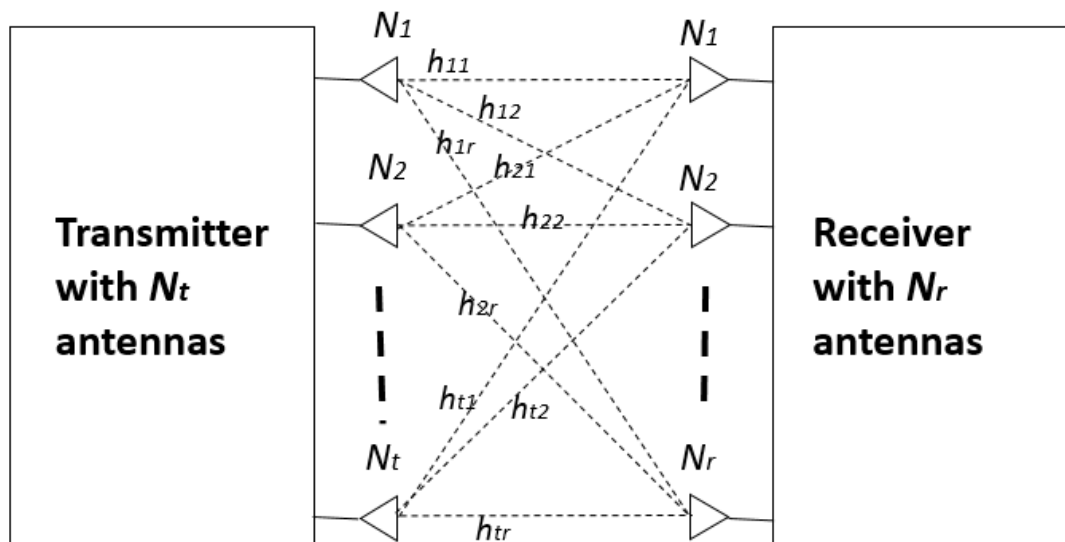


Figure 2.2 MIMO system model with  $N_t$  transmit antennas and  $N_r$  receive antennas

In figure 2.2, we consider a MIMO system with  $N_t$  transmit antennas and  $N_r$  receive antennas, where  $N_t \leq N_r$ . The MIMO channel is modeled as an uncorrelated Rayleigh

flat fading channel and can be denoted by a  $N_r \times N_t$  matrix  $\mathbf{H}$ . If  $h_{ij}$  denotes a function of fading coefficient is employed, we can express the channel matrix as:

$$\mathbf{H} = \begin{bmatrix} h_{11} & h_{12} & \cdots & h_{1t} \\ h_{21} & h_{22} & \cdots & h_{2t} \\ \vdots & \vdots & \vdots & \vdots \\ h_{r1} & h_{r2} & \cdots & h_{rt} \end{bmatrix} \quad (2.1)$$

then the received signal vector  $\mathbf{r}$  can be expressed as:

$$\mathbf{r} = \mathbf{H}\mathbf{x} + \mathbf{n} \quad (2.2)$$

where  $\mathbf{x}$  is the transmitted data with  $\mathbf{x} = [x_1 \ x_2 \ \dots \ x_t]$  and  $\mathbf{n}$  is the Gaussian noise. Equation 2.2 gives a general expression of the received signal for a MIMO system experiencing flat-fading channel.

### 2.3.2. MIMO Diversity

In single input and multiple output (SIMO) systems, the multiple receive antennas can see independently faded signal from the same transmit signal, and the received signals are then combined those faded signal to obtain a resulting signal with reduced fading [15]. The maximum receive diversity order with SIMO system is equal to the receive antennas number. Similarly, in multiple input and single output (MISO) systems, the same signal is transmitted through multiple fading paths which achieve the transmit diversity [16], and the maximum transmit diversity order is equal to the transmit antennas number. For a general MIMO system, the maximum diversity order can be obtained by:

$$D_{MIMO} = N_t \times N_r \quad (2.3)$$

where  $N_t$  is the number of transmit antennas and  $N_r$  is the number of receive antennas.

### 2.3.3. Channel Model

In wireless communications, the fading happens when there has reflection and scattering when transmit the signal, and this might affect the result of signal transmission: the amplitude and phase of the received signals could be suffered from fluctuations, and we named this channel model with multipath fading. With channel fading, we consider path loss, shadowing fading and multi-path fading. Besides, in this thesis, we always assume the channel state information (CSI) is known perfectly at the receiver.

#### ► Rayleigh Fading Channel

Rayleigh fading models assume that the magnitude of a signal that passes through a communication channel with fading according to a Rayleigh distribution shows in equation 2.4. Rayleigh fading is a reasonable model to represent the communication scenario when the transmitted signal is scattered by many objects before it arrives at the receiver. With sufficient scattering, the channel impulse response will be modelled as a Gaussian process irrespective of the distribution of the individual components. With no dominant component to the scattering, the process will result zero mean and phase that distributed between 0 and  $2\pi$  radians. The envelope of the channel response will therefore be Rayleigh distributed, which is defined by [17]:

$$f_{rayleigh}(x) = \frac{2x}{\Omega} e^{-\frac{x^2}{\Omega}} u(x) \quad (2.4)$$

where  $\Omega$  is the average power of received signal and  $u(x)$  is the step function. Note that the Rayleigh distribution can be expressed by two independent and identically

distributed zero mean Gaussian random variables as real and imaginary parts of a complex number and then taking its magnitude [17].

### ► Rician Channel

Rician fading is a channel model for the radio propagation caused by partial cancellation, which transmits the signal with several paths. One of the paths is much stronger than the others, which typically a line of sight (LoS) path, and the other paths are scatter paths. The amplitude gain can be characterized by a Rician distribution.

A Rician fading channel can be expressed by two parameters:  $K$  and  $\Omega$ .  $K$  is the ratio between the power in the direct path and the power in the other scattered paths.  $\Omega$  is the total power from all paths including direct path and the scattered paths ( $\Omega = v^2 + 2\sigma^2$ ) and acts as a scaling factor to the distribution,  $v^2$  and  $\sigma^2$  can be obtained by [18] [19]:

$$v^2 = \frac{K}{1+K} \Omega \quad (2.5)$$

$$\sigma^2 = \frac{\Omega}{2(1+K)} \quad (2.6)$$

The PDF with rician fading is given by:

$$f_{rician}(x) = \frac{2(K+1)x}{\Omega} \exp\left(-K - \frac{(K+1)x^2}{\Omega}\right) I_0\left(2\sqrt{\frac{K(K+1)}{\Omega}}x\right) \quad (2.7)$$

where  $I_0$  is the  $0th$  order modified Bessel function of the first kind.

When  $K = 0$ , the Rician distribution becomes the Rayleigh distribution; when  $K = +\infty$ , the channel does not exhibit fading, then Rician distribution considers with the Gaussian distribution.

## 2.4. Detection Techniques

A challenge in the practical realization of MIMO wireless systems lies in the efficient implementation of the detector which needs to separate the spatially multiplexed data streams. This section introduces the algorithms of Zero-Forcing (ZF), Minimum Mean Square Error (MMSE), and Maximum likelihood (ML). These detection techniques will be applied to the system in chapter 3, and the BER performance with multiple levels of quantizer will be explored.

### 2.4.1. Zero-Forcing

The Zero-Forcing technique is a standard linear detection method [21] [22]. If perfect CSI is available at the receiver, the zero-forcing estimate of the transmitted symbol vector can be written as:

$$\tilde{\mathbf{r}}_{ZF} = \mathbf{G}_{ZF} (\mathbf{H}\mathbf{s} + \mathbf{n}) = \mathbf{s} + \mathbf{G}_{ZF} \mathbf{n} , \quad (2.8)$$

where  $\mathbf{G}_{ZF} = \mathbf{H}^\dagger = (\mathbf{H}^H \mathbf{H})^{-1} \mathbf{H}^H$ ,  $\dagger$  denotes the pseudo-inverse operation.  $\tilde{\mathbf{r}}_{ZF}$  is the recovered data vector of the transmitted symbol vector  $\mathbf{s}$ .

$\tilde{\mathbf{r}}_{ZF}$  consists of the decoded vector  $\mathbf{s}$  plus a combination of the inverted channel matrix and the unknown noise vector. Because the pseudo-inverse of the channel matrix may causes noise amplification when the channel matrix is ill conditioned, the noise variance is consequently increased and the performance is degraded. To alleviate the noise enhancement introduced by the ZF detector, the MMSE detector was proposed, where the noise variance is considered in the construction of the filtering matrix [23].

### 2.4.2 Minimum Mean Square Error

The Minimum Mean Square Error (MMSE) approach alleviates the noise enhancement problem by taking into consideration the noise power when constructing the filtering matrix using the MMSE performance-based criterion [23, 24].

In order to maximize the post-detection signal-to-interference plus noise ratio (SINR), the MMSE weight matrix is given as [23]:

$$\mathbf{G}_{MMSE} = (\mathbf{H}^H \mathbf{H} + \sigma^2 \mathbf{I})^{-1} \mathbf{H}^H \quad (2.9)$$

Note that the MMSE receiver requires the statistical information of the noise  $\sigma^2$ . Then we obtain the following relationship:

$$\tilde{\mathbf{r}}_{MMSE} = \mathbf{G}_{MMSE} (\mathbf{H}\mathbf{s} + \mathbf{n}) = \mathbf{s} + \mathbf{G}_{MMSE} \mathbf{n} \quad (2.10)$$

where  $\tilde{\mathbf{r}}_{MMSE}$  is the recovered symbol vector of  $\mathbf{s}$ . The term  $(1/\text{SNR} = \sigma^2)$  offers a trade-off between the residual interference and the noise enhancement. As the SNR grows large, the MMSE detector converges to the ZF detector.

### 2.4.3 Maximum Likelihood

Maximum likelihood (ML) detection calculates the Euclidean distance between the received signal vector and the product of all possible transmitted signal vectors with the given channel  $\mathbf{H}$ , and finds the one with the minimum distance [23]. Let  $\mathbf{C}$  denote a set of signal constellation symbol points and  $N_T$  denote a number of transmit antennas. Then, the estimated transmitted signal vector  $\mathbf{x}$  can be determined with ML detection as [23]:

$$\hat{\mathbf{x}}_{ML} = \arg \min(\|\mathbf{r} - \mathbf{H}\mathbf{x}\|^2), \mathbf{x} \in \mathbf{C}^{N_T} \quad (2.11)$$

where  $\|\mathbf{r} - \mathbf{H}\mathbf{x}\|^2$  corresponds to the ML metric. The ML method can achieve the optimal performance when all the transmitted vectors are equally likely. However, as modulation order and the transmit antennas number increases, the system complexity increases exponentially. We can define the required number of ML metric as  $C^{N_r}$ , the complexity of calculation largely increases with the number of antennas. Although the ML detection method suffers from computational complexity, the achieved performance can be served as a reference to other detection methods since it corresponds to the optimal performance [21, 23].

## 2.5. Quantization

Quantization is involved in nearly all digital signal processing, which is a process to represent a signal in digital form involves rounding. Quantization replaces each number with an approximation level from a set of discrete levels, and then convert to digital number for storage and processing. When quantizing a sequence of numbers, the system generates quantization errors that is modelled as an additive random signal, which is called as quantization noise. The more levels a quantizer uses, the lower its quantization noise power [25].

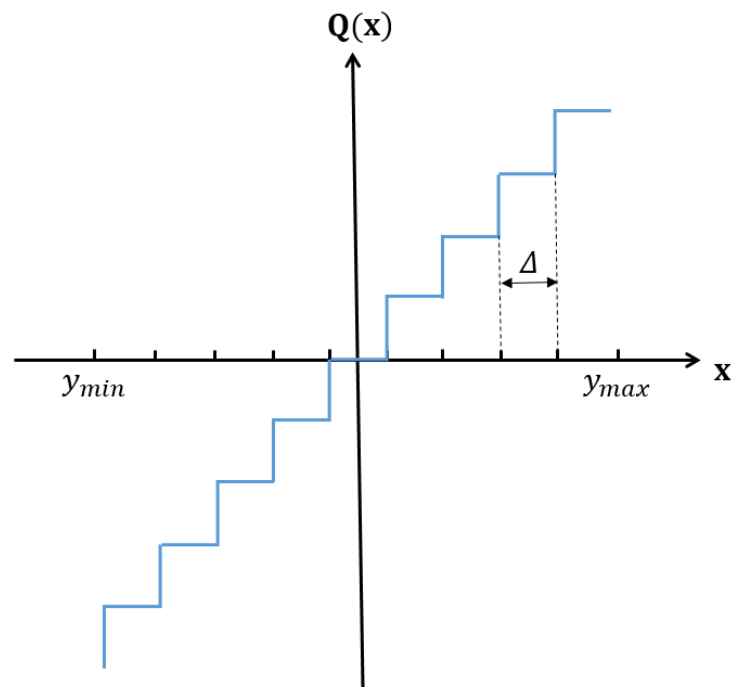


**Figure 2.3 Uniform quantization**

In figure 2.3, the signal has a finite range from  $y_{min}$  to  $y_{max}$ .  $Q(x)$  is the quantization output which can be converted to digital number in transmission. Then the entire data is divided into  $l$  equal intervals of length  $\Delta$  which known as the quantization step-size. The interval can be represented by:

$$l = \frac{y_{max} - y_{min}}{\Delta} \quad (2.12)$$

## 2.6. Combiner

When wireless signals travel from a single transmit antenna to multiple receive antennas they experience different fading conditions. While the signal from one path may experience a deep fade the signal from another path may be stronger [28]. Therefore selecting the stronger of the two signals (selection combining, threshold combining) or adding the signals (equal gain combining, maximal ratio combining)

would always yield much better results (lower bit error rate). However, there must be sufficient spacing between the different receive antennas for the received signals to be dissimilar (uncorrelated). Here we consider the equal gain combining or maximal ratio combining to combine the received signals in our future system design [28].

### 2.6.1 Equal-gain Combining

Equal-gain combining (EGC) is of practical interest because it achieves a comparable performance to the optimal maximal ratio combining receiver but with less complexity. Suppose the transmitted signal is subjected to multipath fading and is perturbed by additive white Gaussian noise (AWGN), the received signal at the  $l$ th antenna ( $l \in \{1, 2\}$ ) can be expressed in complex form as [28]:

$$s_l(t) = \text{Re}\{\alpha_l(t)e^{j(\varepsilon_l(t)+\theta_l(t))} + N_l(t)\} \quad (2.13)$$

where  $\text{Re}\{\cdot\}$  denotes the real part of its argument,  $\alpha_l(t)$  and  $\varepsilon_l(t)$  correspond to fading amplitude and uniformly distributed random phase processes respectively,  $\theta_l(t)$  denotes the desired phase modulation and  $N_l(t)$  is the zero mean complex AWGN process with a power spectral density  $N_0$  (W/Hz).

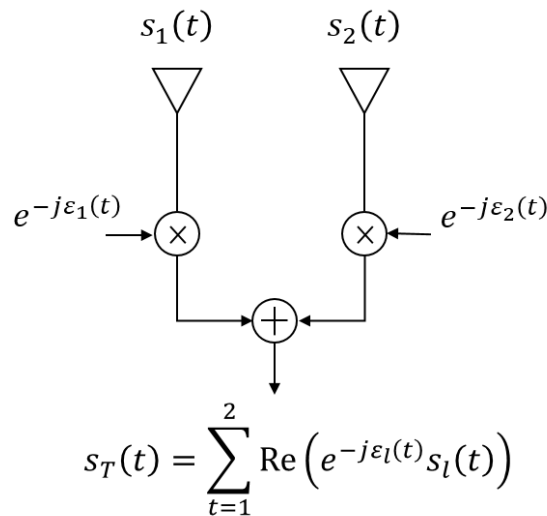


Figure 2.4 Equal-gain combiner

In contrast to the maximum-ratio combining (MRC) technique, the EGC combiner adds the co-phased signals from the two antennas in a linear fashion to produce the decision statistic [28].

### 2.6.2 Maximum-ratio Combining

In MRC, different weight factor are applied to the corresponding signal branch that is proportional to the signal amplitude, which result branches with strong signals are amplified, while weak signals are attenuated [29]. MRC is the optimum combiner for independent AWGN channels [29]. In MRC, the signals from all of the branches are weighted according to their individual SNRs and then summed. Here the individual signals need to be brought into phase alignment before summing [29].

The output of the combiner at the  $l$ th antenna ( $l \in \{1, 2\}$ ) can be obtained by:

$$S_{MRC} = x \sum_{l=1}^L w_l h_l + \sum_{l=1}^L w_l n_l \quad (2.14)$$

where  $x$  is the amplitude,  $w_l$  is the combining weights,  $h_l$  is the channel, and  $n_l$  is AWGN noise.

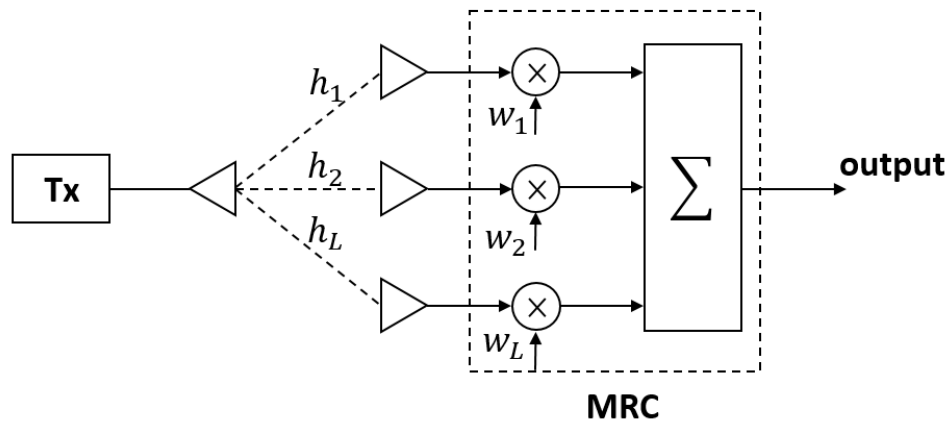
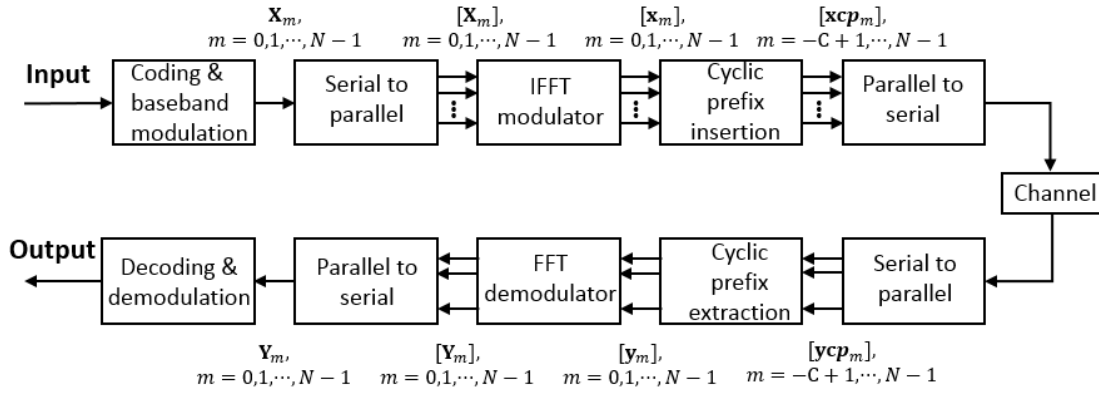


Figure 2.5 Maximum-ratio combining structure

## 2.7. OFDM

Orthogonal Frequency Division Multiplexing (OFDM) is a method of encoding digital data on multiple carrier frequencies. OFDM is a special case of Frequency Division Multiplex (FDM) which uses a large number of closely spaced orthogonal sub-carrier signals to carry data on several parallel data streams or channels. Each sub-carrier is modulated at a low symbol rate and has the total data rates similar with single-carrier schemes in the same bandwidth [30, 31, 41].

In OFDM, the sub-carrier frequencies are chosen and the sub-carriers are orthogonal to each other, meaning that cross-talk between the sub-channels is eliminated and inter-carrier guard bands are not required, that greatly simplifies the design of both the transmitter and the receiver.



**Figure 2.6 Block diagram of an OFDM system**

In figure 2.6, the input data is modulated by using a digital modulation scheme such as Binary Phase Shift Keying (BPSK), Quadrature Phase Shift Keying (QPSK) and different constellation levels of Quadrature Amplitude Modulation (QAM). Then the data symbols are parallelized in  $N$  different sub-streams. Each sub-stream will modulate a separate carrier through the Inverse Fast Fourier Transform (IFFT) modulation block. A cyclic prefix is inserted in order to avoid inter-symbol interference (ISI) and inter-block interference (IBI). This cyclic prefix of length  $C$  is a circular extension of the IFFT-modulated symbol, obtained by copying the last  $C$  samples of the symbol in front of it. Next, the data are converted back to serial and forming an OFDM symbol that will modulate a high-frequency carrier before its transmission through the channel. At the receiver, the system will perform the inverse operations [41].

## 2.8. Information Theory

### 2.8.1. Entropy

Entropy is a measurement of the uncertainty with a random variable, and it defines the limitation of lossless compression. For a random variable  $X$ , its entropy is defined as [35]

$$H(X) = -\sum_{x \in \mathcal{X}} p(x) \log p(x) \quad (2.15)$$

where  $p(x) = \Pr\{X = x\}, x \in \mathcal{X}$  is the probability mass function. In the digital system, the log is usually to the base 2 and entropy is expressed in bits. The entropy of continuous random variable is infinite, because the possible values are infinite.

### 2.8.2. Joint Entropy

The uncertainty of a pair of random variables can be measured with joint entropy. For a given pair of discrete random variables  $(X, Y)$ , their joint entropy is defined as [35]:

$$H(X, Y) = -\sum_{x \in \mathcal{X}} \sum_{y \in \mathcal{Y}} p(x, y) \log p(x, y) \quad (2.16)$$

where  $p(x, y)$  is the joint distribution probability.

Furthermore, the conditional entropy of a pair of discrete random variables  $(X, Y)$  can be defined as [35]:

$$\begin{aligned} H(Y | X) &= \sum_{x \in \mathcal{X}} p(x) H(Y | X = x) \\ &= -\sum_{x \in \mathcal{X}} p(x) \sum_{y \in \mathcal{Y}} p(y | x) \log p(y | x) \\ &= -\sum_{x \in \mathcal{X}} \sum_{y \in \mathcal{Y}} p(x, y) \log p(y | x) \end{aligned} \quad (2.17)$$

The joint entropy of a pair of random variables can be expressed with the entropy of  $X$  plus the conditional entropy of the other variable  $Y$ .

$$H(X, Y) = H(X) + H(Y | X) \quad (2.18)$$

we can also expand the rule to three random variables:

$$H(X, Y | Z) = H(X | Z) + H(Y | X, Z) \quad (2.19)$$

### 2.8.3. Mutual Information

Mutual information measures the similarity between a pair of random variables. For a pair of discrete random variables  $(X, Y)$ , the mutual information can be expressed as [35]:

$$I(x; y) = \sum_{x \in X} \sum_{y \in Y} p(x, y) \log \frac{p(x, y)}{p(x)p(y)} \quad (2.20)$$

where  $p(x, y)$  is the joint probability mass function and  $p(x)$ ,  $p(y)$  are marginal probability mass functions.

For random variables  $X$  and  $Y$  given  $Z$ , the conditional mutual information can be defined by:

$$\begin{aligned} I(X; Y | Z) &= H(X | Z) - H(X | Y, Z) \\ &= \sum_{x \in X, y \in Y, z \in Z} p(x, y, z) \log \frac{p(x, y | z)}{p(x | z)p(y | z)} \end{aligned} \quad (2.21)$$

### 2.8.4. Mutual Information and Entropy

$$\begin{aligned} I(X; Y) &= H(X) - H(X | Y) \\ I(X; Y) &= H(Y) - H(Y | X) \\ I(X; Y) &= H(X) + H(Y) - H(X, Y) \\ I(X; Y) &= I(Y; X) \end{aligned} \quad (2.22)$$

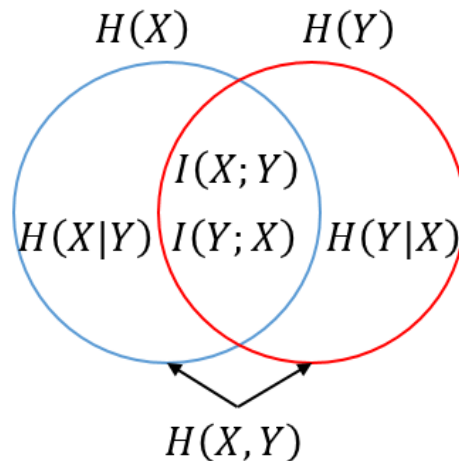


**Figure 2.7 Relationship between entropy and mutual information**

## 2.9. Slepian-Wolf Code

The Slepian-Wolf theorem was introduced by David Slepian and Jack Wolf in 1973 [45]. The theorem deals with the lossless compression of distributed correlated sources, and it also indicates that each of the correlated sources can be encoded separately without knowledge of the other sources and the compressed data from all these sources can be jointly decoded with arbitrarily small error probability [87]. Slepian-Wolf coding can achieve the same compression rate as the optimal joint compression. In Figure 2.8, sources  $X_1$  and  $X_2$  are two correlated sources, if  $X_1, X_2$  are separately encoded without exploiting the correlated information, we can constrain the achievable rate pair  $(R_1, R_2)$  by [87]:

$$\begin{aligned}
 R_1 + R_2 &\geq H(X_1) + H(X_2) \\
 R_1 &\geq H(X_1) \\
 R_2 &\geq H(X_2)
 \end{aligned}
 \tag{2.23}$$

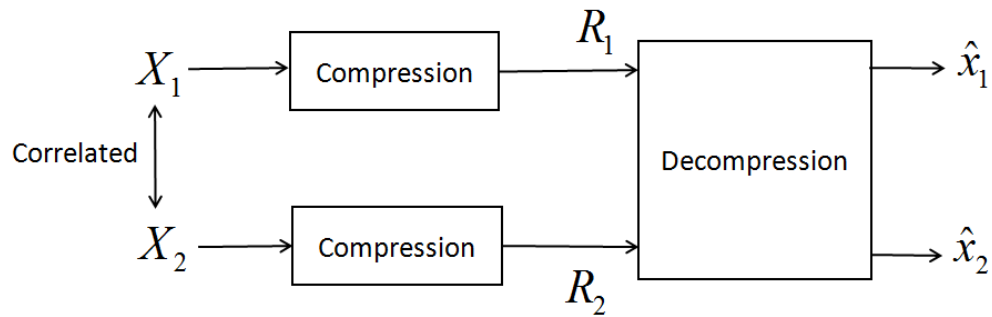


**Figure 2.8 Slepian-Wolf concept,  $\hat{x}_1$  and  $\hat{x}_2$  are the estimation of source  $x_1$  and  $x_2$**

The Slepian-Wolf region and non Slepian-Wolf region are shown in figure 2.9. By implementing a Slepian-Wolf code, the system require less transmit rate, and future reduce the channel capacity [87].

$$\begin{aligned}
 R_1 + R_2 &\geq H(X_1, X_2) \\
 R_1 &\geq H(X_1 / X_2) \\
 R_2 &\geq H(X_2 / X_1)
 \end{aligned}
 \tag{2.24}$$

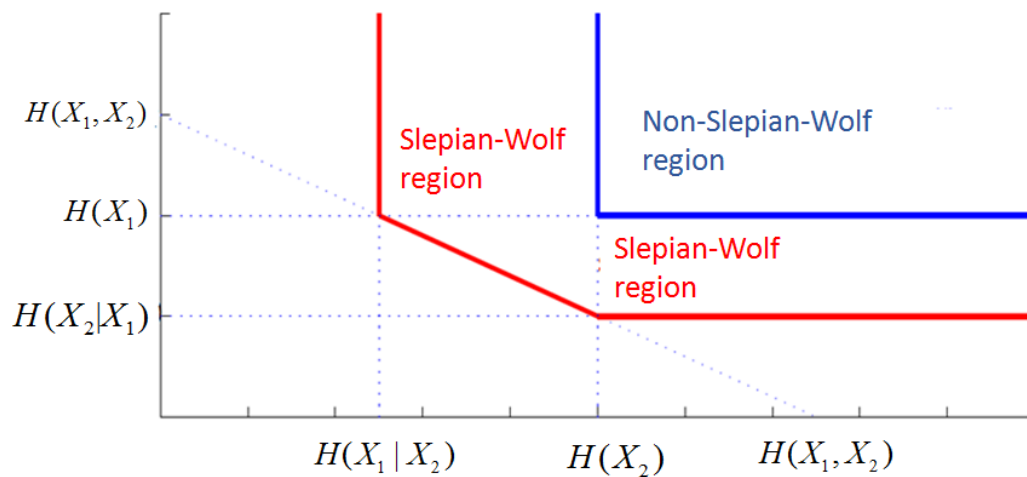


**Figure 2.9. Slepian-Wolf rate region**

## 2.10. Chapter Summary

In this chapter, we have introduced the definition and architectures of C-RAN and the basic structure of traditional MIMO and channel models. These system structures are helpful to build up the systems in our following chapters. We have also introduced the detection techniques that will be used for the designing with BBU. Then the quantization and combiner are introduced which will also be used in our future system development. Finally, the information theory with compression techniques are introduced which relate to the system development of constrained fronthaul.

---

## Chapter 3 Detection Techniques with Quantization at Receiver in Single Carrier Scheme

### 3.1. Introduction

In a C-RAN system, more than one BS forwards multiple users' signal to the BBU simultaneously, all of the base stations using the same spectral bandwidth. This causes interference between neighbouring cells. In this chapter, we will explore the detection techniques used in the central processors at the BBU. Those detectors remove the interference and separate the user signals. The advanced detection techniques we introduce in this chapter are: ZF, MMSE and ML, also discussed in [36, 37, 75]. Each of the detectors will recover the quantized signals which are sent from the RRUs. We will analyse the effect of quantization on BPSK and QPSK with ML and ZF detection methods. Besides, due to the constrained-fronthaul network between RRUs and BBU, multiple levels of quantization at RRUs will be deployed. We will then analyse the impact of the quantization level on the fronthaul load and the BER performance with each detection technique.

### 3.2. System Model

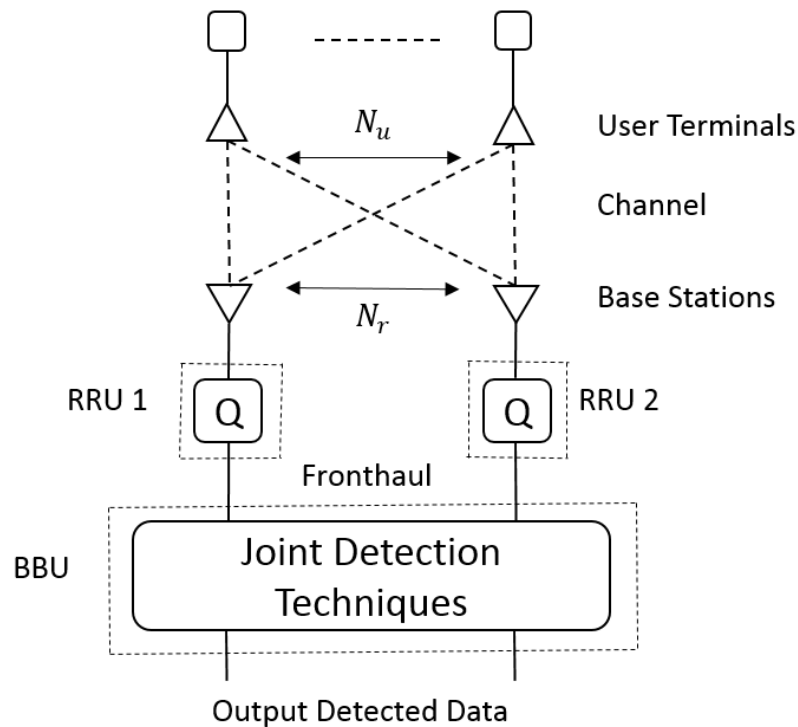


**Figure 3.1 System model of a basic C-RAN system**

In this system, an uplink MIMO system is considered. In Figure 3.1, the system has two user terminals and two base stations. Each user terminal has one transmit antenna, and each BS contains one receive antenna. Thus we have  $N_u = 2$  and  $N_r = 2$ . In this model we assume perfect CSI. At each receive antenna, the complex signal data is quantized: here we use uniform quantization. The quantized data is then input to detection filters and the recovered data of the two users is output. The structure is shown in Figure 3.2.

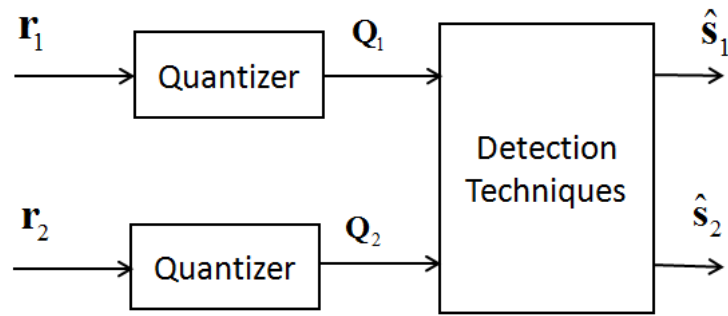


**Figure 3.2** Detection techniques after quantizer.  $r_1$  and  $r_2$  represent the received signal at each base station.  $Q_1$  and  $Q_2$  represent the quantized signals.  $\hat{s}_1$  and  $\hat{s}_2$  represent the recovered signal with two users.

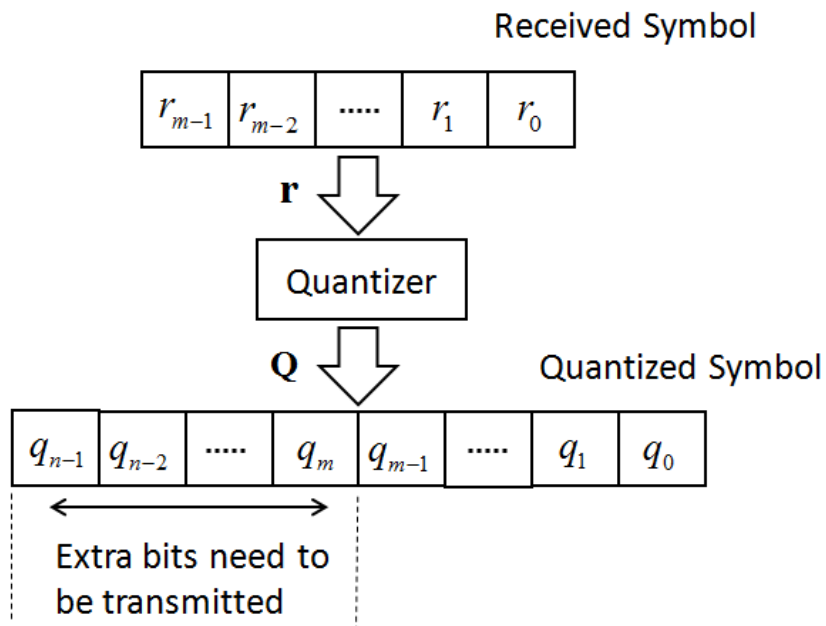


**Figure 3.3** Extra quantization index bits need to be transmitted in fronthaul

The quantization level affects the fronthaul load and transmission efficiency. If the quantization level is much higher than the modulation level of the system, the RRU will need to transmit more binary bits with each quantized symbol than the unquantized symbol. The extra bits  $N_{extra}$  which need to be transmitted can be defined as:

$$\begin{aligned}
N_{extra} &= n - m - 2 \\
n &= \log_2(L_Q) \\
m &= \log_2(L_M)
\end{aligned} \tag{3.1}$$

where  $L_Q$  is the quantization level, and  $L_M$  is the modulation level. In practice,  $N_{extra}$  should be kept as low as we can, to avoid too much fronthaul load with transmission. For the system design and simulation, we investigate the minimum number of extra bits required to achieve an accredited BER performance. In the following simulation, the performance should be close to the optimal BER performance with which unquantized data can be decoded. However, the unquantized case is not practical as it would require an effectively infinitely fronthaul load. We assume the channel between user terminals and base stations is a multipath Rayleigh fading channel. We also assume that the channel between RRUs and BBU is a "bit pipe", which delivers the signal bits without any losses.

### 3.3. Theory Analysis

In this section, we will explore the effect of quantization on BPSK and QPSK with ML and ZF detection methods, and compare the theoretical results with the simulation results in MATLAB.

The basic idea to explore the effect of quantization on the received signal at BBU is to estimate the probability of failure to recover the desired data from multiple sources, and the recovery failure will also generate erroneous bits at the BBU, and we call it outage probability. By analysing the outage cases with the quantized data, we can estimate the overall bit error rate (BER) at BBU.

#### 3.3.1 Quantization with BPSK Modulation Scheme

##### ➤ BPSK on real-only channel

Let data vector be:

$$\mathbf{x} = [x_1 \quad x_2], x_1, x_2 \in \{-1, 1\} \quad (3.2)$$

Received signal, neglecting noise:

$$y = \mathbf{h}\mathbf{x} = h_1x_1 + h_2x_2 \quad (3.3)$$

We assume that some form of automatic gain control adjusts the maximum signal  $y_{max}$  at the access point to correspond to the maximum quantization centre, then:

$$y_{max} = |h_1| + |h_2| = (l-1) \frac{\Delta}{2} \quad (3.4)$$

where  $l$  is the number of quantization steps, and  $\Delta$  is the quantization interval which can be expressed as:

$$\Delta = \frac{2y_{max}}{l-1} = \frac{2(|h_1| + |h_2|)}{l-1} \quad (3.5)$$

With different numbers of quantization levels, the quantization threshold  $q_{th}$  shown in figure 3.4 can be defined with:

$$q_{th} = y_{max} - \frac{y_{max}}{\frac{(l-1) \times 2}{2}} = y_{max} - \frac{y_{max}}{l-1} \quad (3.6)$$

The quantizer is a one-domain mid-rise quantizer, and the output of the quantizer rounds to the nearest quantization point (positive or negative). Assuming  $|h_1| > |h_2|$ , for  $h_1 = 1, h_2 = 0.8$ , with  $l = 4$ , the received constellation is:

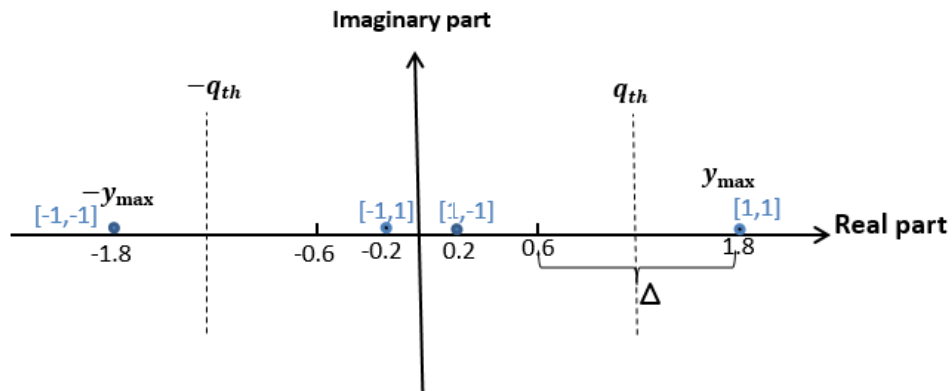


**Figure 3.4 Constellation of received points with  $h_1 = 1, h_2 = 0.8$**

which quantizes as follows (with  $\Delta = 1.2$ ):

$x$	<b>[-1,-1]</b>	<b>[-1,1]</b>	<b>[1,-1]</b>	<b>[1,1]</b>
$y$	-1.8	-0.2	0.2	1.8
$Q$	-1.8	-0.6	0.6	1.8

**Table 3.1 Quantization results of received signal with  $h_1 = 1, h_2 = 0.8$**

In figure 3.4,  $Q$  is the quantization output of  $y$ . The received point  $[1, 1]$  is great than the threshold  $q_{th}$ , and  $[1,-1]$  is less than  $q_{th}$ , which results in  $[1, 1]$  and  $[1,-1]$  being quantised to different quantization points corresponding to the results shows in Table 3.1. Similarly received points  $[-1, -1]$  and  $[-1, 1]$  are quantized to different quantization points. Thus  $Q$  can be decoded perfectly using ML detection, and the transmitted signal can be fully recovered without errors.

With another example, for  $h_1 = 1.6, h_2 = 0.2$ , and  $l = 4$ , the received constellation is:

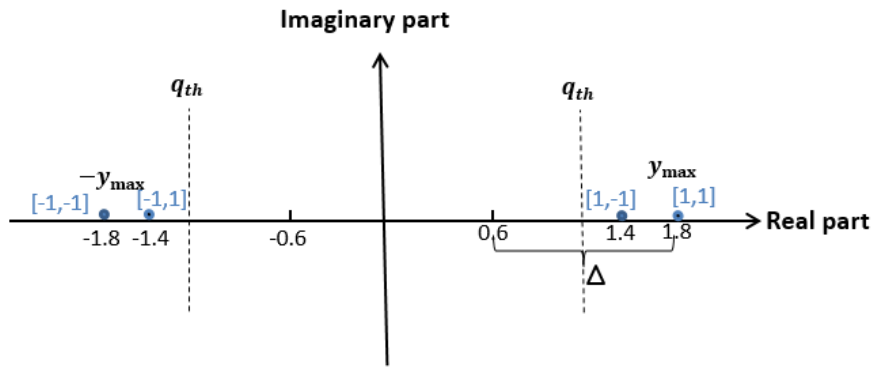


**Figure 3.5 Constellation of received points with  $h_1 = 1.6, h_2 = 0.2$**

Comparing figure 3.5 with figure 3.4,  $h_1 = 1.6, h_2 = 0.2$  and  $h_1 = 1, h_2 = 0.8$  have the same quantization step  $l$  and length of quantization interval  $\Delta$ , however, the results for  $Q$  are different, as shown in Table 3.2, which quantizes as follows (with  $\Delta = 1.2$ ):

$x$	<b>[-1,-1]</b>	<b>[-1,1]</b>	<b>[1,-1]</b>	<b>[1,1]</b>
$y$	-1.8	-1.4	1.4	1.8
$Q$	-1.8	-1.8	1.8	1.8

**Table 3.2 Quantization results of received signal with  $h_1 = 1.6, h_2 = 0.2$**

In figure 3.5, the transmitted data vector  $[1, 1]$  and  $[1, -1]$  are both greater than the threshold  $q_{th}$ , so that both of the vectors are quantized to the same quantization point. Similarly, the transmitted data vectors  $[-1, -1]$  and  $[-1, 1]$  are quantized to the same quantization point  $-1.8$ , as shown in Table 3.2. Using the ML detection method expressed in equation 2.11, thus the vector  $[1, -1]$  will be decoded to  $[1, 1]$ , and hence  $x_2$  will be decoded incorrectly. In figure 3.4 and 3.5, we can also notice the symmetry of the coordinate axis: if  $[1, -1]$  and  $[1, 1]$  in the positive side are in outage, then  $[-1, 1]$  and  $[-1, -1]$  will be in outage. Thus we only need to consider the outage probability on one side.

Assume  $|h_1| > |h_2|$ , with  $l = 4$  the distance between quantization threshold  $q_{th}$  and

$y_{\max}$  can be defined with  $\frac{|h_1| + |h_2|}{3}$ , we can express the condition for the outage

probability:

$$\begin{aligned}
 P_{outage} &= P\left(\left(|h_1| + |h_2|\right) - \left(|h_1| - |h_2|\right) < \frac{|h_1| + |h_2|}{3}\right) \\
 &= P\left(2|h_2| < \frac{|h_1| + |h_2|}{3}\right) \\
 &= P\left(5|h_2| < |h_1|\right) \\
 &= P\left(|h_2| < \frac{|h_1|}{5}\right)
 \end{aligned} \tag{3.7}$$

Thus the PDF for the outage probability can be expressed as:

$$P\left(|h_2| < \frac{|h_1|}{5}\right) = \int_0^\infty p(|h_1|) \int_0^{\frac{|h_1|}{5}} p(|h_2|) d|h_2| d|h_1| \tag{3.8}$$

Thus a common condition of outage probability with quantization step  $l$  can be expressed as:

$$\begin{aligned}
 P_{outage} &= P\left(\left(|h_1| + |h_2|\right) - \left(|h_1| - |h_2|\right) < \frac{|h_1| + |h_2|}{l-1}\right) \\
 &= P\left(2|h_2| < \frac{|h_1| + |h_2|}{l-1}\right) \\
 &= P\left((2l-3)|h_2| < |h_1|\right) \\
 &= P\left(|h_2| < \frac{|h_1|}{2l-3}\right)
 \end{aligned} \tag{3.9}$$

and the outage probability can be expressed as:

$$\begin{aligned}
 P_{outage} &= \int_0^\infty p(|h_1|) \int_0^{\frac{|h_1|}{2l-3}} p(|h_2|) d|h_2| d|h_1| \\
 &= \frac{\operatorname{atan}\left(\frac{1}{2 \times l - 3}\right)}{\pi}
 \end{aligned} \tag{3.10}$$

Which takes into account both cases  $|h_1| > |h_2|$  and  $|h_1| < |h_2|$ .

Once the outage condition occurs, the symbol will have the second bit in error ( $|h_1| > |h_2|$ ) or first bit in error ( $|h_1| < |h_2|$ ), and thus we have:

$$\text{BER} = \frac{P_{\text{outage}}}{2} \quad (3.11)$$

To calculate the outage probability, we derive equation (3.10) in Wolfram Mathematica. By giving multiple numbers of quantization levels, the theoretical results are shown in Table 3.3:

Number of Quantization Level	Theoretical Results	Simulation Results
4	0.0628	0.0631
8	0.0244	0.0244
16	0.0110	0.0113
64	0.0026	0.0025

**Table 3.3 Comparison between the theoretical and simulation results for BPSK with real-only channel**

In Table 3.3, the simulation results are simulated in MATLAB. We set up a system transmitting binary data bit from two sources through a real-only channel, next quantize the received signal with a one domain mid-rise quantizer, then the quantized data is recovered by using ML detection, and finally we can count the number of erroneous bits and calculate the overall BER. From the results shown in Table 3.3, it can be seen that the theoretical results and simulation results are very close.

► **BPSK on complex channel**

For the complex channel, we assume that the quantization is a two-domain mid-rise quantizer, and rounds the outputs to the nearest complex quantization point. The outage conditions in equation 3.10 could apply to either the real or the imaginary part, or to both of the parts, and the maximum quantization centre  $y_{max}$  can be defined as:

$$y_{max} = |\text{Re}[h_1]| + |\text{Re}[h_2]| + j(|\text{Im}[h_1]| + |\text{Im}[h_2]|) \quad (3.12)$$

and then:

$$\begin{aligned} y_{max}^{real} &= |\text{Re}[h_1]| + |\text{Re}[h_2]| \\ y_{max}^{imag} &= |\text{Im}[h_1]| + |\text{Im}[h_2]| \end{aligned} \quad (3.13)$$

With the number of quantization levels  $L_Q$ , the quantization step  $l$  can be denoted as

$\sqrt{L_Q}$ , and thus the threshold  $q_{th}$  can be denoted for the real and imaginary parts:

$$\begin{aligned} q_{th}^{real} &= y_{max}^{real} - \frac{y_{max}^{real}}{(l-1)} \\ q_{th}^{imag} &= y_{max}^{imag} - \frac{y_{max}^{imag}}{(l-1)} \end{aligned} \quad (3.14)$$

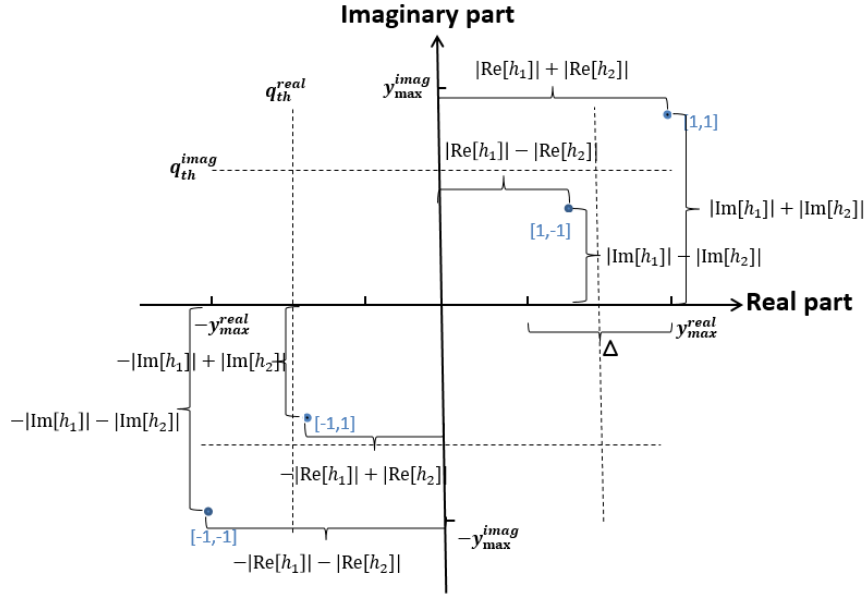


**Figure 3.6 Constellation of received points with two-domain quantizer**

The common outage probability with quantization step  $l$  can be expressed as:

$$P_{outage}^{real} = P\left(|\text{Re}[h_2]| < \frac{|\text{Re}[h_1]|}{2l-3}\right) \quad (3.15)$$

$$P_{outage}^{imag} = P\left(|\text{Im}[h_2]| < \frac{|\text{Im}[h_1]|}{2l-3}\right)$$

Note that the received signal must meet the outage condition in both real and imaginary parts, and thus the total outage probability condition can be expressed as:

$$P_{outage} = P_{outage}^{real} \times P_{outage}^{imag} = P\left(|\text{Re}[h_2]| < \frac{|\text{Re}[h_1]|}{2l-3}\right) \times P\left(|\text{Im}[h_2]| < \frac{|\text{Im}[h_1]|}{2l-3}\right) \quad (3.16)$$

Similar to equation 3.11, we also have the BER for the complex channel:

$$\text{BER} = \frac{P_{outage}}{2} = \frac{P_{outage}^{real} \times P_{outage}^{imag}}{2} \quad (3.17)$$

For ML detection, all the possible transmitted symbols should be quantized, and the ML detection equation can be expressed with:

$$\hat{\mathbf{x}}_{ML} = \min \left( \left\| \mathbf{Q} - \mathbf{q}(\mathbf{H}\mathbf{x}) \right\|^2 \right) \quad (3.18)$$

where  $\mathbf{x} \in \{+1, -1\}$  and,  $\mathbf{q}(\mathbf{H}\mathbf{x})$  denotes the quantization of all the possible transmitted symbols. In this case, the ML detector outputs the recovered vector which has minimum distance between the received quantizing symbol and all of the possible quantizing symbols. Note that, the minimum distance is 0 from the desired symbols. In an outage case there will be more than one symbol having the minimum distance. Thus any bits which are different in the two symbol labels will be in error with probability 0.5 if there are two symbols at the same distance.

An alternative approach to ML detection might compare the received signal to unquantized signal values, expressed as:

$$\hat{\mathbf{x}}_{ML} = \min \left( \left\| \mathbf{Q} - \mathbf{H}\mathbf{x} \right\|^2 \right) \quad (3.19)$$

In this case, the system will have another outage case when  $|\text{Re}_1| + |\text{Re}_2|$  is much greater than  $|\text{Im}_1| + |\text{Im}_2|$ , or  $|\text{Im}_1| + |\text{Im}_2|$  is much greater than  $|\text{Re}_1| + |\text{Re}_2|$ , as shown in figure 3.7:

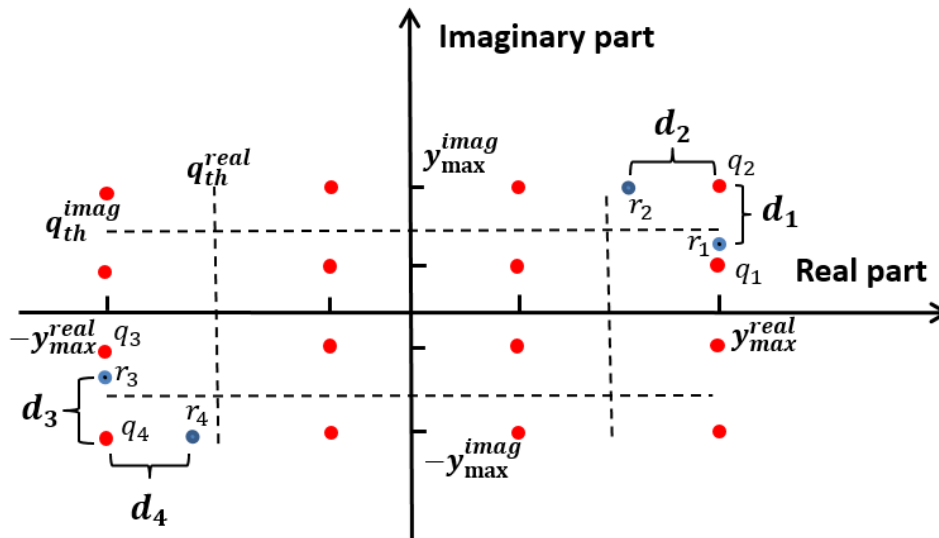


**Figure 3.7** Outage case with ML detection without quantize the possible received symbol

In figure 3.7, the blue points  $r_1, r_2, r_3, r_4$  are the four possible received symbol, and the red points are the 16 quantization points. After quantizing the 4 possible symbols,  $r_1$  is quantized to quantization point  $q_1$ , and  $r_2$  is quantized to quantization point  $q_2$ . The distance between the quantization point  $q_2$  and the received symbol  $r_1$  is  $d_1$ , and the distance between  $q_2$  and  $r_2$  is  $d_2$ . If  $r_2$  is the desired symbol, then  $q_2$  will be the target point which is to be compared with the distances from all the possible received points. We assume  $|\text{Re}_1| + |\text{Re}_2|$  is much greater than  $|\text{Im}_1| + |\text{Im}_2|$ , and this could give  $d_1 < d_2$ , then the target point will be recovered to symbol  $r_1$  instead of  $r_2$ , which generates errors in the recovered data bits. A similar outage case occurs when  $|\text{Im}_1| + |\text{Im}_2|$  is much greater than  $|\text{Re}_1| + |\text{Re}_2|$ .

This outage case occurs when the real part is in outage and the imaginary part is not in outage, or vice versa. Besides, it also need to meet  $d_1 < d_2$  or  $d_2 < d_1$

corresponding to two cases. Thus it can be seen that ML method with un-quantized possible received symbol will generate more error to the recovered symbol.

The theoretical results can be calculated in Wolfram Mathematica using equation (3.16) and equation (3.17). To develop the simulation system, we extend the channel to complex channel. Note that the real and imaginary part separately are the same as for the real only case shows in Table 3.3, thus we have the results shown in Table 3.4:

Number of Quantization Level	Theoretical Results	Simulation Results (ML with quantize the possible received symbol)
16	0.0076	0.0078
64	0.0011	0.0011
256	0.00021	0.00024
1024	0.000058	0.000054

**Table 3.4 Comparison between the theoretical and simulation results for BPSK with complex channel**

In Table 3.4, the simulation results for the ideal case give the same value as the theoretical result for different quantization levels. Simulation results with non-ideal case has a higher outage probability to generate errors in the recovered data bits.

Furthermore, with more APs, we assume the channels are independent, thus the outage probability at each AP is independent. If the transmitted signal at the first AP is in outage, then the system can still recover the data vector correctly by using the quantized symbol at second AP. When the quantized symbol at both APs are in outage, then the recovered bits will have errors. Thus we can calculate the outage probability for a two

APs system by squaring the outage probability for only one AP. With  $N$  APs we can express the total outage probability as:

$$P_{outage2 \times N} = P_{outage2 \times 1}^N \quad (3.20)$$

The results of a two APs system are shown in Table 3.5:

Number of Quantization Level	Theoretical Results	Simulation Results (ML with quantize the possible received symbol)
16	0.000125	0.000154
64	$1.15 \times 10^{-7}$	0

**Table 3.5 Comparison between the theoretical and simulation results for BPSK with complex channel with two APs**

### ➤ Effect of quantization in Zero Forcing

In this part we will analysis the outage cases with quantization in Zero Forcing. The fundamental idea is to represent the effect of transmission from two sources over the channel pair (represented by the vector  $\mathbf{h}$ ), then quantization at an AP, as equivalent to multiplication of the vector of source data  $\mathbf{x}$  by an integer vector representing the joint effect of channel and quantization. Assuming there are two APs, this forms a  $2 \times 2$  matrix: successful reception of both sources requires that this be full rank.

We assume the quantizer is a mid-rise quantizer with integer output, and therefore rounds to the nearest odd integer (positive or negative), which we will denote by:

$$y^q = Q_{odd} \left( \frac{2y}{\Delta} \right) \quad (3.21)$$

Note that  $y^q$  is different from  $Q$  in previous section, and  $Q$  can be obtain by  $\frac{y_q \times \Delta}{2}$ .

For example, for  $h_1 = 1, h_2 = 0.8$ , which quantizes as follows (with  $\Delta = 1.2$ ):

$x$	<b>[-1,-1]</b>	<b>[-1,1]</b>	<b>[1,-1]</b>	<b>[1,1]</b>
$y$	-1.8	-0.2	0.2	1.8
$y^q$	-3	-1	1	3

**Table 3.6 Integer quantization results of received signal with  $h_1 = 1, h_2 = 0.8$**

The same result would be obtained from  $y^q = \mathbf{x}\mathbf{h}^q$  with  $\mathbf{h}^q = [2,1]$ , so this can be regarded as the equivalent integer channel vector.

For  $l = 4$  the same vector will apply for any channel coefficients such that the received signals quantize to the same values, i.e. provided:

$$\begin{aligned} \frac{|h_1| + |h_2|}{|h_1| - |h_2|} &> \frac{l-1}{l-2} = \frac{3}{2} \\ |h_2| &> \frac{|h_1|}{5} \end{aligned} \quad (3.22)$$

and assuming  $|h_1| > |h_2|$ . If  $|h_2| < \frac{|h_1|}{5}$ , then the values will quantize as follows:

$x$	<b>[-1,-1]</b>	<b>[-1,1]</b>	<b>[1,-1]</b>	<b>[1,1]</b>
$y^q$	-3	-3	3	3

**Table 3.7 Integer quantization results of received signal with  $|h_2| < \frac{|h_1|}{5}$**

which is equivalent to the integer channel vector  $[3, 0]$ . There are other possibilities, depending on the sign of  $h_1$  and  $h_2$  are shown in Table 3.8:

$h_1 > 0, h_2 > 0,$ $5h_1 > h_2 > h_1/5$	<b>x</b>	[-1,-1]	[-1,1]	[1,-1]	[1,1]	<b>h<sup>q</sup></b>	<b>Condition</b>
	<b>y<sup>q</sup></b>	-3	-1	1	3	[2,1]	<b>Probability</b> $p_1 = 0.0936$
$h_1 > 0$ $ h_2  < h_1/5$	<b>x</b>	[-1,-1]	[-1,1]	[1,-1]	[1,1]		
	<b>y<sup>q</sup></b>	-3	-3	3	3	[3,0]	$p_2 = 0.0628$
$h_1 > 0, h_2 < 0,$ $-5h_1 < h_2 < -h_1/5$	<b>x</b>	[-1,-1]	[-1,1]	[1,-1]	[1,1]		
	<b>y<sup>q</sup></b>	-1	-3	3	1	[2,-1]	$p_3 = 0.0936$
$h_1 < 0, h_2 > 0,$ $-5h_1 > h_2 > -h_1/5$	<b>x</b>	[-1,-1]	[-1,1]	[1,-1]	[1,1]		
	<b>y<sup>q</sup></b>	1	3	-3	-1	[-2,1]	$p_4 = 0.0936$
$h_1 < 0, h_2 < 0,$ $5h_1 < h_2 < h_1/5$	<b>x</b>	[-1,-1]	[-1,1]	[1,-1]	[1,1]		
	<b>y<sup>q</sup></b>	3	1	-1	-3	[-2,-1]	$p_5 = 0.0936$
$h_1 < 0$ $ h_2  <  h_1 /5$	<b>x</b>	[-1,-1]	[-1,1]	[1,-1]	[1,1]		
	<b>y<sup>q</sup></b>	3	3	-3	-3	[-3,0]	$p_6 = 0.0628$

**Table 3.8 Integer quantization results and condition probability with sign of  $h_1$  and  $h_2$**

In Table 3.8, the condition probability for each case can be expressed as:

$$p_1 = \frac{1}{2} \int_0^\infty p(h_1) \int_{\frac{h_1}{2l-3}}^{(2l-3)h_1} p(h_2) dh_2 dh_1 = \frac{\text{atan}\left(\frac{12}{2l-3}\right)}{4\pi}, \quad (3.23)$$

$$p_2 = 2 \int_0^\infty p(h_1) \int_0^{\frac{h_1}{2l-3}} p(h_2) dh_2 dh_1 = \frac{\text{atan}\left(\frac{1}{2l-3}\right)}{4\pi}, \quad (3.24)$$

$$p_3 = \frac{1}{2} \int_0^\infty p(h_1) \int_{-\frac{h_1}{2l-3}}^{-(2l-3)h_1} p(h_2) dh_2 dh_1 = \frac{\text{atan}\left(\frac{12}{2l-3}\right)}{4\pi}, \quad (3.25)$$

$$p_4 = \frac{1}{2} \int_{-\infty}^0 p(h_1) \int_{-\frac{h_1}{2l-3}}^{-(2l-3)h_1} p(h_2) dh_2 dh_1 = \frac{\text{atan}\left(\frac{12}{2l-3}\right)}{4\pi}, \quad (3.26)$$

$$p_5 = \frac{1}{2} \int_{-\infty}^0 p(h_1) \int_{\frac{h_1}{2l-3}}^{(2l-3)h_1} p(h_2) dh_2 dh_1 = \frac{\text{atan}\left(\frac{12}{2l-3}\right)}{4\pi} \quad \text{and} \quad (3.27)$$

$$p_6 = 2 \int_{-\infty}^0 p(h_1) \int_0^{-\frac{h_1}{2l-3}} p(h_2) dh_2 dh_1 = \frac{\text{atan}\left(\frac{1}{2l-3}\right)}{4\pi} \quad (3.28)$$

where  $l$  is the number of quantization steps which is 4. Note that the probability results with  $p_1$ ,  $p_3$ ,  $p_4$  and  $p_5$  are the common cases for both  $|h_1| > |h_2|$  and  $|h_1| < |h_2|$ , thus for only  $|h_1| > |h_2|$ , the result is half of the probability. Then equation 3.23 to equation 3.28 can be calculated in Wolfram Mathematica. These results correspond to  $|h_1| > |h_2|$ , and the sum of the probability of conditions is equal to 0.5; there is a corresponding set, with all vectors reversed, corresponding to  $|h_1| < |h_2|$ , and the sum of probability of conditions is another half of the total probability. It is possible to calculate the probability of each of these conditions, and hence the corresponding integer vectors for each access point. We assume that the channels are independent for each access point, so the integer vectors are also independent.

These vectors form the columns of the equivalent integer channel matrix, which should be full rank for correct decoding. Hence an outage will occur (usually for both sources) if the matrix is rank-deficient. This will occur if one column is a multiple of the other. For example, if the integer channel vector with first AP is  $[2, 1]$ , and the integer channel vector with second AP is  $[-2, -1]$ , then the channel matrix is rank-deficient, which

results the recovered results by ZF is in outage. The probability of this rank-deficient channel matrix appears is  $0.0936 \times 0.0936 = 0.0087$ . Thus, we can calculate the total outage probability for the rank-deficient channel matrix with:

$$P_{|h_1|>|h_2|} = (p_1p_1 + p_1p_5) + (p_2p_2 + p_2p_6) + (p_3p_3 + p_3p_4) + \dots \quad (3.29)$$

$$(p_4p_4 + p_4p_3) + (p_5p_5 + p_5p_2) + (p_6p_6 + p_6p_2)$$

where  $P_{|h_1|>|h_2|}$  is the outage probability for  $|h_1|>|h_2|$ , and the result is 0.0859. Thus the total outage probability is  $P_{|h_1|>|h_2|} + P_{|h_1|<|h_2|} = 2 \times P_{|h_1|>|h_2|} = 0.1718$ . The comparison of the theoretical results and simulation results are shown in Table 3.9:

Condition $ h_1  >  h_2 $	Theoretical Results	Simulation results with $ h_1  >  h_2 $	Condition $ h_1  <  h_2 $	Simulation results with $ h_1  <  h_2 $
$h_1 > 0, h_2 > 0,$ $5h_1 > h_2 > h_1/5$	0.0175	0.0169	$h_1 > 0, h_2 > 0,$ $5h_2 > h_1 > h_2/5$	0.0168
$h_1 > 0$ $ h_2  < h_1/5$	0.0078	0.0075	$h_2 > 0$ $ h_1  < h_2/5$	0.0080
$h_1 > 0, h_2 < 0,$ $-5h_1 < h_2 < -h_1/5$	0.0175	0.0165	$h_1 < 0, h_2 > 0,$ $-5h_2 < h_1 < -h_2/5$	0.0173
$h_1 < 0, h_2 > 0,$ $-5h_1 > h_2 > -h_1/5$	0.0175	0.0167	$h_1 > 0, h_2 < 0,$ $-5h_2 > h_1 > -h_2/5$	0.0163
$h_1 < 0, h_2 < 0,$ $5h_1 < h_2 < h_1/5$	0.0175	0.0172	$h_1 < 0, h_2 < 0,$ $5h_2 < h_1 < h_2/5$	0.0175
$h_1 < 0$ $ h_2  <  h_1 /5$	0.0078	0.0080	$h_2 < 0$ $ h_1  <  h_2 /5$	0.0081
Total	0.0856	0.0828		0.0839

**Table 3.9 Comparison between the theoretical and simulation results for the outage probability in different conditions**

Table 3.9 shows the outage probability comparison in different cases. The simulation results are achieved by counting the number of integer channel matrices which are rank-deficient, and each of them will corresponding to one of the conditions. It can be seen that the simulation results with  $|h_1| > |h_2|$  and  $|h_1| < |h_2|$  both match with the theoretical results.

### 3.3.2 Quantization with QPSK Modulation Scheme

In this section, we will analyse the outage probability for QPSK. With BPSK, when two received symbol locate at the same quantization region, the outage will occurs. With QPSK, there are 16 possible received symbols shows in figure 3.8, thus it could have more than two symbol lie in the same quantization region. Here we explore three outage scenarios: four points, three points and two points lie in the same region. Each scenario includes several cases in which a different set of points lies in the same region, for different regions. Furthermore, we explore the conditions for each case, and then apply these conditions using Monte Carlo integration [92]. Finally, we compare these numerical results and the simulation results in MATLAB.

Let the data vector be:

$$\mathbf{x} = [x_1 \quad x_2], x_1, x_2 \in \left\{ \frac{-1-j}{\sqrt{2}}, \frac{-1+j}{\sqrt{2}}, \frac{1-j}{\sqrt{2}}, \frac{1+j}{\sqrt{2}} \right\} \quad (3.30)$$

According to equation 3.12, the quantization centre  $y_{\max}$  can be expressed as:

$$\begin{aligned}
y_{\max} &= \max\left(\frac{\pm 1 \pm j}{\sqrt{2}} h_1 + \frac{\pm 1 \pm j}{\sqrt{2}} h_2\right) \\
&= \max\left(\frac{1}{\sqrt{2}}(\pm 1 \pm j)(\operatorname{Re}[h_1] + j \operatorname{Im}[h_1]) + \frac{1}{\sqrt{2}}(\pm 1 \pm j)(\operatorname{Re}[h_2] + j \operatorname{Im}[h_2])\right) \quad (3.31) \\
&= \max\left(\frac{1}{\sqrt{2}}((\pm \operatorname{Re}[h_1] \mp \operatorname{Im}[h_1]) + j(\pm \operatorname{Re}[h_1] \pm \operatorname{Im}[h_1])) + \right. \\
&\quad \left. \frac{1}{\sqrt{2}}((\pm \operatorname{Re}[h_2] \mp \operatorname{Im}[h_2]) + j(\pm \operatorname{Re}[h_2] \pm \operatorname{Im}[h_2]))\right)
\end{aligned}$$

and the real part and imaginary part of  $y_{\max}$  can be expressed as:

$$y_{\max}^{\text{real}} = y_{\max}^{\text{imag}} = \frac{1}{\sqrt{2}}(|\operatorname{Re}[h_1]| + |\operatorname{Im}[h_1]| + |\operatorname{Re}[h_2]| + |\operatorname{Im}[h_2]|) \quad (3.32)$$

For QPSK, there are 16 desired data vectors:

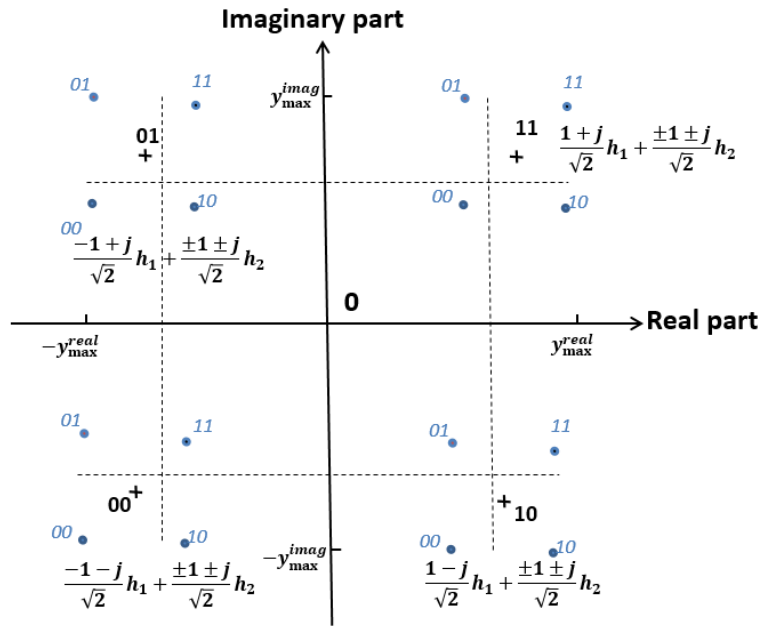


**Figure 3.8 Constellation of received points for QPSK**

We will assume that  $|h_1| > |h_2|$ , without loss of generality since results on this assumption can be converted to the opposite assumption by reversing these two symbols. Because these variables are identically distributed, and because the two cases are mutually

exclusive, the probabilities of results obtained in one case is the same as those obtained in the other case, and we can also obtain the total probability in both cases by doubling the probability for one.

Note that the symmetry of the diagram means we need only consider one cluster of the points in the constellation, corresponding to one of the symbols of source 1. We will consider the cluster around a point in the top right hand quadrant (TRHQ). We will further assume without loss of generality that these correspond to  $d_1 = 11, s_1 = (1+j)/\sqrt{2}$ .

This implies that the received signal due to this source:

$$r_1 = \frac{1}{\sqrt{2}}(1+j)h_1 = \frac{1}{\sqrt{2}}(\text{Re}[h_1] - \text{Im}[h_1] + j(\text{Re}[h_1] + \text{Im}[h_1])) \quad (3.33)$$

(which we will subsequently write  $1/\sqrt{2}(\text{Re}_1 - \text{Im}_1 + j(\text{Re}_1 + \text{Im}_1))$ ). For this to be in the TRHQ implies that:

$$(\text{Re}_1 > \text{Im}_1) \& (\text{Re}_1 > -\text{Im}_1) \quad (3.34)$$

and hence that

$$\text{Re}_1 > 0$$

Generality is preserved by this assumption since if these conditions on  $\text{Re}_1$  and  $\text{Im}_1$  do not apply for this source data, there will be another source data symbol (equally probable) for which they do.

In general also two of the four points in this cluster will be closest to the boundary set by the overall maximum of real or imaginary part: one of these will lie on the boundary. We will assume, again without loss of generality, that these two points correspond to source 2 data 11 and 10, and hence that:

$$\begin{aligned} \text{Re}_2 + \text{Im}_2 > \text{Re}_2 - \text{Im}_2 &\rightarrow \text{Im}_2 > 0 \\ \text{Re}_2 + \text{Im}_2 > \text{Im}_2 - \text{Re}_2 &\rightarrow \text{Re}_2 > 0 \end{aligned} \quad (3.35)$$

Again, if this is not the case then there will be another source 2 symbol for which it is.

There are then two cases, depending on which of these two points lies on the boundary:

Case 1:  $\text{Re}[r(1110)] > \text{Im}[r(1111)]$ , and thus 1110 lies on the boundary.

(where we note that  $r(1110)$  denotes the received signal when  $s_1 = 11$  and  $s_2 = 10$ ).

Then:

$$\frac{1}{\sqrt{2}}(\text{Re}_1 - \text{Im}_1 + \text{Re}_2 + \text{Im}_2) > \frac{1}{\sqrt{2}}(\text{Re}_1 + \text{Im}_1 + \text{Re}_2 + \text{Im}_2) \quad (3.36)$$

and hence  $\text{Im}_1 < 0$

The boundary is then given by  $\frac{1}{\sqrt{2}}(\text{Re}_1 - \text{Im}_1 + \text{Re}_2 + \text{Im}_2)$ . The next quantization threshold value is then:

$$q_{th} = q_{th}^{real} = q_{th}^{imag} = \frac{1}{\sqrt{2}}(\text{Re}_1 - \text{Im}_1 + \text{Re}_2 + \text{Im}_2) \left(1 - \frac{1}{l-1}\right) \quad (3.37)$$

where  $l = \sqrt{L}$  is the number of quantization levels.

Case 2:  $\text{Im}[r(1111)] > \text{Re}[r(1110)]$ , and thus 1111 lies on the boundary. Then:

$$\frac{1}{\sqrt{2}}(\text{Re}_1 + \text{Im}_1 + \text{Re}_2 + \text{Im}_2) > \frac{1}{\sqrt{2}}(\text{Re}_1 - \text{Im}_1 + \text{Re}_2 + \text{Im}_2) \quad (3.38)$$

Hence

$$\text{Im}_1 > 0$$

The boundary is then given by  $\frac{1}{\sqrt{2}}(\text{Re}_1 + \text{Im}_1 + \text{Re}_2 + \text{Im}_2)$ . The next quantization threshold value is then:

$$q_{th} = \frac{1}{\sqrt{2}}(\text{Re}_1 + \text{Im}_1 + \text{Re}_2 + \text{Im}_2) \left(1 - \frac{1}{l-1}\right) \quad (3.39)$$

We assume the number of quantization levels  $L$  is 16, thus we can denote the quantization step  $l = \sqrt{L} = 4$ . We also define the regions A, B, C and D as shown in figure 3.9:

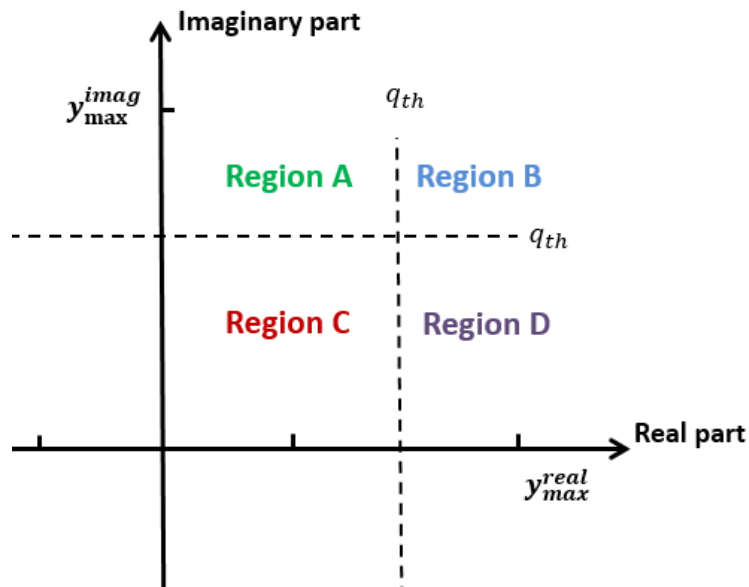
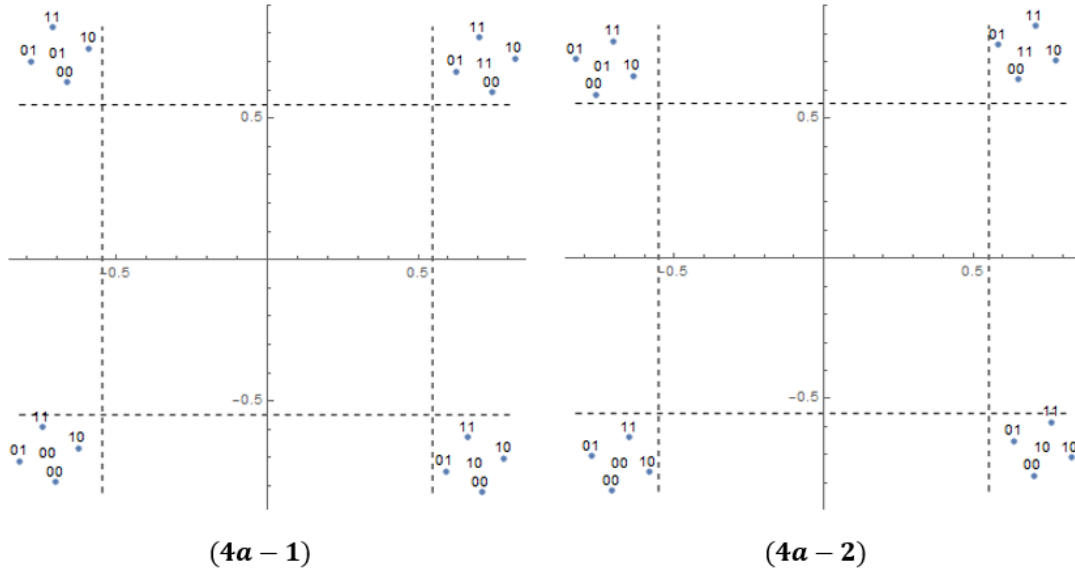


Figure 3.9 Define the region positions

Below we will explore all of the outage cases with different numbers of points in outage, located in different regions.

► **Four Points in outage**

There are two cases: four points in region B, and four points in edge region D or region A.



**Figure 3.10 Case with four points in region B**

In Figure 3.10, with case 4a-1, 1110 is on border; 1111 is not (and note  $\text{Im}_1 < 0$ ). Hence if  $\text{Re}[1100]$  is within the threshold,  $\text{Im}[1101]$  certainly is. Thus we only have one threshold:

$$\begin{aligned} \text{Im}[1100] &> q_{th} \\ \frac{1}{\sqrt{2}}(\text{Re}_1 + \text{Im}_1 - \text{Re}_2 - \text{Im}_2) &> \frac{1}{\sqrt{2}}(\text{Re}_1 - \text{Im}_1 + \text{Re}_2 + \text{Im}_2) \left(1 - \frac{1}{l-1}\right) \\ (l-1)(\text{Re}_1 + \text{Im}_1 - \text{Re}_2 - \text{Im}_2) &> (\text{Re}_1 - \text{Im}_1 + \text{Re}_2 + \text{Im}_2)(l-2) \\ \text{Re}_1 + (2l-3)(\text{Im}_1 - \text{Re}_2 - \text{Im}_2) &> 0 \end{aligned} \quad (3.40)$$

For case 4a-2, 1111 is on border; 1110 is not (and note  $\text{Im}_1 > 0$ ). Hence if  $\text{Re}[1101]$  is within the threshold,  $\text{Im}[1100]$  certainly is. Thus we again have only one condition:

$$\text{Re}[1101] > q_{th}$$

$$\frac{1}{\sqrt{2}}(\text{Re}_1 - \text{Im}_1 - \text{Re}_2 - \text{Im}_2) > \frac{1}{\sqrt{2}}(\text{Re}_1 + \text{Im}_1 + \text{Re}_2 + \text{Im}_2) \left(1 - \frac{1}{l-1}\right) \quad (3.41)$$

$$(l-1)(\text{Re}_1 - \text{Im}_1 - \text{Re}_2 - \text{Im}_2) > (\text{Re}_1 + \text{Im}_1 + \text{Re}_2 + \text{Im}_2)(l-2)$$

$$\text{Re}_1 + (2l-3)(-\text{Im}_1 - \text{Re}_2 - \text{Im}_2) > 0$$

This is in fact identical to case 4a-1, note that the sign of  $\text{Im}_1$  is different in the two cases.

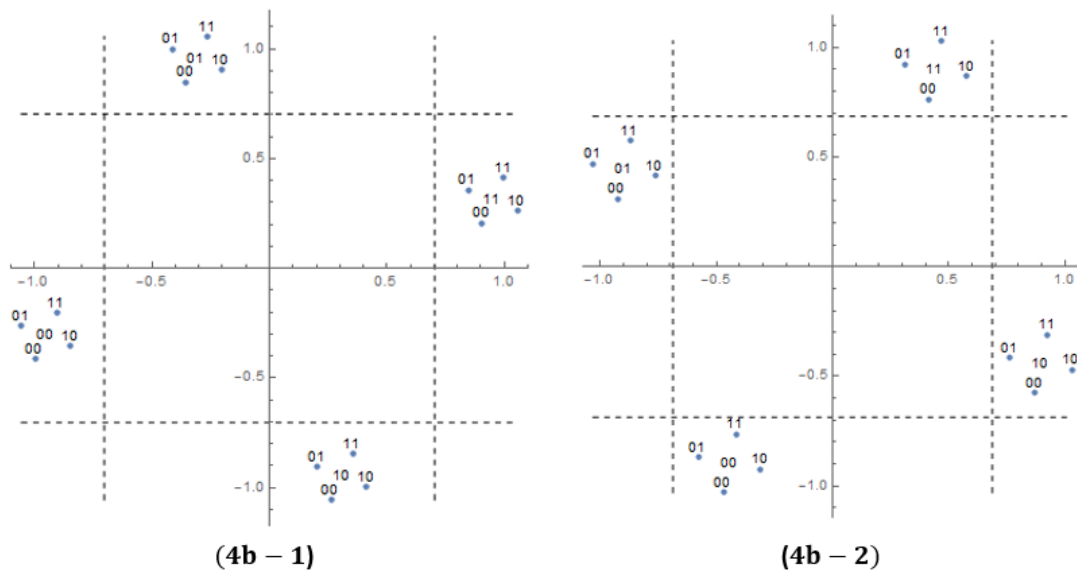


**Figure 3.11 Case with four points in region A and D**

In figure 3.11, for 4b-1, 1110 is on the border, which means that the four points must be in region D. Outage occurs if:

$$\begin{aligned}
& \text{Im}[1111] < q_{th} \ \& \ \text{Im}[1100] > 0 \ \& \ \text{Re}[1101] > q_{th} \\
& \text{Re}_1 + \text{Im}_1 + \text{Re}_2 + \text{Im}_2 < (\text{Re}_1 - \text{Im}_1 + \text{Re}_2 + \text{Im}_2) \left(1 - \frac{1}{l-1}\right) \ \& \\
& \text{Re}_1 + \text{Im}_1 - \text{Re}_2 - \text{Im}_2 > 0 \ \& \\
& \text{Re}_1 - \text{Im}_1 - \text{Re}_2 - \text{Im}_2 > (\text{Re}_1 - \text{Im}_1 + \text{Re}_2 + \text{Im}_2) \left(1 - \frac{1}{l-1}\right); \\
& (l-1)(\text{Re}_1 + \text{Im}_1 + \text{Re}_2 + \text{Im}_2) < (\text{Re}_1 - \text{Im}_1 + \text{Re}_2 + \text{Im}_2)(l-2) \ \& \quad (3.42) \\
& \text{Re}_1 + \text{Im}_1 - \text{Re}_2 - \text{Im}_2 > 0 \ \& \\
& (l-1)(\text{Re}_1 - \text{Im}_1 - \text{Re}_2 - \text{Im}_2) > (\text{Re}_1 - \text{Im}_1 + \text{Re}_2 + \text{Im}_2)(l-2); \\
& \text{Re}_1 + \text{Re}_2 + \text{Im}_2 + (2l-3)\text{Im}_1 < 0 \ \& \\
& \text{Re}_1 + \text{Im}_1 - \text{Re}_2 - \text{Im}_2 > 0 \ \& \\
& \text{Re}_1 - \text{Im}_1 - (2l-3)(\text{Re}_2 + \text{Im}_2) > 0
\end{aligned}$$

For case 4b-2, 1111 is on the border, which means that the four points must be in region

A. Outage occurs if:

$$\begin{aligned}
& \text{Re}[1110] < q_{th} \ \& \ \text{Re}[1101] > 0 \ \& \ \text{Im}[1100] > q_{th} \\
& \text{Re}_1 - \text{Im}_1 + \text{Re}_2 + \text{Im}_2 < (\text{Re}_1 + \text{Im}_1 + \text{Re}_2 + \text{Im}_2) \left(1 - \frac{1}{l-1}\right) \ \& \\
& \text{Re}_1 - \text{Im}_1 - \text{Re}_2 - \text{Im}_2 > 0 \ \& \\
& \text{Re}_1 + \text{Im}_1 - \text{Re}_2 - \text{Im}_2 > (\text{Re}_1 + \text{Im}_1 + \text{Re}_2 + \text{Im}_2) \left(1 - \frac{1}{l-1}\right); \\
& (l-1)(\text{Re}_1 - \text{Im}_1 + \text{Re}_2 + \text{Im}_2) < (\text{Re}_1 + \text{Im}_1 + \text{Re}_2 + \text{Im}_2)(l-2) \ \& \quad (3.43) \\
& \text{Re}_1 - \text{Im}_1 - \text{Re}_2 - \text{Im}_2 > 0 \ \& \\
& (l-1)(\text{Re}_1 + \text{Im}_1 - \text{Re}_2 - \text{Im}_2) > (\text{Re}_1 + \text{Im}_1 + \text{Re}_2 + \text{Im}_2)(l-2); \\
& \text{Re}_1 + \text{Re}_2 + \text{Im}_2 - (2l-3)\text{Im}_1 < 0 \ \& \\
& \text{Re}_1 - \text{Im}_1 - \text{Re}_2 - \text{Im}_2 > 0 \ \& \\
& \text{Re}_1 + \text{Im}_1 - (2l-3)(\text{Re}_2 + \text{Im}_2) > 0
\end{aligned}$$

Again, the conditions for case 4b-2 are identical to case 4b-1. Because of the complexity with the integrals of the conditions, we calculate the outage probability by using Monte Carlo integration. Monte Carlo methods are numerical techniques which rely on random sampling to approximate their results. Monte Carlo integration applies this

process to the numerical estimation of integrals [92]. The basic idea is to count the number of the sampling points which meet the conditions, then calculate the percentage of these points of the total number of sample points.

According to equation (3.34) and (3.35), we can define the range for  $h_1$  and  $h_2$ , as shown in figure 3.12:

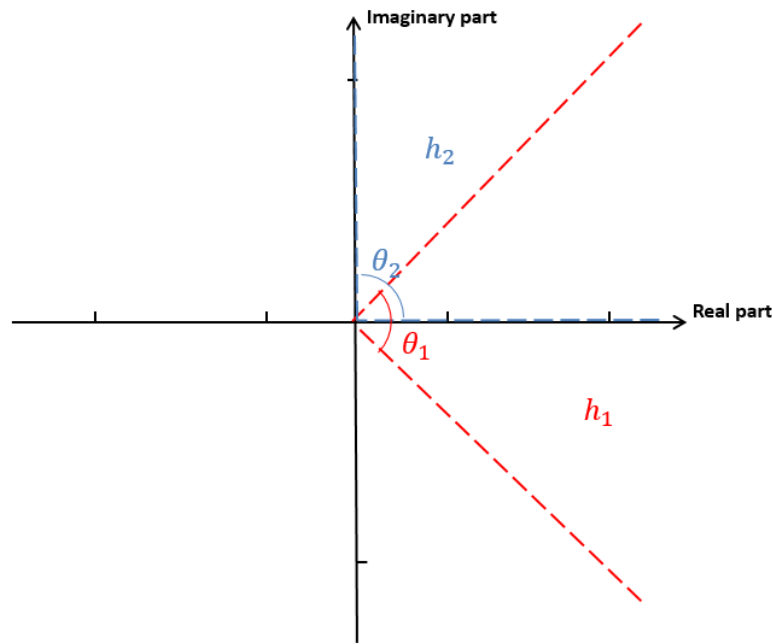


**Figure 3.12 Monte Carlo sampling range with  $h_1$  and  $h_2$**

In figure 3.12, when 1110 is on the boundary,  $\text{Im}_1 < 0$ , and we define  $\theta_1 \in [-\frac{\pi}{4}, 0]$ .

When 1111 is on the boundary,  $\text{Im}_1 > 0$ , and we have  $\theta_1 \in [0, \frac{\pi}{4}]$ . According to

equation (3.35), hence  $\theta_2 \in [0, \frac{\pi}{2}]$ .

To generate the sampling points of  $h_1$  and  $h_2$ . The real part and imaginary part can be generated separately with:

$$\begin{aligned}
 \text{Re}_1 &= a_1 \cos \theta_1 \\
 \text{Im}_1 &= a_1 \sin \theta_1 \\
 \text{Re}_2 &= a_2 \cos \theta_2 \\
 \text{Im}_2 &= a_2 \sin \theta_2
 \end{aligned}
 \tag{3.44}$$

where  $a_1$  and  $a_2$  represent the amplitudes of  $h_1$  and  $h_2$ .

Then we can count the number of sampling pairs of  $h_1$  and  $h_2$  which meet the conditions above, and calculate the probability of these pairs as a proportion of the total number of sample pairs.

We also simulate the outage cases in MATLAB: we assume that each region has a corresponding quantization point. For the 16 desired transmitted symbol of QPSK, if some of them are quantized to the same quantization point, then we can count the number with same quantization point and locate the region position. For the outage case with four points locate at the same region, the comparison results are shown in Table 3.10:

Four points in outage					
Region A	Region B	Region C	Region D	Simulation Results	Monte Carlo Results
-	-	4	-	0	0
-	4	-	-	0.0045	0.0042
4	-	-	-	0.0229	0.0231
-	-	-	4	0.0228	0.0233
Total outage probability				0.0502	0.0506

**Table 3.10 Comparison between simulation and Monte Carlo results with four points in different region**

Note that the outage probability show in Table 3.10 denotes the four points in outage case, to convert from outage probability to BER, we need to estimate the error probability for each bit.

	00	01	10	11
00	0	1	1	2
01	1	0	2	1
10	1	2	0	1
11	2	1	1	0

**Table 3.11 Number of erroneous bit table for desired bits and transmitted bits for  $s_2$  with four points in outage**

For the case of four points in outage, if the desired vector of  $s_2$  is  $[0, 0]$ , it has equal probability to be recovered as  $[0, 0]$ ,  $[0, 1]$ ,  $[1, 0]$  and  $[1, 1]$ . If the recovered vector is  $[0, 0]$ , the vector is recovered without any errors. If the recovered vector is  $[0, 1]$ , this will generate one bit error. If the recovered vector is  $[1, 1]$ , it will generate two bit errors. Similarly the other desired vectors, will generate different numbers of error bits with different recovered vectors. The average number of bit errors listed in Table 3.11 is 1 out of two bits transmitted, hence BER is half outage probability. Thus we can estimate the BER by counting the number of bit errors over the total number of bits:

$$BER_{four} = \frac{1}{2} P_{four} \quad (3.45)$$

Thus the theoretical BER with four points in outage is 0.0253.

► **Three points in outage**

There are seven cases with three points in outage: one case with three outage points in region B, three cases with three outage points in region A and D, and three cases with three outage points in region C.

Figure 3.13 and 3.14 show two cases for three points in outage; see more cases with three points in outage in the appendix.

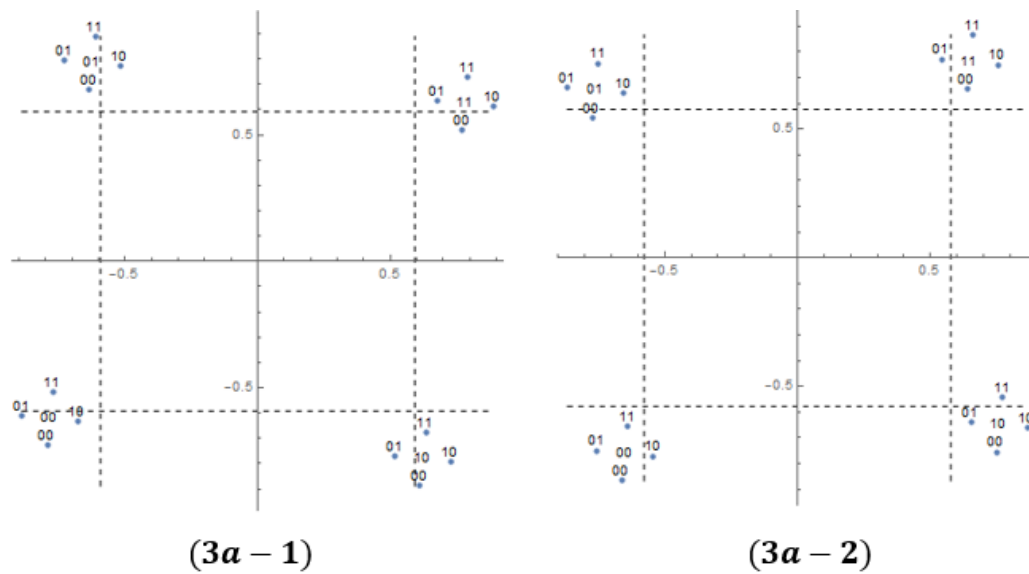


**Figure 3.13 Three points in outage in region B**

In figure 3.13, with case 3a-1, 1110 is on border; 1111 is not (and note  $\text{Im}_1 < 0$ ), 1100 in region D and 1101, 1110 and 1111 located in region B. Thus we have the conditions:

$$\text{Im}[1100] < q_{ih} \ \& \ \text{Im}[1101] > q_{ih} \ \& \ \text{Re}[1101] > q_{ih} \ \& \ \text{Im}[1110] > q_{ih}$$

$$\begin{aligned} \frac{1}{\sqrt{2}}(\text{Re}_1 + \text{Im}_1 - \text{Re}_2 - \text{Im}_2) &< \frac{1}{\sqrt{2}}(\text{Re}_1 - \text{Im}_1 + \text{Re}_2 + \text{Im}_2) \left(1 - \frac{1}{l-1}\right) \ \& \\ \frac{1}{\sqrt{2}}(\text{Re}_1 + \text{Im}_1 + \text{Re}_2 - \text{Im}_2) &> \frac{1}{\sqrt{2}}(\text{Re}_1 - \text{Im}_1 + \text{Re}_2 + \text{Im}_2) \left(1 - \frac{1}{l-1}\right) \ \& \\ \frac{1}{\sqrt{2}}(\text{Re}_1 - \text{Im}_1 - \text{Re}_2 - \text{Im}_2) &> \frac{1}{\sqrt{2}}(\text{Re}_1 - \text{Im}_1 + \text{Re}_2 + \text{Im}_2) \left(1 - \frac{1}{l-1}\right) \ \& \\ \frac{1}{\sqrt{2}}(\text{Re}_1 + \text{Im}_1 - \text{Re}_2 + \text{Im}_2) &> \frac{1}{\sqrt{2}}(\text{Re}_1 - \text{Im}_1 + \text{Re}_2 + \text{Im}_2) \left(1 - \frac{1}{l-1}\right); \end{aligned}$$

$$\begin{aligned} (l-1)(\text{Re}_1 + \text{Im}_1 - \text{Re}_2 - \text{Im}_2) &< (\text{Re}_1 - \text{Im}_1 + \text{Re}_2 + \text{Im}_2)(l-2) \ \& \\ (l-1)(\text{Re}_1 + \text{Im}_1 + \text{Re}_2 - \text{Im}_2) &> (\text{Re}_1 - \text{Im}_1 + \text{Re}_2 + \text{Im}_2)(l-2) \ \& \\ (l-1)(\text{Re}_1 - \text{Im}_1 - \text{Re}_2 - \text{Im}_2) &> (\text{Re}_1 - \text{Im}_1 + \text{Re}_2 + \text{Im}_2)(l-2) \ \& \\ (l-1)(\text{Re}_1 + \text{Im}_1 - \text{Re}_2 + \text{Im}_2) &> (\text{Re}_1 - \text{Im}_1 + \text{Re}_2 + \text{Im}_2)(l-2); \end{aligned}$$

$$\begin{aligned} \text{Re}_1 + (2l-3)(\text{Im}_1 - \text{Re}_2 - \text{Im}_2) &< 0 \ \& \\ \text{Re}_1 + \text{Re}_2 + (2l-3)(\text{Im}_1 - \text{Im}_2) &> 0 \ \& \\ \text{Re}_1 - \text{Im}_1 + (2l-3)(-\text{Re}_2 - \text{Im}_2) &> 0 \ \& \\ \text{Re}_1 + \text{Im}_2 + (2l-3)(\text{Im}_1 - \text{Re}_2) &> 0 \end{aligned} \tag{3.46}$$

For case 3a-2, 1111 is on border and 1110 is not (and note  $\text{Im}_1 > 0$ ), 1101 in region A and 1111, 1100 and 1110 in region B. Thus we have the conditions:

$$\text{Re}[1101] < q_{th} \ \& \ \text{Im}[1100] > q_{th} \ \& \ \text{Re}[1100] > q_{th} \ \& \ \text{Re}[1111] > q_{th}$$

$$\begin{aligned} \frac{1}{\sqrt{2}}(\text{Re}_1 - \text{Im}_1 - \text{Re}_2 - \text{Im}_2) &< \frac{1}{\sqrt{2}}(\text{Re}_1 + \text{Im}_1 + \text{Re}_2 + \text{Im}_2) \left(1 - \frac{1}{l-1}\right) \ \& \\ \frac{1}{\sqrt{2}}(\text{Re}_1 + \text{Im}_1 - \text{Re}_2 - \text{Im}_2) &> \frac{1}{\sqrt{2}}(\text{Re}_1 + \text{Im}_1 + \text{Re}_2 + \text{Im}_2) \left(1 - \frac{1}{l-1}\right) \ \& \\ \frac{1}{\sqrt{2}}(\text{Re}_1 - \text{Im}_1 - \text{Re}_2 + \text{Im}_2) &> \frac{1}{\sqrt{2}}(\text{Re}_1 + \text{Im}_1 + \text{Re}_2 + \text{Im}_2) \left(1 - \frac{1}{l-1}\right) \ \& \\ \frac{1}{\sqrt{2}}(\text{Re}_1 - \text{Im}_1 + \text{Re}_2 - \text{Im}_2) &> \frac{1}{\sqrt{2}}(\text{Re}_1 + \text{Im}_1 + \text{Re}_2 + \text{Im}_2) \left(1 - \frac{1}{l-1}\right); \end{aligned}$$

$$\begin{aligned} (l-1)(\text{Re}_1 - \text{Im}_1 - \text{Re}_2 - \text{Im}_2) &< (\text{Re}_1 + \text{Im}_1 + \text{Re}_2 + \text{Im}_2)(l-2) \ \& \\ (l-1)(\text{Re}_1 + \text{Im}_1 - \text{Re}_2 - \text{Im}_2) &> (\text{Re}_1 + \text{Im}_1 + \text{Re}_2 + \text{Im}_2)(l-2) \ \& \\ (l-1)(\text{Re}_1 - \text{Im}_1 - \text{Re}_2 + \text{Im}_2) &> (\text{Re}_1 + \text{Im}_1 + \text{Re}_2 + \text{Im}_2)(l-2) \ \& \\ (l-1)(\text{Re}_1 - \text{Im}_1 + \text{Re}_2 - \text{Im}_2) &> (\text{Re}_1 + \text{Im}_1 + \text{Re}_2 + \text{Im}_2)(l-2); \end{aligned}$$

$$\begin{aligned} \text{Re}_1 + (2l-3)(-\text{Im}_1 - \text{Re}_2 - \text{Im}_2) &< 0 \ \& \\ \text{Re}_1 + \text{Im}_1 + (2l-3)(-\text{Re}_2 - \text{Im}_2) &> 0 \ \& \\ \text{Re}_1 + \text{Im}_2 + (2l-3)(-\text{Im}_1 - \text{Re}_2) &> 0 \ \& \\ \text{Re}_1 + \text{Re}_2 + (2l-3)(-\text{Im}_1 - \text{Im}_2) &> 0 \end{aligned} \tag{3.47}$$

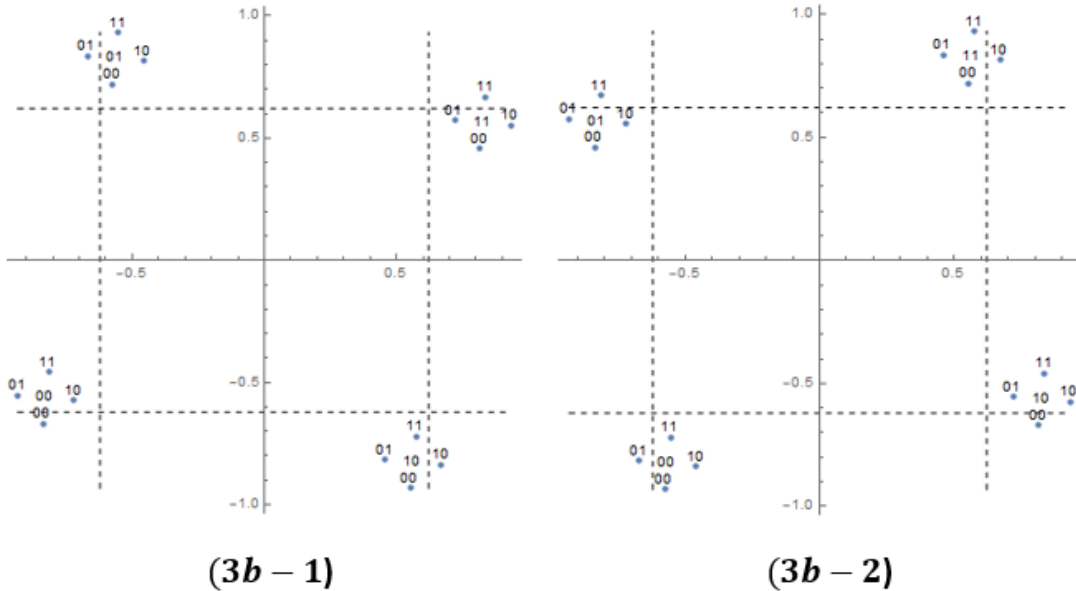


Figure 3.14 Three points in outage in region A and D

In figure 3.14, with case 3b-1, 1110 is on the border, and 1101, 1110 and 1100 in the region D, 1111 in region B. Thus we have the conditions:

$$\text{Im}[1111] > q_{th} \ \& \ \text{Im}[1101] < q_{th} \ \& \ \text{Re}[1101] > q_{th} \ \& \ \text{Im}[1110] < q_{th}$$

$$\begin{aligned} \frac{1}{\sqrt{2}}(\text{Re}_1 + \text{Im}_1 + \text{Re}_2 + \text{Im}_2) &> \frac{1}{\sqrt{2}}(\text{Re}_1 - \text{Im}_1 + \text{Re}_2 + \text{Im}_2) \left(1 - \frac{1}{l-1}\right) \ \& \\ \frac{1}{\sqrt{2}}(\text{Re}_1 + \text{Im}_1 + \text{Re}_2 - \text{Im}_2) &< \frac{1}{\sqrt{2}}(\text{Re}_1 - \text{Im}_1 + \text{Re}_2 + \text{Im}_2) \left(1 - \frac{1}{l-1}\right) \ \& \\ \frac{1}{\sqrt{2}}(\text{Re}_1 - \text{Im}_1 - \text{Re}_2 - \text{Im}_2) &> \frac{1}{\sqrt{2}}(\text{Re}_1 - \text{Im}_1 + \text{Re}_2 + \text{Im}_2) \left(1 - \frac{1}{l-1}\right) \ \& \\ \frac{1}{\sqrt{2}}(\text{Re}_1 + \text{Im}_1 - \text{Re}_2 + \text{Im}_2) &< \frac{1}{\sqrt{2}}(\text{Re}_1 - \text{Im}_1 + \text{Re}_2 + \text{Im}_2) \left(1 - \frac{1}{l-1}\right); \end{aligned}$$

$$\begin{aligned} (l-1)(\text{Re}_1 + \text{Im}_1 + \text{Re}_2 + \text{Im}_2) &> (\text{Re}_1 - \text{Im}_1 + \text{Re}_2 + \text{Im}_2)(l-2) \ \& \\ (l-1)(\text{Re}_1 + \text{Im}_1 + \text{Re}_2 - \text{Im}_2) &< (\text{Re}_1 - \text{Im}_1 + \text{Re}_2 + \text{Im}_2)(l-2) \ \& \\ (l-1)(\text{Re}_1 - \text{Im}_1 - \text{Re}_2 - \text{Im}_2) &> (\text{Re}_1 - \text{Im}_1 + \text{Re}_2 + \text{Im}_2)(l-2) \\ (l-1)(\text{Re}_1 + \text{Im}_1 - \text{Re}_2 + \text{Im}_2) &< (\text{Re}_1 - \text{Im}_1 + \text{Re}_2 + \text{Im}_2)(l-2); \end{aligned}$$

$$\begin{aligned} \text{Re}_1 + \text{Re}_2 + \text{Im}_2 + (2l-3)(\text{Im}_1) &> 0 \ \& \\ \text{Re}_1 + \text{Re}_2 + (2l-3)(\text{Im}_1 - \text{Im}_2) &< 0 \ \& \\ \text{Re}_1 - \text{Im}_1 + (2l-3)(-\text{Re}_2 - \text{Im}_2) &> 0 \ \& \\ \text{Re}_1 + \text{Im}_2 + (2l-3)(\text{Im}_1 - \text{Re}_2) &< 0 \end{aligned} \tag{3.48}$$

For case 3b-2, 1111 is on the border, 1111, 1101, 1100 in region A, 1110 in region B.

Thus the conditions with this case are:

$$\text{Re}[1110] > q_{th} \ \& \ \text{Im}[1100] > q_{th} \ \& \ \text{Re}[1100] < q_{th} \ \& \ \text{Re}[1111] < q_{th}$$

$$\begin{aligned} \frac{1}{\sqrt{2}}(\text{Re}_1 - \text{Im}_1 + \text{Re}_2 + \text{Im}_2) &> \frac{1}{\sqrt{2}}(\text{Re}_1 + \text{Im}_1 + \text{Re}_2 + \text{Im}_2) \left(1 - \frac{1}{l-1}\right) \ \& \\ \frac{1}{\sqrt{2}}(\text{Re}_1 + \text{Im}_1 - \text{Re}_2 - \text{Im}_2) &> \frac{1}{\sqrt{2}}(\text{Re}_1 + \text{Im}_1 + \text{Re}_2 + \text{Im}_2) \left(1 - \frac{1}{l-1}\right) \ \& \\ \frac{1}{\sqrt{2}}(\text{Re}_1 - \text{Im}_1 - \text{Re}_2 + \text{Im}_2) &< \frac{1}{\sqrt{2}}(\text{Re}_1 + \text{Im}_1 + \text{Re}_2 + \text{Im}_2) \left(1 - \frac{1}{l-1}\right) \ \& \\ \frac{1}{\sqrt{2}}(\text{Re}_1 - \text{Im}_1 + \text{Re}_2 - \text{Im}_2) &< \frac{1}{\sqrt{2}}(\text{Re}_1 + \text{Im}_1 + \text{Re}_2 + \text{Im}_2) \left(1 - \frac{1}{l-1}\right); \end{aligned}$$

$$\begin{aligned} (l-1)(\text{Re}_1 - \text{Im}_1 + \text{Re}_2 + \text{Im}_2) &> (\text{Re}_1 + \text{Im}_1 + \text{Re}_2 + \text{Im}_2)(l-2) \ \& \\ (l-1)(\text{Re}_1 + \text{Im}_1 - \text{Re}_2 - \text{Im}_2) &> (\text{Re}_1 + \text{Im}_1 + \text{Re}_2 + \text{Im}_2)(l-2) \ \& \\ (l-1)(\text{Re}_1 - \text{Im}_1 - \text{Re}_2 + \text{Im}_2) &< (\text{Re}_1 + \text{Im}_1 + \text{Re}_2 + \text{Im}_2)(l-2) \ \& \\ (l-1)(\text{Re}_1 - \text{Im}_1 + \text{Re}_2 - \text{Im}_2) &< (\text{Re}_1 + \text{Im}_1 + \text{Re}_2 + \text{Im}_2)(l-2); \end{aligned}$$

$$\begin{aligned} \text{Re}_1 + \text{Re}_2 + \text{Im}_2 + (2l-3)(-\text{Im}_1) &> 0 \ \& \\ \text{Re}_1 + \text{Im}_1 + (2l-3)(-\text{Re}_2 - \text{Im}_2) &> 0 \ \& \\ \text{Re}_1 + \text{Im}_2 + (2l-3)(-\text{Im}_1 - \text{Re}_2) &< 0 \ \& \\ \text{Re}_1 + \text{Re}_2 + (2l-3)(-\text{Im}_1 - \text{Im}_2) &< 0 \end{aligned} \tag{3.49}$$

More cases are shown in the appendix. We sum the outage probability with three points in the same region and list the results in Table 3.12:

Three points in outage					
Region A	Region B	Region C	Region D	Simulation Results	Monte Carlo Results
-	-	3	-	0.0706	0.0714
-	3	-	-	0.0027	0.0028
3	-	-	-	0.0221	0.0223
-	-	-	3	0.0225	0.0223
Total outage probability				0.1179	0.1188

**Table 3.12 Comparison between simulation and Monte Carlo results with three points in different region**

In Table 3.12, it can be seen that the Monte Carlo results and the simulation results are matched in each region. The outage probability for three points in outage is 0.1188. To calculate the BER from the outage probability, similar to Table 3.11, we can derive the erroneous bit table for desired bits and transmitted bits as shown in Table 3.13:

	01	10	11		00	01	10
01	0	2	1	00	0	1	1
10	2	0	1	01	1	0	2
11	1	1	0	10	1	2	0
	00	10	11		00	01	11
00	0	1	2	00	0	1	2
10	1	0	1	01	1	0	1
11	2	1	0	11	2	1	0
	0110	1101	1111		0110	0100	1111
0110	0	3	2	0110	0	1	2
1101	3	0	1	0100	1	0	3
1111	2	1	0	1111	2	3	0
	1111	0110	1011				
1111	0	2	1				
0110	2	0	3				
1011	1	3	0				

**Table 3.13** Number of erroneous bit table for desired bits and transmitted bits for  $s_2$  with three points in outage

Table 3.13 shows the number of erroneous bit in each case for three points in outage, noting that the outage points could include the points from the other clusters with  $s_1$

except  $s_1 = [1, 1]$ . Thus when two points from different cluster are in outage, the recovered bits for  $s_1$  and  $s_2$  can both be in error.

Thus the BER for each case can be computed and shows in Table 3.14:

Region	Case number	Symbol outage probability	Bit error rate per symbol	Bit error probability
B	3-a	0.0028	4/9	0.0012
A&D	3-b	0.0040	4/9	0.0018
A&D	3-c	0.0325	4/9	0.0144
A&D	3-d	0.0081	4/9	0.0036
C	3-e	0.0612	1/3	0.0204
C	3-f	0.0013	1/3	0.0004
C	3-g	0.0090	1/3	0.0030
	Total			0.0448

**Table 3.14 Bit outage probability with each case for three points in outage**

Thus we have that the total bit outage probability for three points is 0.0448.

### ➤ Two points in outage

For the two points in outage case, we have explored 13 cases for two received symbols in the same region.

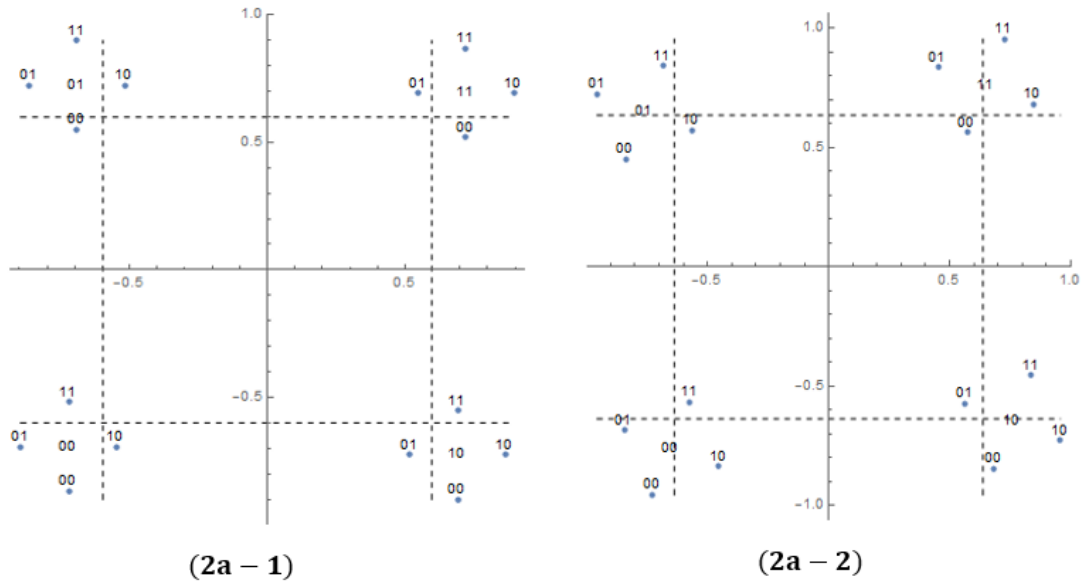


**Figure 3.15 Two points in outage in region B**

With case 2a-1. 1110 is on the border, and 1111 is not. 1110 and 1111 will lie in the quantization region B if:

$$\begin{aligned}
 & \operatorname{Re}[r(1111)] > q_{th} \ \& \ \operatorname{Im}[r(1110)] > q_{th} \\
 & \operatorname{Re}_1 - \operatorname{Im}_1 + \operatorname{Re}_2 - \operatorname{Im}_2 > \left(1 - \frac{1}{l-1}\right) (\operatorname{Re}_1 - \operatorname{Im}_1 + \operatorname{Re}_2 + \operatorname{Im}_2) \ \& \\
 & \operatorname{Re}_1 + \operatorname{Im}_1 - \operatorname{Re}_2 + \operatorname{Im}_2 > \left(1 - \frac{1}{l-1}\right) (\operatorname{Re}_1 - \operatorname{Im}_1 + \operatorname{Re}_2 + \operatorname{Im}_2); \\
 & (l-1)(\operatorname{Re}_1 - \operatorname{Im}_1 + \operatorname{Re}_2 - \operatorname{Im}_2) > (l-2)(\operatorname{Re}_1 - \operatorname{Im}_1 + \operatorname{Re}_2 + \operatorname{Im}_2) \ \& \\
 & (l-1)(\operatorname{Re}_1 + \operatorname{Im}_1 - \operatorname{Re}_2 + \operatorname{Im}_2) > (l-2)(\operatorname{Re}_1 - \operatorname{Im}_1 + \operatorname{Re}_2 + \operatorname{Im}_2); \\
 & (\operatorname{Re}_1 - \operatorname{Im}_1 + \operatorname{Re}_2) - (2l-3)\operatorname{Im}_2 > 0 \ \& \\
 & (\operatorname{Re}_1 + \operatorname{Im}_2) + (2l-3)(\operatorname{Im}_1 - \operatorname{Re}_2) > 0
 \end{aligned} \tag{3.50}$$

With case 2a-2. 1111 is on the border, and 1110 is not. 1110 and 1111 will lie in the quantization region B if:

$$\operatorname{Re}[r(1111)] > q_{th} \ \& \ \operatorname{Im}[r(1110)] > q_{th}$$

$$\operatorname{Re}_1 - \operatorname{Im}_1 + \operatorname{Re}_2 - \operatorname{Im}_2 > \left(1 - \frac{1}{l-1}\right)(\operatorname{Re}_1 + \operatorname{Im}_1 + \operatorname{Re}_2 + \operatorname{Im}_2) \ \&$$

$$\operatorname{Re}_1 + \operatorname{Im}_1 - \operatorname{Re}_2 + \operatorname{Im}_2 > \left(1 - \frac{1}{l-1}\right)(\operatorname{Re}_1 + \operatorname{Im}_1 + \operatorname{Re}_2 + \operatorname{Im}_2);$$

(3.51)

$$(l-1)(\operatorname{Re}_1 - \operatorname{Im}_1 + \operatorname{Re}_2 - \operatorname{Im}_2) > (l-2)(\operatorname{Re}_1 + \operatorname{Im}_1 + \operatorname{Re}_2 + \operatorname{Im}_2) \ \&$$

$$(l-1)(\operatorname{Re}_1 + \operatorname{Im}_1 - \operatorname{Re}_2 + \operatorname{Im}_2) > (l-2)(\operatorname{Re}_1 + \operatorname{Im}_1 + \operatorname{Re}_2 + \operatorname{Im}_2);$$

$$(\operatorname{Re}_1 + \operatorname{Re}_2) + (2l-3)(-\operatorname{Im}_1 - \operatorname{Im}_2) > 0 \ \&$$

$$(\operatorname{Re}_1 + \operatorname{Im}_1 + \operatorname{Im}_2) + (2l-3)(-\operatorname{Re}_2) > 0$$

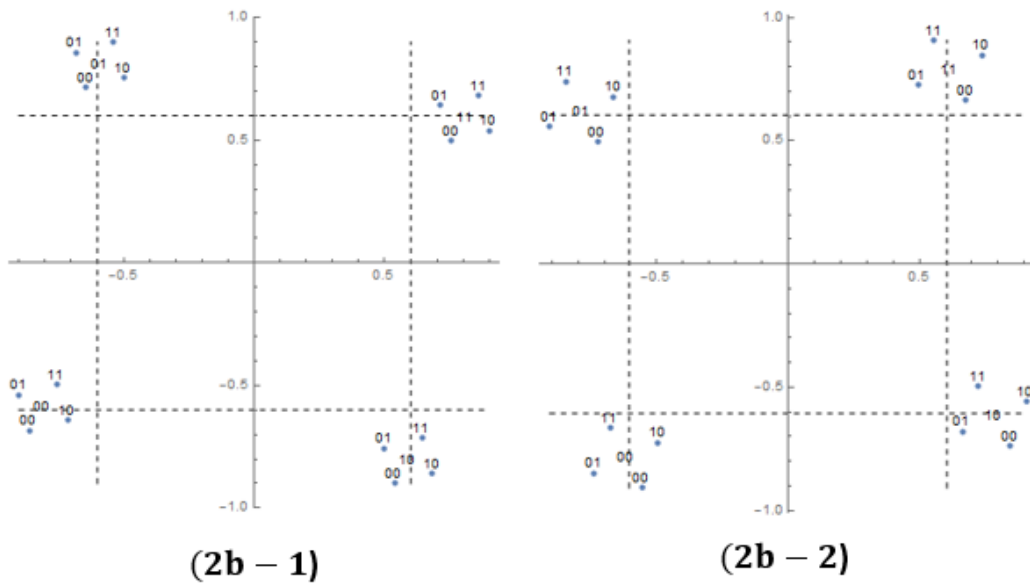


**Figure 3.16 Two points in outage in region B**

With case 2b-1, 1110 is on the border, and 1111 is not. 1110 and 1111 will lie in region B if:

$$\begin{aligned}
& \text{Re}[1111] > q_{th} \ \& \ \text{Im}[1111] < q_{th} \ \& \ \text{Im}[1110] > 0 \\
& \text{Re}_1 - \text{Im}_1 + \text{Re}_2 - \text{Im}_2 > \left(1 - \frac{1}{l-1}\right) (\text{Re}_1 - \text{Im}_1 + \text{Re}_2 + \text{Im}_2) \ \& \\
& \text{Re}_1 + \text{Im}_1 + \text{Re}_2 + \text{Im}_2 < \left(1 - \frac{1}{l-1}\right) (\text{Re}_1 - \text{Im}_1 + \text{Re}_2 + \text{Im}_2) \ \& \\
& \text{Re}_1 + \text{Im}_1 - \text{Re}_2 + \text{Im}_2 > 0; \\
& (l-1)(\text{Re}_1 - \text{Im}_1 + \text{Re}_2 - \text{Im}_2) > (l-2)(\text{Re}_1 - \text{Im}_1 + \text{Re}_2 + \text{Im}_2) \ \& \tag{3.52} \\
& (l-1)(\text{Re}_1 + \text{Im}_1 + \text{Re}_2 + \text{Im}_2) < (l-2)(\text{Re}_1 - \text{Im}_1 + \text{Re}_2 + \text{Im}_2) \ \& \\
& \text{Re}_1 + \text{Im}_1 - \text{Re}_2 + \text{Im}_2 > 0; \\
& (\text{Re}_1 - \text{Im}_1 + \text{Re}_2) - (2l-3)\text{Im}_2 > 0 \ \& \\
& (\text{Re}_1 + \text{Re}_2 + \text{Im}_2) + (2l-3)(\text{Im}_1) < 0 \ \& \\
& \text{Re}_1 + \text{Im}_1 - \text{Re}_2 + \text{Im}_2 > 0
\end{aligned}$$

Case 2b-2. 1111 is on the border, and 1110 is not. 1110 and 1111 will lie in the quantization region B if:

$$\begin{aligned}
& \text{Re}[1111] > 0 \ \& \ \text{Re}[1110] < q_{th} \ \& \ \text{Im}[1110] > q_{th} \\
& \text{Re}_1 - \text{Im}_1 + \text{Re}_2 - \text{Im}_2 > 0 \ \& \\
& \text{Re}_1 - \text{Im}_1 + \text{Re}_2 + \text{Im}_2 < \left(1 - \frac{1}{l-1}\right) (\text{Re}_1 + \text{Im}_1 + \text{Re}_2 + \text{Im}_2) \ \& \\
& \text{Re}_1 + \text{Im}_1 - \text{Re}_2 + \text{Im}_2 > \left(1 - \frac{1}{l-1}\right) (\text{Re}_1 + \text{Im}_1 + \text{Re}_2 + \text{Im}_2); \\
& (\text{Re}_1 - \text{Im}_1 + \text{Re}_2 - \text{Im}_2) > 0 \ \& \tag{3.53} \\
& (l-1)(\text{Re}_1 - \text{Im}_1 + \text{Re}_2 + \text{Im}_2) < (l-2)(\text{Re}_1 + \text{Im}_1 + \text{Re}_2 + \text{Im}_2) \ \& \\
& (l-1)(\text{Re}_1 + \text{Im}_1 - \text{Re}_2 + \text{Im}_2) > (l-2)(\text{Re}_1 + \text{Im}_1 + \text{Re}_2 + \text{Im}_2); \\
& (\text{Re}_1 - \text{Im}_1 + \text{Re}_2 - \text{Im}_2) > 0 \ \& \\
& (\text{Re}_1 + \text{Re}_2 + \text{Im}_2) - (2l-3)(\text{Im}_1) < 0 \ \& \\
& (\text{Re}_1 + \text{Im}_1 + \text{Im}_2) - (2l-3)(\text{Re}_2) > 0
\end{aligned}$$

See appendix for more cases. Thus the sum of outage case in each region are shown in Table 3.15:

Two points in outage					
Region A	Region B	Region C	Region D	Simulation Results	Monte Carlo Results
-	-	2	-	0.5411	0.5404
-	2	-	-	0.0144	0.0139
2	-	-	-	0.1384	0.1281
-	-	-	2	0.1389	0.1281
Total outage probability				0.7309	-

**Table 3.15 Comparison between simulation and Monte Carlo results with two points in different region**

In Table 3.15, the outage probability with Monte Carlo results are very close to the simulation results, the slight difference in the results for region A and D shows that there may be some cases missed which results the Monte Carlo result is less than the simulation result. Besides, there are also cases in which two points are in outage in one region, and at the same time two points are in outage in another region (as shown in 2b-1), and thus the outage probability with two points in one region will also include part of the outage probability with another two points in outage with their region. This means these outage events are not mutually exclusive, so their probabilities cannot simply be summed to obtain the overall outage probability. Therefore, in the Monte Carlo results, the sum of the outage probabilities from all the regions is not calculated.

	10	11		00	10		00	01		01	11
10	0	1		00	0	1		00	0	1	
11	1	0		10	1	0		01	1	0	

	0110	1111		0111	1111		0110	1011
0110	0	2	0111	0	1	0110	0	3
1111	2	0	1111	1	0	1011	3	0
	0100	1111		0110	1101			
0100	0	3	0110	0	3			
1111	3	0	1101	3	0			

**Table 3.16** Number of erroneous bit table for desired bits and transmitted bits for  $s_2$  with two points in outage

Region	Case number	Symbol outage probability	Bit error rate per symbol	Bit error probability
B	2-a	0.0103	1/4	0.0025
B	2-b	0.0034	1/4	0.00085
A&D	2-c	0.1115	1/4	0.0279
A&D	2-d	0.0739	1/4	0.0185
A&D	2-e	0.0043	1/4	0.00095
A&D	2-f	0.0035	1/4	0.00073
A&D	2-g	0.0608	1/4	0.0152
A&D	2-h	0.0033	1/8	0.0004
C	2-i	0.0683	1/4	0.0171
C	2-j	0.0665	1/4	0.0166
C	2-k	0.0432	3/8	0.0162
C	2-l	0.1096	3/8	0.0411
C	2-m	0.2533	3/8	0.09499

**Table 3.17** Bit outage probability with each case for two points in outage

In Table 3.17, the bit error probability with each case is calculated according to different bit error rate per symbol in different cases. However, as we have noted, we cannot

calculate straightforwardly the total bit error probability with two points in outage. Nevertheless in view of the results in Table 3.15, the Monte Carlo result for each region is very close to the simulation result. Hence we can estimate that the simulation and Monte Carlo will produce the same results for total bit error probability for two points in outage case, which is 0.2224, noting that the simulation process can easily achieve the computation by counting the number of incorrect bits for only the two points in outage case.

Thus we can sum the bit error probability for three outage cases with different number of points in the same region, and the comparison between theoretical and simulation results are shown in Table 3.18:

Number of Quantization Level	Theoretical Results (BER)	Simulation Results (BER)
16	0.2928	0.2922

**Table 3.18 BER comparison between theoretical and simulation results for QPSK modulation scheme and ML detection method**

In this section, we have analysed the effect of quantization on ML detection with BPSK and QPSK, due to the complexity of the outage cases for QPSK, we have only explored the 16 level quantization. For the effect of quantization on ZF detection, we have explored the real-only channel case, and compared the outage cases under different conditions.

With a higher order quantization, the received symbols have smaller probability to lie in the same region, which further reduces the outage probability, and hence this will reduce the BER of the recovered data bits and improve the detection performance at the BBU. In this section, we have calculated the probability that two or more symbols cannot be distinguished in the absence of noise, and this determines the error floor

which applies at high  $E_b/N_0$ . Thus we can conclude that increasing the quantization order can reduce the outage probability, and hence the level of the error floor, but does not eliminate it.

### 3.4. Simulations with C-RAN

In this section, we will evaluate multiple quantization levels at the RRU with multiple detection techniques in the BBU. The detection techniques which will be used in the simulations are ZF, MMSE and ML. We will also explore the minimum number of extra bits required with multiple modulation levels such as BPSK, QPSK, 16QAM and 64QAM [49, 50]. The expected BER performance to achieve is  $10^{-4}$ .

#### 3.4.1. ZF Signal Detection

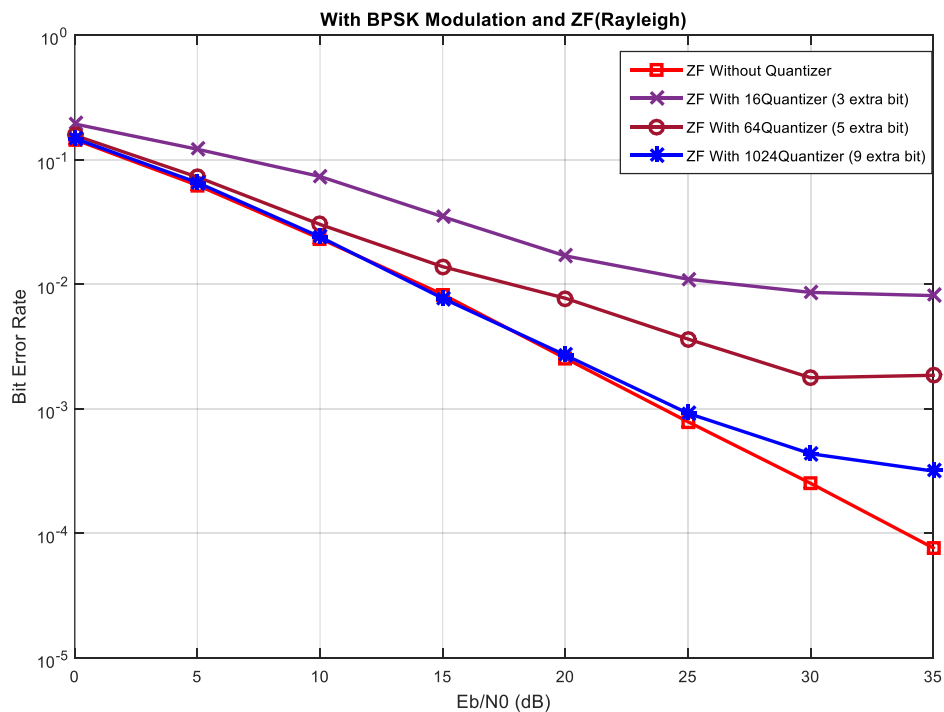
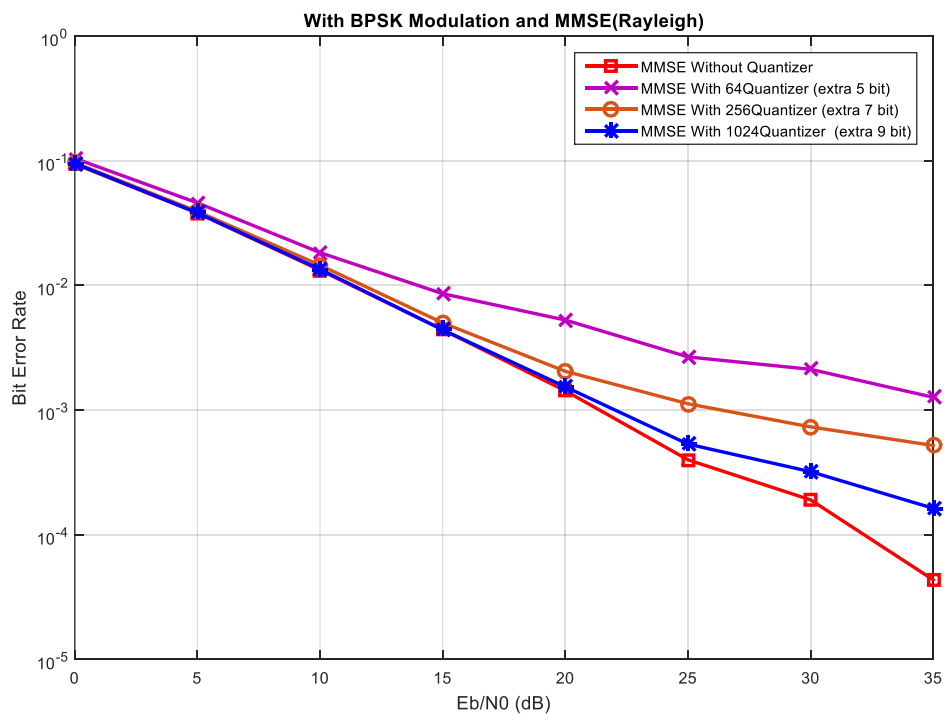


Figure 3.17 BER performance comparison with Zero Forcing

Figure. 3.17 shows the BER performance with Zero-Forcing detection with multiple levels of quantization, and also compare the performance without quantization. When quantization is processed, it shows that an error floor occurs, at which increasing SNR on access links no longer improves the BER. To reduce this noise floor to a low enough level requires 10 quantization bits (1024) for BPSK, which means the quantized signal required at least 9 extra quantized bits to be conveyed to reach the performance of un-quantized signal. The BER of un-quantized signal reaches  $10^{-4}$  at 34dB with SINR.

### 3.4.2. MMSE Signal Detection



**Figure 3.18 BER performance comparison with MMSE**

Figure 3.18 shows the BER performance with MMSE detection and different levels of quantization. Similarly to the ZF detection approach, the error floor also occurs when quantization is processed. Besides, the quantized signal required at least 10 extra quantized bits to be conveyed to reach the performance of the un-quantized signal. The

optimal BER performance of the un-quantized signal reaches  $10^{-4}$  at 32dB SNR. The performance has slight improvement compared with ZF. This is because the MMSE approach includes the statistical information of the noise when separating the spatially multiplexed data. (See equation 2.10)

### 3.4.3. Maximum Likelihood Signal Detection

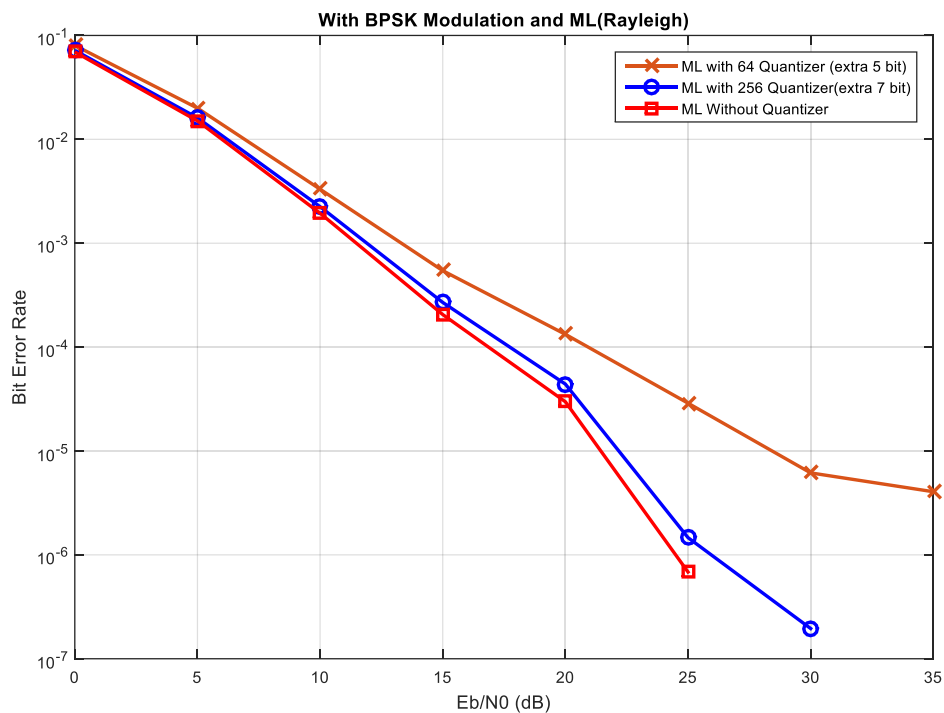
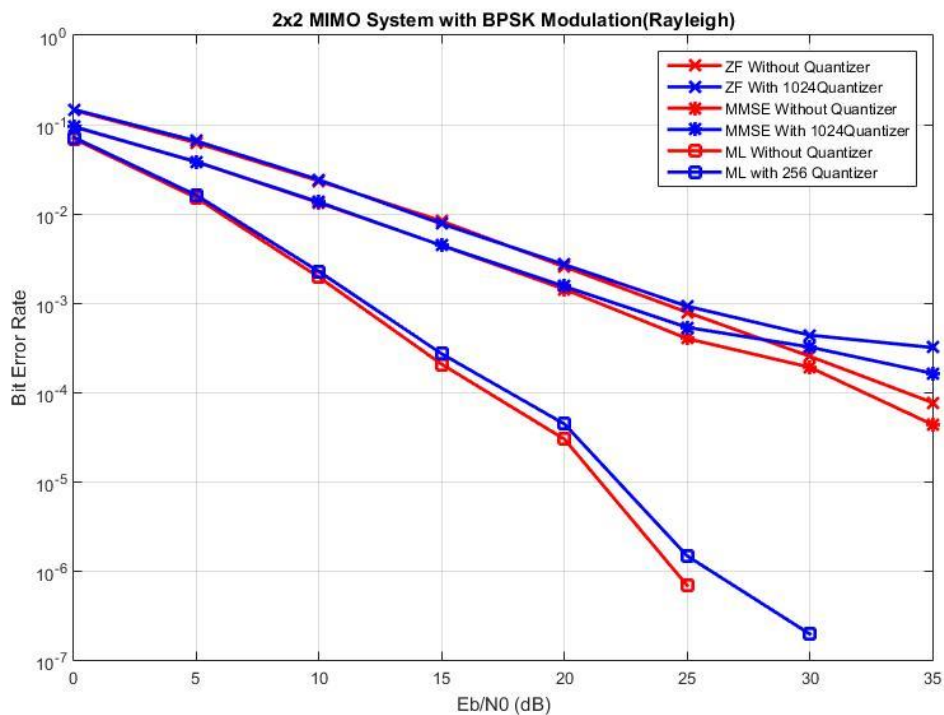


**Figure 3.19 BER performance comparison with ML**

Figure 3.19 shows the BER performance with ML detection with different levels of quantization. It can be clearly seen that the BER performance of the un-quantized signal is significantly improved, and the optimal BER reaches  $10^{-4}$  at around 16.5dB SNR. However, the error floor still occurs with the quantized signal. The quantization degrades the BER performance noticeably with a low level quantizer (5 extra bits). As the level of quantization increases, the BER performance improves rapidly. With 8 bits

quantized signal (7 extra bit), the BER performance is almost the same as the BER performance of the un-quantized signal.

### 3.4.4. Comparisons



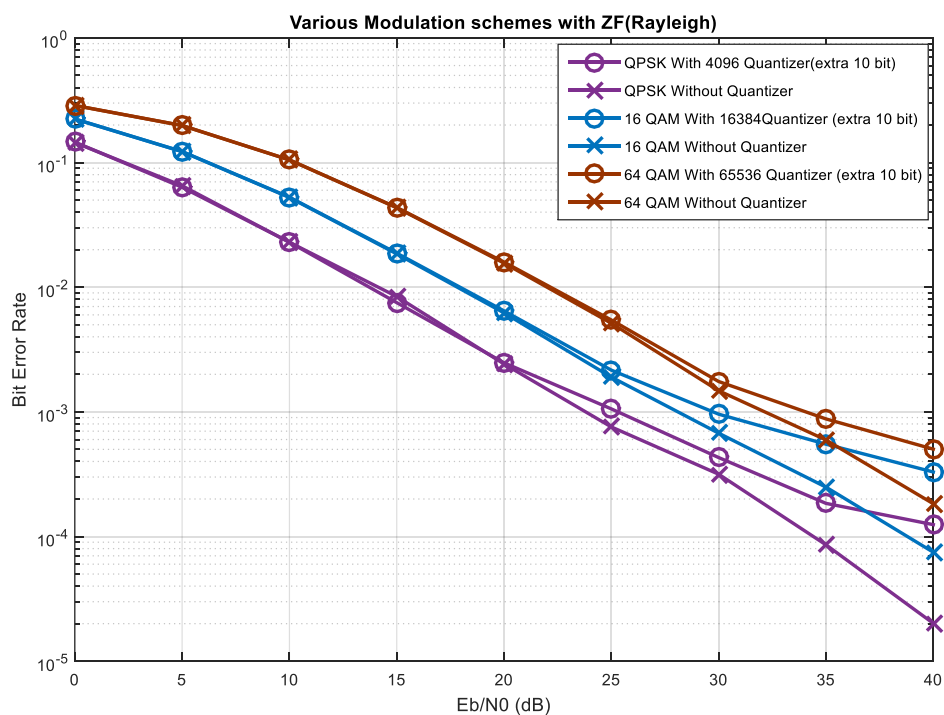
**Figure 3.20 BER performance comparison with multiple detection approaches**

Figure 3.20 shows the performance of ZF, MMSE and ML. With MMSE, the term  $(1/\text{SNR} = \sigma^2)$  offers a trade-off between the residual interference and the noise enhancement, when  $E_b/N_0$  at low level, the BER of MMSE is lower than ZF, and when  $E_b/N_0$  at high level, MMSE detection generates a BER performance very close to ZF detection. It can be seen that at high  $E_b/N_0$ , error floor still exist with each detection approach. Thus we can also conclude that the detection techniques cannot eliminate the error floor.

Detection Methods	ZF	MMSE	ML
Extra Bit Required per Symbol	9 bit	9 bit	7 bit
Detection Efficiency	High	High	Low

**Table 3.19 Comparison the performance with multiple detection methods**

### 3.4.5. Modulation Schemes



**Figure 3.21 BER performance with Zero-Forcing detection in different modulation level**

Figure 3.21 shows the BER performance with various modulation schemes. With higher level modulation scheme, the system needs a higher level quantizer to achieve

the expected BER performance. With a 64 QAM modulation scheme, the quantization level needs to reach 65536. However, even though the required quantization level increases as the modulation level increases, the number of extra bits required with the various modulation schemes remains the same. All of the modulation schemes require at least 10 extra bits to transmit the quantized signal. This results in an improvement of transmission efficiency as the modulation level increases, as shown in Table 3.20.

<b>Modulation Scheme</b>	<b>BPSK</b>	<b>QPSK</b>	<b>16 QAM</b>	<b>64 QAM</b>
Extra Bit Required per Symbol	9 bit	10 bit	10 bit	10 bit
Total Transmitted bit per Symbol	10 bit	12 bit	14 bit	16 bit
Transmission Efficiency	10%	17%	28%	37.5%

**Table 3.20 Transmission efficiency with various modulation schemes**

### 3.5. Chapter Summary

In this chapter, we have built up a single carrier C-RAN system with fronthaul network. The effect of quantization on BPSK and QPSK modulation scheme with ML and ZF detection methods have been explored and analyzed, we conclude that when quantization is applied, no matter what the quantization level is, erroneous bits can still exist in the recovered data bits, and an error floor will occur with the BER performance. However, this error floor level can be reduced by increasing the quantization level.

Then multiple detection techniques are simulated and various modulation schemes are explored with the system. The ML detection method gives significant improvement of the BER performance compared with ZF and MMSE, and also ML need 2 fewer extra bits than ZF and MMSE. However, the ML implementation is computationally infeasible, the processing time to separate the complex baseband signals from multiple

users is too long, which will increase the fronthaul latency. Therefore, for the further work of system design, we will apply ZF or MMSE to separate the complex signals from multiple user terminals.

With various modulation schemes, we have explored BPSK, QPSK, 16 QAM and 64 QAM in the system, and find that the number of minimum extra bits required with each modulation scheme is the same, which is 10. Thus when a higher level modulation scheme is applied to the system, the transmission efficiency in the fronthaul can be improved. However, when the modulation level is low, this system has insufficient transmission efficiency, and furthermore produces more fronthaul load.

As we have noticed that the error floor causes an irreducible BER which remains significant however high the signal to noise ratio (SNR) on the radio access links. This effect is however eliminated if user signals are separated before quantization: in this case there is no error floor provided the quantization is correctly applied, since the spurious components do not occur if there is no noise. The level of the error floor can also be reduced to negligible levels if the user signals are partly separated, in the sense that a component from another user may remain in a first user's signal, but this component is relatively small. In Chapter 4, we will design the system to reduce the fronthaul load caused by quantization.

# Chapter 4 Quantization Position Design with C-RAN Fronthaul in Multiple Carrier Scheme

## 4.1. Introduction

In chapter 3 we have investigated a C-RAN system using single carrier modulation, considering especially quantization in the fronthaul network. In this chapter, we will design a system with a multi-carrier scheme using orthogonal frequency-division multiplexing (OFDM). Furthermore, we will develop the system and improve the transmission efficiency, especially at low modulation order.

As we discussed in sections 3.3 - 3.4, the quantized signal with detection techniques generates error floors which are caused by the self-interference due to intermodulation produced by quantizing the mixed signals from multiple user terminals. Therefore, at the RRU, following RF processing then fast Fourier transformation (FFT) to separate data sub-channels of the orthogonal OFDM signal, a beam-former or other appropriate spatial filter can be applied to the signals from the multiple antennas of the RRU to separate to some degree signals from different users, which are either located in different directions or received via radio channels with different amplitudes and phases, which can be exploited to assist in the separation. The corresponding signals are then quantized to only that precision which is required according to the modulation being used by the user and on the sub-channels in question. The separation process gives each signal quantized contains mainly the signal from one user, with component signals from other users being reduced to low levels. This reduces the intermodulation effect due to quantization of a mixture of signals.

The bits representing the quantized signals are then transmitted over the fronthaul network to the BBU. At the BBU signals corresponding to the same user via different RRUs are combined in relative proportions according to the strength and accuracy of the signals. The remaining demodulation, decoding and other processing is performed at the BBU on the combined signals.

In this chapter, using a multi-carrier scheme, we will investigate a system with quantization before FFT, and a system with quantization after beamformer. The transmission efficiency result for each system and the BER performance will be evaluated and compared.

Furthermore, we will introduce three different channel models to the system: Rayleigh fading channel, Rician channel and Frequency Selective channel. We also develop the system by increasing the antenna diversity at each base station, and analyse how the diversity order will affect the error floor.

## **4.2. System Design**

This section introduces two systems with C-RAN and fronthaul networks: quantize before FFT and quantize after beamformer. The former system is similar to the system introduced in chapter 3 but with a multi-carrier scheme. The latter system is developed based on the former system by choosing the quantizer and beamformer positions.

### **4.2.1. Quantization before FFT**

Quantization before FFT, or signal sampling, is close to what we might describe as “classical” C-RAN: the signal is sampled directly at the antenna, or rather after down conversion to complex baseband, at a sample rate determined by the bandwidth of the OFDM multiplex. (Note that here we assume that the entire multiplex is used, and that all users employ the same modulation constellation). All baseband processing is then performed at the BBU on digitised signals from all RRUs which serve a given user or

group of users. First the FFT operation demodulates the OFDM multiplex, and following this we assume that a joint zero-forcing operation is performed on all signals from all cooperating RRUs, after which the signals are demodulated. (Here we assume, for simplicity, that forward error correction (FEC) coding is not used). This approach clearly minimizes the complexity of the BBU.

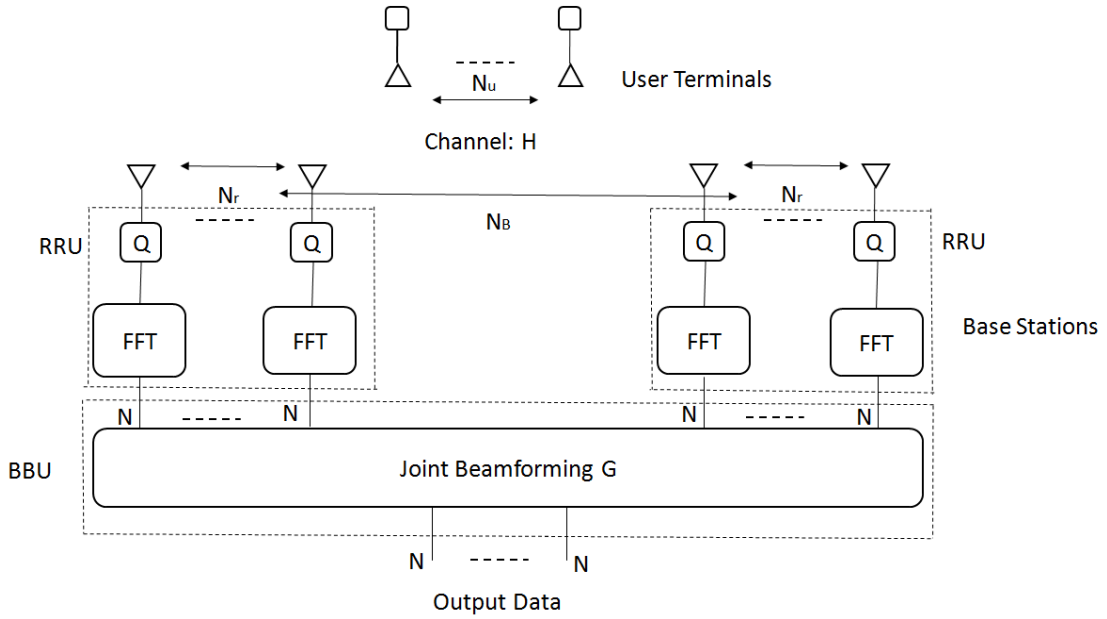


**Figure 4.1 C-RAN system with quantize before FFT**

The system is illustrated in figure 4.1, in which we assume that user terminals having a total of  $N_u$  antennas are served by  $N_B$  RRUs each with  $N_r$  antennas. Note that the  $N_u$  antennas may in general be single antennas attached to  $N_u$  user terminals, or alternatively some terminals may have more than one antenna, in which each transmits an independent data stream using spatial multiplexing.

The channel between the user terminals and the RRU antennas can in this case be described by a single  $(N_r N_B \times N_u)$  matrix  $\mathbf{H}$ . The joint beamforming matrix  $\mathbf{G}$  using zero-forcing is then given by the pseudo-inverse of this matrix, i.e.

$$\mathbf{G} = (\mathbf{H}^H \mathbf{H})^{-1} \mathbf{H}^H \quad (4.1)$$

#### 4.2.2. Quantize after Beamformer

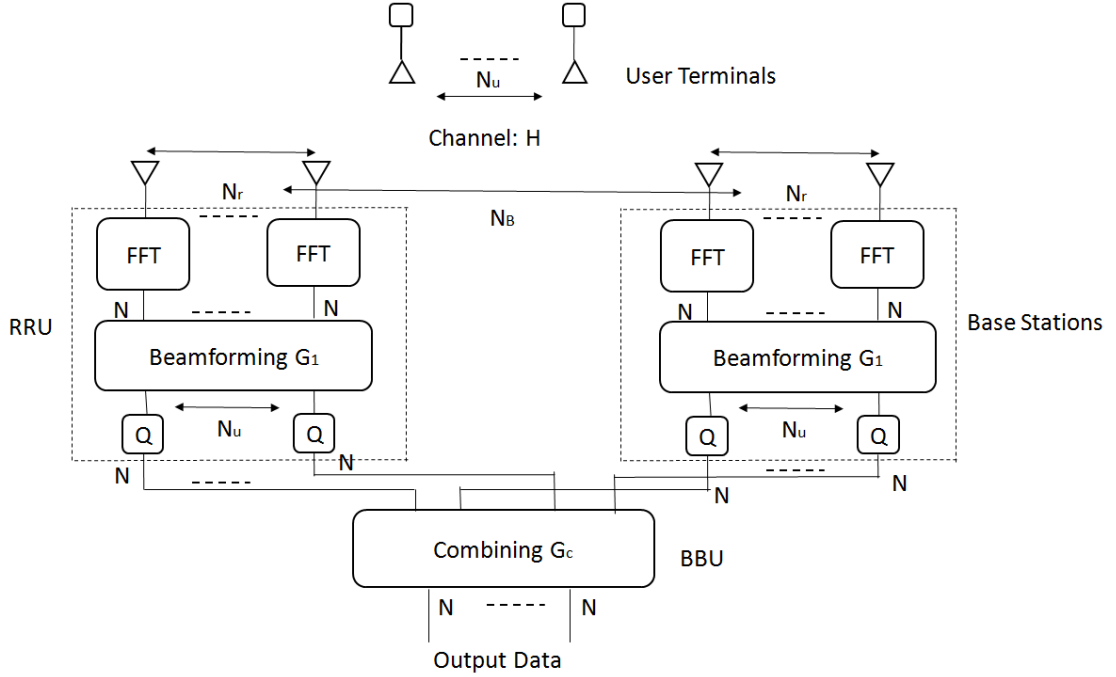


Figure 4.2 C-RAN with quantize after beamformer

In this system we assume that some of the baseband processing functions are performed at the RRUs. This is sometimes described as a split of the physical layer between the RRUs and the BBU. It has the disadvantage of increasing the complexity of the RRU. In this case we assume that each RRU includes the FFT, and then, operating on a per-subcarrier basis, performs beamforming in order to separate the signals from different user terminals. Different beamformer algorithms are deployed in [84, 85]. Here we assume the beamformer operates a zero-forcing (ZF) algorithm [86], which nulls the interference between each user, potentially at the cost of enhancement of the thermal noise. If the matrix between the user terminals and the  $i^{\text{th}}$  RRU is  $\mathbf{H}_i, i = 1 \dots N_B$ , then the beamformer matrix in the  $i^{\text{th}}$  RRU is

$$\mathbf{G}_i = (\mathbf{H}_i^H \mathbf{H}_i) \mathbf{H}_i^H \quad (4.2)$$

This forms an estimate  $\hat{\mathbf{s}}_i = \mathbf{G}_i \mathbf{r}_i$  of the data symbols of each user at the  $i^{\text{th}}$  RRU, where  $\mathbf{r}_i$  is the vector of received signals on the antennas of this RRU.

The quantizer then operates on the signals corresponding to each user and each subcarrier. At the BBU the recovered signals from each RRU corresponding to the same user are combined according to the degree of noise enhancement that each has suffered: a maximum ratio combiner is used, in the sense that it maximizes the signal to noise ratio of the combined signal.

Then the combined estimate:

$$\hat{\mathbf{s}} = \begin{bmatrix} \hat{\mathbf{s}}_1 \\ \hat{\mathbf{s}}_2 \\ \vdots \\ \hat{\mathbf{s}}_L \end{bmatrix} = \mathbf{G} \mathbf{r} = \begin{bmatrix} \mathbf{G}_1 & & \mathbf{0} \\ & \mathbf{G}_2 & \\ & & \ddots \\ \mathbf{0} & & & \mathbf{G}_L \end{bmatrix} \begin{bmatrix} \mathbf{r}_1 \\ \mathbf{r}_2 \\ \vdots \\ \mathbf{r}_L \end{bmatrix} \quad (4.3)$$

where:

$$\mathbf{G}_C = [\mathbf{A}_1 \ \mathbf{A}_2 \ \cdots \ \mathbf{A}_L]; \text{ with } \mathbf{A}_i = \text{diag} \left( \left( \text{diag}(\mathbf{G}_i \mathbf{G}_i^H) \right)^{-1} \right) \quad (4.4)$$

Note that  $\text{diag}(\square)$  here has the same properties as the MATLAB function: that is,  $\text{diag}(\mathbf{A})$  where  $\mathbf{A}$  is a matrix returns the diagonal as vector, and  $\text{diag}(\mathbf{a})$  where  $\mathbf{a}$  is a vector returns a diagonal matrix with  $\mathbf{a}$  as its diagonal. The inverse operation returns the element-by-element inverse. The combining matrix  $\mathbf{G}_C$  is a block diagonal matrix which operates on a stacked vector containing all the signal estimates from the RRUs.

### 4.3. Performance on Rayleigh Channel

We evaluate the performance of the two systems by simulation, determining the end-to-end BER of each. First we assume a frequency-flat Rayleigh channel for the access links, with various modulation schemes, without FEC coding.

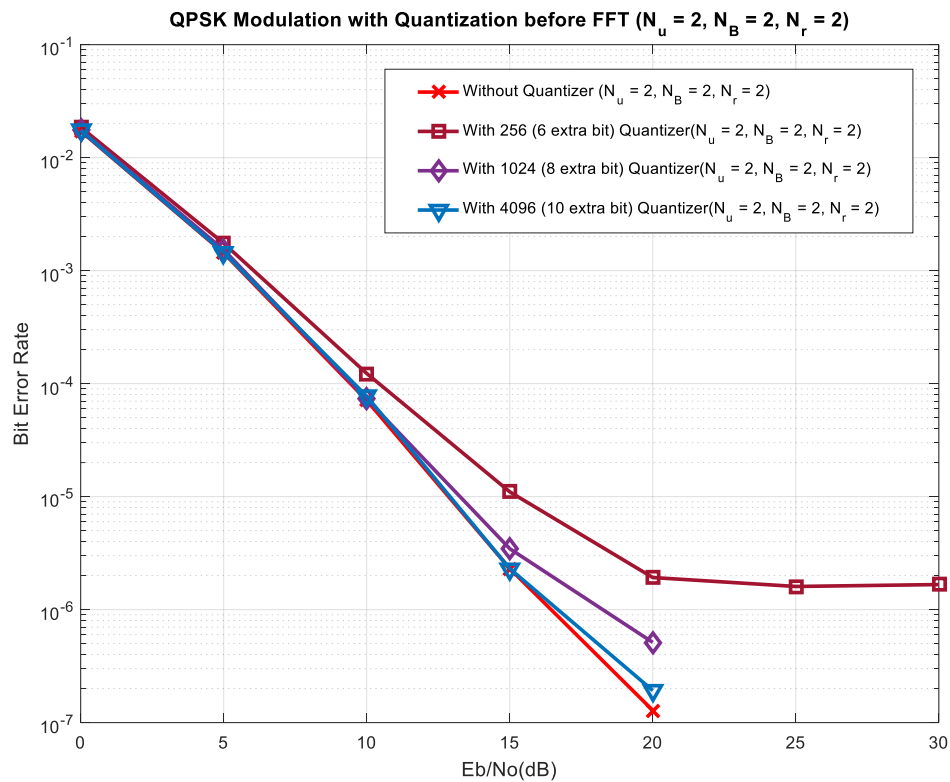


**Figure 4.3 Quantize before FFT:  $N_u = N_B = N_r = 2$ ; QPSK modulation with 6-10 extra bits**

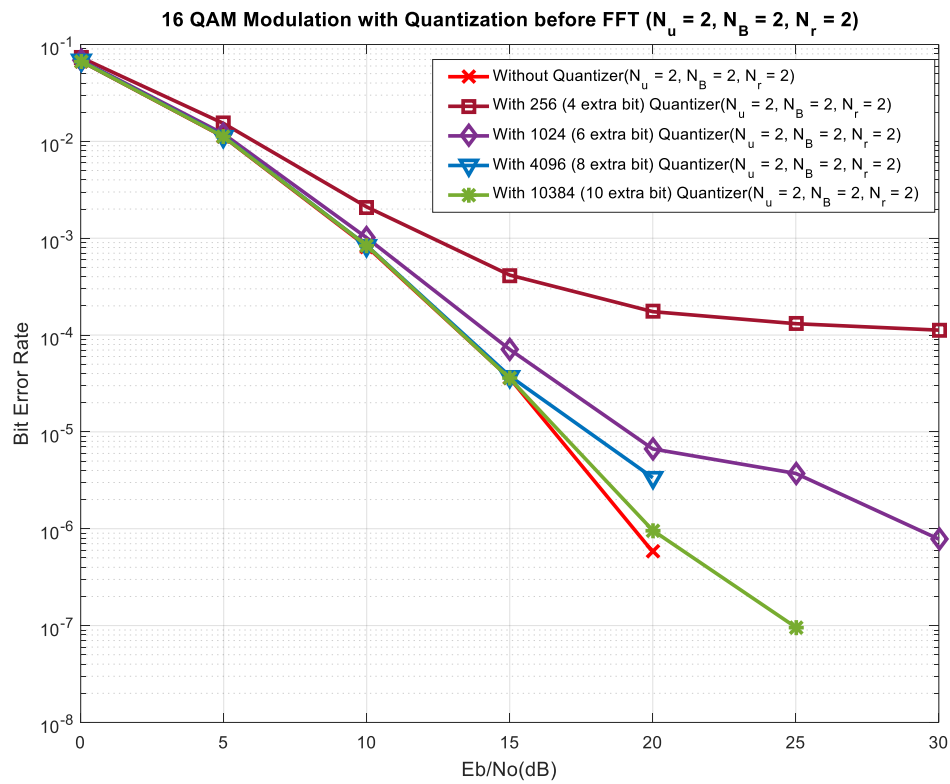


**Figure 4.4 Quantize before FFT:  $N_u = N_B = N_r = 2$ ; 16QAM modulation with 4-10 extra bits**

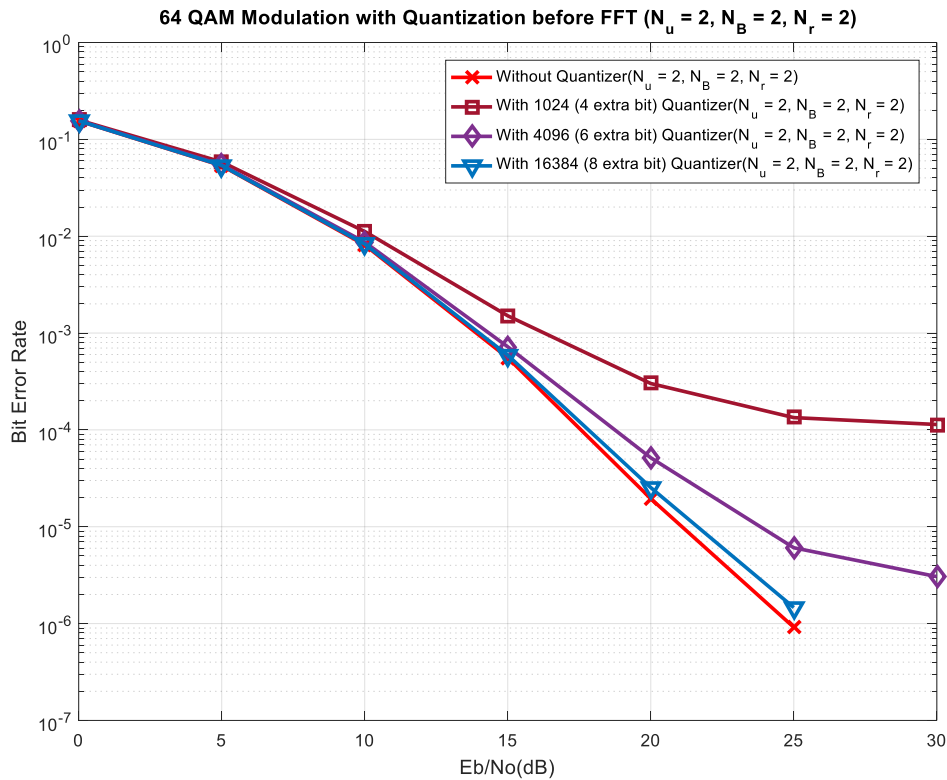


**Figure 4.5 Quantize before FFT:  $N_u = N_B = N_r = 2$ ; 64QAM modulation with 4-8 extra bits**

Figs 4.3-4.5 shows the BER performance versus  $E_b/N_0$  on the access links with quantize-before-FFT, followed by joint beamforming, in this case with  $N_u = N_B = N_r = 2$ , for simplicity, and for QPSK, 16QAM and 64QAM. It shows that an error floor occurs, at which increasing  $E_b/N_0$  on access links no longer improves BER. The error floors are generated with the same reason with the system described in chapter 3: the signals on the antennas contain mixed signals from multiple terminals, and generate self-interference due to intermodulation, which degrades BER performance even in the absence of noise. To reduce this noise floor to a low enough level requires 12 quantization bits for QPSK, 14 for 16QAM and 16 for 64QAM, which in each case means 10 extra bits on the fronthaul on top of the information bits conveyed. In each case the results are compared with the unquantized case to show the extent of the

degradation due to quantization. Of course the unquantized case is not practical as it would require an effectively infinite fronthaul load.

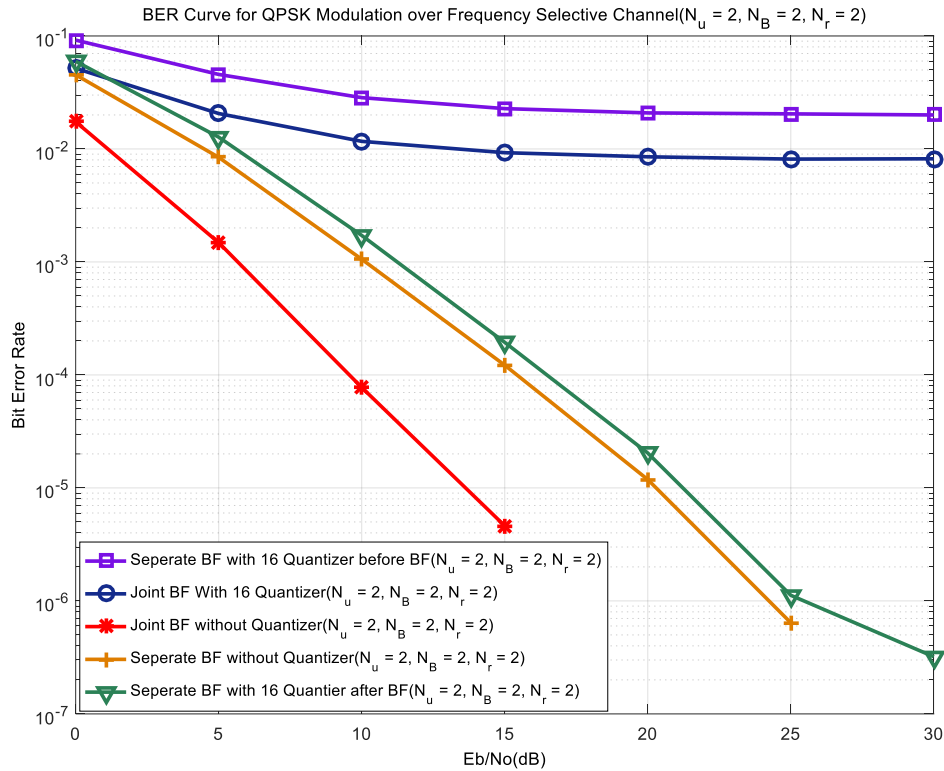


**Figure 4.6 Comparison of quantizer before FFT and after separate beamformer, and of joint and separate beamformer without quantization;  $N_u = N_B = N_r = 2$ ; QPSK with 16-level quantization (2 extra bits)**

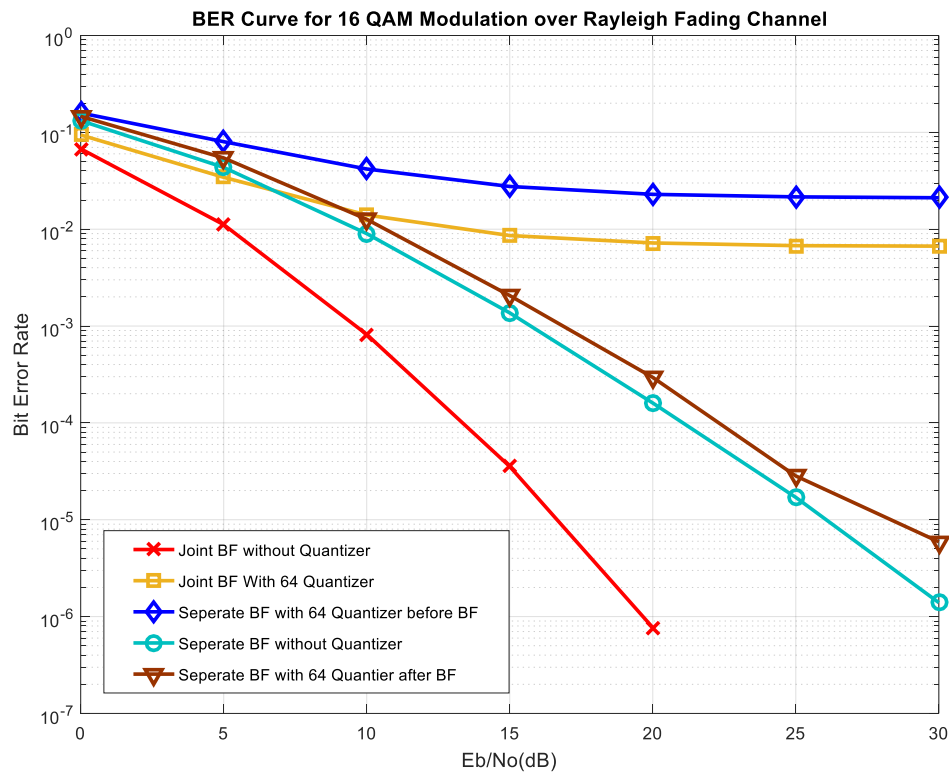


**Figure 4.7 Comparison of quantizer before FFT and after (separate) beamformer, and of joint and separate beamformer without quantization;  $N_u = N_B = N_r = 2$ ; 16QAM with 64-level quantization (2 extra bits)**

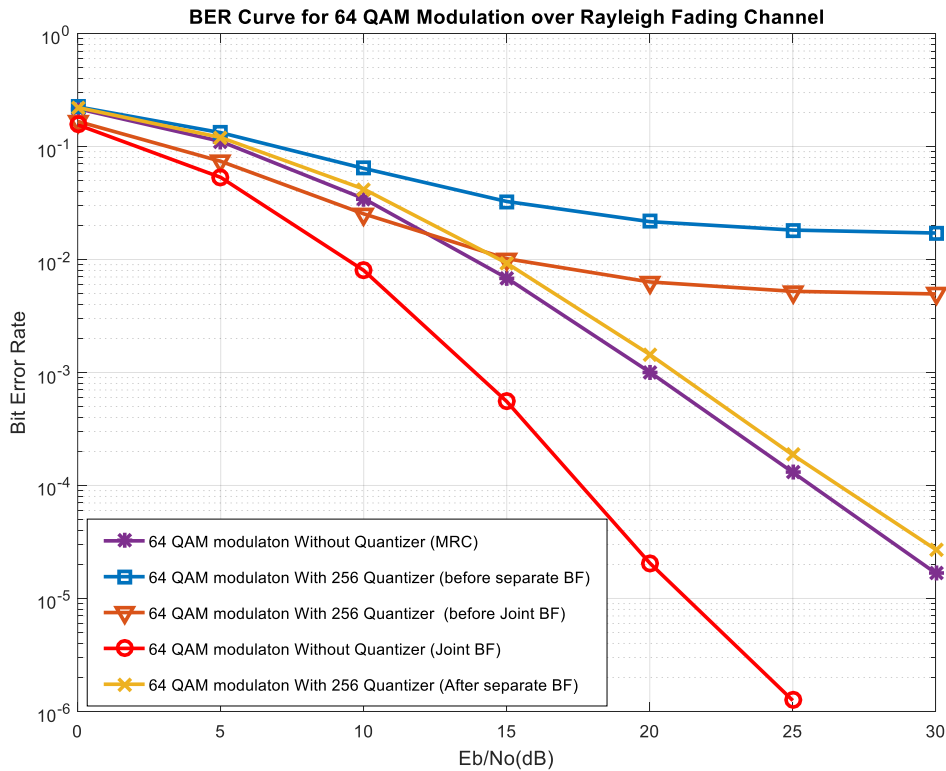


**Figure 4.8 Comparison of quantizer before FFT and after beamformer, and of joint and separate beamformer without quantization;  $N_u = N_B = N_r = 2$ ; 64QAM with 256-level quantization (2 extra bits)**

Figs 4.6 - 4.8 compare the performance of the separate beamformers and combiner and the joint beamformer, and the effect of quantization in the two schemes with two extra bits, for QPSK, 16QAM and 64QAM respectively. They show that the joint beamformer has the better performance without quantization. This is because it achieves higher diversity: the joint processing means that the detector effectively has a total of  $N_r \times N_B$  antennas, and hence the diversity order obtainable with linear detection is  $N_r N_B - N_u + 1$ . For the separate beamformer and combiner, however, the linear detector at each RRU can achieve diversity  $N_r - N_u + 1$ , and optimum combining at the BBU then gives a total diversity  $(N_r - N_u + 1)N_B$ . However, with quantization

the latter has a very small performance degradation, of less than 2 dB with two extra quantization bits, whereas the former has a very high error floor. This is because quantization after beamformer separates the user signals before they are quantized, greatly reducing the intermodulation distortion. In terms of the outage analysis in section 3 above, quantization after beamforming does not suffer from outage, because the separate data streams do not interfere, and different combinations of symbols from two sources will not therefore fall into the same quantization region.

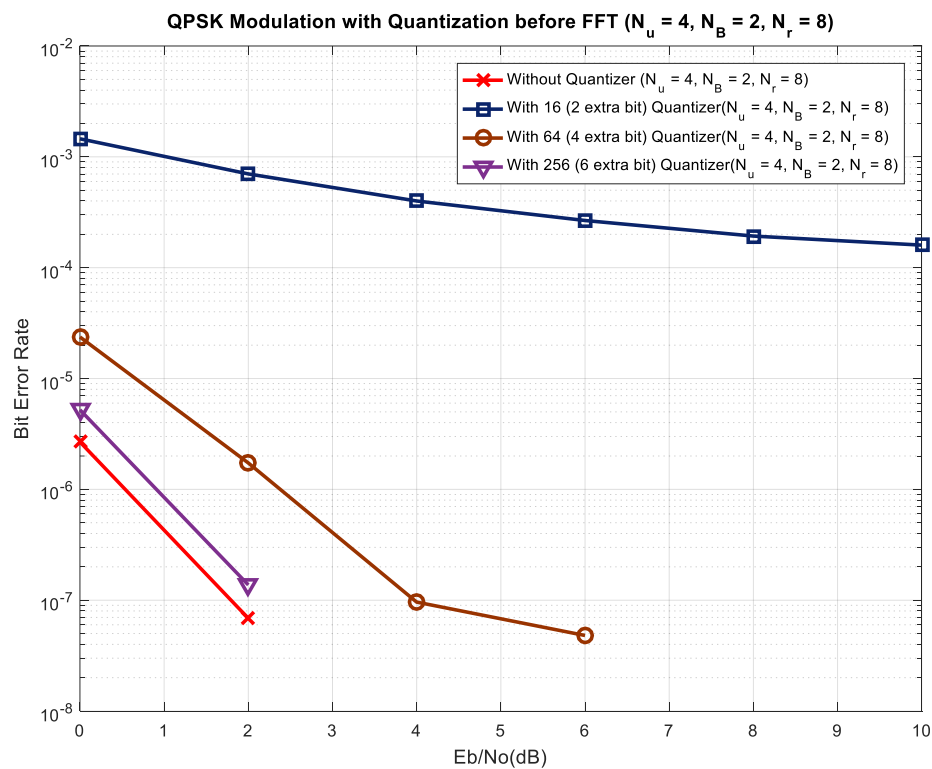


**Figure 4.9 Quantize-before-FFT (with joint beamformer):  $N_u = 4, N_B = 2, N_r = 8$ ;**

**QPSK modulation with 2-6 extra bits**

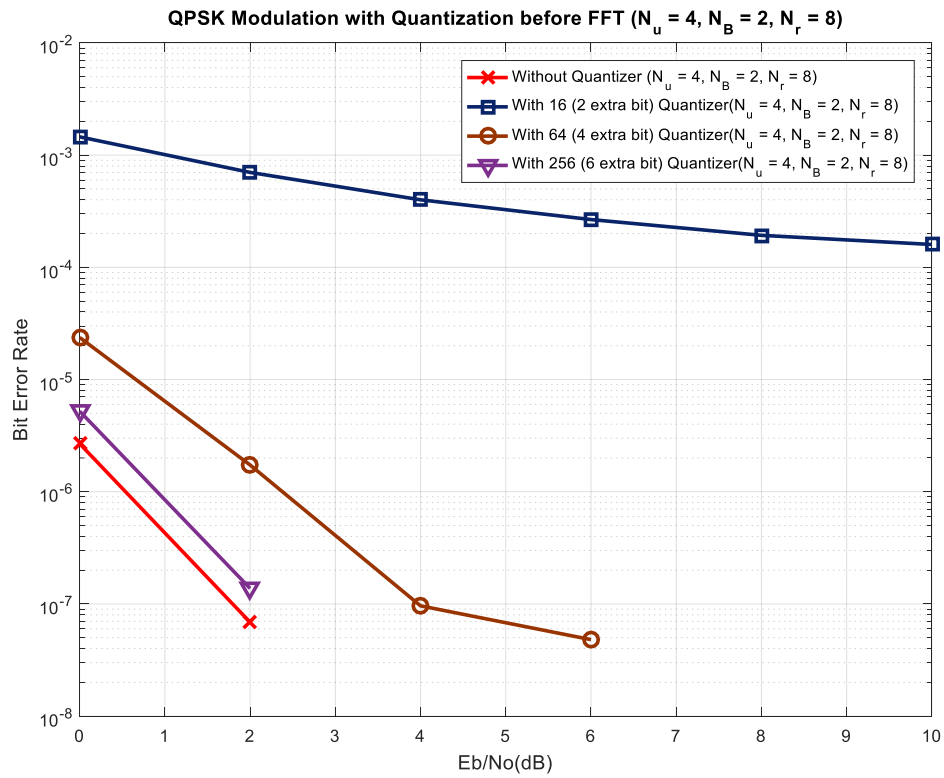


**Figure 4.10 Quantize-before-FFT:  $N_u = 4, N_B = 2, N_r = 8$ ; 16QAM modulation with 2-6 extra bits**

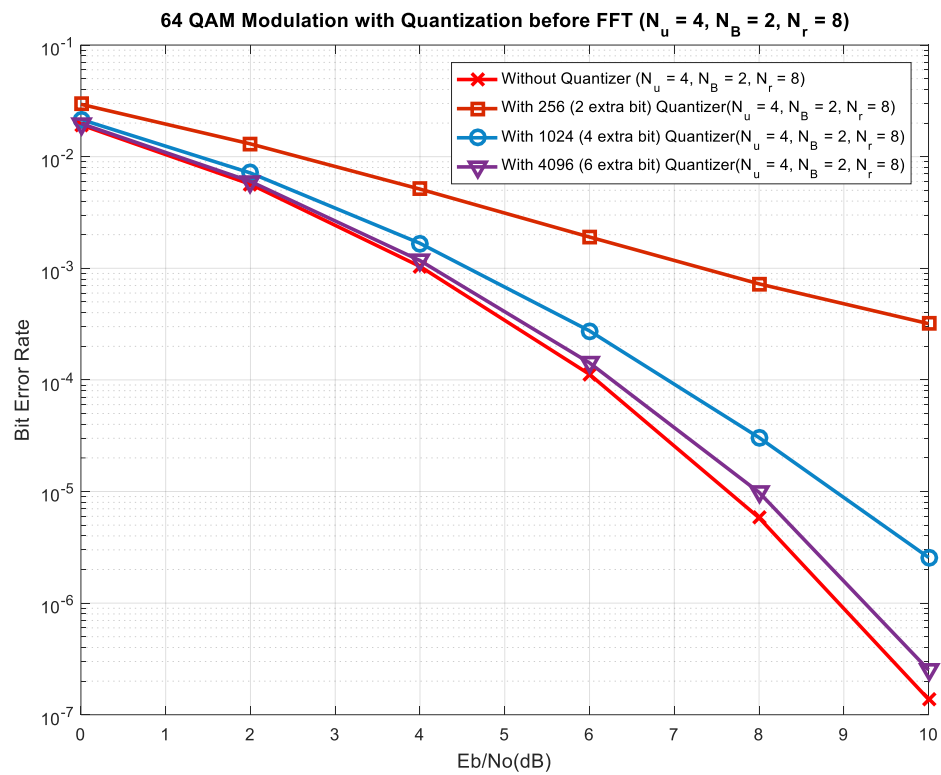


**Figure 4.11 Quantize-before-FFT:  $N_u = 4, N_B = 2, N_r = 8$ ; 64QAM modulation with 2-6 extra bits**

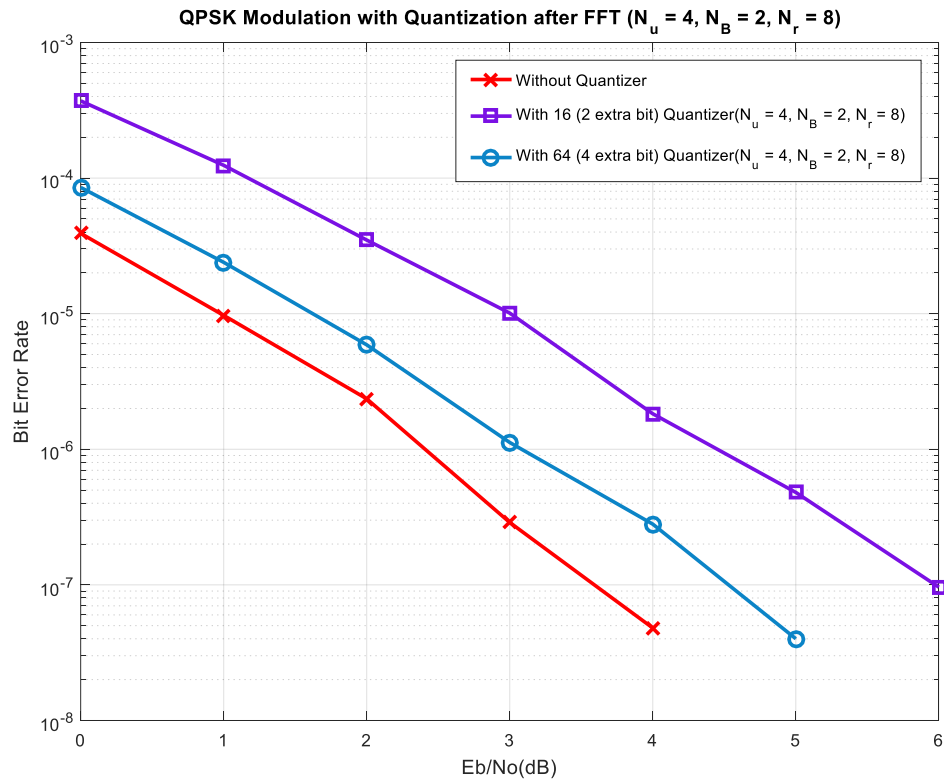


**Figure 4.12 Quantize after (separate) beamformer:  $N_u = 4, N_B = 2, N_r = 8$ ; QPSK modulation with 2-4 extra bits**

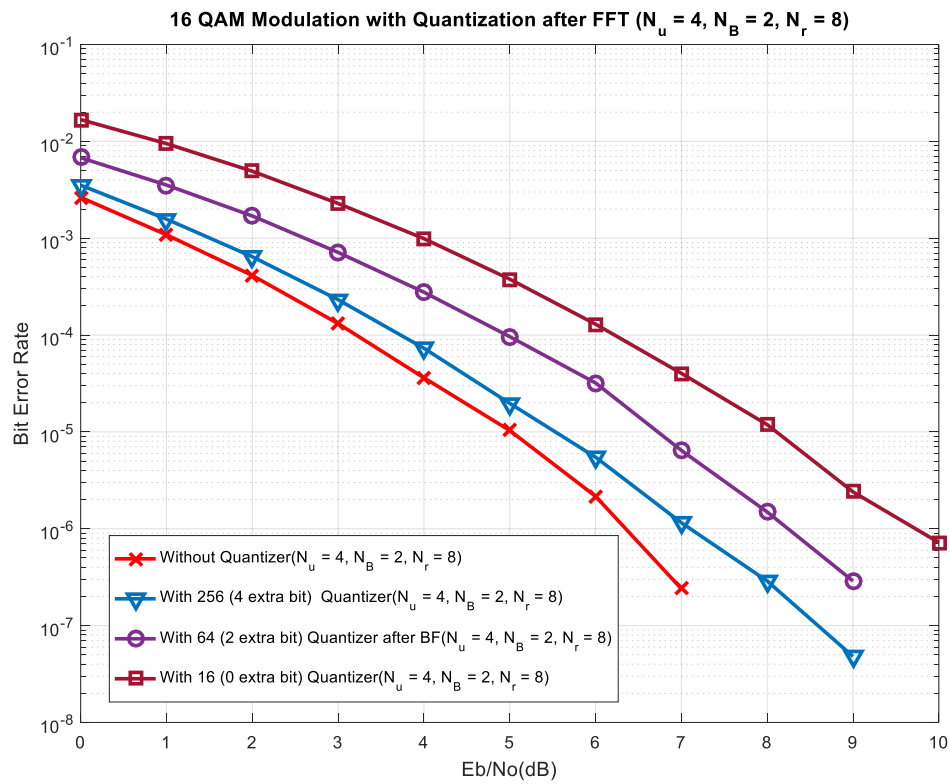


**Figure 4.13 Quantize after beamformer:  $N_u = 4, N_B = 2, N_r = 8$ ; 64QAM modulation with 0-4 extra bits**

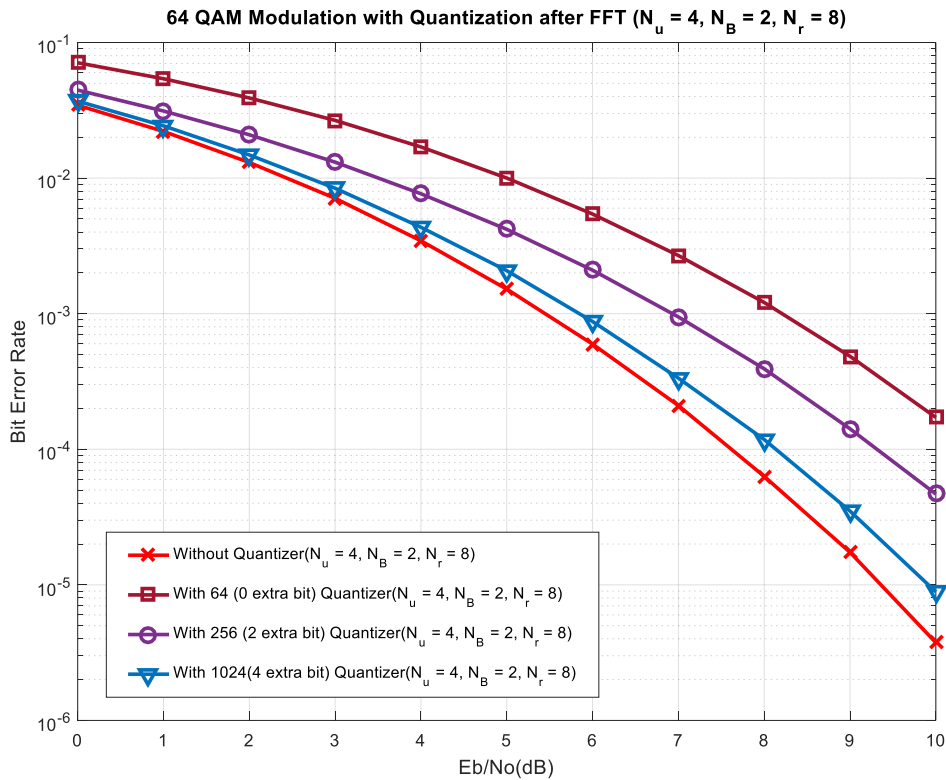


**Figure 4.14 Quantize-after-beamformer:  $N_u = 4, N_B = 2, N_r = 8$ ; 64QAM modulation with 0-4 extra bits**

Figures 4.9-4.14 give the same comparisons for a more realistic scenario with 8 antennas per RRU, still with two RRUs, but now with four user terminals. This yields significantly larger diversity, which also reduces the error floor in the quantize-before-FFT case. Now the error floor is sufficiently low (below  $10^{-6}$ ) in this case with only 4 extra bits, but there is a loss of around 3 dB at  $10^{-6}$ , while with 6 extra bits this is largely eliminated. We also investigate the effect of different numbers of extra bits in the quantize-after-beamforming scheme: we observe that there is a trade-off between the loss (compared to no quantization) and the number of extra bits. It is even possible to use zero extra bits without giving rise to an error floor, but the loss is then around 3 dB. We should note also that the extra diversity provided by the joint beamformer gives rise to approximately 4 dB improvement in performance (at  $10^{-6}$ ), so that the BER

performance with 4 extra bits in the two schemes is then roughly comparable at this BER. However in this scenario, because the number of antennas is twice the number of users, the fronthaul load in the quantize-before-FFT scheme is twice that of the quantize-after-beamformer, even for the same number of extra bits.

Scenario	Modulation	Scheme	$b_e$	$b_t$	$E_b/N_0$ (dB)	Transmission Efficiency
$N_u = 2,$ $N_B = 2,$ $N_r = 2$	QPSK	QbFFT	8 bits	10 bits	18	20%
		QaBF	2 bits	4 bits	25	50%
	16QAM	QbFFT	8 bits	12 bits	23	33.3%
		QaBF	2 bits	6 bits	32	66.7%
	64QAM	QbFFT	8 bits	14 bits	26	42.9%
		QaBF	2 bits	8 bits	37	75%
$N_u = 4,$ $N_B = 2,$ $N_r = 8$	QPSK	QbFFT	4 bits	6 bits	2.3	33.3%
		QaBF	2 bits	4 bits	4.4	50%
	16QAM	QbFFT	4 bits	8 bits	7	50%
		QaBF	2 bits	6 bits	8.2	66.7%
	64QAM	QbFFT	4 bits	10 bits	11	60%
		QaBF	2 bits	8 bits	13	75%

**Table 4.1: Comparison of Quantize-before-FFT (QbFFT) and Quantize-after-Beamformer (QaBF) for the two different scenarios and various modulation schemes, showing number of extra bits be used by quantizer, total transmitted bits for each symbol  $b_t$ , required  $E_b/N_0$  for BER  $10^{-6}$ , and fronthaul transmission efficiency**

Table 4.1 summarizes the results for the two scenarios we have considered, comparing the transmission efficiency for the two schemes: that is, the ratio of total user data rate of users served by each RRU to the fronthaul load of that RRU. We observe that the quantize-after-beamformer scheme improves the transmission efficiency by a ratio between 30% and 32.1% with the scenario  $N_u = 2, N_B = 2, N_r = 2$ , and an improved ratio between 15% and 16.7% with the scenario  $N_u = 4, N_B = 2, N_r = 8$ . So that the additional overhead due to quantization is typically less than 50%. There is however a penalty in the required  $E_b/N_0$  on the access link for the latter scheme: for the scenario  $N_u = 4, N_B = 2, N_r = 8$  this is only 1-2 dB; for  $N_u = 2, N_B = 2, N_r = 2$  it is between 7 and 9 dB, largely due to the greater diversity available using the joint beamformer.

#### 4.4. Performance on Rician and Frequency-selective Channels

Since in most cases a line-of-sight (LOS) signal will be available on the access links, the channels will be Rician rather than Rayleigh fading [52, 54]. Hence also it is necessary to account for the location of the user terminals and of the RRUs. This is illustrated in Fig. 4.15: we assume the terminals are uniformly distributed along a street between two RRUs, which are a distance  $a$  from the centre of the street, and a distance  $d$  apart. The  $i^{\text{th}}$  terminal is a distance  $x_i$  along the street from one of the RRUs (which we will call the left hand RRU) and therefore a distance  $d - x_i$  from the other. The antenna spacing at the RRUs is  $l$  and the wavelength is  $\lambda$ .

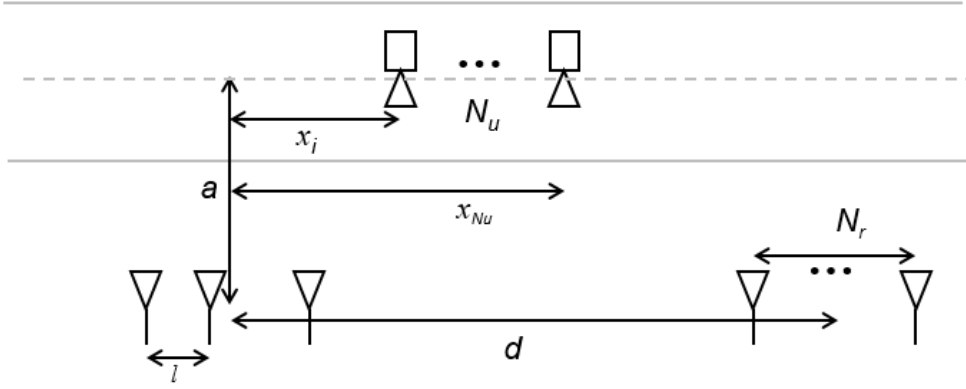


**Figure 4.15 Location of RRUs and terminals in Rician channel**

The response vector for the LOS component of the signal at the left hand RRU from the  $i^{\text{th}}$  user terminal is given by:

$$\mathbf{h}_{i,LOS} = \left\{ \exp\left(2\pi j \frac{l \sin \theta_i}{\lambda}\right), i = 0 \dots N_r - 1 \right\} \quad (4.5)$$

where the angle of arrival at the left hand RRU:

$$\theta_i = \tan^{-1}\left(\frac{x_i}{a}\right) \quad (4.6)$$

The vectors  $\mathbf{h}_{i,LOS}$  then form the columns of the LOS channel matrix  $\mathbf{H}_{LOS}$  for this RRU. The matrix for the right hand RRU can be obtained using the same equations and substituting  $d - x_i$  for  $x_i$ . The complete Rician channel matrix is then:

$$\mathbf{H}_{Rice} = \sqrt{\frac{K}{K+1}} \mathbf{H}_{LOS} + \sqrt{\frac{1}{K+1}} \mathbf{H}_{Ray} \quad (4.7)$$

where  $K$  is the Rice factor of the channel, which is the ratio of the power of the LOS component to the multipath component, and  $\mathbf{H}_{Ray}$  denotes a matrix with independent complex Gaussian entries representing the Rayleigh fading channel.

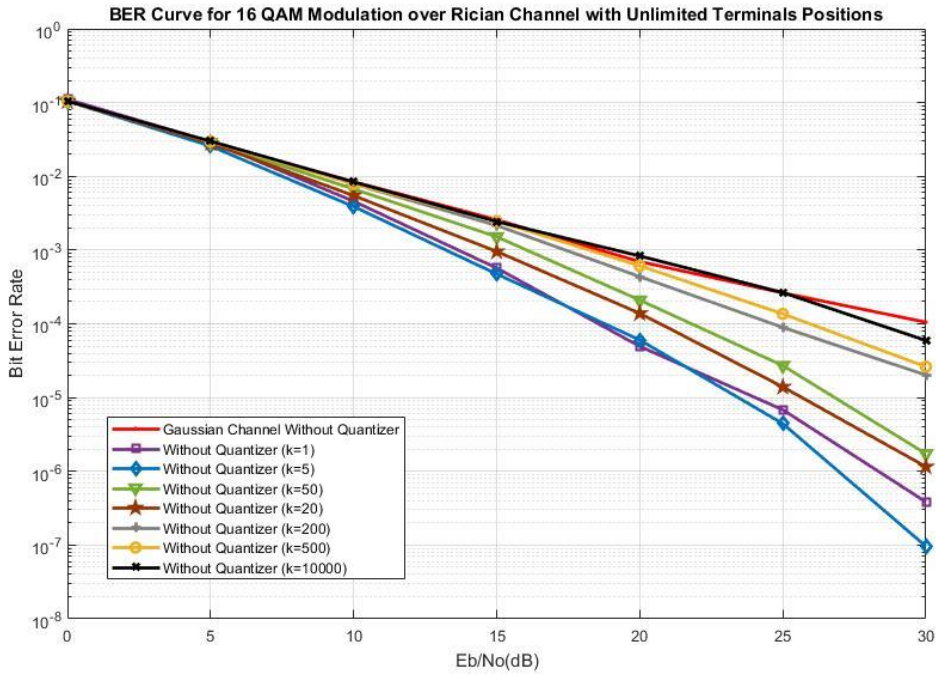


**Figure 4.16 BER on Rician channel, random terminal positions, with different  $K$ -factors**

Figure 4.16 shows the BER performance with ZF beamforming, in this case without quantization. With unlimited terminal positions, here the user terminal positions are random, uniformly distributed along the street. It shows, somewhat unexpectedly, that

performance degrades as  $K$ -factor increases, and reach the poorest performance with a pure Gaussian noise channel. However, this is because of the correlation between the response vectors from different users when the terminals are close together, which means that ZF results in large noise enhancement, as shown in figure 4.17. Here the signals from two users are correlated when the angles of arrival of their LOS components are very similar, which means that their LOS response vectors are very similar. It is low if the distance between them is more than 10 m, and rises again beyond 40 m due to a grating lobe.

Note that in Fig. 4.16 and all subsequent plots,  $N_u = N_B = N_r = 2$ , distance between RRUs is  $d = 50\text{m}$ , distance  $a$  of RRUs from centre of street is 20m, and antenna spacing at RRUs  $l$  is equal to the wavelength  $\lambda$ .

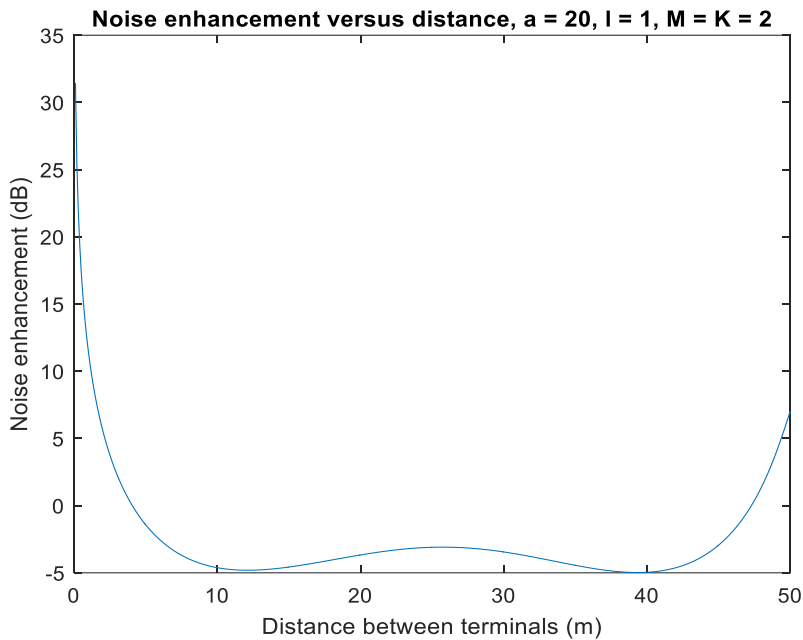


**Figure 4.17 Noise enhancement factor in Gaussian channel *versus* distance between terminals**

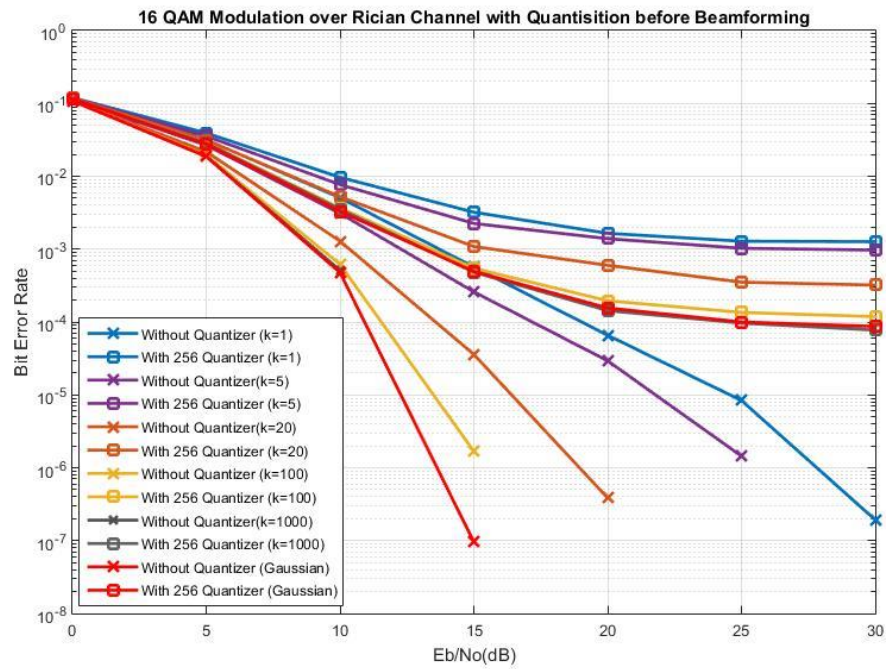


Figure 4.18 Quantize before FFT, Rician channel with various  $K$ -factors, 16QAM modulation with 4 extra bits

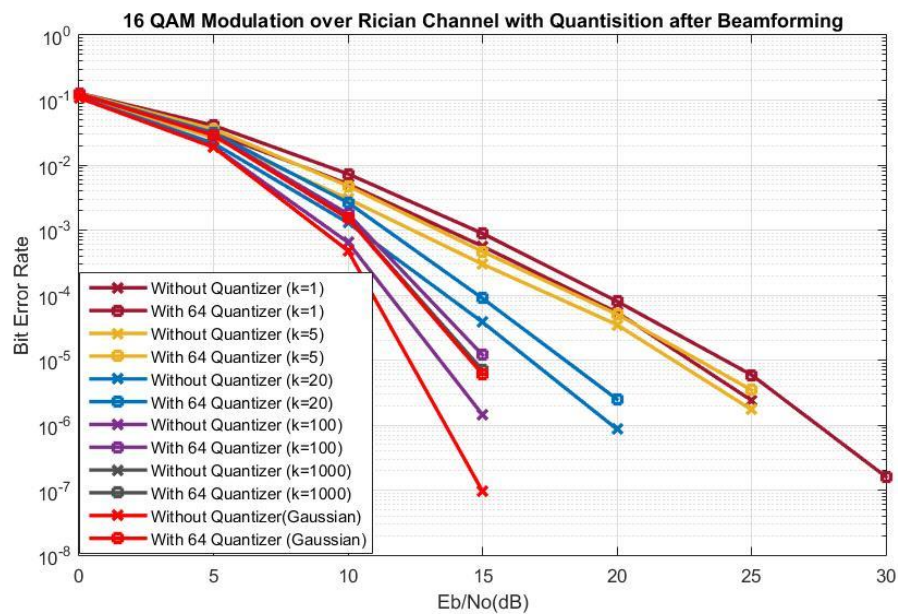
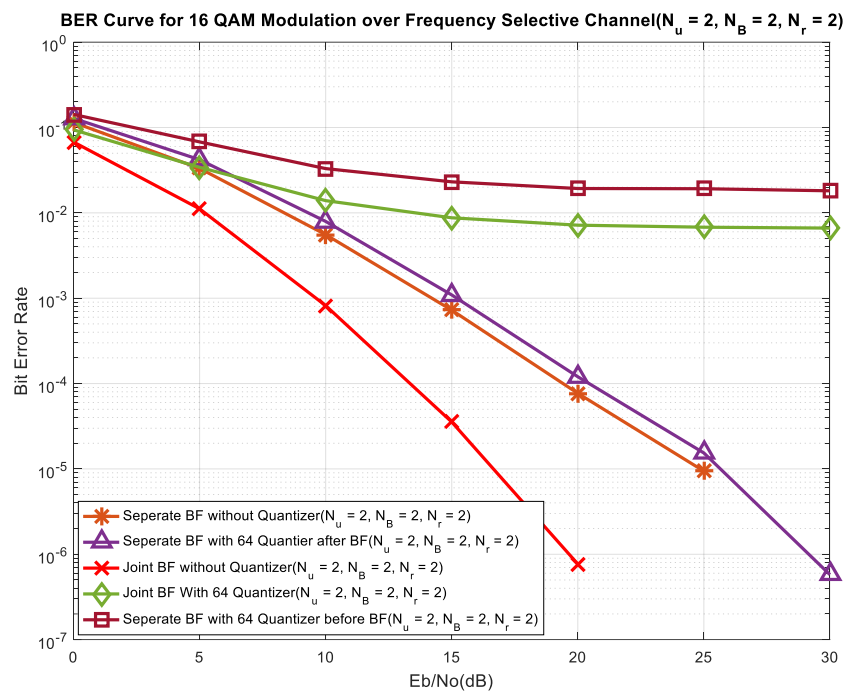
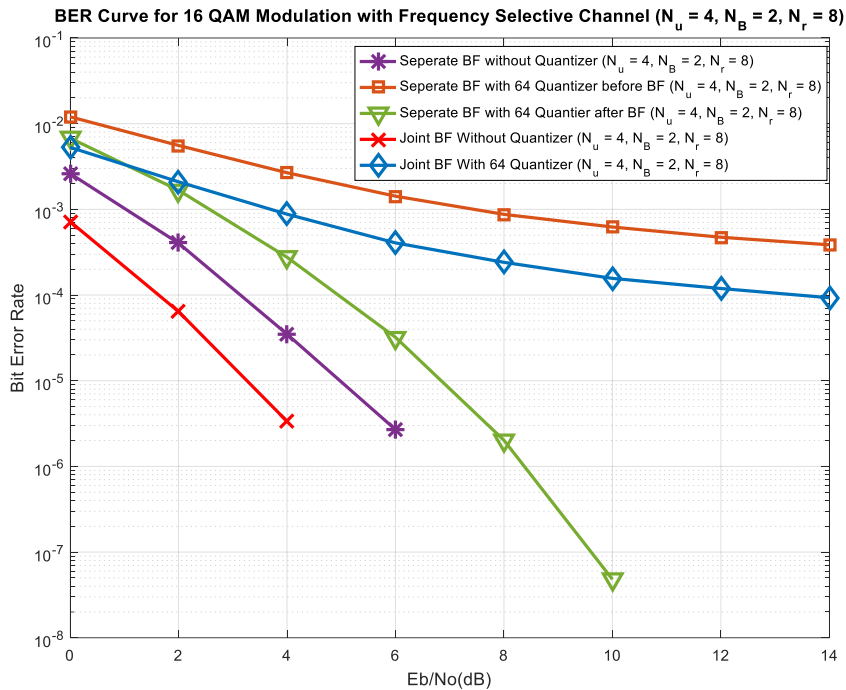


Figure 4.19 Quantize after beamformer, Rician channel with various  $K$ -factors, 16QAM modulation with 2 extra bits



**Figure 4.20 Comparison of quantizer positions on frequency-selective channel, Rayleigh fading,  $N_u = 2, N_B = 2, N_r = 2$ ; 16QAM modulation with 2 extra bits**



**Figure 4.21 Comparison of quantizer positions on frequency-selective channel, Rayleigh fading,  $N_u = 4$ ,  $N_B = 2$ ,  $N_r = 8$ ; 16QAM modulation with 2 extra bits**

Fig 4.18 shows the performance in this case for quantize-before-FFT, with 16QAM modulation and 4 extra bits, where a substantial error floor is visible. Fig. 4.19 shows the result for quantize-after-beamformer, with 2 extra bits. Here an error floor is avoided, although a performance loss occurs with quantization which increases with  $K$ -factor, reaching 3-4 dB for the Gaussian channel. This confirms the benefit of quantize-after-beamformer also in the Rician case, for the full range of  $K$ -factors. With a limit terminal positions, we propose that the distance between terminals sharing the same resources should be limited to a minimum of 10m, by reassigning resource blocks for closer users. This avoids excessive noise enhancement, and means that channels with higher  $K$ -factor give better BER.

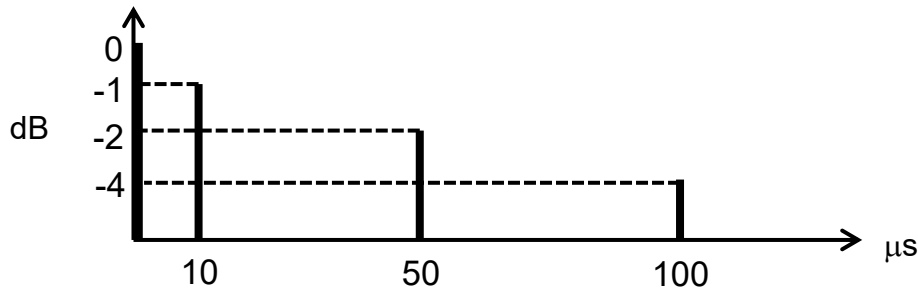


**Figure 4.22 Channel power-delay profile for frequency-selective channel**

Finally Figure 4.20 and figure 4.21 shows the BER performance for both quantizer positions for a frequency-selective Rayleigh fading channel with different antenna diversity, with an arbitrarily-chosen power-delay profile, shown in Figure 4.22. It suggests a similar comparison between the two schemes as for frequency-flat fading.

#### 4.5. Chapter Conclusion

This chapter explored two C-RAN systems in fronthaul networks: quantize before FFT and quantize after beamformer. Each system is evaluated with multiple modulation schemes: QPSK, 16 QAM and 64 QAM. Additionally, a greater diversity scenario was considered in practice and simulated. Finally, the end to end BER performance for each system and scenario has been compared and analysed.

For the system with quantize before FFT, with first scenario ( $N_u = 2, N_B = 2, N_r = 2$ ), because of the error floor which occurs, increasing  $E_b/N_0$  no longer improves BER and each BBU needs to transmit 8-10 extra bits to reduce the error floor to a low enough level ( $10^{-6}$  with BER). The number of required extra bits remain unchanged as higher and higher modulation levels are applied, thus the transmission efficiency improves. With the second scenario ( $N_u = 4, N_B = 2, N_r = 8$ ), the extra bits required are reduced by 4 bits (4-6 bits) compared with first scenario, resulting in an improvement of

transmission efficiency in the fronthaul network. Moreover, a higher diversity can greatly improve the BER performance.

For the system with quantization after beamformer, in the first scenario ( $N_u = 2$ ,  $N_B = 2$ ,  $N_r = 2$ ), the beamformer separates the user signals before they are quantized, and hence the error floor is removed. Two extra bits can easily achieve the required BER performance level (zero extra bits can also achieve the BER level, but requires higher  $E_b/N_0$ ), and improves the transmission efficiency significantly, especially with low level modulation schemes. When the system modulation level increases, the required extra bits still remains the same. As a result, a higher level modulation scheme also improves the transmission efficiency with this system. With the second scenario ( $N_u = 4$ ,  $N_B = 2$ ,  $N_r = 8$ ), this system can also achieve the BER performance level with only 0-2 bits, furthermore, the higher antenna diversity also improves the BER performance significantly.

Moreover, two systems are evaluated with Rician channel and FSC channel. We conclude that the BER performances also benefit from the system with quantization after beamformer. With Rician channel, the BER performance is also affected by the K factor and the distance between terminal positions.

Through the comparison of the performance results between two systems, on the one hand, one solution for improving the transmission efficiency is to increase the antenna diversity at each RRU, since we have observed that the extra bits required has dropped from 8-10 bits to 4-6 bits if we increases the number of receive antennas at each BBU. But increasing the antenna diversity also increases the complexity of the base stations. On the other hand, the second system with quantization after beamformer provides an obvious improvement of transmission efficiency, and the transmission efficiency at low modulation level is greatly enhanced. However, the second system also requires separation of the user signals by using a beamformer before quantization at each RRU,

which increases the complexity and costs for the base stations. Besides, as higher and higher modulation schemes are applied, the improvement rate of the transmission efficiency with the second system becomes diminished. If we assume the modulation level can be extremely high, the difference of transmission efficiency between two systems is negligible. However if this assumption is unrealistic and high modulation level also increases the fronthaul load, we will not accept the solution which increases the modulation level with first system. As a result, the second C-RAN system gives outstanding improvement on transmission efficiency in the fronthaul and will be used in the following work.

---

# Chapter 5 Physical Layer: Error Control in Fronthaul

## 5.1. Introduction

In the previous system design, we assumed the transmission between RRUs and BBU is a lossless "bit pipe". In this chapter we will introduce errors and investigate the effect of errors in transmission of the quantized data over the fronthaul network, to evaluate the error rate requirements for this network as well as its capacity requirements. It may be appropriate to combine the quantized data into packets for transmission over the fronthaul network, especially for the purposes of error control. This packetization may cause additional latency, and so we also address here the effectiveness of error control [59] measures such as error detection and error correction coding [58] as a function of packet length. Error correction coding results in increased fronthaul load because of the additional code parity bits required, but the throughput efficiency is increased with increased packet length. This results in a trade-off between throughput efficiency and increased latency [59].

## 5.2. System Structure

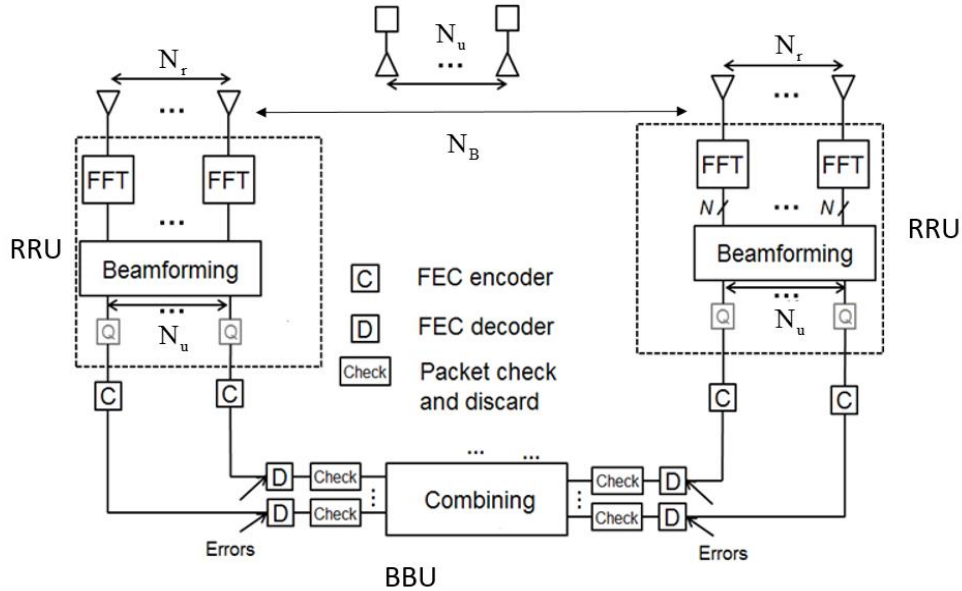


**Figure 5.1 Fronthaul error handling**

Figure 5.1 shows the error-handling options for fronthaul. We consider two methods of error control, both based on packetization of the fronthaul data. The first is to detect packet errors using error-detection coding (such as cyclic redundancy check – CRC [56]) and to discard any erroneous packets; the second is to apply error correction coding. Note that if a packet is discarded from one RRU, the BBU may still be able to recover the transmitted data using the corresponding packet from another RRU. These methods are compared with no error control: allowing erroneous packets to be forwarded and combined.

Note that all the simulations reported in the following system design use 16 QAM modulation and 4 extra bits of quantization (256 levels). We assume that an end-to-end error floor of  $10^{-6}$  is acceptable.

### 5.2.1. Error Detection Coding Approach

The first method of error control is to apply an error detection code to the system, which only detects the errors from the received packets at the BBU. Once any packet errors are detected, the system will discard the erroneous packet and use the corresponding packet from the other RRUs. If all of the corresponding packets contains errors, then the system will discard all of these packets, which results information loss of user signals. The system will need to re-transmit these packets. The system flowchart is illustrated in figure 5.3.

The cyclic redundancy check, or CRC, is a technique for detecting errors in digital data, but not for making corrections when errors are detected. It is used primarily in data transmission. In the CRC method, a certain number of check bits, often called a checksum, are appended to the message being transmitted. The receiver can determine whether or not the check bits agree with the data, to ascertain with a certain degree of probability whether or not an error occurred in transmission. If an error occurs, the receiver at the BBU will consider asking the sender to retransmit the message or just discard the erroneous data.

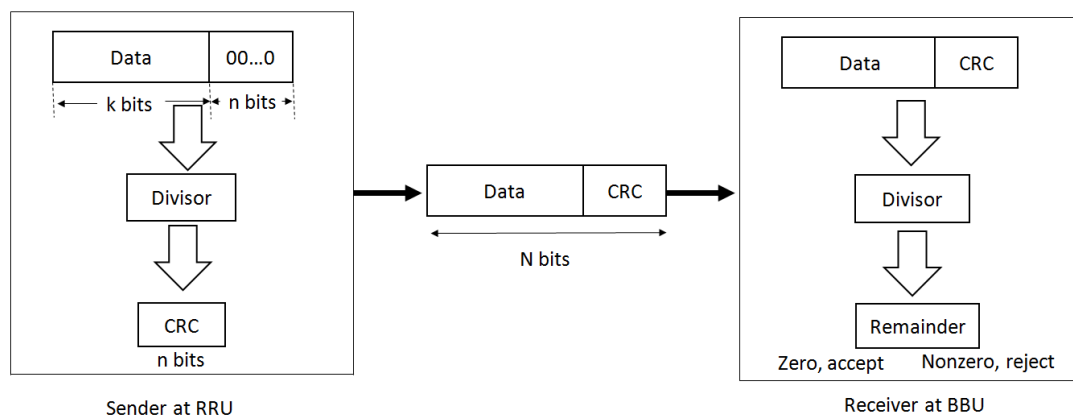


**Figure 5.2 CRC generator and checker**

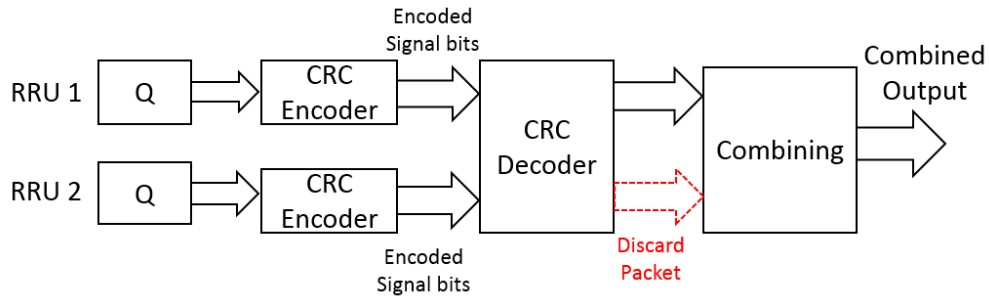


**Figure 5.3 System flowchart with CRC codes**

In figure 5.2, the system first computes an  $n$  bit binary CRC, then  $k$  data bits are encoded into  $N$  code bits by appending the  $n$  bit code and forming the codeword. Once the codeword is received at the BBU node, the system computes the remainder by using the whole codeword and the same polynomial as at transmitter. If the remainder is zero, this means the data is received without any errors. If the remainder is not zero, it means that the received data contains errors [59].

If  $\alpha$  is a prime number, then a field consists of a set of  $\alpha^k$  elements for any  $k$ , which known as Galois fields and denoted with  $GF(\alpha^k)$ . Then each element can be represented by a polynomial expression:

$$\alpha^k = a_{k-1}x^{k-1} + a_{k-2}x^{k-2} + \dots + a_1x + a_0 \quad (5.1)$$

where the coefficients  $a_{k-1}$  to  $a_0$  take the values in the set  $\{0, 1, \dots, \alpha - 1\}$ . In coding applications,  $\alpha$  is commonly 2, thus the coefficients are taken from the binary digits  $\{0, 1\}$ . Thus  $2^k$  field elements correspond to the  $2^k$  combinations of the  $k$ -bit number.

The addition of two field elements can be represented with [59]:

$$\begin{aligned} & (a_{k-1}x^{k-1} + a_{k-2}x^{k-2} + \dots + a_1x + a_0) + (b_{k-1}x^{k-1} + b_{k-2}x^{k-2} + \dots + b_1x + b_0) \\ & = c_{k-1}x^{k-1} + c_{k-2}x^{k-2} + \dots + c_1x + c_0 \end{aligned} \quad (5.2)$$

where  $c_i = a_i + b_i$ . Because the coefficients only take values 0 and 1, we have:

$$\begin{cases} c_i = 0 & \text{for } a_i = b_i \\ c_i = 1 & \text{for } a_i \neq b_i \end{cases} \quad (5.3)$$

which producing the bit-by-bit exclusive-OR function of two binary numbers. With CRC code, the data bits:  $\mathbf{m} = [m_{k-1}m_{k-2}\dots m_1m_0]$  can be represented with [59]:

$$\mathbf{m}(x) = m_{k-1}x^{k-1} + m_{k-2}x^{k-2} + \dots m_1x + m_0 \quad (5.4)$$

while appended bits:  $\mathbf{R} = [r_{k-1}r_{k-2}\dots r_1r_0]$  can be represented with [59]:

$$\mathbf{R}(x) = r_{k-1}x^{k-1} + r_{k-2}x^{k-2} + \dots r_1x + r_0 \quad (5.5)$$

and hence codeword bits [59]:

$$\mathbf{C} = [c_{k-1}c_{k-2}\dots c_1c_0] = [m_{k-1}m_{k-2}\dots m_1m_0r_{k-1}r_{k-2}\dots r_1r_0] \quad (5.6)$$

which can be represented by [59]:

$$\begin{aligned} \mathbf{C}(x) &= c_{k-1}x^{k-1} + c_{k-2}x^{k-2} + \dots c_1x + c_0 \\ &= x^n \mathbf{m}(x) + \mathbf{R}(x) \end{aligned} \quad (5.7)$$

### 5.2.2. Error Correction Coding Approach

The second method of error control is to apply forward error correction (FEC) techniques, which encodes the message in a redundant way by using an error correction code (ECC). Many different ECC types can be used to correct the errors occur in transmission, however, Reed-Solomon code (RSC) is introduced with [60, 61], which provides a good compromise between transmission efficiency (the proportion of redundant part required) and complexity (the difficulty of encoding and decoding).

The Reed-Solomon code is a block code, which divides the transmitted message into separate blocks of data. Each separate block is encoded by adding parity protection symbols: the structure is shown in figure. 5.4.

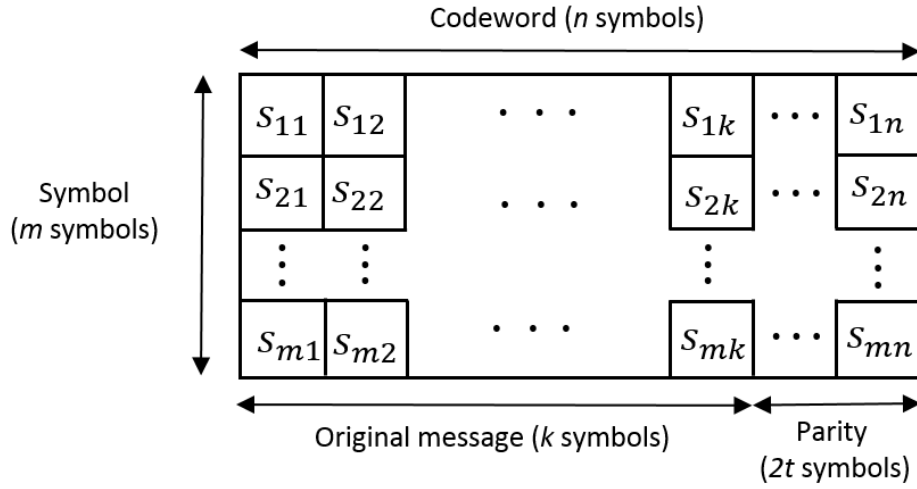


**Figure 5.4 Reed-Solomon code definitions**

In figure 5.4, the encoder inputs with  $k$  symbols of  $m$  bits each, then adds the parity symbols and outputs the  $n$  symbol codeword. At the decoder, the Reed-Solomon code can correct up to  $t$  symbols which contain errors in the received codeword. The error correction capacity (ECC)  $t$  can be represented with [60]:

$$t = \frac{n - k}{2} \quad (5.8)$$

where  $n$  is the codeword length and  $k$  is the number of transmitted symbols. The encoder and decoder of the Reed-Solomon code is based on Galois (Finite) fields, which carry out the arithmetic operations such as addition, subtraction, multiplication and division.

The received codeword  $R(x)$  can be represented with [60]:

$$R(x) = T(x) + E(x) \quad (5.9)$$

where  $E(x)$  is an error polynomial can be represented with [60]:

$$E(x) = E_{n-1}x^{n-1} + \dots + E_1x + E_0 \quad (5.10)$$

Each of the coefficients is an  $m$ -bit value, represented by an element of  $\text{GF}(2^m)$ . If more than  $t$  of the  $E$  values are non-zero, then the error number exceeds the correction capacity and those errors cannot be corrected.

Similarly with CRC encoder, remainders can be calculated by dividing a generator polynomial. The syndromes can be calculated by substituting the  $2t$  roots of the generator polynomial into  $R(x)$ .

To find the symbol error location, the Reed-Solomon decoder uses several algorithms such as the Euclidean algorithm and the Chien search algorithm [63]. Euclid's method [59] [60] is used to find the error locator polynomial, and the Chien search algorithm is used to find the roots of this polynomial. To calculate the error values, the Forney algorithm can be used [71]. The process of decoding to use these algorithms is illustrated in figure 5.5.

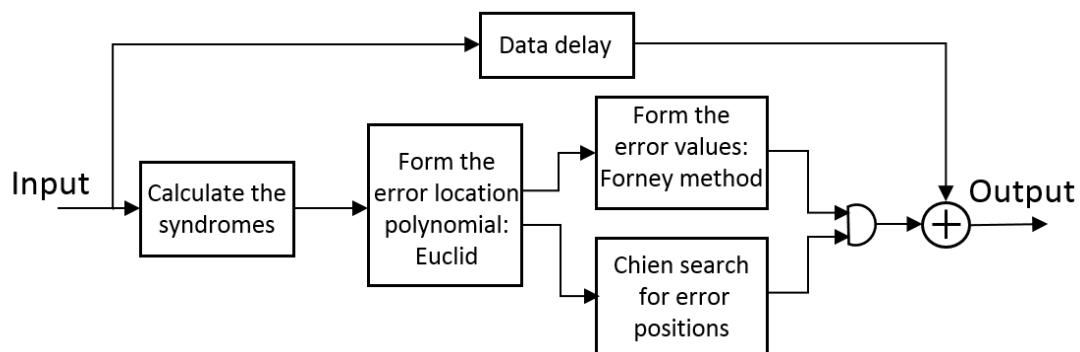


**Figure 5.5 Main processes of a Reed-Solomon decoder**

After applying Reed-Solomon codes to the system, since the error correction capacity might be exceeded and the errors might not be corrected, we still need to apply the CRC code to detect if any errors still exist after the correction approach. Figure 5.6 illustrates the flowchart applied with RSC and CRC codes.

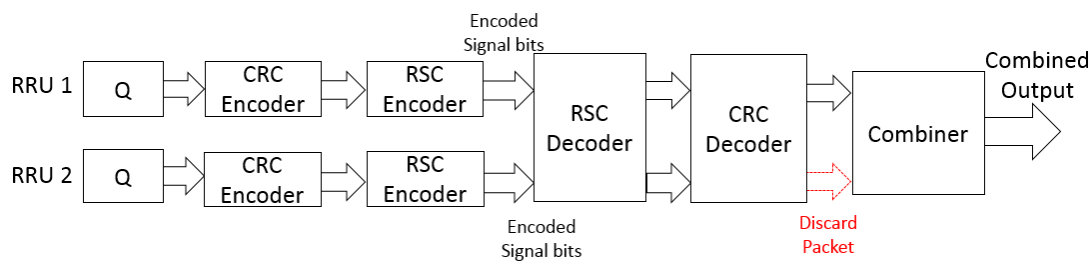


**Figure 5.6 System flowchart applying RSC and CRC codes**

### 5.3. Simulation Results

In this section, we have evaluated the two error control systems in section 5.2 by giving multiple BER levels in fronthaul network: the higher the fronthaul BER, the more errors are generated with transmission. With the first system, we compare the end-to-end BER performance when discarding or forwarding the erroneous packets. With the second system, we explore the performance obtained by giving different ECC (Error Correction Capacity) with RSC code, also with different numbers of symbols to be encoded. In this way, we will test the throughput efficiency in those scenarios. Furthermore, we will evaluate these two systems by improving the antenna diversity at each RRU.

### 5.3.1. Simulation Results with CRC code

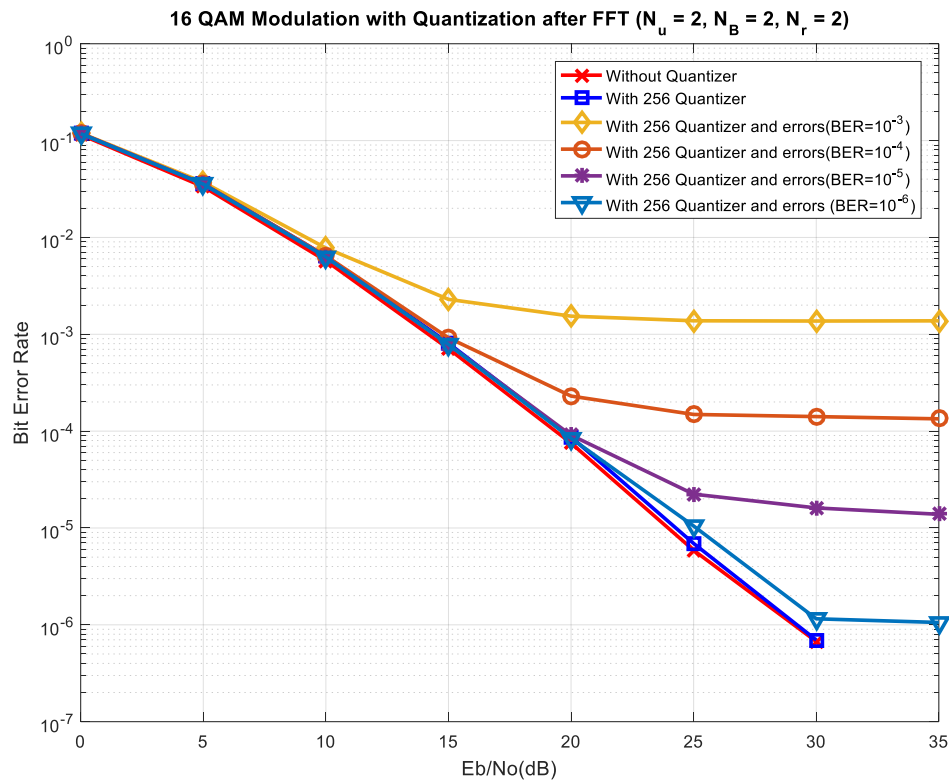


**Figure 5.7 Comparison with different BER level in fronthaul; Without error correction code; Quantize-after-beamformer;  $N_u = 2, N_B = 2, N_r = 2$**

Figure 5.7 shows the end-to-end BER performance with different error rates in the fronthaul, assuming that the system transmits and combines the erroneous packets with the other packets directly with no error control. Obviously, the BER performance degrades as the fronthaul error rate increases. We note that the end-to-end error floor is slightly above the fronthaul BER: the error floor is acceptable (below  $10^{-6}$ ) only when the fronthaul BER is less than  $10^{-6}$ .

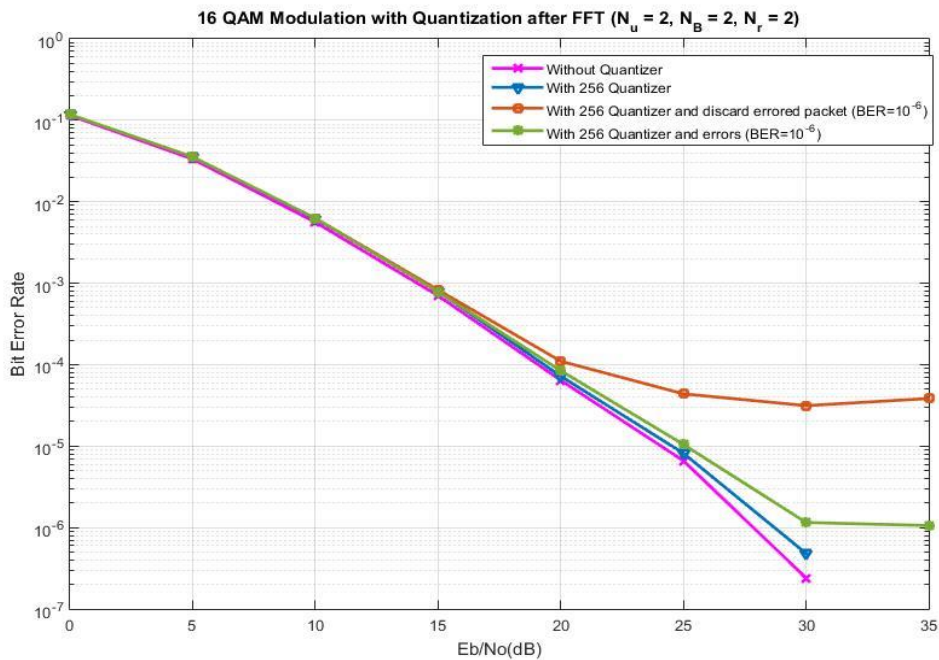


**Figure 5.8 With and without erroneous packets discarded; Quantize-after-beamformer;  $N_u = 2, N_b = 2, N_r = 2$**

Figure 5.8 shows the BER performance with the system discard erroneous packets. It can be observed that this gives significantly worse end-to-end performance than no error control. Discarding a whole erroneous packet means discarding many correct bits along with a few erroneous ones. Furthermore, if the packets from both RRUs contain errors, the entire source data packet will be lost. The green line shows the scenario with fronthaul BER reach to  $10^{-6}$ , and it can be seen that the BER performance is very close to the scenario without any fronthaul errors. Thus we conclude that if the fronthaul BER is better than  $10^{-6}$ , then no error control is required. This also means that no additional latency need be introduced due to fronthaul packetization.

### 5.3.2. Simulation Results with RSC code

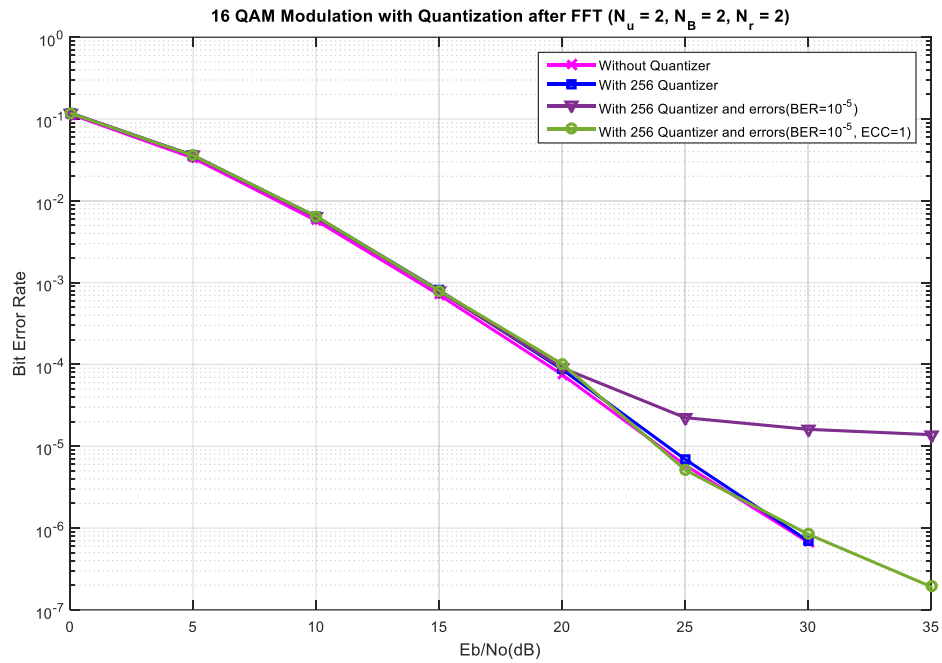


Figure 5.9 With error correction code; Quantize-after-beamformer;  $N_u = 2, N_B = 2,$   
 $N_r = 2$

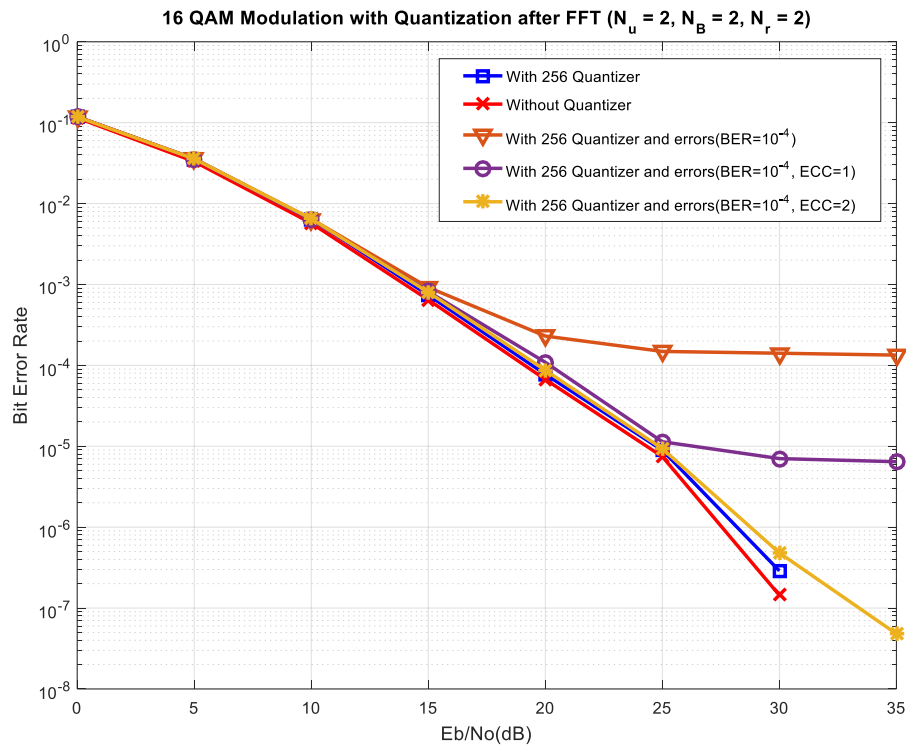
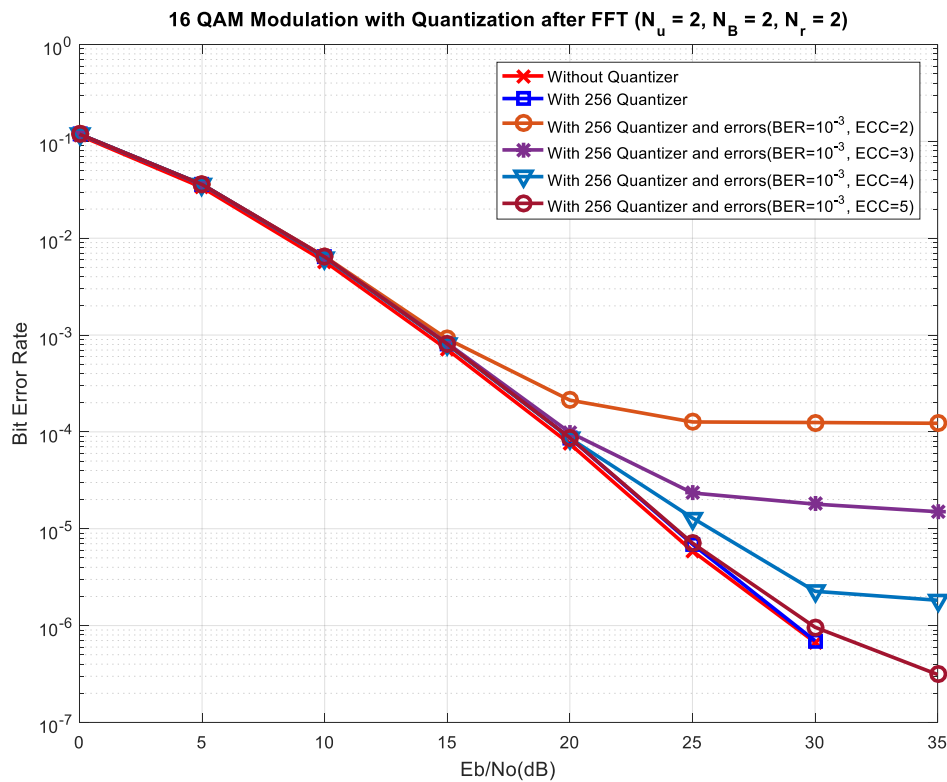


Figure 5.10 With error correction code; Quantize-after-beamformer;  $N_u = 2, N_B = 2,$   
 $N_r = 2$



**Figure 5.11 With error correction code; Quantize-after-beamformer;  $N_u = 2, N_B = 2, N_r = 2$**

Figure 5.9 - Figure 5.11 show the BER performances with error correction codes for different fronthaul error rates. We use Reed-Solomon codes (RSC) here to correct the errors with different error correction capacities (ECC), see equation 5.8. Here we compare the performance with different ECC of the RSC, that is where different numbers of bit errors can be corrected: with fronthaul error rate  $10^{-5}$ , only single bit error correction is required to reach the required end-to-end BER ( $10^{-6}$ ), while error rate  $10^{-4}$  will require ECC of at least 2 and error rate  $10^{-3}$  will require at least 5. Clearly the higher the fronthaul error rate, the greater the ECC is required.

### 5.3.3. Simulation Results with Different Scenarios

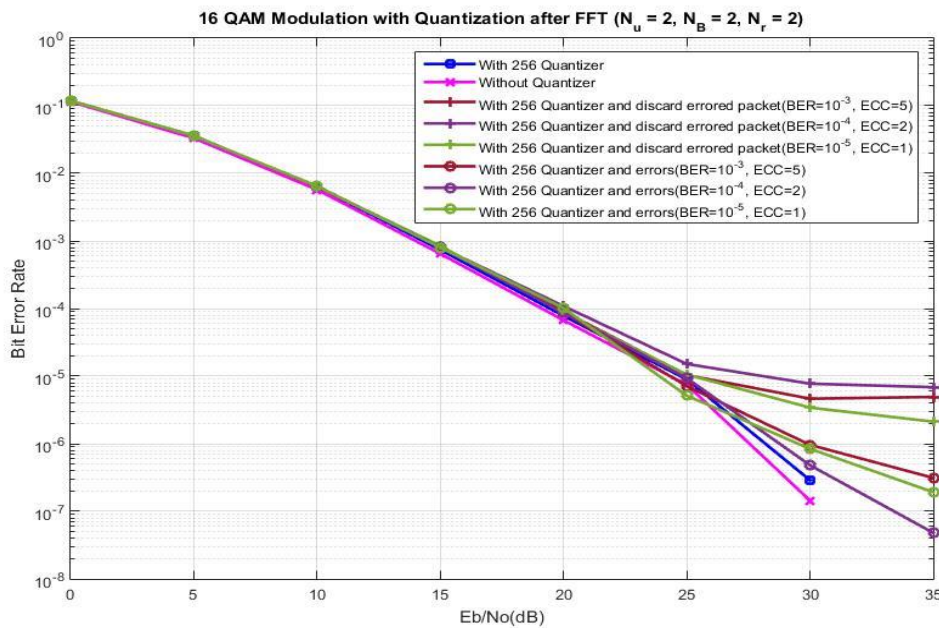


**Figure 5.12 With and without erroneous packets discarded; With error correction code; Quantize-after-beamformer;  $N_u = 2, N_B = 2, N_r = 2$**

Figure 5.12 shows the effect of discarding packets which still contain errors after error correction, due to the limited ECC. It shows again that discarding errored packets results in further degradation of the end-to-end BER performance. It shows also a small variation in the required  $E_b/N_0$  on the access network to achieve end-to-end BER  $10^{-6}$ .

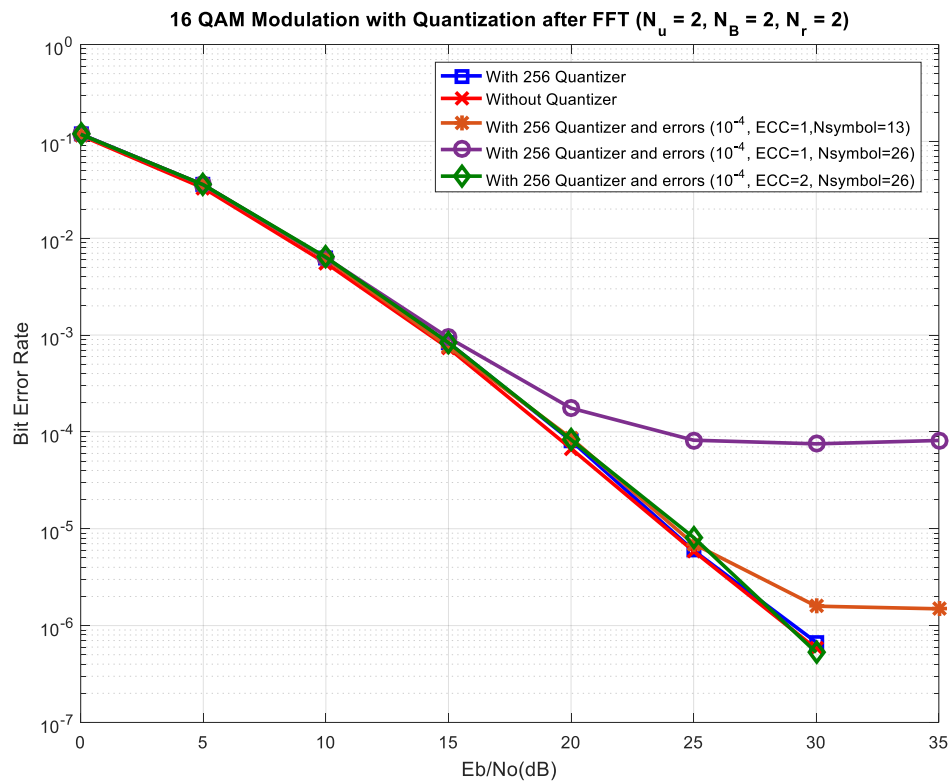


**Figure 5.13 Comparison with different length of transmitted data. With error correction code; Quantize-after-beamformer;  $N_u = 2, N_B = 2, N_r = 2$**

Figure 5.13 shows the end-to-end BER performance as a function of the data length and ECC. For a given ECC, increasing data length degrades performance: hence larger ECC is required for longer data. If the packet contains 13 symbols data, ECC of 1 can meet the required BER. If the data length increases to 26 symbols, it will require ECC of at least 2. Note however that for a given code rate, the longer the data, the greater the ECC can be achieved.

BER	Number of data symbols in each packet	Error correction capacity required	Codeword length required	Throughput efficiency	$E_b/N_0$ (dB)
$10^{-5}$	13	1	15	86.67%	30
$10^{-5}$	26	1	28	92.86%	35
$10^{-5}$	35	2	39	89.74%	30
$10^{-5}$	52	2	56	92.86%	35
$10^{-4}$	13	2	17	76.47%	29
$10^{-4}$	26	2	30	86.67%	29
$10^{-4}$	35	3	41	85.37%	29
$10^{-4}$	52	3	58	89.66%	32
$10^{-3}$	13	4	21	61.90%	31
$10^{-3}$	26	5	36	72.22%	30
$10^{-3}$	35	6	47	74.46%	33
$10^{-3}$	52	7	66	78.79%	32

**Table 5.1 Comparison of throughput efficiency with different data lengths and fronthaul error rate, giving minimum error correction capacity and minimum  $E_b/N_0$  to meet the required BER**

Table 5.1 shows the relationship between fronthaul BER, data length and throughput efficiency, defined as the ratio of quantization bits to the total number of bits transmitted on the fronthaul (including the code parity bits). The effect of error correction coding will be to further increase the fronthaul load by the inverse of the throughput efficiency. Note that in general the required number of code parity bits depends on the ECC, and hence for given ECC the throughput efficiency increases with data length.

For a given fronthaul error rate, the longer the packet length, the higher the throughput efficiency that can be achieved, and so the smaller the increase in required fronthaul capacity. However the packetization will result in additional latency. There may also be a small increase (of a few dB) in the required  $E_b/N_0$  on the access network.

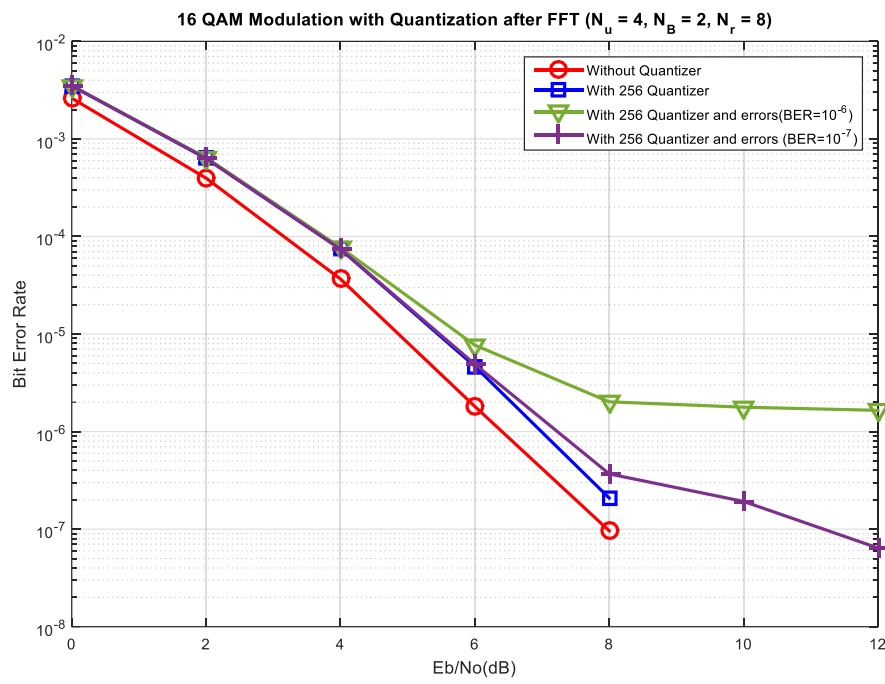
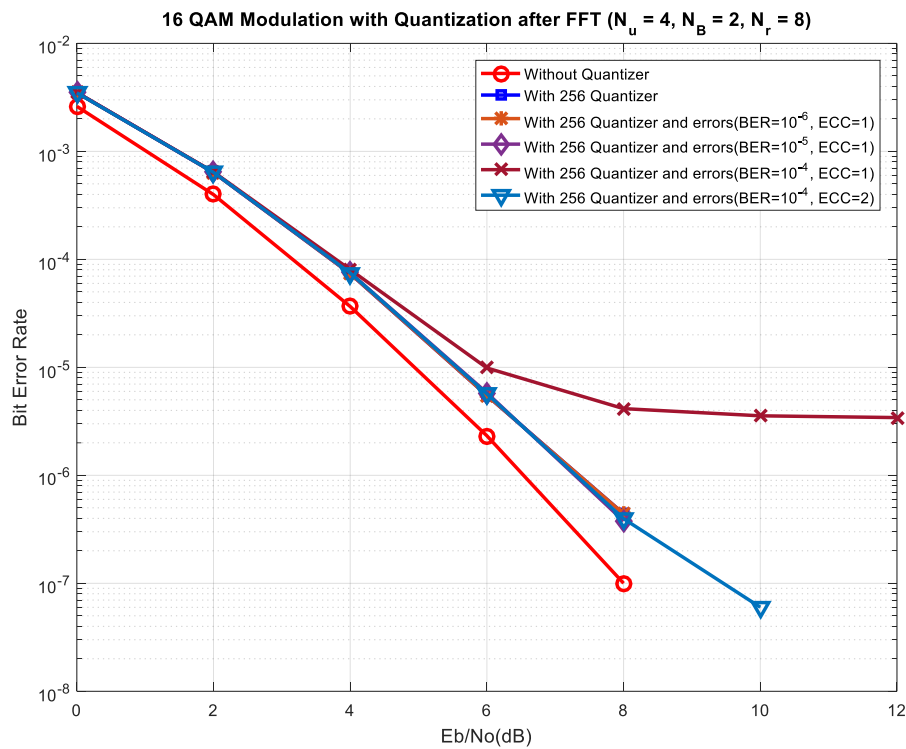


Figure 5.14 Without error correction code; Quantize-after-beamformer;  $N_u = 4$ ,  
 $N_B = 2, N_r = 8$



**Figure 5.15 With error correction code; Quantize-after-beamformer;  $N_u = 4, N_B = 2,$   
 $N_r = 8$**

Figure 5.14 and figure 5.15 give the BER performance for a more realistic scenario with four antennas per RRU, two RRUs and four user terminals. Figure 5.14 shows the effect of different fronthaul error rates, without and with error correction respectively, which gives a similar BER performance as that of the previous scenario shown in 5.7. Figure 5.15 shows the minimum ECC required with different fronthaul error rates. After applying error correction technique to the system, with adequate ECC, the performance can always meet the required end-to-end BER.

#### 5.4. Chapter Summary

Therefore, we can conclude that, if the fronthaul error rate is lower than  $10^{-6}$ , the system can transmit and combine the erroneous packets without any error detection or correction techniques, and can still meet the required end-to-end BER. If the fronthaul

---

error rate is higher than  $10^{-6}$ , then to achieve the required end-to-end BER fronthaul error correction coding is necessary. Erroneous packets, either in the uncoded case or after error correction decoding, should not be discarded since this always degrades performance. Where error correction is necessary, increased data length will increase throughput efficiency (and thus reduce fronthaul load), but will increase latency.

---

## Chapter 6 Compression Techniques

### 6.1. Introduction

The data received at each RRU are sent by the same user terminals. We can consider the received data at each RRU are correlated with each other. With this scenario, a Slepian-Wolf code can be applied to the system which allows the data from each RRU to be compressed and transmitted to the BBU, which increases the spectral efficiency and further reduces the fronthaul load. In this chapter, we will implement a Slepian-Wolf code to the RRU and BBU, and test the transmission rate of the system.

The Accumulate-Repeat-Accumulate code (ARA) [68] and the Super-Turbo code [66] are two methods to implement Slepian-Wolf code, that use different methods to reduce the transmit rate: the ARA code uses CNE (see section 6.3.1) to reduce the transmit rate and the Super-Turbo code uses puncturing to reduce its transmit rate. According to [66, 68], Super-Turbo has greater complexity and very close compression rate with ARA code, we decide to use ARA code to implement the Slepian-Wolf code[87].

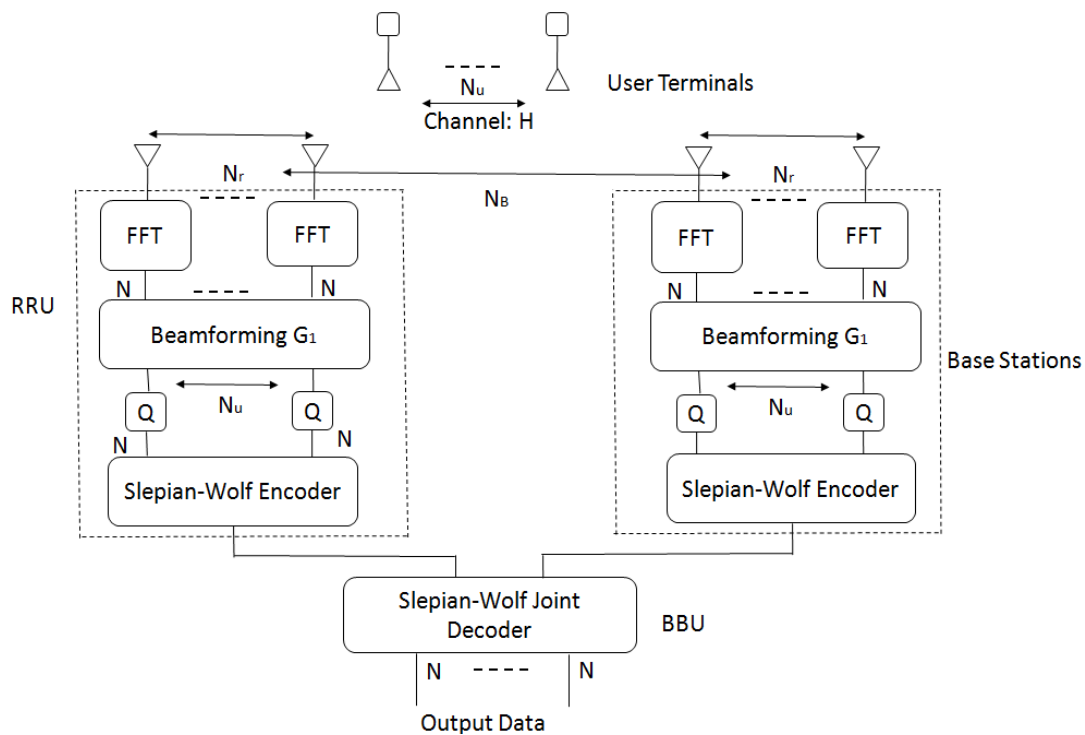


**Figure 6.1 System structure with Slepian-Wolf code applied**

In figure 6.1, at RRU, with each base station, the quantized signals are compressed by the Slepian-Wolf encoder. Then the signals from stations are transmitted simultaneously to the BBU. At the BBU, the compressed data are detected and decompressed by the Slepian-Wolf decoder.

For the following design work, we consider only a 2x2 MIMO system model between the user terminals and RRUs. Thus we have two users and two RRUs. The channel we assume is independent Rayleigh fading, with perfect CSI at receiver.

## 6.2. Slepian-Wolf Overall Structure

The Slepian-Wolf code generally includes following structure: (details are introduced in [48, 66, 67, 68, 69]):

- The sources from different base stations are randomly interleaved before being independently encoded (see Figure 6.2).

- At BBU, a joint decoder performs iterative decoding with soft-in and soft-out decoders [70] (See Figure 6.3).
- Each source has a separate iterative decoder, then exchange the extrinsic information between the decoders in each source by using the Log likelihood Ratio (LLR) updating function. (See equation 6.1 and 6.2).

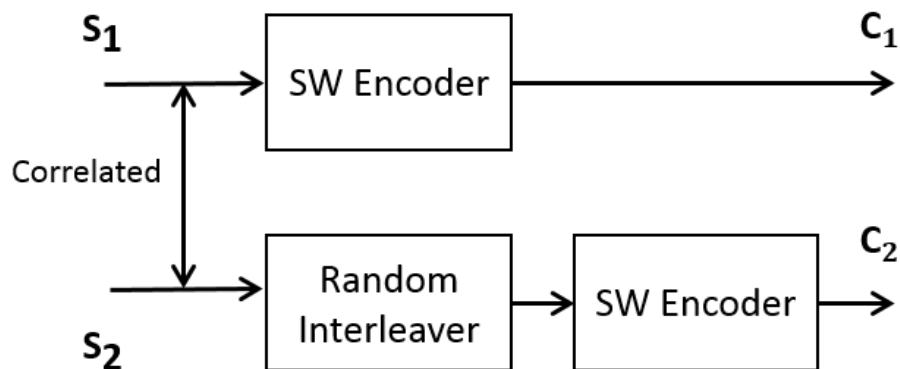


Figure 6.2 Slepian-Wolf encoder implementation

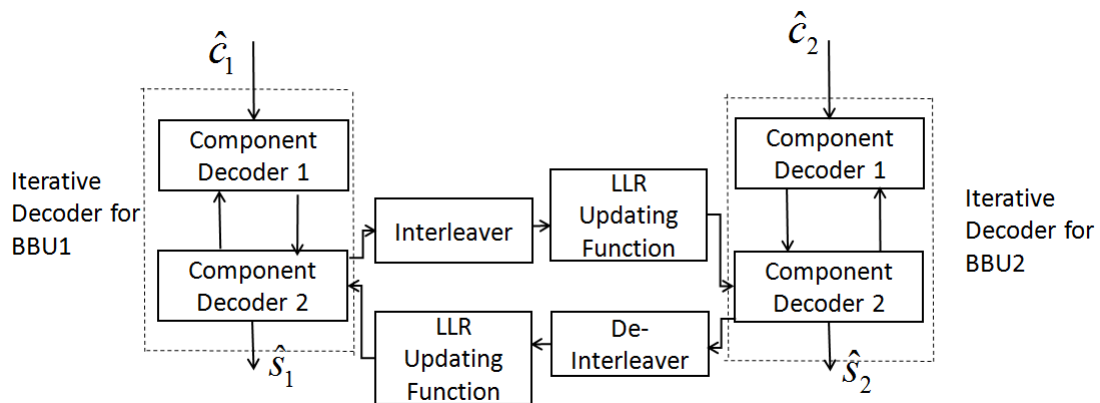


Figure 6.3 Slepian-Wolf decoder implementation;  $\hat{C}_1$  and  $\hat{C}_2$  are the coded messages  $C_1$  and  $C_2$  in Figure 6.2.  $\hat{S}_1$  and  $\hat{S}_2$  are the estimated output of data  $S_1$  and  $S_2$  in Figure 6.2

In figure 6.3, the LLR updating function is one of the most crucial steps in Slepian-Wolf code implementation. When the corresponding extrinsic information from each source are worked by the iterative decoder, the system will input the extrinsic information to the LLR updating function, which will produce the priori information for the other source. The LLR updating algorithms are defined with [68, 87]

$$Pr(\hat{b} = 0) = (1 - p)Pr(b = 0) + pPr(b = 1) \quad (6.1)$$

$$Pr(\hat{b} = 1) = (1 - p)Pr(b = 1) + pPr(b = 0) \quad (6.2)$$

where

$$p = \frac{\text{Number of bits that are different between detected messages}}{\text{Length of the overall message}} \quad (6.3)$$

is the bit difference probability between two base stations,  $Pr(b=0)$  and  $Pr(b=1)$  are the probability of a particular bit being 0 and 1 in one source,  $Pr(\hat{b} = 0)$  and  $Pr(\hat{b} = 1)$  are the probability of the corresponding bit being 0 and 1 in the other source [87].

For the iterative soft-in/soft-out decoders, the LLR updating function can be rewritten as [68]

$$L^{\hat{b}} = \ln \frac{(1 - p)\exp(L^b) + p}{(1 - p) + p\exp(L^b)} \quad (6.4)$$

where  $L^{\hat{b}}$  and  $L^b$  are bit log likelihood ratio from each base station.

The probability of difference  $p$  in equation (6.4) can be estimated by the following algorithm [68]:

$$p = \frac{1}{N} \sum_{n=1}^N \frac{\exp(L^b) + \exp(\hat{L}^b)}{(1 + \exp(L^b))(1 + \exp(\hat{L}^b))} \quad (6.5)$$

where  $N$  is the number of bits in one frame.

### 6.3. Accumulate-Repeat-Accumulate Code

The Accumulate-Repeat-Accumulate (ARA) code is built base on the Repeat-Accumulate (RA) code [69]. The ARA code contains two part codes: outer code and inner code, the outer code is structured with the variable node encoder (VNE) and the doped accumulator and inner code is structured with the check node encoder (CNE). Finally, the outer code and the inner code are connected by an interleaver [87]. The ARA encoder and decoder structures are shown in Figure 6.4 and Figure 6.6.

#### 6.3.1. Accumulate-Repeat-Accumulate Encoder

The encoder of the ARA code consists three components: doped accumulator, variable node encoder (VNE) and check node encoder (CNE).

The accumulator is a memory one recursive convolution encoder [72], that by using doping technique to improve the decoding convergence in the iterative decoding procedure. The output of a doped accumulator consists of the original information bit from  $S$  and coded bits from  $C$ : if doping period is  $P$  (positive integer), the output is  $S$  with every  $P_{th}$  bit replaced by the corresponding bit in  $C$ . ARA encoder has two doped accumulators: outer accumulator and inner accumulator. The outer accumulator is attached to the source and only be activated when the correlation of two sources is low. The inner accumulator is attached to the antenna and only be activated when SNR is low [48, 87]. The structure of the doped accumulator is shown in Figure 6.5.

The VNE is a repetition code, which repeats the input bits for multiple times and then outputs them. The repeat times of the input bits is named as the degree. If a different

portion of the input bits are repeated in different repetition numbers, this kind of VNE is called an irregular VNE [87].

The CNE is a parity check code. It takes the input bits and output the results by performing modulo 2 addition on them. The number of bits that participate in the modulo 2 addition is called the degree. Similar with VNE, if a different portion of the input bits have different degrees, then this kind of CNE is referred to as an irregular CNE [87].

The interleaver used in figure 6.4 is a random interleaver defined with  $\pi$ ,  $\pi_1$  and  $\pi_2$ ,  $\pi_1$  and  $\pi_2$  takes the output of the VNE and randomly shuffles the input bits, then outputs the results to the CNE [87].

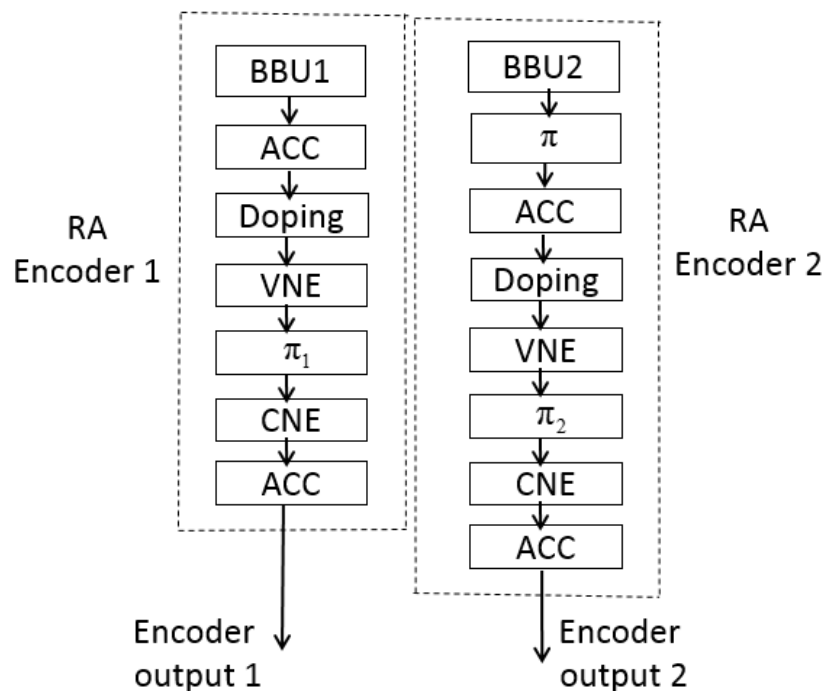


**Figure 6.4** Accumulate-Repeat-Accumulate encoder,  $\pi$ ,  $\pi_1$  and  $\pi_2$  are interleavers

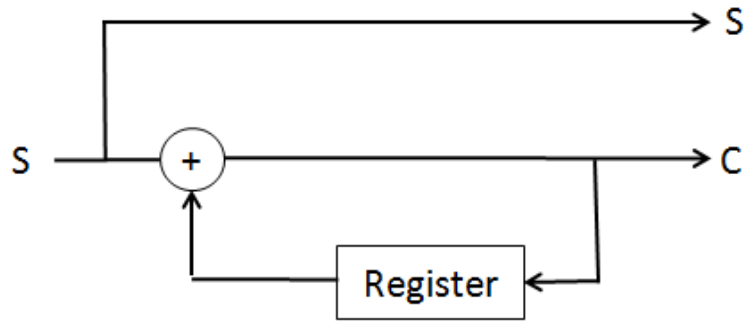


**Figure 6.5 Doped accumulator**

### 6.3.2. Accumulate-Repeat-Accumulate Decoder

The decoder of the ARA code consists four components: de-accumulator, variable node decoder (VND), check node decoder (CND) and LLR updating function. Each of these component decoders takes the LLR as input and output.

The de-accumulator is the decoder for the accumulator. Here the de-accumulator can use the simplified version of the Bahl-Cocke-Jelinek-Raviv (BCJR) algorithm [74].

A degree  $n$  variable node decoder takes  $n+1$  inputs, which consists one information bit and  $n$  coded bits. The corresponding output value  $L_{i,out}$  is to add the rest of the input values  $L_{j,in}$  together [87].

$$L_{i,out} = \sum_{j \neq i} L_{j,in} \quad (6.6)$$

A degree  $n$  check node decoder takes  $n+1$  inputs which consists one coded bit and  $n$  information bits. The corresponding output  $L_{i,out}$  applies the "box plus" function [76] to the rest of the input values  $L_{j,in}$

$$L_{i,out} = \sum_{j \neq i} \boxplus(L_{j,in}) \quad (6.7)$$

The rules for "box plus" are defined as [76, 87]:

$$(L_u) \boxplus (\infty) = L_u$$

$$(L_u) \boxplus (-\infty) = -L_u$$

$$(L_u) \boxplus (0) = 0$$

$$\sum_{j=1}^J \boxplus L(u_j) = \log \frac{1 + \prod_{j=1}^J \tanh(L(u_j)/2)}{1 - \prod_{j=1}^J \tanh(L(u_j)/2)} \quad (6.8)$$

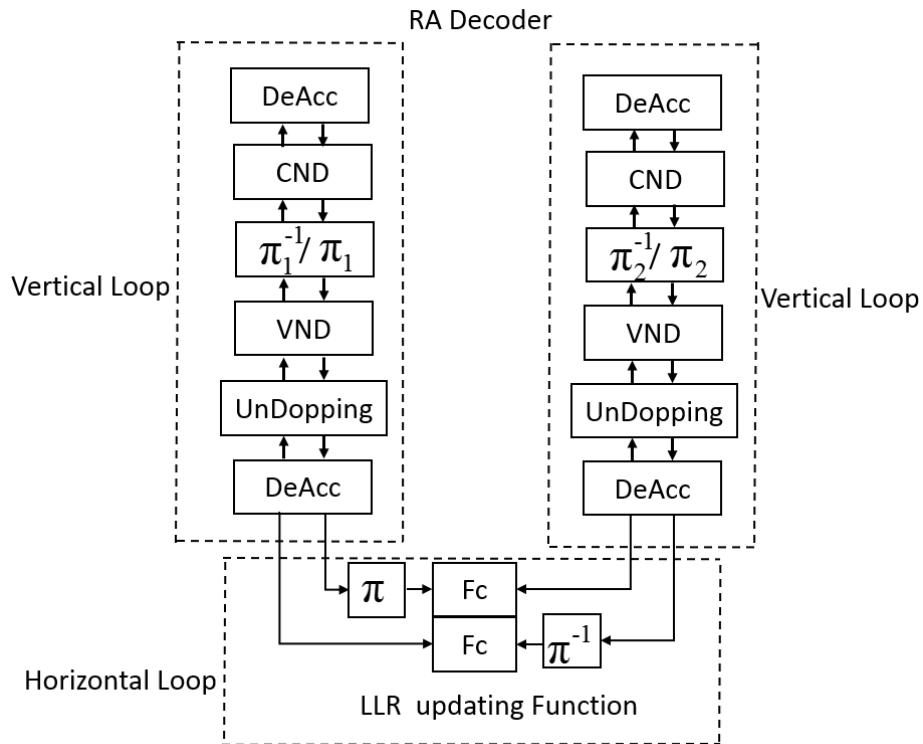


**Figure 6.6 Accumulate-Repeat-Accumulate decoder,  $\pi$ ,  $\pi_1$  and  $\pi_2$  are interleavers, and  $\pi^{-1}$ ,  $\pi_1^{-1}$  and  $\pi_2^{-1}$  are de-interleavers**

In figure 6.6, the vertical loop represents the separate decoding at each BBU, whereas the horizontal loop represents the exchange of extrinsic information between two individual decoders.

In the ARA decoding process, each individual vertical loop takes place several times, and then a horizontal loop takes place once between two vertical loop outputs. This process is regarded as one joint decoding loop. In order to decode a frame successfully, the system normally needs several joint decoding loops, and the number of loops depends on the compression rate and the SNR [87].

#### 6.4. Simulation Results and Analysis

To analyse the performance of Slepian-Wolf code in the system, we compute the total transmission rate  $T_r$  as:

$$T_r = \frac{N_{c1} + N_{c2}}{N_{s1} + N_{s2}} \quad (6.9)$$

and the compression rate  $C_r$  as:

$$C_r = \frac{N_{s1} + N_{s2}}{N_{c1} + N_{c2}} \quad (6.10)$$

where  $N_{c1}$  and  $N_{c2}$  are the size of compressed bits for each source.  $N_{s1}$  and  $N_{s2}$  are the size of uncompressed data bits for each source.

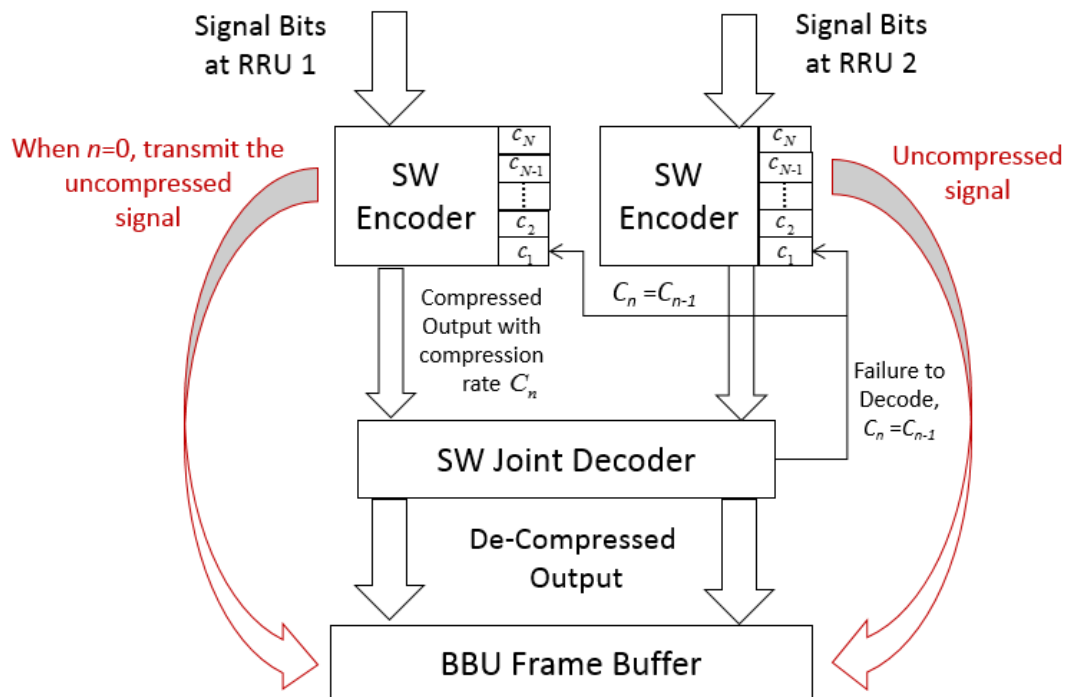


**Figure 6.7 Program design flowchart**

Figure 6.7 illustrates the flowchart of program design. At the Slepian-Wolf encoder of each source, the system has set compression parameters with  $N$  level compression ratios from  $C_1$  to  $C_N$ , and outputs the compressed data with compression ratio  $C_n$ ,  $n \in \{0, 1, 2, 3, \dots, N\}$ .  $C_1$  has the least compression ratio and  $C_N$  has the greatest compression ratio. Each time signal bits are input to the encoder. It starts to compress the signal bits with the largest compression ratio  $C_N$ . Then the compressed signal is sent to the joint Slepian-Wolf decoder. The joint decoder de-compresses the received signals and detects the bit errors. If the number of detected errors is over the threshold limit (here we use 100 bit errors as the threshold), the system defines this compression ratio  $C_N$  as too high and the compression process as failed. Next the system sends feedback to the encoders to activate a lower level compression ratio  $C_{N-1}$ . The system will repeat this loop until the number of detected errors at the decoder is below the threshold, and finally the joint decoder stores the de-compressed signal bits at a frame

buffer. However, the system may still fail the compression with the least compression ratio, especially with very low correlation between two sources. For this case, each RRU will transmit the uncompressed signal frame to the BBU, and we define the probability of these uncompressed frames occurring as "compression failure rate".

To simulate the Slepian-Wolf code in our system, BPSK modulation and an 8 level (3 bit) quantizer are used in the following simulations. Each user terminal sends 10000 binary bits. After the quantizer at each RRU, there are 60000 bits before compression.

The data transmission rate from RRUs to BBU is shown in Figure 6.8. The red line represents the actual data transmission rate and the blue line represents the joint entropy with two sources. As SNR increases the transmitted data from the two sources become highly correlated with each other, which improve the mutual information and lowers the joint entropy [See equation 2.21]. The highest compression rate reaches 1.4 at 40dB. Therefore, as the formation in common between the two sources increases, the compression rate of Slepian-Wolf code increases. Figure 6.9 shows the compression failure rate against SNR. When the SNR is less than 15dB, the data from the two sources has low correlation, and thus the system is unable to compress and de-compress the data.

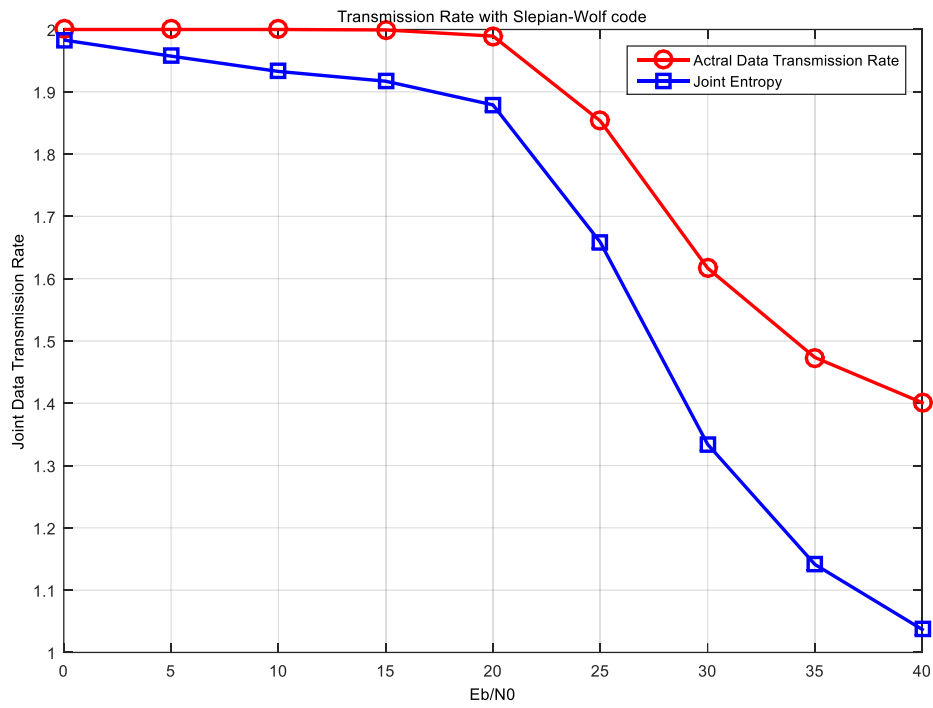


Figure 6.8 Compression rate with Slepian-Wolf code

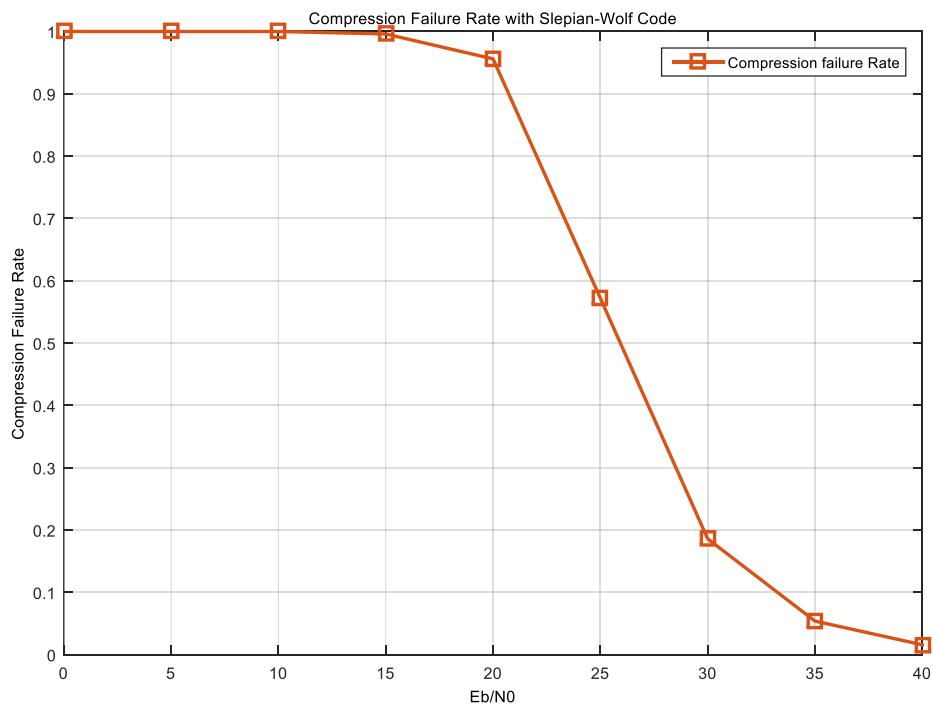
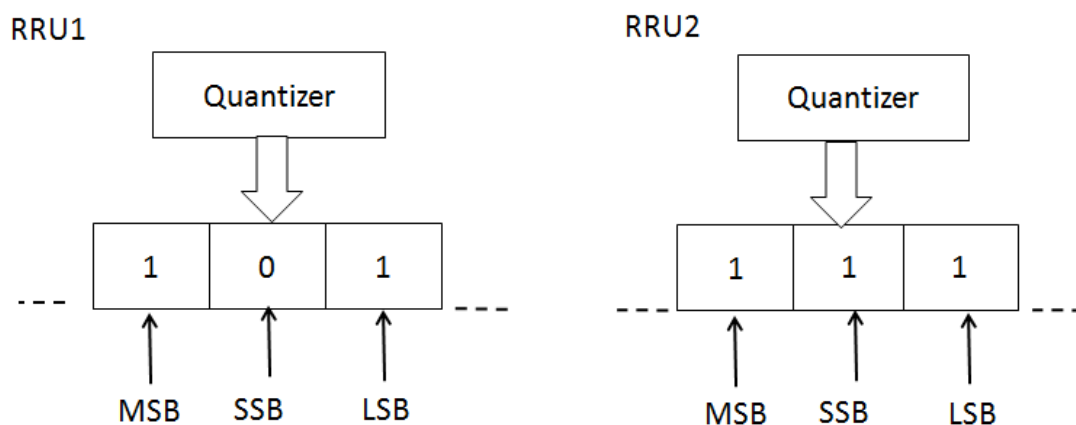


Figure 6.9 Compression failure rate with Slepian-Wolf code

## 6.5. System Development

In the previous simulations, the system tried to compress the binary data from two sources simultaneously, and the binary bits in each source are compressed with equal compression ratio. The compression ratio is defined by the parameters at the VNE and CNE. For example, if we define the parameter of the VNE as  $(30\%(2), 70\%(3))$ , this means that 30% of the bits at VNE in each source will do the repetition process twice, and 70% of binary bits will do the repetition process three times. The ratio and repetition numbers produce different numbers of output bits. In the system design, the VNE process increases the data size, while the CNE reduces the data size and compresses the signal. Once the VNE parameters are fixed, the system will try to compress the two correlated sources by adjusting the CNE parameters.

Assuming the system uses an 8 level quantizer, each quantized signal can be represented with 3 bits, and all of them are compressed with equal compression ratio. However, these three bits have different significance. We say the first bit is the most significant bit (MSB), the second bit is the second significant bit (SSB) and the third bit is the least significant bit (LSB). The structure is shown in Figure 6.10.



**Figure 6.10** Each symbol is quantized with 8 level quantizer and output 3 binary bits: MSB, SSB and LSB

MSB, SSB, and LSB can be compressed with different compression ratio by giving different parameters with VNE. In system design and simulations, they can be separately compressed and de-compressed.

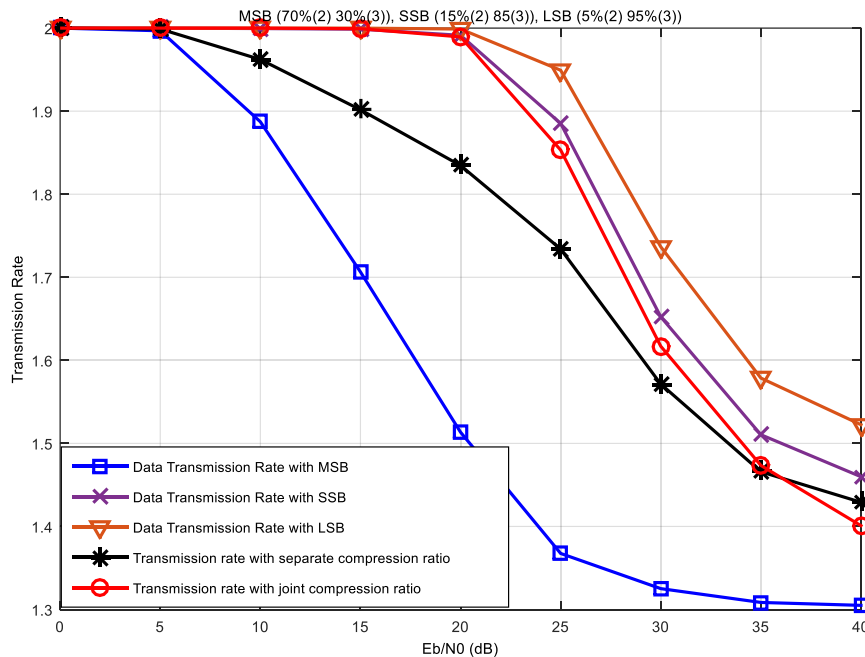


**Figure 6.11 Compression rate comparison between joint transmission ratio and separate transmission ratios. The joint transmission uses the VNE parameters (30%(2) 70%(3)), and the separate compression uses the VNE parameters with MSB(70%(2) 30%(3)), SSB(15%(2) 85%(3)) and LSB (5%(2) 95%(3)).**

In Figure 6.11, the black line represents the overall transmission ratio with different compression ratios for MSB, SSB and LSB, and the red line represents the transmission ratio with joint compression. At low SNR, the separate transmission ratio scheme improves the transmission rate significantly and efficiently, and the two correlated sources are compressed successfully from 5dB. The blue line represents the compression rate with MSB, due to the larger significance of the MSB, the common information in the MSBs from two sources has greatly increased, which results in greater compression of the two sources.

## 6.6. Chapter Summary

Based on the simulation results from this chapter, with the joint compression scheme, the compression ratio can achieve up to 1.4 at 40dB which means that 30% of the data bits are compressed from the two correlated sources. The deficiency of this scheme is that the system is unable to compress the sources at low SNR properly. With the separate compression ratio scheme, even if the SSB and LSB parts cannot be compressed by the system at low SNR, due to the greater robustness of the MSB part, which causes high correlation between the two MSB parts from each source, the binary data from two sources can still be partly compressed at low SNR.

For the future work of this chapter, more VNE parameters will be tested, and the compression bound of this compression scheme will be explored. As part of the potential development of the separate compression scheme, the system can consider to discard the LSB frames even the second least significant bit (SLSB) frames, especially with higher level of quantization, because the LSB frames have very little impact on the constellation of quantized symbols.

## Chapter 7 Conclusions and Further Work

### 7.1 Summary of the Achievements

In this section we review the previous work in this project and summarise the contributions made for C-RAN system design in fronthaul network.

- In chapter 3, we have set up the basic C-RAN system and analysed the effect of quantization with different modulation schemes and detection techniques. We concluded that quantization of the received symbol will cause an error floor in the BER performance to the recovered data bits. Then we have evaluated different detection techniques that are located at the BBU processing centre. Multiple levels of quantization at each RRUs are tested with different detection approaches. Finally ZF is chosen to be applied in the following system design because of its low complexity and acceptable end-to-end BER performance. Moreover, we determine that with the ZF detection approach, the system needs to transmit at least 10 more extra bits to low the error floor and achieve the expected end-to-end BER performance. A higher level of modulation scheme can improve the transmission efficiency but it still suffers a high fronthaul load.
- In chapter 4, we have developed and proposed two C-RAN system by changing the positions of quantization in RRUs: quantize before FFT and quantize after beamformer. The system with quantize after beamfomer finally removes the error floor occurs in the system which occurs with quantize before FFT (as in chapter 3), and the extra bits required with this system have been reduced to 2. The transmission efficiency is significantly improved, especially for low modulation levels.

- In chapter 5, we have explored and evaluated two error control approaches in the fronthaul network. The first approach only detects errors from received frames using a CRC code. The second approach detects and corrects errors using both CRC code and RS code. We have also explored the two approaches and tested the system with erroneous packets being discarded or not discarded. Finally we conclude that if the fronthaul error rate is lower than  $10^{-6}$ , the system can transmit and combine the erroneous packets without any error detection or correction techniques, and can still meet the required end-to-end BER. Erroneous packets, either in the uncoded case or after error correction decoding, it should not be discarded since this always degrades performance.
- In chapter 6, we have designed and applied a compression technique (Slepian-Wolf code) to the C-RAN system. The compression rate for the system has been evaluated. The deficiency of this scheme is that the system is unable to compress the sources at low SNR properly, because of low correlation between the two sources. When  $E_b/N_0$  reaches 40dB, the transmission rate can achieve 1.4 after compression, which reduces the fronthaul load by 30%.

We have proposed a C-RAN system exploring the quantization level and positions, modulation schemes, antenna diversity, error control methods (error detection and correction codes) and compression techniques (Slepian-Wolf), and give solutions to improve the transmission efficiency and reduce the fronthaul load. However, there are still some aspects that can be improved with our design.

## 7.2 Future Work

- For the system model we current set up in chapter 4, we evaluated performance with 2 and 4 antennas at each base station: a larger number of antennas diversity can be applied to the system, and also with more user terminals may be included.
- For the quantization design, we use uniform quantization in our system. A more advance quantizer such as lattice quantizer [91] can be applied to the system.

- For the theoretical analysis, the quantization effect on ZF detection method with complex channel can be developed.
- More advanced beamformer algorithms [83, 84] can be applied to the system with quantize after beamformer.
- For the compression scheme with C-RAN system, more parameters with VNE and CNE should be tested: the combination between the two parameter settings will produce different transmission rate. To maximum the compression rate, Curve-Fitting method can be studied and designed in our system [37].
- As regards compression techniques, a Wyner-Ziv compression approach [88, 89] can be designed and applied to the system. Different from lossless compression in Slepian-Wolf theorem, Wyner-Ziv theorem looked into the lossy compression case. The Wyner-Ziv theorem presents the achievable lower bound for the bit rate at given distortion. It was found that for Gaussian memoryless sources and mean-squared error distortion, the lower bound for the bit rate remains the same no matter whether the side information  $Y$  is available at the encoder or not. The approach of Wyner-Ziv is illustrated in figure 7.1

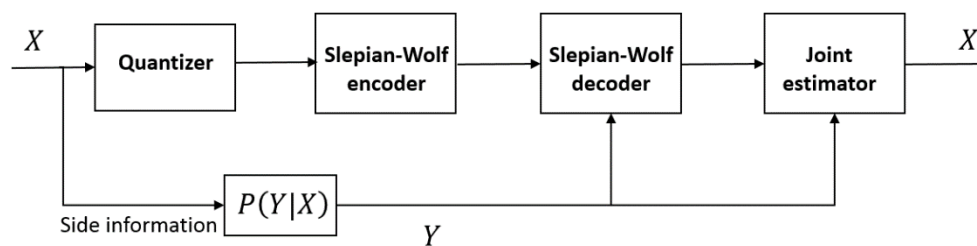


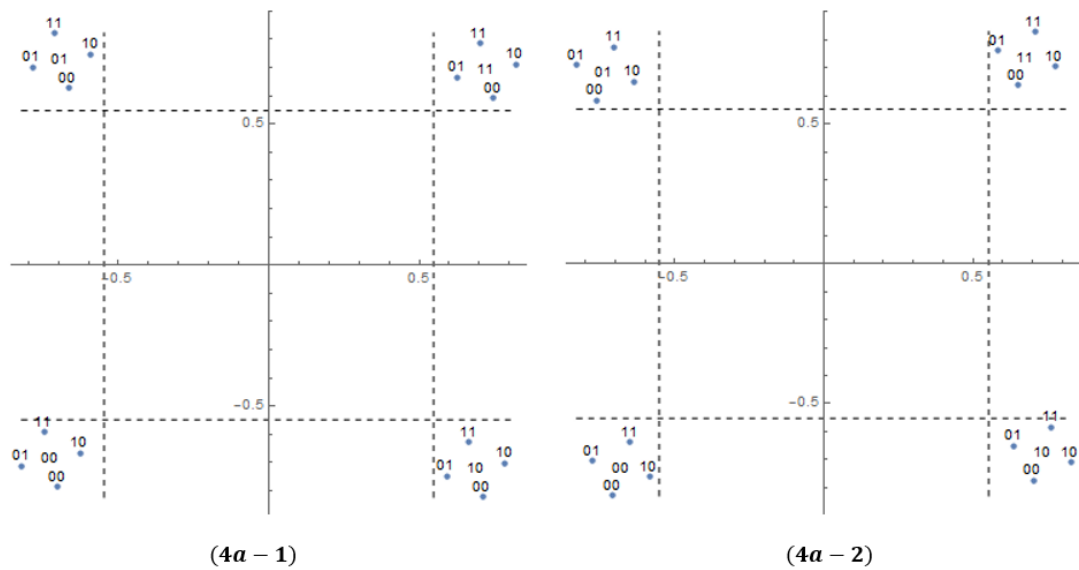
**Figure 7.1 Wyner-Ziv compression approach**

## Appendix

### ► Four Points in outage

There are two cases: four points in region B, and four points in edge region D or region A.

#### Case 4a



Case (4a-1):

1110 is on border; 1111 is not (and note  $\text{Im}_1 < 0$ ). Hence if  $\text{Re}[1100]$  is within the threshold,  $\text{Im}[1101]$  certainly is. Thus we only have one threshold:

$$\text{Im}[1100] > q_{th}$$

$$\frac{1}{\sqrt{2}}(\text{Re}_1 + \text{Im}_1 - \text{Re}_2 - \text{Im}_2) > \frac{1}{\sqrt{2}}(\text{Re}_1 - \text{Im}_1 + \text{Re}_2 + \text{Im}_2) \left(1 - \frac{1}{l-1}\right)$$

$$(l-1)(\text{Re}_1 + \text{Im}_1 - \text{Re}_2 - \text{Im}_2) > (\text{Re}_1 - \text{Im}_1 + \text{Re}_2 + \text{Im}_2)(l-2)$$

$$\text{Re}_1 + (2l-3)(\text{Im}_1 - \text{Re}_2 - \text{Im}_2) > 0$$

Case (4a-2):

1111 is on border; 1110 is not (and note  $\text{Im}_1 > 0$ ). Hence if  $\text{Re}[1101]$  is within the threshold,  $\text{Im}[1100]$  certainly is. Thus we again have only one condition:

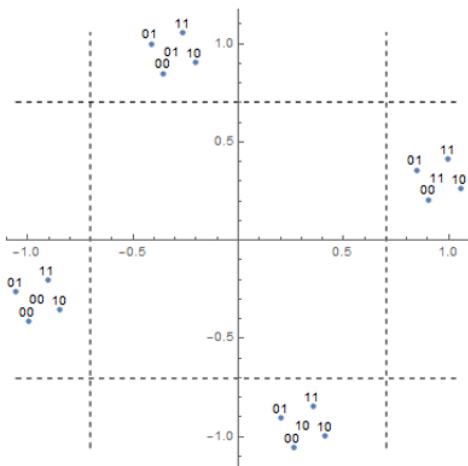
$$\text{Re}[1101] > q_{th}$$

$$\frac{1}{\sqrt{2}}(\text{Re}_1 - \text{Im}_1 - \text{Re}_2 - \text{Im}_2) > \frac{1}{\sqrt{2}}(\text{Re}_1 + \text{Im}_1 + \text{Re}_2 + \text{Im}_2) \left(1 - \frac{1}{l-1}\right)$$

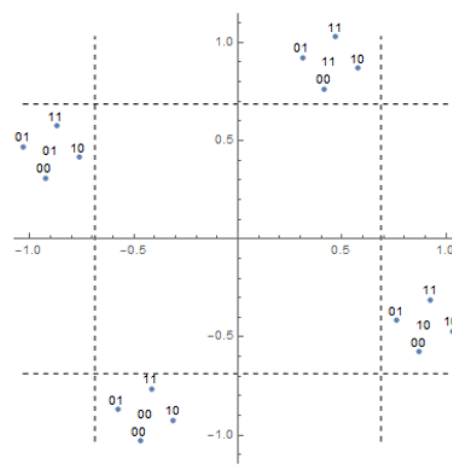
$$(l-1)(\text{Re}_1 - \text{Im}_1 - \text{Re}_2 - \text{Im}_2) > (\text{Re}_1 + \text{Im}_1 + \text{Re}_2 + \text{Im}_2)(l-2)$$

$$\text{Re}_1 + (2l-3)(-\text{Im}_1 - \text{Re}_2 - \text{Im}_2) > 0$$

**Case 4b**



(4b - 1)



(4b - 2)

Case (4b-1):

1110 is on the border, which means that the four points must be in region D. Outage occurs if:

$$\begin{aligned}
& \text{Im}[1111] < q_{th} \ \& \ \text{Im}[1100] > 0 \ \& \ \text{Re}[1101] > q_{th} \\
& \text{Re}_1 + \text{Im}_1 + \text{Re}_2 + \text{Im}_2 < (\text{Re}_1 - \text{Im}_1 + \text{Re}_2 + \text{Im}_2) \left(1 - \frac{1}{l-1}\right) \ \& \\
& \text{Re}_1 + \text{Im}_1 - \text{Re}_2 - \text{Im}_2 > 0 \ \& \\
& \text{Re}_1 - \text{Im}_1 - \text{Re}_2 - \text{Im}_2 > (\text{Re}_1 - \text{Im}_1 + \text{Re}_2 + \text{Im}_2) \left(1 - \frac{1}{l-1}\right); \\
& (l-1)(\text{Re}_1 + \text{Im}_1 + \text{Re}_2 + \text{Im}_2) < (\text{Re}_1 - \text{Im}_1 + \text{Re}_2 + \text{Im}_2)(l-2) \ \& \\
& \text{Re}_1 + \text{Im}_1 - \text{Re}_2 - \text{Im}_2 > 0 \ \& \\
& (l-1)(\text{Re}_1 - \text{Im}_1 - \text{Re}_2 - \text{Im}_2) > (\text{Re}_1 - \text{Im}_1 + \text{Re}_2 + \text{Im}_2)(l-2); \\
& \text{Re}_1 + \text{Re}_2 + \text{Im}_2 + (2l-3)\text{Im}_1 < 0 \ \& \\
& \text{Re}_1 + \text{Im}_1 - \text{Re}_2 - \text{Im}_2 > 0 \ \& \\
& \text{Re}_1 - \text{Im}_1 - (2l-3)(\text{Re}_2 + \text{Im}_2) > 0
\end{aligned}$$

Case (4b-2):

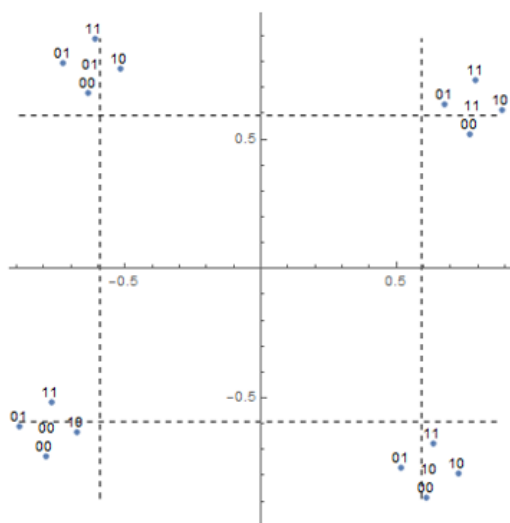
1111 is on the border, which means that the four points must be in region A. Outage occurs if:

$$\begin{aligned}
& \text{Re}[1110] < q_{th} \ \& \ \text{Re}[1101] > 0 \ \& \ \text{Im}[1100] > q_{th} \\
& \text{Re}_1 - \text{Im}_1 + \text{Re}_2 + \text{Im}_2 < (\text{Re}_1 + \text{Im}_1 + \text{Re}_2 + \text{Im}_2) \left(1 - \frac{1}{l-1}\right) \ \& \\
& \text{Re}_1 - \text{Im}_1 - \text{Re}_2 - \text{Im}_2 > 0 \ \& \\
& \text{Re}_1 + \text{Im}_1 - \text{Re}_2 - \text{Im}_2 > (\text{Re}_1 + \text{Im}_1 + \text{Re}_2 + \text{Im}_2) \left(1 - \frac{1}{l-1}\right); \\
& (l-1)(\text{Re}_1 - \text{Im}_1 + \text{Re}_2 + \text{Im}_2) < (\text{Re}_1 + \text{Im}_1 + \text{Re}_2 + \text{Im}_2)(l-2) \ \& \\
& \text{Re}_1 - \text{Im}_1 - \text{Re}_2 - \text{Im}_2 > 0 \ \& \\
& (l-1)(\text{Re}_1 + \text{Im}_1 - \text{Re}_2 - \text{Im}_2) > (\text{Re}_1 + \text{Im}_1 + \text{Re}_2 + \text{Im}_2)(l-2); \\
& \text{Re}_1 + \text{Re}_2 + \text{Im}_2 - (2l-3)\text{Im}_1 < 0 \ \& \\
& \text{Re}_1 - \text{Im}_1 - \text{Re}_2 - \text{Im}_2 > 0 \ \& \\
& \text{Re}_1 + \text{Im}_1 - (2l-3)(\text{Re}_2 + \text{Im}_2) > 0
\end{aligned}$$

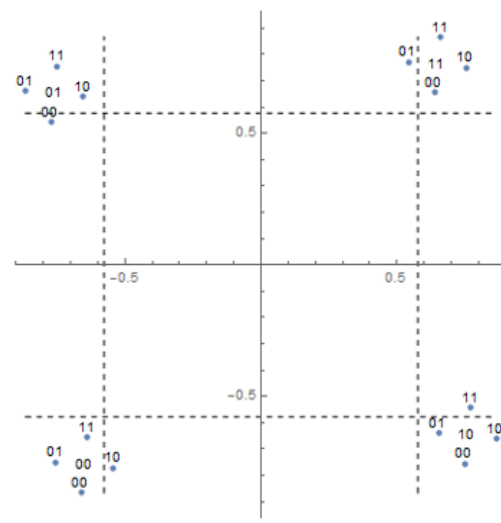
### Three points in outage

For the three points in outage case, there are 7 cases for three possible received symbols in the same region.

#### Case 3a



(3a - 1)



(3a - 2)

Case (3a-1):

1110 is on border; 1111 is not (and note  $\text{Im}_1 < 0$ ), 1100 will lie in region D and 1101, 1110 and 1111 will lie in region B if:

$$\text{Im}[1100] < q_{th} \ \& \ \text{Im}[1101] > q_{th} \ \& \ \text{Re}[1101] > q_{th} \ \& \ \text{Im}[1110] > q_{th}$$

$$\begin{aligned} \frac{1}{\sqrt{2}}(\text{Re}_1 + \text{Im}_1 - \text{Re}_2 - \text{Im}_2) &< \frac{1}{\sqrt{2}}(\text{Re}_1 - \text{Im}_1 + \text{Re}_2 + \text{Im}_2) \left(1 - \frac{1}{l-1}\right) \ \& \\ \frac{1}{\sqrt{2}}(\text{Re}_1 + \text{Im}_1 + \text{Re}_2 - \text{Im}_2) &> \frac{1}{\sqrt{2}}(\text{Re}_1 - \text{Im}_1 + \text{Re}_2 + \text{Im}_2) \left(1 - \frac{1}{l-1}\right) \ \& \\ \frac{1}{\sqrt{2}}(\text{Re}_1 - \text{Im}_1 - \text{Re}_2 - \text{Im}_2) &> \frac{1}{\sqrt{2}}(\text{Re}_1 - \text{Im}_1 + \text{Re}_2 + \text{Im}_2) \left(1 - \frac{1}{l-1}\right) \ \& \\ \frac{1}{\sqrt{2}}(\text{Re}_1 + \text{Im}_1 - \text{Re}_2 + \text{Im}_2) &> \frac{1}{\sqrt{2}}(\text{Re}_1 - \text{Im}_1 + \text{Re}_2 + \text{Im}_2) \left(1 - \frac{1}{l-1}\right); \end{aligned}$$

$$\begin{aligned} (l-1)(\text{Re}_1 + \text{Im}_1 - \text{Re}_2 - \text{Im}_2) &< (\text{Re}_1 - \text{Im}_1 + \text{Re}_2 + \text{Im}_2)(l-2) \ \& \\ (l-1)(\text{Re}_1 + \text{Im}_1 + \text{Re}_2 - \text{Im}_2) &> (\text{Re}_1 - \text{Im}_1 + \text{Re}_2 + \text{Im}_2)(l-2) \ \& \\ (l-1)(\text{Re}_1 - \text{Im}_1 - \text{Re}_2 - \text{Im}_2) &> (\text{Re}_1 - \text{Im}_1 + \text{Re}_2 + \text{Im}_2)(l-2) \ \& \\ (l-1)(\text{Re}_1 + \text{Im}_1 - \text{Re}_2 + \text{Im}_2) &> (\text{Re}_1 - \text{Im}_1 + \text{Re}_2 + \text{Im}_2)(l-2); \end{aligned}$$

$$\begin{aligned} \text{Re}_1 + (2l-3)(\text{Im}_1 - \text{Re}_2 - \text{Im}_2) &< 0 \ \& \\ \text{Re}_1 + \text{Re}_2 + (2l-3)(\text{Im}_1 - \text{Im}_2) &> 0 \ \& \\ \text{Re}_1 - \text{Im}_1 + (2l-3)(-\text{Re}_2 - \text{Im}_2) &> 0 \ \& \\ \text{Re}_1 + \text{Im}_2 + (2l-3)(\text{Im}_1 - \text{Re}_2) &> 0 \end{aligned}$$

Case (3a-2):

1111 is on border and 1110 is not (and note  $\text{Im}_1 > 0$ ). 1101 will lie in region A and

1111, 1100 and 1110 will lie in region B if:

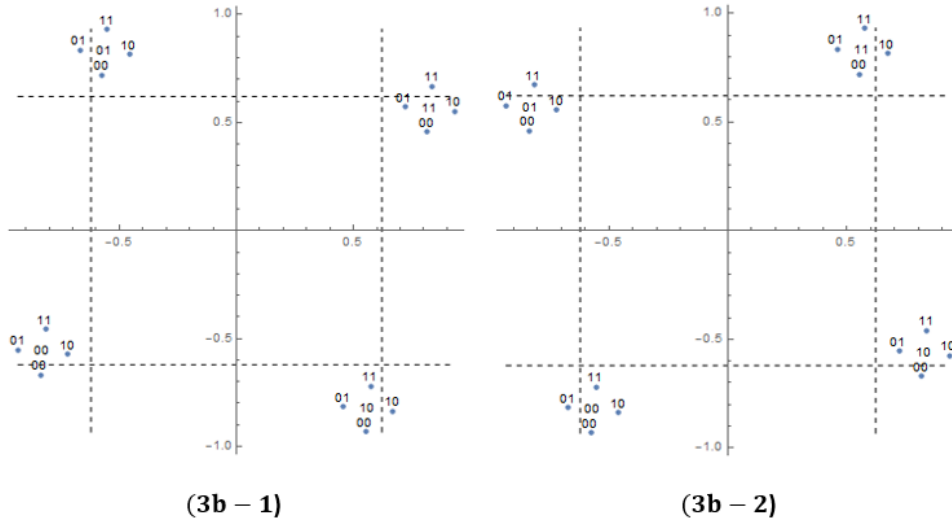
$$\operatorname{Re}[1101] < q_{th} \ \& \ \operatorname{Im}[1100] > q_{th} \ \& \ \operatorname{Re}[1100] > q_{th} \ \& \ \operatorname{Re}[1111] > q_{th}$$

$$\begin{aligned} \frac{1}{\sqrt{2}}(\operatorname{Re}_1 - \operatorname{Im}_1 - \operatorname{Re}_2 - \operatorname{Im}_2) &< \frac{1}{\sqrt{2}}(\operatorname{Re}_1 + \operatorname{Im}_1 + \operatorname{Re}_2 + \operatorname{Im}_2) \left(1 - \frac{1}{l-1}\right) \ \& \\ \frac{1}{\sqrt{2}}(\operatorname{Re}_1 + \operatorname{Im}_1 - \operatorname{Re}_2 - \operatorname{Im}_2) &> \frac{1}{\sqrt{2}}(\operatorname{Re}_1 + \operatorname{Im}_1 + \operatorname{Re}_2 + \operatorname{Im}_2) \left(1 - \frac{1}{l-1}\right) \ \& \\ \frac{1}{\sqrt{2}}(\operatorname{Re}_1 - \operatorname{Im}_1 - \operatorname{Re}_2 + \operatorname{Im}_2) &> \frac{1}{\sqrt{2}}(\operatorname{Re}_1 + \operatorname{Im}_1 + \operatorname{Re}_2 + \operatorname{Im}_2) \left(1 - \frac{1}{l-1}\right) \ \& \\ \frac{1}{\sqrt{2}}(\operatorname{Re}_1 - \operatorname{Im}_1 + \operatorname{Re}_2 - \operatorname{Im}_2) &> \frac{1}{\sqrt{2}}(\operatorname{Re}_1 + \operatorname{Im}_1 + \operatorname{Re}_2 + \operatorname{Im}_2) \left(1 - \frac{1}{l-1}\right); \end{aligned}$$

$$\begin{aligned} (l-1)(\operatorname{Re}_1 - \operatorname{Im}_1 - \operatorname{Re}_2 - \operatorname{Im}_2) &< (\operatorname{Re}_1 + \operatorname{Im}_1 + \operatorname{Re}_2 + \operatorname{Im}_2)(l-2) \ \& \\ (l-1)(\operatorname{Re}_1 + \operatorname{Im}_1 - \operatorname{Re}_2 - \operatorname{Im}_2) &> (\operatorname{Re}_1 + \operatorname{Im}_1 + \operatorname{Re}_2 + \operatorname{Im}_2)(l-2) \ \& \\ (l-1)(\operatorname{Re}_1 - \operatorname{Im}_1 - \operatorname{Re}_2 + \operatorname{Im}_2) &> (\operatorname{Re}_1 + \operatorname{Im}_1 + \operatorname{Re}_2 + \operatorname{Im}_2)(l-2) \ \& \\ (l-1)(\operatorname{Re}_1 - \operatorname{Im}_1 + \operatorname{Re}_2 - \operatorname{Im}_2) &> (\operatorname{Re}_1 + \operatorname{Im}_1 + \operatorname{Re}_2 + \operatorname{Im}_2)(l-2); \end{aligned}$$

$$\begin{aligned} \operatorname{Re}_1 + (2l-3)(-\operatorname{Im}_1 - \operatorname{Re}_2 - \operatorname{Im}_2) &< 0 \ \& \\ \operatorname{Re}_1 + \operatorname{Im}_1 + (2l-3)(-\operatorname{Re}_2 - \operatorname{Im}_2) &> 0 \ \& \\ \operatorname{Re}_1 + \operatorname{Im}_2 + (2l-3)(-\operatorname{Im}_1 - \operatorname{Re}_2) &> 0 \ \& \\ \operatorname{Re}_1 + \operatorname{Re}_2 + (2l-3)(-\operatorname{Im}_1 - \operatorname{Im}_2) &> 0 \end{aligned}$$

### Case 3b



Case (3b-1):

1110 is on the border. 1101, 1110 and 1100 will lie in the region D, and 1111 will lie in region B if:

$$\text{Im}[1111] > q_{th} \ \& \ \text{Im}[1101] < q_{th} \ \& \ \text{Re}[1101] > q_{th} \ \& \ \text{Im}[1110] < q_{th}$$

$$\begin{aligned} \frac{1}{\sqrt{2}}(\text{Re}_1 + \text{Im}_1 + \text{Re}_2 + \text{Im}_2) &> \frac{1}{\sqrt{2}}(\text{Re}_1 - \text{Im}_1 + \text{Re}_2 + \text{Im}_2) \left(1 - \frac{1}{l-1}\right) \ \& \\ \frac{1}{\sqrt{2}}(\text{Re}_1 + \text{Im}_1 + \text{Re}_2 - \text{Im}_2) &< \frac{1}{\sqrt{2}}(\text{Re}_1 - \text{Im}_1 + \text{Re}_2 + \text{Im}_2) \left(1 - \frac{1}{l-1}\right) \ \& \\ \frac{1}{\sqrt{2}}(\text{Re}_1 - \text{Im}_1 - \text{Re}_2 - \text{Im}_2) &> \frac{1}{\sqrt{2}}(\text{Re}_1 - \text{Im}_1 + \text{Re}_2 + \text{Im}_2) \left(1 - \frac{1}{l-1}\right) \ \& \\ \frac{1}{\sqrt{2}}(\text{Re}_1 + \text{Im}_1 - \text{Re}_2 + \text{Im}_2) &< \frac{1}{\sqrt{2}}(\text{Re}_1 - \text{Im}_1 + \text{Re}_2 + \text{Im}_2) \left(1 - \frac{1}{l-1}\right); \end{aligned}$$

$$\begin{aligned} (l-1)(\text{Re}_1 + \text{Im}_1 + \text{Re}_2 + \text{Im}_2) &> (\text{Re}_1 - \text{Im}_1 + \text{Re}_2 + \text{Im}_2)(l-2) \ \& \\ (l-1)(\text{Re}_1 + \text{Im}_1 + \text{Re}_2 - \text{Im}_2) &< (\text{Re}_1 - \text{Im}_1 + \text{Re}_2 + \text{Im}_2)(l-2) \ \& \\ (l-1)(\text{Re}_1 - \text{Im}_1 - \text{Re}_2 - \text{Im}_2) &> (\text{Re}_1 - \text{Im}_1 + \text{Re}_2 + \text{Im}_2)(l-2) \\ (l-1)(\text{Re}_1 + \text{Im}_1 - \text{Re}_2 + \text{Im}_2) &< (\text{Re}_1 - \text{Im}_1 + \text{Re}_2 + \text{Im}_2)(l-2); \end{aligned}$$

$$\begin{aligned} \text{Re}_1 + \text{Re}_2 + \text{Im}_2 + (2l-3)(\text{Im}_1) &> 0 \ \& \\ \text{Re}_1 + \text{Re}_2 + (2l-3)(\text{Im}_1 - \text{Im}_2) &< 0 \ \& \\ \text{Re}_1 - \text{Im}_1 + (2l-3)(-\text{Re}_2 - \text{Im}_2) &> 0 \ \& \\ \text{Re}_1 + \text{Im}_2 + (2l-3)(\text{Im}_1 - \text{Re}_2) &< 0 \end{aligned}$$

Case (3b-2):

1111 is on the border. Points 1111, 1101 and 1100 will lie in region A, 1110 will lie in region B if:

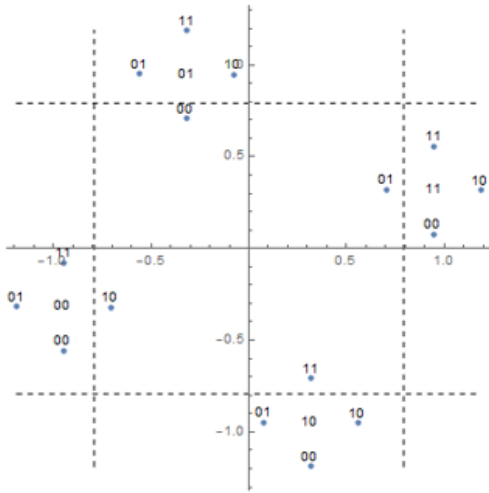
$$\operatorname{Re}[1110] > q_{th} \ \& \ \operatorname{Im}[1100] > q_{th} \ \& \ \operatorname{Re}[1100] < q_{th} \ \& \ \operatorname{Re}[1111] < q_{th}$$

$$\begin{aligned} \frac{1}{\sqrt{2}}(\operatorname{Re}_1 - \operatorname{Im}_1 + \operatorname{Re}_2 + \operatorname{Im}_2) &> \frac{1}{\sqrt{2}}(\operatorname{Re}_1 + \operatorname{Im}_1 + \operatorname{Re}_2 + \operatorname{Im}_2) \left(1 - \frac{1}{l-1}\right) \ \& \\ \frac{1}{\sqrt{2}}(\operatorname{Re}_1 + \operatorname{Im}_1 - \operatorname{Re}_2 - \operatorname{Im}_2) &> \frac{1}{\sqrt{2}}(\operatorname{Re}_1 + \operatorname{Im}_1 + \operatorname{Re}_2 + \operatorname{Im}_2) \left(1 - \frac{1}{l-1}\right) \ \& \\ \frac{1}{\sqrt{2}}(\operatorname{Re}_1 - \operatorname{Im}_1 - \operatorname{Re}_2 + \operatorname{Im}_2) &< \frac{1}{\sqrt{2}}(\operatorname{Re}_1 + \operatorname{Im}_1 + \operatorname{Re}_2 + \operatorname{Im}_2) \left(1 - \frac{1}{l-1}\right) \ \& \\ \frac{1}{\sqrt{2}}(\operatorname{Re}_1 - \operatorname{Im}_1 + \operatorname{Re}_2 - \operatorname{Im}_2) &< \frac{1}{\sqrt{2}}(\operatorname{Re}_1 + \operatorname{Im}_1 + \operatorname{Re}_2 + \operatorname{Im}_2) \left(1 - \frac{1}{l-1}\right); \end{aligned}$$

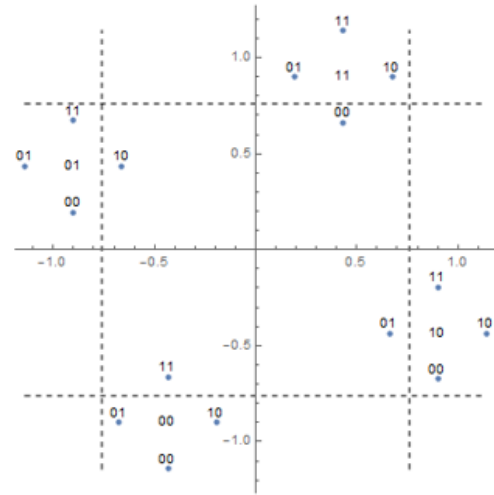
$$\begin{aligned} (l-1)(\operatorname{Re}_1 - \operatorname{Im}_1 + \operatorname{Re}_2 + \operatorname{Im}_2) &> (\operatorname{Re}_1 + \operatorname{Im}_1 + \operatorname{Re}_2 + \operatorname{Im}_2)(l-2) \ \& \\ (l-1)(\operatorname{Re}_1 + \operatorname{Im}_1 - \operatorname{Re}_2 - \operatorname{Im}_2) &> (\operatorname{Re}_1 + \operatorname{Im}_1 + \operatorname{Re}_2 + \operatorname{Im}_2)(l-2) \ \& \\ (l-1)(\operatorname{Re}_1 - \operatorname{Im}_1 - \operatorname{Re}_2 + \operatorname{Im}_2) &< (\operatorname{Re}_1 + \operatorname{Im}_1 + \operatorname{Re}_2 + \operatorname{Im}_2)(l-2) \ \& \\ (l-1)(\operatorname{Re}_1 - \operatorname{Im}_1 + \operatorname{Re}_2 - \operatorname{Im}_2) &< (\operatorname{Re}_1 + \operatorname{Im}_1 + \operatorname{Re}_2 + \operatorname{Im}_2)(l-2); \end{aligned}$$

$$\begin{aligned} \operatorname{Re}_1 + \operatorname{Re}_2 + \operatorname{Im}_2 + (2l-3)(-\operatorname{Im}_1) &> 0 \ \& \\ \operatorname{Re}_1 + \operatorname{Im}_1 + (2l-3)(-\operatorname{Re}_2 - \operatorname{Im}_2) &> 0 \ \& \\ \operatorname{Re}_1 + \operatorname{Im}_2 + (2l-3)(-\operatorname{Im}_1 - \operatorname{Re}_2) &< 0 \ \& \\ \operatorname{Re}_1 + \operatorname{Re}_2 + (2l-3)(-\operatorname{Im}_1 - \operatorname{Im}_2) &< 0 \end{aligned}$$

### Case 3c



(3c - 1)



(3c - 2)

Case (3c-1):

1110 is on the border. Three points (1111, 1110 and 1100) will lie in the region D, 1101 will lie in region C if:

$$\operatorname{Re}[1111] > q_{th} \ \& \ \operatorname{Im}[1111] < q_{th} \ \& \ \operatorname{Re}[1100] > q_{th} \ \& \ \operatorname{Im}[1100] > 0 \ \& \ \operatorname{Re}[1101] < q_{th}$$

$$\operatorname{Re}_1 - \operatorname{Im}_1 + \operatorname{Re}_2 - \operatorname{Im}_2 > (\operatorname{Re}_1 - \operatorname{Im}_1 + \operatorname{Re}_2 + \operatorname{Im}_2) \left(1 - \frac{1}{l-1}\right) \ \&$$

$$\operatorname{Re}_1 + \operatorname{Im}_1 + \operatorname{Re}_2 + \operatorname{Im}_2 < (\operatorname{Re}_1 - \operatorname{Im}_1 + \operatorname{Re}_2 + \operatorname{Im}_2) \left(1 - \frac{1}{l-1}\right) \ \&$$

$$\operatorname{Re}_1 - \operatorname{Im}_1 - \operatorname{Re}_2 + \operatorname{Im}_2 > (\operatorname{Re}_1 - \operatorname{Im}_1 + \operatorname{Re}_2 + \operatorname{Im}_2) \left(1 - \frac{1}{l-1}\right) \ \&$$

$$\operatorname{Re}_1 + \operatorname{Im}_1 - \operatorname{Re}_2 - \operatorname{Im}_2 > 0 \ \&$$

$$\operatorname{Re}_1 - \operatorname{Im}_1 - \operatorname{Re}_2 - \operatorname{Im}_2 < (\operatorname{Re}_1 - \operatorname{Im}_1 + \operatorname{Re}_2 + \operatorname{Im}_2) \left(1 - \frac{1}{l-1}\right);$$

$$(l-1)(\operatorname{Re}_1 - \operatorname{Im}_1 + \operatorname{Re}_2 - \operatorname{Im}_2) > (\operatorname{Re}_1 - \operatorname{Im}_1 + \operatorname{Re}_2 + \operatorname{Im}_2)(l-2) \ \&$$

$$(l-1)(\operatorname{Re}_1 + \operatorname{Im}_1 + \operatorname{Re}_2 + \operatorname{Im}_2) < (\operatorname{Re}_1 - \operatorname{Im}_1 + \operatorname{Re}_2 + \operatorname{Im}_2)(l-2) \ \&$$

$$(l-1)(\operatorname{Re}_1 - \operatorname{Im}_1 - \operatorname{Re}_2 + \operatorname{Im}_2) > (\operatorname{Re}_1 - \operatorname{Im}_1 + \operatorname{Re}_2 + \operatorname{Im}_2)(l-2) \ \&$$

$$\operatorname{Re}_1 + \operatorname{Im}_1 - \operatorname{Re}_2 - \operatorname{Im}_2 > 0 \ \&$$

$$(l-1)(\operatorname{Re}_1 - \operatorname{Im}_1 - \operatorname{Re}_2 - \operatorname{Im}_2) < (\operatorname{Re}_1 - \operatorname{Im}_1 + \operatorname{Re}_2 + \operatorname{Im}_2)(l-2);$$

$$\operatorname{Re}_1 - \operatorname{Im}_1 + \operatorname{Re}_2 - (2l-3)\operatorname{Im}_2 > 0 \ \&$$

$$\operatorname{Re}_1 + \operatorname{Re}_2 + \operatorname{Im}_2 + (2l-3)\operatorname{Im}_1 < 0 \ \&$$

$$\operatorname{Re}_1 - \operatorname{Im}_1 + \operatorname{Im}_2 - (2l-3)\operatorname{Re}_2 > 0 \ \&$$

$$\operatorname{Re}_1 + \operatorname{Im}_1 - \operatorname{Re}_2 - \operatorname{Im}_2 > 0 \ \&$$

$$\operatorname{Re}_1 - \operatorname{Im}_1 - (2l-3)(\operatorname{Re}_2 + \operatorname{Im}_2) < 0$$

Case (3c-2):

1111 is on the border. Three points (1111, 1110 and 1101) will lie in region A, and 1100 will lie in region C if:

$$\operatorname{Re}[1110] < q_{th} \ \& \ \operatorname{Re}[1101] > 0 \ \& \ \operatorname{Im}[1100] < q_{th}$$

$$\operatorname{Re}_1 - \operatorname{Im}_1 + \operatorname{Re}_2 + \operatorname{Im}_2 < (\operatorname{Re}_1 + \operatorname{Im}_1 + \operatorname{Re}_2 + \operatorname{Im}_2) \left(1 - \frac{1}{l-1}\right) \ \&$$

$$\operatorname{Re}_1 - \operatorname{Im}_1 - \operatorname{Re}_2 - \operatorname{Im}_2 > 0 \ \&$$

$$\operatorname{Re}_1 + \operatorname{Im}_1 - \operatorname{Re}_2 - \operatorname{Im}_2 < (\operatorname{Re}_1 + \operatorname{Im}_1 + \operatorname{Re}_2 + \operatorname{Im}_2) \left(1 - \frac{1}{l-1}\right);$$

$$(l-1)(\operatorname{Re}_1 - \operatorname{Im}_1 + \operatorname{Re}_2 + \operatorname{Im}_2) < (\operatorname{Re}_1 + \operatorname{Im}_1 + \operatorname{Re}_2 + \operatorname{Im}_2)(l-2) \ \&$$

$$\operatorname{Re}_1 - \operatorname{Im}_1 - \operatorname{Re}_2 - \operatorname{Im}_2 > 0 \ \&$$

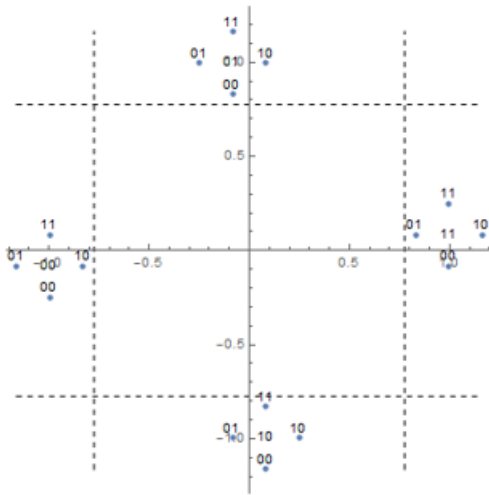
$$(l-1)(\operatorname{Re}_1 + \operatorname{Im}_1 - \operatorname{Re}_2 - \operatorname{Im}_2) < (\operatorname{Re}_1 + \operatorname{Im}_1 + \operatorname{Re}_2 + \operatorname{Im}_2)(l-2);$$

$$\operatorname{Re}_1 + \operatorname{Re}_2 + \operatorname{Im}_2 - (2l-3)\operatorname{Im}_1 < 0 \ \&$$

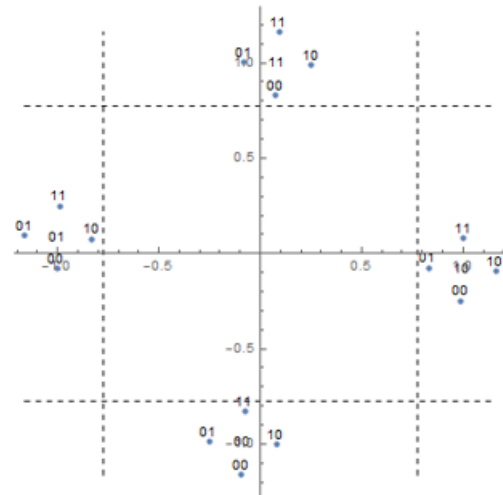
$$\operatorname{Re}_1 - \operatorname{Im}_1 - \operatorname{Re}_2 - \operatorname{Im}_2 > 0 \ \&$$

$$\operatorname{Re}_1 + \operatorname{Im}_1 - (2l-3)(\operatorname{Re}_2 + \operatorname{Im}_2) < 0$$

### Case 3d



(3d - 1)



(3d - 2)

Case (3d-1):

1110 is on the border. Three points (1111, 1110 and 1101) will lie in region D, and 1100 will lie in down right hand edge region if:

$$\text{Im}[1100] < 0 \& \text{Im}[1101] > 0 \& \text{Re}[1101] > q_{th} \& \text{Im}[1110] > 0$$

$$\frac{1}{\sqrt{2}}(\text{Re}_1 + \text{Im}_1 - \text{Re}_2 - \text{Im}_2) < 0 \&$$

$$\frac{1}{\sqrt{2}}(\text{Re}_1 + \text{Im}_1 + \text{Re}_2 - \text{Im}_2) > 0 \&$$

$$\frac{1}{\sqrt{2}}(\text{Re}_1 - \text{Im}_1 - \text{Re}_2 - \text{Im}_2) > \frac{1}{\sqrt{2}}(\text{Re}_1 - \text{Im}_1 + \text{Re}_2 + \text{Im}_2) \left(1 - \frac{1}{l-1}\right) \&$$

$$\frac{1}{\sqrt{2}}(\text{Re}_1 + \text{Im}_1 - \text{Re}_2 + \text{Im}_2) > 0;$$

$$(\text{Re}_1 + \text{Im}_1 - \text{Re}_2 - \text{Im}_2) < 0 \&$$

$$(\text{Re}_1 + \text{Im}_1 + \text{Re}_2 - \text{Im}_2) > 0 \&$$

$$(l-1)(\text{Re}_1 - \text{Im}_1 - \text{Re}_2 - \text{Im}_2) > (\text{Re}_1 - \text{Im}_1 + \text{Re}_2 + \text{Im}_2)(l-2);$$

$$(\text{Re}_1 + \text{Im}_1 - \text{Re}_2 - \text{Im}_2) < 0 \&$$

$$(\text{Re}_1 + \text{Im}_1 + \text{Re}_2 - \text{Im}_2) > 0 \&$$

$$\text{Re}_1 - \text{Im}_1 + (2l-3)(-\text{Re}_2 - \text{Im}_2) > 0 \&$$

$$(\text{Re}_1 + \text{Im}_1 - \text{Re}_2 + \text{Im}_2) > 0;$$

Case (3d-2):

1111 is on the border. Three points (1111, 1110 and 1100) will lie in region A, and

1100 will lie in left upper right hand edge region if:

$$\text{Re}[1101] < 0 \ \& \ \text{Im}[1100] > q_{th} \ \& \ \text{Re}[1100] > 0 \ \& \ \text{Re}[1111] > 0$$

$$\frac{1}{\sqrt{2}}(\text{Re}_1 - \text{Im}_1 - \text{Re}_2 - \text{Im}_2) < 0 \ \&$$

$$\frac{1}{\sqrt{2}}(\text{Re}_1 + \text{Im}_1 - \text{Re}_2 - \text{Im}_2) > \frac{1}{\sqrt{2}}(\text{Re}_1 + \text{Im}_1 + \text{Re}_2 + \text{Im}_2) \left(1 - \frac{1}{l-1}\right) \ \&$$

$$\frac{1}{\sqrt{2}}(\text{Re}_1 - \text{Im}_1 - \text{Re}_2 + \text{Im}_2) > 0 \ \&$$

$$\frac{1}{\sqrt{2}}(\text{Re}_1 - \text{Im}_1 + \text{Re}_2 - \text{Im}_2) > 0;$$

$$(\text{Re}_1 - \text{Im}_1 - \text{Re}_2 - \text{Im}_2) < 0 \ \&$$

$$(l-1)(\text{Re}_1 + \text{Im}_1 - \text{Re}_2 - \text{Im}_2) > (\text{Re}_1 + \text{Im}_1 + \text{Re}_2 + \text{Im}_2)(l-2) \ \&$$

$$(\text{Re}_1 - \text{Im}_1 - \text{Re}_2 + \text{Im}_2) > 0;$$

$$(\text{Re}_1 - \text{Im}_1 - \text{Re}_2 - \text{Im}_2) < 0 \ \&$$

$$\text{Re}_1 + \text{Im}_1 + (2l-3)(-\text{Re}_2 - \text{Im}_2) > 0 \ \&$$

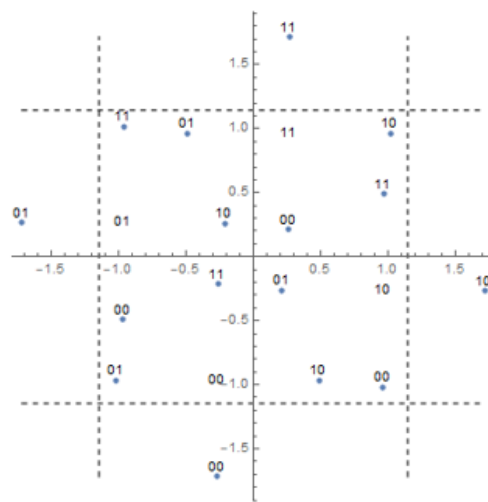
$$(\text{Re}_1 - \text{Im}_1 - \text{Re}_2 + \text{Im}_2) > 0 \ \&$$

$$(\text{Re}_1 - \text{Im}_1 + \text{Re}_2 - \text{Im}_2) > 0$$

**Case 3e**



**(3e - 1)**



**(3e - 2)**

Case (3e-1):

1110 is on the border. Three points (1111, 1101 and 0110) will lie in region C if:

$$\text{Im}[1111] < q_{th} \ \& \ \text{Re}[1111] < q_{th} \ \& \ \text{Re}[1101] > 0 \ \& \ \text{Im}[1101] > 0 \ \& \ \text{Re}[0110] > 0 \ \& \ \text{Im}[0110] < q_{th}$$

$$\begin{aligned} \frac{1}{\sqrt{2}}(\text{Re}_1 + \text{Im}_1 + \text{Re}_2 + \text{Im}_2) &< \frac{1}{\sqrt{2}}(\text{Re}_1 - \text{Im}_1 + \text{Re}_2 + \text{Im}_2) \left(1 - \frac{1}{l-1}\right) \ \& \\ \frac{1}{\sqrt{2}}(\text{Re}_1 - \text{Im}_1 + \text{Re}_2 - \text{Im}_2) &< \frac{1}{\sqrt{2}}(\text{Re}_1 - \text{Im}_1 + \text{Re}_2 + \text{Im}_2) \left(1 - \frac{1}{l-1}\right) \ \& \\ \frac{1}{\sqrt{2}}(\text{Re}_1 - \text{Im}_1 - \text{Re}_2 - \text{Im}_2) &> 0 \ \& \\ \frac{1}{\sqrt{2}}(\text{Re}_1 + \text{Im}_1 + \text{Re}_2 - \text{Im}_2) &> 0 \ \& \\ \frac{1}{\sqrt{2}}(-\text{Re}_1 - \text{Im}_1 + \text{Re}_2 + \text{Im}_2) &> 0 \ \& \\ \frac{1}{\sqrt{2}}(\text{Re}_1 - \text{Im}_1 - \text{Re}_2 + \text{Im}_2) &< \frac{1}{\sqrt{2}}(\text{Re}_1 - \text{Im}_1 + \text{Re}_2 + \text{Im}_2) \left(1 - \frac{1}{l-1}\right); \end{aligned}$$

$$\begin{aligned} (l-1)(\text{Re}_1 + \text{Im}_1 + \text{Re}_2 + \text{Im}_2) &< (l-2)(\text{Re}_1 - \text{Im}_1 + \text{Re}_2 + \text{Im}_2) \ \& \\ (l-1)(\text{Re}_1 - \text{Im}_1 + \text{Re}_2 - \text{Im}_2) &< (l-2)(\text{Re}_1 - \text{Im}_1 + \text{Re}_2 + \text{Im}_2) \ \& \\ (\text{Re}_1 - \text{Im}_1 - \text{Re}_2 - \text{Im}_2) &> 0 \ \& \\ (\text{Re}_1 + \text{Im}_1 + \text{Re}_2 - \text{Im}_2) &> 0 \ \& \\ (-\text{Re}_1 - \text{Im}_1 + \text{Re}_2 + \text{Im}_2) &> 0 \ \& \\ (l-1)(\text{Re}_1 - \text{Im}_1 - \text{Re}_2 + \text{Im}_2) &< (l-2)(\text{Re}_1 - \text{Im}_1 + \text{Re}_2 + \text{Im}_2); \end{aligned}$$

$$\begin{aligned} \text{Re}_1 + \text{Re}_2 + \text{Im}_2 + (2l-3)\text{Im}_1 &< 0 \ \& \\ \text{Re}_1 - \text{Im}_1 + \text{Re}_2 + (2l-3)(-\text{Im}_2) &< 0 \ \& \\ (\text{Re}_1 - \text{Im}_1 - \text{Re}_2 - \text{Im}_2) &> 0 \ \& \\ (\text{Re}_1 + \text{Im}_1 + \text{Re}_2 - \text{Im}_2) &> 0 \ \& \\ (-\text{Re}_1 - \text{Im}_1 + \text{Re}_2 + \text{Im}_2) &> 0 \ \& \\ \text{Re}_1 - \text{Im}_1 + \text{Im}_2 + (2l-3)(-\text{Re}_2) &< 0; \end{aligned}$$

Case (3e-2)

1111 is on the border. Three points (1110, 1100 and 1011) will lie in region C if:

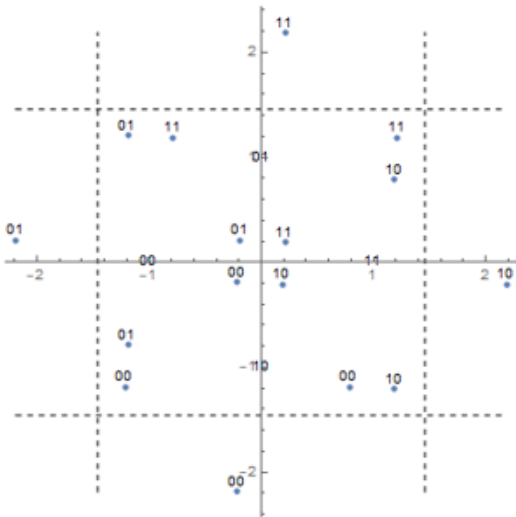
$$\text{Im}[1110] < q_{hh} \ \& \ \text{Re}[1110] < q_{hh} \ \& \ \text{Re}[1100] > 0 \ \& \ \text{Im}[1100] > 0 \ \& \ \text{Re}[1011] < q_{hh} \ \& \ \text{Im}[1011] > 0$$

$$\begin{aligned} \frac{1}{\sqrt{2}}(\text{Re}_1 + \text{Im}_1 - \text{Re}_2 + \text{Im}_2) &< \frac{1}{\sqrt{2}}(\text{Re}_1 + \text{Im}_1 + \text{Re}_2 + \text{Im}_2) \left(1 - \frac{1}{l-1}\right) \ \& \\ \frac{1}{\sqrt{2}}(\text{Re}_1 - \text{Im}_1 + \text{Re}_2 + \text{Im}_2) &< \frac{1}{\sqrt{2}}(\text{Re}_1 + \text{Im}_1 + \text{Re}_2 + \text{Im}_2) \left(1 - \frac{1}{l-1}\right) \ \& \\ \frac{1}{\sqrt{2}}(\text{Re}_1 - \text{Im}_1 - \text{Re}_2 + \text{Im}_2) &> 0 \ \& \\ \frac{1}{\sqrt{2}}(\text{Re}_1 + \text{Im}_1 - \text{Re}_2 - \text{Im}_2) &> 0 \ \& \\ \frac{1}{\sqrt{2}}(\text{Re}_1 + \text{Im}_1 + \text{Re}_2 - \text{Im}_2) &< \frac{1}{\sqrt{2}}(\text{Re}_1 + \text{Im}_1 + \text{Re}_2 + \text{Im}_2) \left(1 - \frac{1}{l-1}\right) \ \& \\ \frac{1}{\sqrt{2}}(-\text{Re}_1 + \text{Im}_1 + \text{Re}_2 + \text{Im}_2) &> 0; \end{aligned}$$

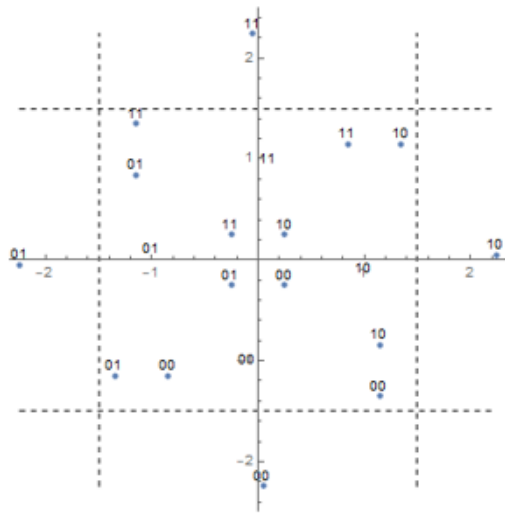
$$\begin{aligned} (l-1)(\text{Re}_1 + \text{Im}_1 - \text{Re}_2 + \text{Im}_2) &< (l-2)(\text{Re}_1 + \text{Im}_1 + \text{Re}_2 + \text{Im}_2) \ \& \\ (l-1)(\text{Re}_1 - \text{Im}_1 + \text{Re}_2 + \text{Im}_2) &< (l-2)(\text{Re}_1 + \text{Im}_1 + \text{Re}_2 + \text{Im}_2) \ \& \\ (\text{Re}_1 - \text{Im}_1 - \text{Re}_2 + \text{Im}_2) &> 0 \ \& \\ (\text{Re}_1 + \text{Im}_1 - \text{Re}_2 - \text{Im}_2) &> 0 \ \& \\ (l-1)(\text{Re}_1 + \text{Im}_1 + \text{Re}_2 - \text{Im}_2) &< (l-2)(\text{Re}_1 + \text{Im}_1 + \text{Re}_2 + \text{Im}_2) \ \& \\ (-\text{Re}_1 + \text{Im}_1 + \text{Re}_2 + \text{Im}_2) &> 0; \end{aligned}$$

$$\begin{aligned} \text{Re}_1 + \text{Im}_1 + \text{Im}_2 + (2l-3)(-\text{Re}_2) &< 0 \ \& \\ \text{Re}_1 + \text{Re}_2 + \text{Im}_2 + (2l-3)(-\text{Im}_1) &< 0 \ \& \\ (\text{Re}_1 - \text{Im}_1 - \text{Re}_2 + \text{Im}_2) &> 0 \ \& \\ (\text{Re}_1 + \text{Im}_1 - \text{Re}_2 - \text{Im}_2) &> 0 \ \& \\ \text{Re}_1 + \text{Im}_1 + \text{Re}_2 + (2l-3)(-\text{Im}_2) &< 0 \ \& \\ (-\text{Re}_1 + \text{Im}_1 + \text{Re}_2 + \text{Im}_2) &> 0; \end{aligned}$$

### Case 3f



(3f - 1)



(3f - 2)

Case (3f-1):

1110 is on the border. Three points (1111, 0110 and 1011) will lie in region C if:

$$\text{Im}[1111] < q_{th} \ \& \ \text{Re}[1111] < q_{th} \ \& \ \text{Re}[1011] > 0 \ \& \ \text{Im}[1011] > 0$$

$$\frac{1}{\sqrt{2}}(\text{Re}_1 + \text{Im}_1 + \text{Re}_2 + \text{Im}_2) < \frac{1}{\sqrt{2}}(\text{Re}_1 - \text{Im}_1 + \text{Re}_2 + \text{Im}_2) \left(1 - \frac{1}{l-1}\right) \ \&$$

$$\frac{1}{\sqrt{2}}(\text{Re}_1 - \text{Im}_1 + \text{Re}_2 - \text{Im}_2) < \frac{1}{\sqrt{2}}(\text{Re}_1 - \text{Im}_1 + \text{Re}_2 + \text{Im}_2) \left(1 - \frac{1}{l-1}\right) \ \&$$

$$\frac{1}{\sqrt{2}}(\text{Re}_1 + \text{Im}_1 + \text{Re}_2 - \text{Im}_2) > 0 \ \&$$

$$\frac{1}{\sqrt{2}}(-\text{Re}_1 + \text{Im}_1 + \text{Re}_2 + \text{Im}_2) > 0;$$

$$(l-1)(\text{Re}_1 + \text{Im}_1 + \text{Re}_2 + \text{Im}_2) < (l-2)(\text{Re}_1 - \text{Im}_1 + \text{Re}_2 + \text{Im}_2) \ \&$$

$$(l-1)(\text{Re}_1 - \text{Im}_1 + \text{Re}_2 - \text{Im}_2) < (l-2)(\text{Re}_1 - \text{Im}_1 + \text{Re}_2 + \text{Im}_2) \ \&$$

$$(\text{Re}_1 + \text{Im}_1 + \text{Re}_2 - \text{Im}_2) > 0 \ \&$$

$$(-\text{Re}_1 + \text{Im}_1 + \text{Re}_2 + \text{Im}_2) > 0;$$

$$\text{Re}_1 + \text{Re}_2 + \text{Im}_2 + (2l-3)\text{Im}_1 < 0 \ \&$$

$$\text{Re}_1 - \text{Im}_1 + \text{Re}_2 + (2l-3)(-\text{Im}_2) < 0 \ \&$$

$$(\text{Re}_1 + \text{Im}_1 + \text{Re}_2 - \text{Im}_2) > 0 \ \&$$

$$(-\text{Re}_1 + \text{Im}_1 + \text{Re}_2 + \text{Im}_2) > 0$$

Case (3f-2):

1111 is on the border. Three points (1110, 0110 and 1011) will lie in region C if:

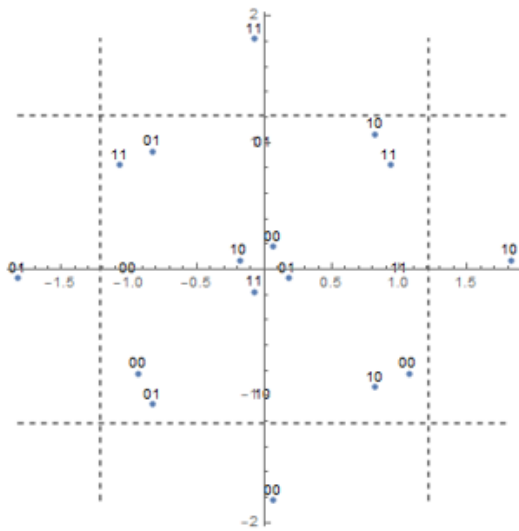
$$\text{Im}[1110] < q_{th} \ \& \ \text{Re}[1110] < q_{th} \ \& \ \text{Re}[0110] > 0 \ \& \ \text{Im}[0110] > 0$$

$$\begin{aligned} \frac{1}{\sqrt{2}}(\text{Re}_1 + \text{Im}_1 - \text{Re}_2 + \text{Im}_2) &< \frac{1}{\sqrt{2}}(\text{Re}_1 + \text{Im}_1 + \text{Re}_2 + \text{Im}_2) \left(1 - \frac{1}{l-1}\right) \ \& \\ \frac{1}{\sqrt{2}}(\text{Re}_1 - \text{Im}_1 + \text{Re}_2 + \text{Im}_2) &< \frac{1}{\sqrt{2}}(\text{Re}_1 + \text{Im}_1 + \text{Re}_2 + \text{Im}_2) \left(1 - \frac{1}{l-1}\right) \ \& \\ \frac{1}{\sqrt{2}}(-\text{Re}_1 - \text{Im}_1 + \text{Re}_2 + \text{Im}_2) &> 0 \ \& \\ \frac{1}{\sqrt{2}}(\text{Re}_1 - \text{Im}_1 - \text{Re}_2 + \text{Im}_2) &> 0; \end{aligned}$$

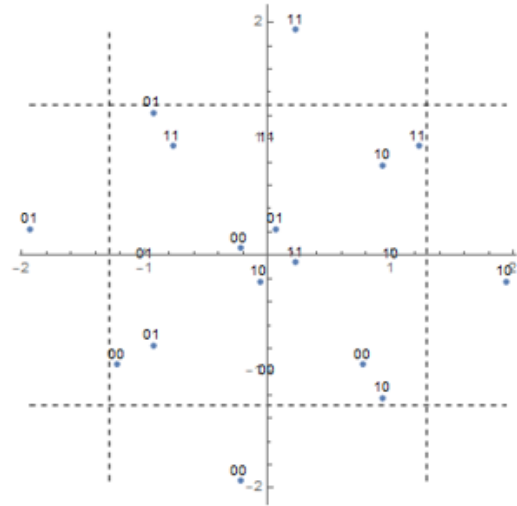
$$\begin{aligned} (l-1)(\text{Re}_1 + \text{Im}_1 - \text{Re}_2 + \text{Im}_2) &< (l-2)(\text{Re}_1 + \text{Im}_1 + \text{Re}_2 + \text{Im}_2) \ \& \\ (l-1)(\text{Re}_1 - \text{Im}_1 + \text{Re}_2 + \text{Im}_2) &< (l-2)(\text{Re}_1 + \text{Im}_1 + \text{Re}_2 + \text{Im}_2) \ \& \\ (-\text{Re}_1 - \text{Im}_1 + \text{Re}_2 + \text{Im}_2) &> 0 \ \& \\ (\text{Re}_1 - \text{Im}_1 - \text{Re}_2 + \text{Im}_2) &> 0; \end{aligned}$$

$$\begin{aligned} \text{Re}_1 + \text{Im}_1 + \text{Im}_2 + (2l-3)(-\text{Re}_2) &< 0 \ \& \\ \text{Re}_1 + \text{Re}_2 + \text{Im}_2 + (2l-3)(-\text{Im}_1) &< 0 \ \& \\ (-\text{Re}_1 - \text{Im}_1 + \text{Re}_2 + \text{Im}_2) &> 0 \ \& \\ (\text{Re}_1 - \text{Im}_1 - \text{Re}_2 + \text{Im}_2) &> 0 \end{aligned}$$

### Case 3g



**(3g - 1)**



**(3g - 2)**

Case (3g-1):

1110 is on the border. Three points (1111, 0110, and 0100) will lie in region C if:

$$\operatorname{Re}[1111] < q_{hh} \ \& \ \operatorname{Im}[0110] < q_{hh} \ \& \ \operatorname{Re}[0100] > 0 \ \& \ \operatorname{Im}[0100] > 0$$

$$\frac{1}{\sqrt{2}}(\operatorname{Re}_1 - \operatorname{Im}_1 + \operatorname{Re}_2 - \operatorname{Im}_2) < \frac{1}{\sqrt{2}}(\operatorname{Re}_1 - \operatorname{Im}_1 + \operatorname{Re}_2 + \operatorname{Im}_2) \left(1 - \frac{1}{l-1}\right) \ \&$$

$$\frac{1}{\sqrt{2}}(\operatorname{Re}_1 - \operatorname{Im}_1 - \operatorname{Re}_2 + \operatorname{Im}_2) < \frac{1}{\sqrt{2}}(\operatorname{Re}_1 - \operatorname{Im}_1 + \operatorname{Re}_2 + \operatorname{Im}_2) \left(1 - \frac{1}{l-1}\right) \ \&$$

$$\frac{1}{\sqrt{2}}(-\operatorname{Re}_1 - \operatorname{Im}_1 - \operatorname{Re}_2 + \operatorname{Im}_2) > 0 \ \&$$

$$\frac{1}{\sqrt{2}}(\operatorname{Re}_1 - \operatorname{Im}_1 - \operatorname{Re}_2 - \operatorname{Im}_2) > 0;$$

$$(l-1)(\operatorname{Re}_1 - \operatorname{Im}_1 + \operatorname{Re}_2 - \operatorname{Im}_2) < (l-2)(\operatorname{Re}_1 - \operatorname{Im}_1 + \operatorname{Re}_2 + \operatorname{Im}_2) \ \&$$

$$(l-1)(\operatorname{Re}_1 - \operatorname{Im}_1 - \operatorname{Re}_2 + \operatorname{Im}_2) < (l-2)(\operatorname{Re}_1 - \operatorname{Im}_1 + \operatorname{Re}_2 + \operatorname{Im}_2) \ \&$$

$$(-\operatorname{Re}_1 - \operatorname{Im}_1 - \operatorname{Re}_2 + \operatorname{Im}_2) > 0 \ \&$$

$$(\operatorname{Re}_1 - \operatorname{Im}_1 - \operatorname{Re}_2 - \operatorname{Im}_2) > 0;$$

$$\operatorname{Re}_1 - \operatorname{Im}_1 + \operatorname{Re}_2 + (2l-3)(-\operatorname{Im}_2) < 0 \ \&$$

$$\operatorname{Re}_1 - \operatorname{Im}_1 + \operatorname{Im}_2 + (2l-3)(-\operatorname{Re}_2) < 0 \ \&$$

$$(-\operatorname{Re}_1 - \operatorname{Im}_1 - \operatorname{Re}_2 + \operatorname{Im}_2) > 0 \ \&$$

$$(\operatorname{Re}_1 - \operatorname{Im}_1 - \operatorname{Re}_2 - \operatorname{Im}_2) > 0$$

Case (3g-2):

1111 is on the border. Three points (1110, 1011, and 1001) will lie in region C if:

$$\text{Re}[1011] < q_{th} \ \& \ \text{Re}[1001] > 0 \ \& \ \text{Im}[1001] > 0$$

$$\frac{1}{\sqrt{2}}(\text{Re}_1 + \text{Im}_1 + \text{Re}_2 - \text{Im}_2) < \frac{1}{\sqrt{2}}(\text{Re}_1 + \text{Im}_1 + \text{Re}_2 + \text{Im}_2) \left(1 - \frac{1}{l-1}\right) \ \&$$

$$\frac{1}{\sqrt{2}}(\text{Re}_1 + \text{Im}_1 - \text{Re}_2 - \text{Im}_2) > 0 \ \&$$

$$\frac{1}{\sqrt{2}}(-\text{Re}_1 + \text{Im}_1 + \text{Re}_2 - \text{Im}_2) > 0;$$

$$(l-1)(\text{Re}_1 + \text{Im}_1 + \text{Re}_2 - \text{Im}_2) < (l-2)(\text{Re}_1 + \text{Im}_1 + \text{Re}_2 + \text{Im}_2) \ \&$$

$$(\text{Re}_1 + \text{Im}_1 - \text{Re}_2 - \text{Im}_2) > 0 \ \&$$

$$(-\text{Re}_1 + \text{Im}_1 + \text{Re}_2 - \text{Im}_2) > 0;$$

$$\text{Re}_1 + \text{Im}_1 + \text{Re}_2 + (2l-3)(-\text{Im}_2) < 0 \ \&$$

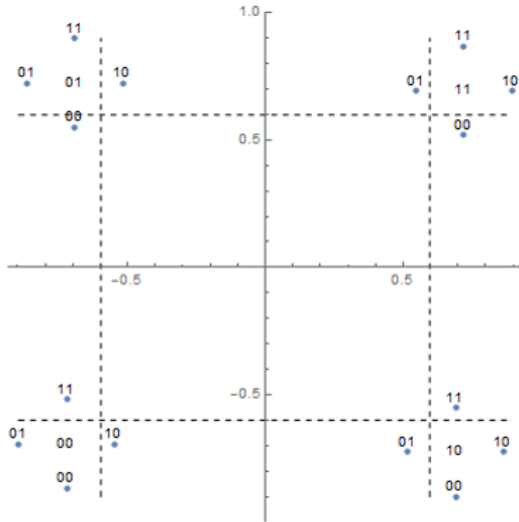
$$(\text{Re}_1 + \text{Im}_1 - \text{Re}_2 - \text{Im}_2) > 0 \ \&$$

$$(-\text{Re}_1 + \text{Im}_1 + \text{Re}_2 - \text{Im}_2) > 0$$

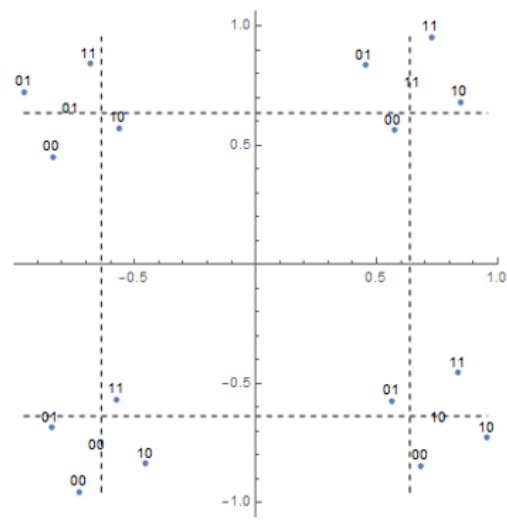
### Two points in outage

For the two points in outage case, there are 13 cases for two possible received symbols in the same region.

#### Case 2a



(2a - 1)



(2a - 2)

Case (2a-1):

1110 is on the border, and 1111 is not. 1110 and 1111 will lie in region B if:

$$\operatorname{Re}[r(1111)] > q_{th} \ \& \ \operatorname{Im}[r(1110)] > q_{th}$$

$$\operatorname{Re}_1 - \operatorname{Im}_1 + \operatorname{Re}_2 - \operatorname{Im}_2 > \left(1 - \frac{1}{l-1}\right)(\operatorname{Re}_1 - \operatorname{Im}_1 + \operatorname{Re}_2 + \operatorname{Im}_2) \ \&$$

$$\operatorname{Re}_1 + \operatorname{Im}_1 - \operatorname{Re}_2 + \operatorname{Im}_2 > \left(1 - \frac{1}{l-1}\right)(\operatorname{Re}_1 - \operatorname{Im}_1 + \operatorname{Re}_2 + \operatorname{Im}_2);$$

$$(l-1)(\operatorname{Re}_1 - \operatorname{Im}_1 + \operatorname{Re}_2 - \operatorname{Im}_2) > (l-2)(\operatorname{Re}_1 - \operatorname{Im}_1 + \operatorname{Re}_2 + \operatorname{Im}_2) \ \&$$

$$(l-1)(\operatorname{Re}_1 + \operatorname{Im}_1 - \operatorname{Re}_2 + \operatorname{Im}_2) > (l-2)(\operatorname{Re}_1 - \operatorname{Im}_1 + \operatorname{Re}_2 + \operatorname{Im}_2);$$

$$(\operatorname{Re}_1 - \operatorname{Im}_1 + \operatorname{Re}_2) - (2l-3)\operatorname{Im}_2 > 0 \ \&$$

$$(\operatorname{Re}_1 + \operatorname{Im}_2) + (2l-3)(\operatorname{Im}_1 - \operatorname{Re}_2) > 0$$

Case (2a-2):

1111 is on the border, and 1110 is not. 1110 and 1111 will lie in region B if:

$$\operatorname{Re}[r(1111)] > q_{th} \ \& \ \operatorname{Im}[r(1110)] > q_{th}$$

$$\operatorname{Re}_1 - \operatorname{Im}_1 + \operatorname{Re}_2 - \operatorname{Im}_2 > \left(1 - \frac{1}{l-1}\right)(\operatorname{Re}_1 + \operatorname{Im}_1 + \operatorname{Re}_2 + \operatorname{Im}_2) \ \&$$

$$\operatorname{Re}_1 + \operatorname{Im}_1 - \operatorname{Re}_2 + \operatorname{Im}_2 > \left(1 - \frac{1}{l-1}\right)(\operatorname{Re}_1 + \operatorname{Im}_1 + \operatorname{Re}_2 + \operatorname{Im}_2);$$

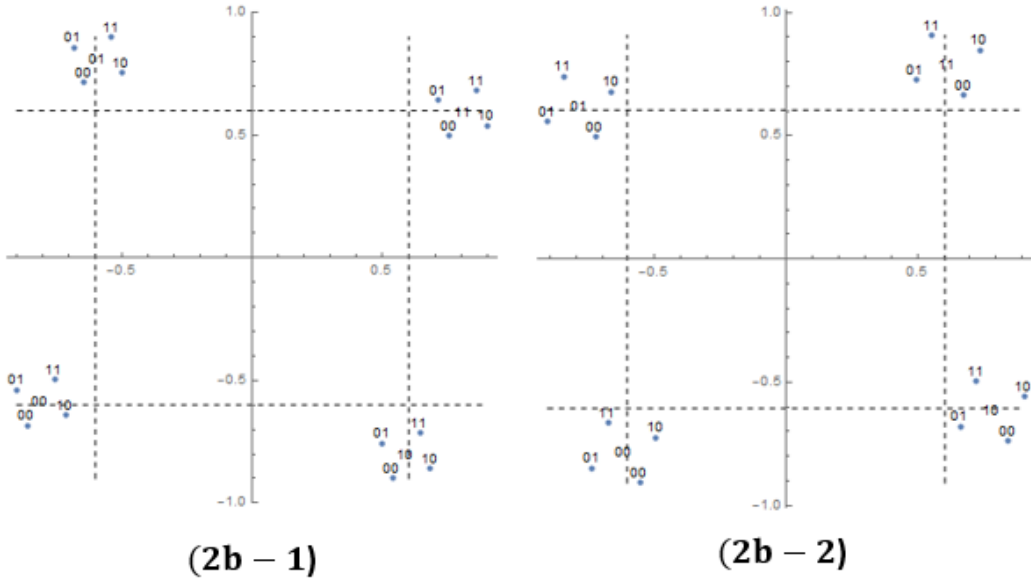
$$(l-1)(\operatorname{Re}_1 - \operatorname{Im}_1 + \operatorname{Re}_2 - \operatorname{Im}_2) > (l-2)(\operatorname{Re}_1 + \operatorname{Im}_1 + \operatorname{Re}_2 + \operatorname{Im}_2) \ \&$$

$$(l-1)(\operatorname{Re}_1 + \operatorname{Im}_1 - \operatorname{Re}_2 + \operatorname{Im}_2) > (l-2)(\operatorname{Re}_1 + \operatorname{Im}_1 + \operatorname{Re}_2 + \operatorname{Im}_2);$$

$$(\operatorname{Re}_1 + \operatorname{Re}_2) + (2l-3)(-\operatorname{Im}_1 - \operatorname{Im}_2) > 0 \ \&$$

$$(\operatorname{Re}_1 + \operatorname{Im}_1 + \operatorname{Im}_2) + (2l-3)(-\operatorname{Re}_2) > 0$$

## Case 2b



Case (2b-1):

1110 is on the border, and 1111 is not. 1101 and 1111 will lie in region B if:

$$\text{Im}[r(1110)] < q_{th} \ \& \ \text{Re}[r(1101)] > q_{th} \ \& \ \text{Im}[r(1101)] > q_{th}$$

$$\text{Re}_1 + \text{Im}_1 - \text{Re}_2 + \text{Im}_2 < \left(1 - \frac{1}{l-1}\right)(\text{Re}_1 + \text{Im}_1 + \text{Re}_2 + \text{Im}_2)$$

$$\text{Re}_1 - \text{Im}_1 - \text{Re}_2 - \text{Im}_2 > \left(1 - \frac{1}{l-1}\right)(\text{Re}_1 - \text{Im}_1 + \text{Re}_2 + \text{Im}_2) \ \&$$

$$\text{Re}_1 + \text{Im}_1 + \text{Re}_2 - \text{Im}_2 > \left(1 - \frac{1}{l-1}\right)(\text{Re}_1 - \text{Im}_1 + \text{Re}_2 + \text{Im}_2);$$

$$(l-1)(\text{Re}_1 + \text{Im}_1 - \text{Re}_2 + \text{Im}_2) < (l-2)(\text{Re}_1 - \text{Im}_1 + \text{Re}_2 + \text{Im}_2) \ \&$$

$$(l-1)(\text{Re}_1 - \text{Im}_1 - \text{Re}_2 - \text{Im}_2) > (l-2)(\text{Re}_1 - \text{Im}_1 + \text{Re}_2 + \text{Im}_2) \ \&$$

$$(l-1)(\text{Re}_1 + \text{Im}_1 + \text{Re}_2 - \text{Im}_2) > (l-2)(\text{Re}_1 - \text{Im}_1 + \text{Re}_2 + \text{Im}_2);$$

$$(\text{Re}_1 + \text{Im}_2) + (2l-3)(\text{Im}_1 - \text{Re}_2) < 0 \ \&$$

$$(\text{Re}_1 - \text{Im}_1) - (2l-3)(\text{Re}_2 + \text{Im}_2) > 0 \ \&$$

$$(\text{Re}_1 + \text{Re}_2) + (2l-3)(\text{Im}_1 - \text{Im}_2) > 0$$

Case (2b-2):

1111 is on the border, and 1110 is not. 1110 and 1100 will lie in region B if:

$$\operatorname{Re}[r(1111)] < q_{th} \ \& \ \operatorname{Re}[r(1100)] > q_{th} \ \& \ \operatorname{Im}[r(1100)] > q_{th}$$

$$\operatorname{Re}_1 - \operatorname{Im}_1 + \operatorname{Re}_2 - \operatorname{Im}_2 < \left(1 - \frac{1}{l-1}\right) (\operatorname{Re}_1 - \operatorname{Im}_1 + \operatorname{Re}_2 + \operatorname{Im}_2) \ \&$$

$$\operatorname{Re}_1 - \operatorname{Im}_1 - \operatorname{Re}_2 + \operatorname{Im}_2 > \left(1 - \frac{1}{l-1}\right) (\operatorname{Re}_1 + \operatorname{Im}_1 + \operatorname{Re}_2 + \operatorname{Im}_2) \ \&$$

$$\operatorname{Re}_1 + \operatorname{Im}_1 - \operatorname{Re}_2 - \operatorname{Im}_2 > \left(1 - \frac{1}{l-1}\right) (\operatorname{Re}_1 + \operatorname{Im}_1 + \operatorname{Re}_2 + \operatorname{Im}_2);$$

$$(l-1)(\operatorname{Re}_1 - \operatorname{Im}_1 + \operatorname{Re}_2 - \operatorname{Im}_2) < (l-2)(\operatorname{Re}_1 + \operatorname{Im}_1 + \operatorname{Re}_2 + \operatorname{Im}_2) \ \&$$

$$(l-1)(\operatorname{Re}_1 - \operatorname{Im}_1 - \operatorname{Re}_2 + \operatorname{Im}_2) > (l-2)(\operatorname{Re}_1 + \operatorname{Im}_1 + \operatorname{Re}_2 + \operatorname{Im}_2) \ \&$$

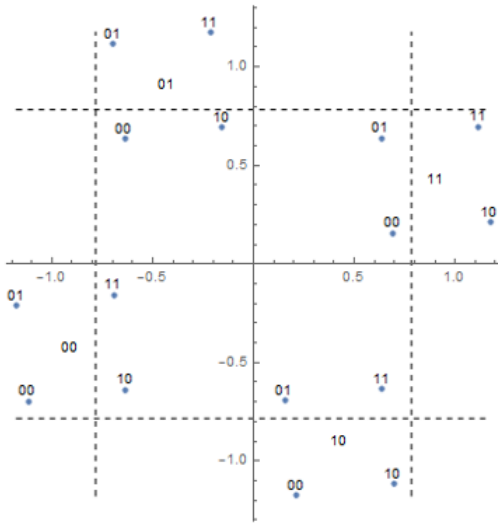
$$(l-1)(\operatorname{Re}_1 + \operatorname{Im}_1 - \operatorname{Re}_2 - \operatorname{Im}_2) > (l-2)(\operatorname{Re}_1 + \operatorname{Im}_1 + \operatorname{Re}_2 + \operatorname{Im}_2);$$

$$(\operatorname{Re}_1 + \operatorname{Re}_2) + (2l-3)(-\operatorname{Im}_1 - \operatorname{Im}_2) < 0 \ \&$$

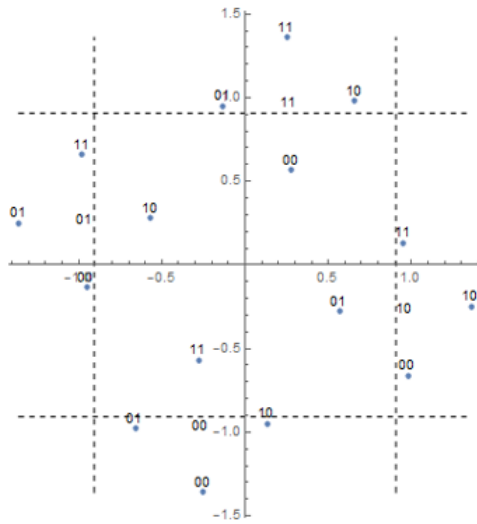
$$(\operatorname{Re}_1 + \operatorname{Im}_2) + (2l-3)(-\operatorname{Im}_1 - \operatorname{Re}_2) > 0 \ \&$$

$$(\operatorname{Re}_1 + \operatorname{Im}_1) + (2l-3)(-\operatorname{Re}_2 - \operatorname{Im}_2) > 0$$

Case 2c



(2c-1)



(2c-2)

Case (2c-1):

1110 is on the border, and 1111 is not. 1110 and 1111 will lie in region D if:

$$\operatorname{Re}[1111] > q_{th} \ \& \ \operatorname{Im}[1111] < q_{th} \ \& \ \operatorname{Im}[1110] > 0$$

$$\operatorname{Re}_1 - \operatorname{Im}_1 + \operatorname{Re}_2 - \operatorname{Im}_2 > \left(1 - \frac{1}{l-1}\right) (\operatorname{Re}_1 - \operatorname{Im}_1 + \operatorname{Re}_2 + \operatorname{Im}_2) \ \&$$

$$\operatorname{Re}_1 + \operatorname{Im}_1 + \operatorname{Re}_2 + \operatorname{Im}_2 < \left(1 - \frac{1}{l-1}\right) (\operatorname{Re}_1 - \operatorname{Im}_1 + \operatorname{Re}_2 + \operatorname{Im}_2) \ \&$$

$$\operatorname{Re}_1 + \operatorname{Im}_1 - \operatorname{Re}_2 + \operatorname{Im}_2 > 0;$$

$$(l-1)(\operatorname{Re}_1 - \operatorname{Im}_1 + \operatorname{Re}_2 - \operatorname{Im}_2) > (l-2)(\operatorname{Re}_1 - \operatorname{Im}_1 + \operatorname{Re}_2 + \operatorname{Im}_2) \ \&$$

$$(l-1)(\operatorname{Re}_1 + \operatorname{Im}_1 + \operatorname{Re}_2 + \operatorname{Im}_2) < (l-2)(\operatorname{Re}_1 - \operatorname{Im}_1 + \operatorname{Re}_2 + \operatorname{Im}_2) \ \&$$

$$\operatorname{Re}_1 + \operatorname{Im}_1 - \operatorname{Re}_2 + \operatorname{Im}_2 > 0;$$

$$(\operatorname{Re}_1 - \operatorname{Im}_1 + \operatorname{Re}_2) - (2l-3)\operatorname{Im}_2 > 0 \ \&$$

$$(\operatorname{Re}_1 + \operatorname{Re}_2 + \operatorname{Im}_2) + (2l-3)(\operatorname{Im}_1) < 0 \ \&$$

$$\operatorname{Re}_1 + \operatorname{Im}_1 - \operatorname{Re}_2 + \operatorname{Im}_2 > 0$$

Case (2c-2):

1111 is on the border, and 1110 is not. 1110 and 1111 will lie in region A if:

$$\operatorname{Re}[1111] > 0 \ \& \ \operatorname{Re}[1110] < q_{th} \ \& \ \operatorname{Im}[1110] > q_{th}$$

$$\operatorname{Re}_1 - \operatorname{Im}_1 + \operatorname{Re}_2 - \operatorname{Im}_2 > 0 \ \&$$

$$\operatorname{Re}_1 - \operatorname{Im}_1 + \operatorname{Re}_2 + \operatorname{Im}_2 < \left(1 - \frac{1}{l-1}\right) (\operatorname{Re}_1 + \operatorname{Im}_1 + \operatorname{Re}_2 + \operatorname{Im}_2) \ \&$$

$$\operatorname{Re}_1 + \operatorname{Im}_1 - \operatorname{Re}_2 + \operatorname{Im}_2 > \left(1 - \frac{1}{l-1}\right) (\operatorname{Re}_1 + \operatorname{Im}_1 + \operatorname{Re}_2 + \operatorname{Im}_2);$$

$$(\operatorname{Re}_1 - \operatorname{Im}_1 + \operatorname{Re}_2 - \operatorname{Im}_2) > 0 \ \&$$

$$(l-1)(\operatorname{Re}_1 - \operatorname{Im}_1 + \operatorname{Re}_2 + \operatorname{Im}_2) < (l-2)(\operatorname{Re}_1 + \operatorname{Im}_1 + \operatorname{Re}_2 + \operatorname{Im}_2) \ \&$$

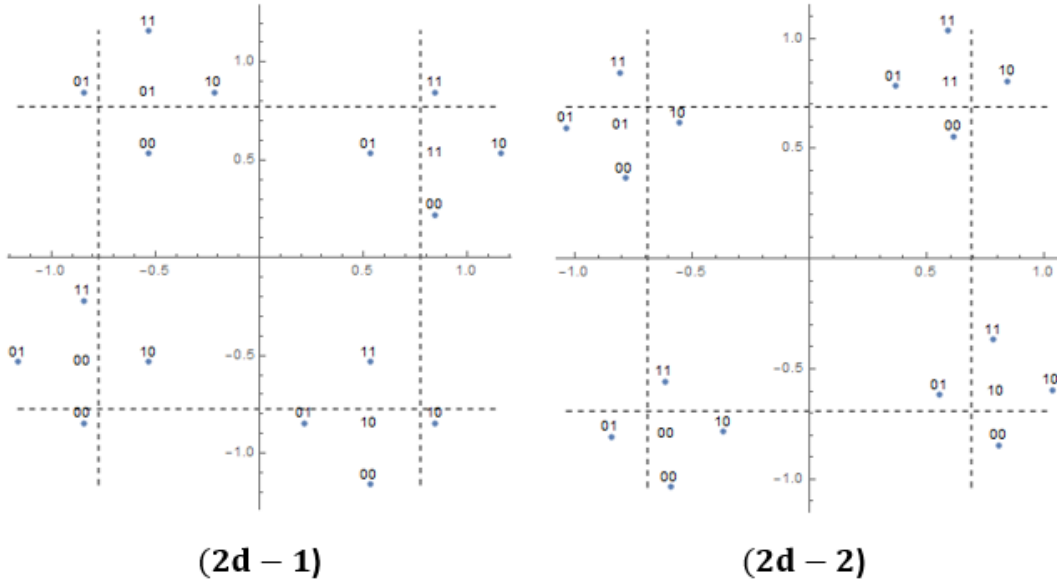
$$(l-1)(\operatorname{Re}_1 + \operatorname{Im}_1 - \operatorname{Re}_2 + \operatorname{Im}_2) > (l-2)(\operatorname{Re}_1 + \operatorname{Im}_1 + \operatorname{Re}_2 + \operatorname{Im}_2);$$

$$(\operatorname{Re}_1 - \operatorname{Im}_1 + \operatorname{Re}_2 - \operatorname{Im}_2) > 0 \ \&$$

$$(\operatorname{Re}_1 + \operatorname{Re}_2 + \operatorname{Im}_2) - (2l-3)(\operatorname{Im}_1) < 0 \ \&$$

$$(\operatorname{Re}_1 + \operatorname{Im}_1 + \operatorname{Im}_2) - (2l-3)(\operatorname{Re}_2) > 0$$

## Case 2d



Case (2d-1):

1110 is on the border, and 1111 is not. 1110 and 1100 will lie in region D if:

$$\operatorname{Re}[1100] > q_{th} \ \& \ \operatorname{Im}[1100] > 0 \ \& \ \operatorname{Im}[1110] < q_{th}$$

$$\operatorname{Re}_1 - \operatorname{Im}_1 - \operatorname{Re}_2 + \operatorname{Im}_2 > \left(1 - \frac{1}{l-1}\right) (\operatorname{Re}_1 - \operatorname{Im}_1 + \operatorname{Re}_2 + \operatorname{Im}_2) \ \&$$

$$\operatorname{Re}_1 + \operatorname{Im}_1 - \operatorname{Re}_2 - \operatorname{Im}_2 > 0 \ \&$$

$$\operatorname{Re}_1 + \operatorname{Im}_1 - \operatorname{Re}_2 + \operatorname{Im}_2 < \left(1 - \frac{1}{l-1}\right) (\operatorname{Re}_1 - \operatorname{Im}_1 + \operatorname{Re}_2 + \operatorname{Im}_2);$$

$$(l-1)(\operatorname{Re}_1 - \operatorname{Im}_1 - \operatorname{Re}_2 + \operatorname{Im}_2) > (l-2)(\operatorname{Re}_1 - \operatorname{Im}_1 + \operatorname{Re}_2 + \operatorname{Im}_2) \ \&$$

$$(\operatorname{Re}_1 + \operatorname{Im}_1 - \operatorname{Re}_2 - \operatorname{Im}_2) > 0 \ \&$$

$$(l-1)(\operatorname{Re}_1 + \operatorname{Im}_1 - \operatorname{Re}_2 + \operatorname{Im}_2) < (l-2)(\operatorname{Re}_1 - \operatorname{Im}_1 + \operatorname{Re}_2 + \operatorname{Im}_2);$$

$$(\operatorname{Re}_1 - \operatorname{Im}_1 + \operatorname{Im}_2) - (2l-3)\operatorname{Re}_2 > 0 \ \&$$

$$(\operatorname{Re}_1 + \operatorname{Im}_1 - \operatorname{Re}_2 - \operatorname{Im}_2) > 0 \ \&$$

$$(\operatorname{Re}_1 + \operatorname{Im}_2) + (2l-3)(\operatorname{Im}_1 - \operatorname{Re}_2) < 0$$

Case (2d-2):

1111 is on the border, and 1110 is not. 1111 and 1101 will lie in region A if:

$$\text{Re}[1101] > 0 \ \& \ \text{Im}[1101] > q_{th} \ \& \ \text{Re}[1111] < q_{th}$$

$$\text{Re}_1 - \text{Im}_1 - \text{Re}_2 - \text{Im}_2 > 0 \ \&$$

$$\text{Re}_1 + \text{Im}_1 + \text{Re}_2 - \text{Im}_2 > \left(1 - \frac{1}{l-1}\right) (\text{Re}_1 + \text{Im}_1 + \text{Re}_2 + \text{Im}_2) \ \&$$

$$\text{Re}_1 - \text{Im}_1 + \text{Re}_2 - \text{Im}_2 < \left(1 - \frac{1}{l-1}\right) (\text{Re}_1 + \text{Im}_1 + \text{Re}_2 + \text{Im}_2);$$

$$(\text{Re}_1 - \text{Im}_1 - \text{Re}_2 - \text{Im}_2) > 0 \ \&$$

$$(l-1)(\text{Re}_1 + \text{Im}_1 + \text{Re}_2 - \text{Im}_2) > (l-2)(\text{Re}_1 + \text{Im}_1 + \text{Re}_2 + \text{Im}_2) \ \&$$

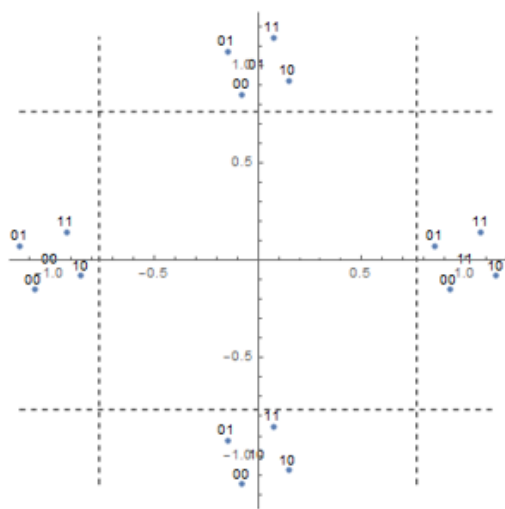
$$(l-1)(\text{Re}_1 - \text{Im}_1 + \text{Re}_2 - \text{Im}_2) < (l-2)(\text{Re}_1 + \text{Im}_1 + \text{Re}_2 + \text{Im}_2);$$

$$(\text{Re}_1 - \text{Im}_1 - \text{Re}_2 - \text{Im}_2) > 0 \ \&$$

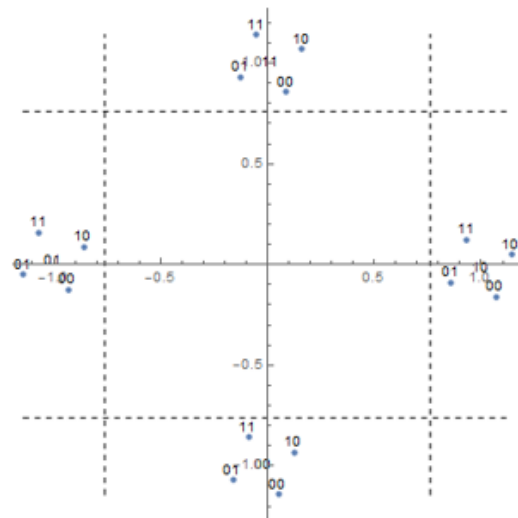
$$(\text{Re}_1 + \text{Im}_1 + \text{Re}_2) - (2l-3)\text{Im}_2 > 0 \ \&$$

$$(\text{Re}_1 + \text{Re}_2) + (2l-3)(-\text{Im}_1 - \text{Im}_2) < 0$$

**Case 2e**



**(2e - 1)**



**(2e - 2)**

Case (2e-1):

1110 is on the border, and 1111 is not. 1111 and 1101 will lie in region D if:

$$\operatorname{Re}[1101] > q_{th} \ \& \ \operatorname{Im}[1101] > 0 \ \& \ \operatorname{Im}[1111] < q_{th}$$

$$\operatorname{Re}_1 - \operatorname{Im}_1 - \operatorname{Re}_2 - \operatorname{Im}_2 > \left(1 - \frac{1}{l-1}\right) (\operatorname{Re}_1 - \operatorname{Im}_1 + \operatorname{Re}_2 + \operatorname{Im}_2) \ \&$$

$$\operatorname{Re}_1 + \operatorname{Im}_1 + \operatorname{Re}_2 - \operatorname{Im}_2 > 0 \ \&$$

$$\operatorname{Re}_1 + \operatorname{Im}_1 + \operatorname{Re}_2 + \operatorname{Im}_2 < \left(1 - \frac{1}{l-1}\right) (\operatorname{Re}_1 - \operatorname{Im}_1 + \operatorname{Re}_2 + \operatorname{Im}_2);$$

$$(l-1)(\operatorname{Re}_1 - \operatorname{Im}_1 - \operatorname{Re}_2 - \operatorname{Im}_2) > (l-2)(\operatorname{Re}_1 - \operatorname{Im}_1 + \operatorname{Re}_2 + \operatorname{Im}_2) \ \&$$

$$(\operatorname{Re}_1 + \operatorname{Im}_1 + \operatorname{Re}_2 - \operatorname{Im}_2) > 0 \ \&$$

$$(l-1)(\operatorname{Re}_1 + \operatorname{Im}_1 + \operatorname{Re}_2 + \operatorname{Im}_2) < (l-2)(\operatorname{Re}_1 - \operatorname{Im}_1 + \operatorname{Re}_2 + \operatorname{Im}_2);$$

$$(\operatorname{Re}_1 - \operatorname{Im}_1) - (2l-3)(\operatorname{Re}_2 + \operatorname{Im}_2) > 0 \ \&$$

$$(\operatorname{Re}_1 + \operatorname{Im}_1 + \operatorname{Re}_2 - \operatorname{Im}_2) > 0 \ \&$$

$$(\operatorname{Re}_1 + \operatorname{Re}_2 + \operatorname{Im}_2) + (2l-3)(\operatorname{Im}_1) < 0$$

Case (2e-2):

1111 is on the border, and 1110 is not. 1100 and 1110 will lie in region A if:

$$\operatorname{Re}[1100] > 0 \ \& \ \operatorname{Im}[1100] > q_{th} \ \& \ \operatorname{Re}[1110] < q_{th}$$

$$\operatorname{Re}_1 - \operatorname{Im}_1 - \operatorname{Re}_2 + \operatorname{Im}_2 > 0 \ \&$$

$$\operatorname{Re}_1 + \operatorname{Im}_1 - \operatorname{Re}_2 - \operatorname{Im}_2 > \left(1 - \frac{1}{l-1}\right) (\operatorname{Re}_1 + \operatorname{Im}_1 + \operatorname{Re}_2 + \operatorname{Im}_2) \ \&$$

$$\operatorname{Re}_1 - \operatorname{Im}_1 + \operatorname{Re}_2 + \operatorname{Im}_2 < \left(1 - \frac{1}{l-1}\right) (\operatorname{Re}_1 + \operatorname{Im}_1 + \operatorname{Re}_2 + \operatorname{Im}_2);$$

$$(\operatorname{Re}_1 - \operatorname{Im}_1 - \operatorname{Re}_2 + \operatorname{Im}_2) > 0 \ \&$$

$$(l-1)(\operatorname{Re}_1 + \operatorname{Im}_1 - \operatorname{Re}_2 - \operatorname{Im}_2) > (l-2)(\operatorname{Re}_1 + \operatorname{Im}_1 + \operatorname{Re}_2 + \operatorname{Im}_2) \ \&$$

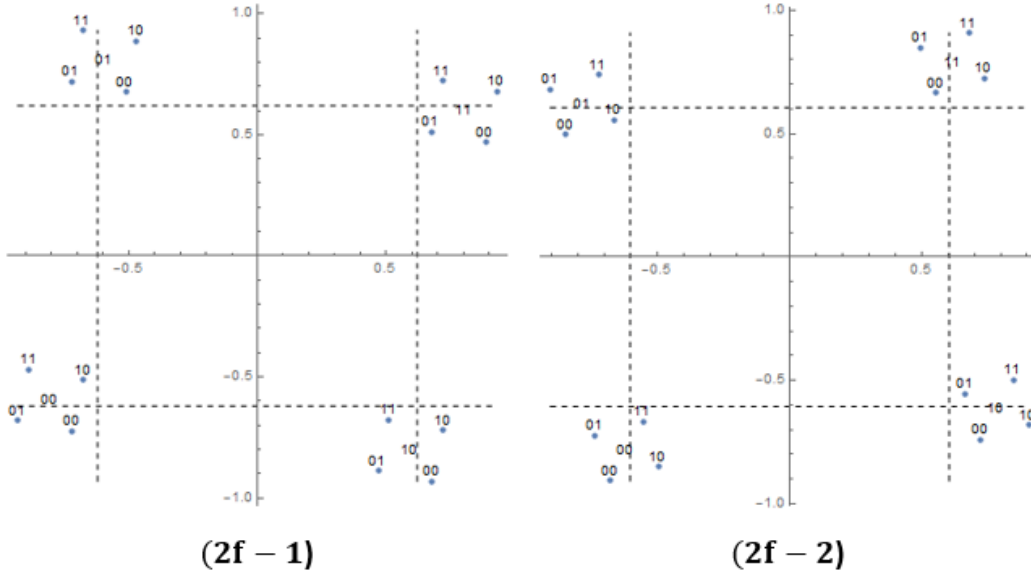
$$(l-1)(\operatorname{Re}_1 - \operatorname{Im}_1 + \operatorname{Re}_2 + \operatorname{Im}_2) < (l-2)(\operatorname{Re}_1 + \operatorname{Im}_1 + \operatorname{Re}_2 + \operatorname{Im}_2);$$

$$(\operatorname{Re}_1 - \operatorname{Im}_1 - \operatorname{Re}_2 + \operatorname{Im}_2) > 0 \ \&$$

$$(\operatorname{Re}_1 + \operatorname{Im}_1) - (2l-3)(\operatorname{Re}_2 + \operatorname{Im}_2) > 0 \ \&$$

$$(\operatorname{Re}_1 + \operatorname{Re}_2 + \operatorname{Im}_2) + (2l-3)(-\operatorname{Im}_1) < 0$$

## Case 2f



Case (2f-1):

1110 is on the border, and 1111 is not. 1101 and 1100 will lie in region D if:

$$\operatorname{Re}[1101] > q_h \ \& \ \operatorname{Im}[1101] < q_h \ \& \ \operatorname{Im}[1100] > 0$$

$$\operatorname{Re}_1 - \operatorname{Im}_1 - \operatorname{Re}_2 - \operatorname{Im}_2 > \left(1 - \frac{1}{l-1}\right) (\operatorname{Re}_1 - \operatorname{Im}_1 + \operatorname{Re}_2 + \operatorname{Im}_2) \ \&$$

$$\operatorname{Re}_1 + \operatorname{Im}_1 + \operatorname{Re}_2 - \operatorname{Im}_2 < \left(1 - \frac{1}{l-1}\right) (\operatorname{Re}_1 - \operatorname{Im}_1 + \operatorname{Re}_2 + \operatorname{Im}_2) \ \&$$

$$\operatorname{Re}_1 + \operatorname{Im}_1 - \operatorname{Re}_2 - \operatorname{Im}_2 > 0;$$

$$(l-1)(\operatorname{Re}_1 - \operatorname{Im}_1 - \operatorname{Re}_2 - \operatorname{Im}_2) > (l-2)(\operatorname{Re}_1 - \operatorname{Im}_1 + \operatorname{Re}_2 + \operatorname{Im}_2) \ \&$$

$$(l-1)(\operatorname{Re}_1 + \operatorname{Im}_1 + \operatorname{Re}_2 - \operatorname{Im}_2) < (l-2)(\operatorname{Re}_1 - \operatorname{Im}_1 + \operatorname{Re}_2 + \operatorname{Im}_2) \ \&$$

$$\operatorname{Re}_1 + \operatorname{Im}_1 - \operatorname{Re}_2 - \operatorname{Im}_2 > 0;$$

$$(\operatorname{Re}_1 - \operatorname{Im}_1) - (2l-3)(\operatorname{Re}_2 + \operatorname{Im}_2) > 0 \ \&$$

$$(\operatorname{Re}_1 + \operatorname{Re}_2) + (2l-3)(\operatorname{Im}_1 - \operatorname{Im}_2) < 0 \ \&$$

$$\operatorname{Re}_1 + \operatorname{Im}_1 - \operatorname{Re}_2 - \operatorname{Im}_2 > 0$$



Case (2g-1):

1110 is on the border, and 1111 is not. 1111 and 0110 will lie in region A if:

$$\operatorname{Re}[1111] > 0 \& \operatorname{Im}[1111] > q_{th} \& \operatorname{Re}[0110] > 0 \& \operatorname{Im}[0110] > q_{th}$$

$$\operatorname{Re}_1 - \operatorname{Im}_1 + \operatorname{Re}_2 - \operatorname{Im}_2 > 0 \&$$

$$\operatorname{Re}_1 + \operatorname{Im}_1 + \operatorname{Re}_2 + \operatorname{Im}_2 > \left(1 - \frac{1}{l-1}\right)(\operatorname{Re}_1 - \operatorname{Im}_1 + \operatorname{Re}_2 + \operatorname{Im}_2) \&$$

$$-\operatorname{Re}_1 - \operatorname{Im}_1 + \operatorname{Re}_2 + \operatorname{Im}_2 > 0 \&$$

$$\operatorname{Re}_1 - \operatorname{Im}_1 - \operatorname{Re}_2 + \operatorname{Im}_2 > \left(1 - \frac{1}{l-1}\right)(\operatorname{Re}_1 - \operatorname{Im}_1 + \operatorname{Re}_2 + \operatorname{Im}_2);$$

$$\operatorname{Re}_1 - \operatorname{Im}_1 + \operatorname{Re}_2 - \operatorname{Im}_2 > 0 \&$$

$$(l-1)(\operatorname{Re}_1 + \operatorname{Im}_1 + \operatorname{Re}_2 + \operatorname{Im}_2) > (l-2)(\operatorname{Re}_1 - \operatorname{Im}_1 + \operatorname{Re}_2 + \operatorname{Im}_2) \&$$

$$-\operatorname{Re}_1 - \operatorname{Im}_1 + \operatorname{Re}_2 + \operatorname{Im}_2 > 0 \&$$

$$(l-1)(\operatorname{Re}_1 - \operatorname{Im}_1 - \operatorname{Re}_2 + \operatorname{Im}_2) > (l-2)(\operatorname{Re}_1 - \operatorname{Im}_1 + \operatorname{Re}_2 + \operatorname{Im}_2);$$

$$\operatorname{Re}_1 - \operatorname{Im}_1 + \operatorname{Re}_2 - \operatorname{Im}_2 > 0 \&$$

$$(\operatorname{Re}_1 + \operatorname{Re}_2 + \operatorname{Im}_2) + (2l-3)\operatorname{Im}_1 > 0 \&$$

$$-\operatorname{Re}_1 - \operatorname{Im}_1 + \operatorname{Re}_2 + \operatorname{Im}_2 > 0 \&$$

$$(\operatorname{Re}_1 - \operatorname{Im}_1 + \operatorname{Im}_2) + (2l-3)(-\operatorname{Re}_2) > 0$$

Case (2g-2):

1111 is on the border, and 1110 is not. 1110 and 1011 will lie in region D if:

$$\text{Im}[1110] > 0 \ \& \ \text{Re}[1110] > q_{th} \ \& \ \text{Im}[1011] > 0 \ \& \ \text{Re}[1011] > q_{th}$$

$$\text{Re}_1 + \text{Im}_1 - \text{Re}_2 + \text{Im}_2 > 0 \ \&$$

$$\text{Re}_1 - \text{Im}_1 + \text{Re}_2 + \text{Im}_2 > \left(1 - \frac{1}{l-1}\right) (\text{Re}_1 + \text{Im}_1 + \text{Re}_2 + \text{Im}_2) \ \&$$

$$-\text{Re}_1 + \text{Im}_1 + \text{Re}_2 + \text{Im}_2 > 0 \ \&$$

$$\text{Re}_1 + \text{Im}_1 + \text{Re}_2 - \text{Im}_2 > \left(1 - \frac{1}{l-1}\right) (\text{Re}_1 + \text{Im}_1 + \text{Re}_2 + \text{Im}_2);$$

$$\text{Re}_1 + \text{Im}_1 - \text{Re}_2 + \text{Im}_2 > 0 \ \&$$

$$(l-1)(\text{Re}_1 - \text{Im}_1 + \text{Re}_2 + \text{Im}_2) > (l-2)(\text{Re}_1 + \text{Im}_1 + \text{Re}_2 + \text{Im}_2) \ \&$$

$$-\text{Re}_1 + \text{Im}_1 + \text{Re}_2 + \text{Im}_2 > 0 \ \&$$

$$(l-1)(\text{Re}_1 + \text{Im}_1 + \text{Re}_2 - \text{Im}_2) > (l-2)(\text{Re}_1 + \text{Im}_1 + \text{Re}_2 + \text{Im}_2);$$

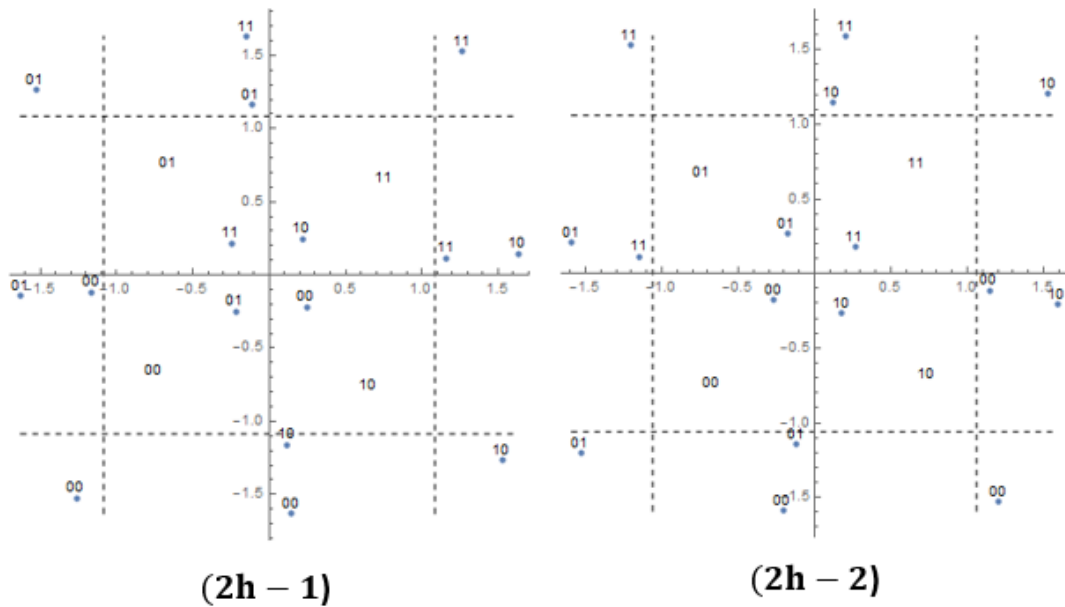
$$\text{Re}_1 + \text{Im}_1 - \text{Re}_2 + \text{Im}_2 > 0 \ \&$$

$$(\text{Re}_1 + \text{Re}_2 + \text{Im}_2) - (2l-3)\text{Im}_1 > 0 \ \&$$

$$-\text{Re}_1 + \text{Im}_1 + \text{Re}_2 + \text{Im}_2 > 0 \ \&$$

$$(\text{Re}_1 + \text{Im}_1 + \text{Re}_2) + (2l-3)(-\text{Im}_2) > 0$$

## Case 2h



Case (2h-1):

1110 is on the border, and 1111 is not. 1110 and 1011 will lie in region D if:

$$\text{Im}[1110] > 0 \ \& \ \text{Im}[1011] > 0 \ \& \ \text{Re}[1011] > q_{th}$$

$$\text{Re}_1 + \text{Im}_1 - \text{Re}_2 + \text{Im}_2 > 0 \ \&$$

$$-\text{Re}_1 + \text{Im}_1 + \text{Re}_2 + \text{Im}_2 > 0 \ \&$$

$$\text{Re}_1 + \text{Im}_1 + \text{Re}_2 - \text{Im}_2 > \left(1 - \frac{1}{l-1}\right)(\text{Re}_1 - \text{Im}_1 + \text{Re}_2 + \text{Im}_2);$$

$$\text{Re}_1 + \text{Im}_1 - \text{Re}_2 + \text{Im}_2 > 0 \ \&$$

$$-\text{Re}_1 + \text{Im}_1 + \text{Re}_2 + \text{Im}_2 > 0 \ \&$$

$$(l-1)(\text{Re}_1 + \text{Im}_1 + \text{Re}_2 - \text{Im}_2) > (l-2)(\text{Re}_1 - \text{Im}_1 + \text{Re}_2 + \text{Im}_2);$$

$$\text{Re}_1 + \text{Im}_1 - \text{Re}_2 + \text{Im}_2 > 0 \ \&$$

$$-\text{Re}_1 + \text{Im}_1 + \text{Re}_2 + \text{Im}_2 > 0 \ \&$$

$$(\text{Re}_1 + \text{Re}_2) + (2l-3)(\text{Im}_1 - \text{Im}_2) > 0$$

Case (2h-2):

1111 is on the border, and 1110 is not. 1111 and 0110 will lie in region A if:

$$\text{Re}[1111] > 0 \ \& \ \text{Re}[0110] > 0 \ \& \ \text{Im}[0110] > q_{th}$$

$$\text{Re}_1 - \text{Im}_1 + \text{Re}_2 - \text{Im}_2 > 0 \ \&$$

$$-\text{Re}_1 - \text{Im}_1 + \text{Re}_2 + \text{Im}_2 > 0 \ \&$$

$$\text{Re}_1 - \text{Im}_1 - \text{Re}_2 + \text{Im}_2 > \left(1 - \frac{1}{l-1}\right)(\text{Re}_1 + \text{Im}_1 + \text{Re}_2 + \text{Im}_2);$$

$$\text{Re}_1 - \text{Im}_1 + \text{Re}_2 - \text{Im}_2 > 0 \ \&$$

$$-\text{Re}_1 - \text{Im}_1 + \text{Re}_2 + \text{Im}_2 > 0 \ \&$$

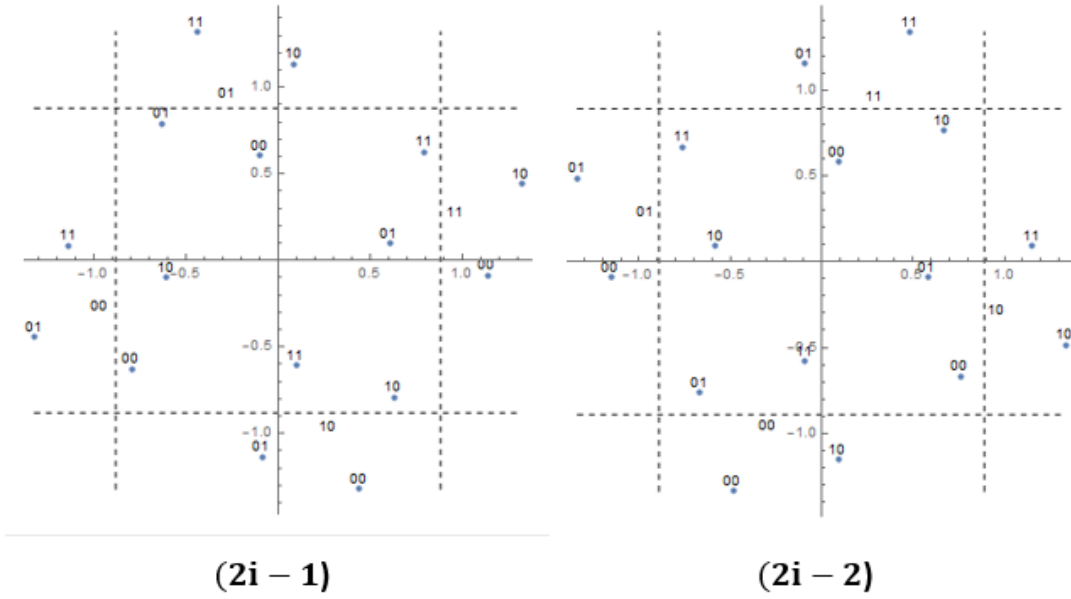
$$(l-1)(\text{Re}_1 - \text{Im}_1 - \text{Re}_2 + \text{Im}_2) > (l-2)(\text{Re}_1 + \text{Im}_1 + \text{Re}_2 + \text{Im}_2);$$

$$\text{Re}_1 - \text{Im}_1 + \text{Re}_2 - \text{Im}_2 > 0 \ \&$$

$$-\text{Re}_1 - \text{Im}_1 + \text{Re}_2 + \text{Im}_2 > 0 \ \&$$

$$(\text{Re}_1 + \text{Im}_2) + (2l-3)(-\text{Im}_1 - \text{Re}_2) > 0$$

## Case 2i



Case (2i-1):

1110 is on the border, and 1111 is not. 1111 and 1101 will lie in region C if:

$$\operatorname{Re}[1111] < q_h \& \operatorname{Im}[1111] < q_h \& \operatorname{Re}[1101] > 0 \& \operatorname{Im}[1101] > 0$$

$$\operatorname{Re}_1 - \operatorname{Im}_1 + \operatorname{Re}_2 - \operatorname{Im}_2 < \left(1 - \frac{1}{l-1}\right) (\operatorname{Re}_1 - \operatorname{Im}_1 + \operatorname{Re}_2 + \operatorname{Im}_2) \&$$

$$\operatorname{Re}_1 + \operatorname{Im}_1 + \operatorname{Re}_2 + \operatorname{Im}_2 < \left(1 - \frac{1}{l-1}\right) (\operatorname{Re}_1 - \operatorname{Im}_1 + \operatorname{Re}_2 + \operatorname{Im}_2) \&$$

$$\operatorname{Re}_1 - \operatorname{Im}_1 - \operatorname{Re}_2 - \operatorname{Im}_2 > 0 \&$$

$$\operatorname{Re}_1 + \operatorname{Im}_1 + \operatorname{Re}_2 - \operatorname{Im}_2 > 0;$$

$$(l-1)(\operatorname{Re}_1 - \operatorname{Im}_1 + \operatorname{Re}_2 - \operatorname{Im}_2) < (l-2)(\operatorname{Re}_1 - \operatorname{Im}_1 + \operatorname{Re}_2 + \operatorname{Im}_2) \&$$

$$(l-1)(\operatorname{Re}_1 + \operatorname{Im}_1 + \operatorname{Re}_2 + \operatorname{Im}_2) < (l-2)(\operatorname{Re}_1 - \operatorname{Im}_1 + \operatorname{Re}_2 + \operatorname{Im}_2) \&$$

$$\operatorname{Re}_1 - \operatorname{Im}_1 - \operatorname{Re}_2 - \operatorname{Im}_2 > 0 \&$$

$$\operatorname{Re}_1 + \operatorname{Im}_1 + \operatorname{Re}_2 - \operatorname{Im}_2 > 0;$$

$$(\operatorname{Re}_1 - \operatorname{Im}_1 + \operatorname{Re}_2) - (2l-3)\operatorname{Im}_2 < 0 \&$$

$$(\operatorname{Re}_1 + \operatorname{Re}_2 + \operatorname{Im}_2) + (2l-3)\operatorname{Im}_1 < 0 \&$$

$$\operatorname{Re}_1 - \operatorname{Im}_1 - \operatorname{Re}_2 - \operatorname{Im}_2 > 0 \&$$

$$\operatorname{Re}_1 + \operatorname{Im}_1 + \operatorname{Re}_2 - \operatorname{Im}_2 > 0$$

Case (2i-2):

1111 is on the border, and 1110 is not. 1110 and 1100 will lie in region C if:

$$\operatorname{Re}[1110] < q_{th} \ \& \ \operatorname{Im}[1110] < q_{th} \ \& \ \operatorname{Re}[1100] > 0 \ \& \ \operatorname{Im}[1100] > 0 \ \& \ \operatorname{Re}[1101] < 0$$

$$\operatorname{Re}_1 - \operatorname{Im}_1 + \operatorname{Re}_2 + \operatorname{Im}_2 < \left(1 - \frac{1}{l-1}\right) (\operatorname{Re}_1 + \operatorname{Im}_1 + \operatorname{Re}_2 + \operatorname{Im}_2) \ \&$$

$$\operatorname{Re}_1 + \operatorname{Im}_1 - \operatorname{Re}_2 + \operatorname{Im}_2 < \left(1 - \frac{1}{l-1}\right) (\operatorname{Re}_1 + \operatorname{Im}_1 + \operatorname{Re}_2 + \operatorname{Im}_2) \ \&$$

$$\operatorname{Re}_1 - \operatorname{Im}_1 - \operatorname{Re}_2 + \operatorname{Im}_2 > 0 \ \&$$

$$\operatorname{Re}_1 + \operatorname{Im}_1 - \operatorname{Re}_2 - \operatorname{Im}_2 > 0 \ \&$$

$$\operatorname{Re}_1 - \operatorname{Im}_1 - \operatorname{Re}_2 - \operatorname{Im}_2 < 0;$$

$$(l-1)(\operatorname{Re}_1 - \operatorname{Im}_1 + \operatorname{Re}_2 + \operatorname{Im}_2) < (l-2)(\operatorname{Re}_1 + \operatorname{Im}_1 + \operatorname{Re}_2 + \operatorname{Im}_2) \ \&$$

$$(l-1)(\operatorname{Re}_1 + \operatorname{Im}_1 - \operatorname{Re}_2 + \operatorname{Im}_2) < (l-2)(\operatorname{Re}_1 + \operatorname{Im}_1 + \operatorname{Re}_2 + \operatorname{Im}_2) \ \&$$

$$\operatorname{Re}_1 - \operatorname{Im}_1 - \operatorname{Re}_2 + \operatorname{Im}_2 > 0 \ \&$$

$$\operatorname{Re}_1 + \operatorname{Im}_1 - \operatorname{Re}_2 - \operatorname{Im}_2 > 0 \ \&$$

$$\operatorname{Re}_1 - \operatorname{Im}_1 - \operatorname{Re}_2 - \operatorname{Im}_2 < 0;$$

$$(\operatorname{Re}_1 + \operatorname{Re}_2 + \operatorname{Im}_2) - (2l-3)\operatorname{Im}_1 < 0 \ \&$$

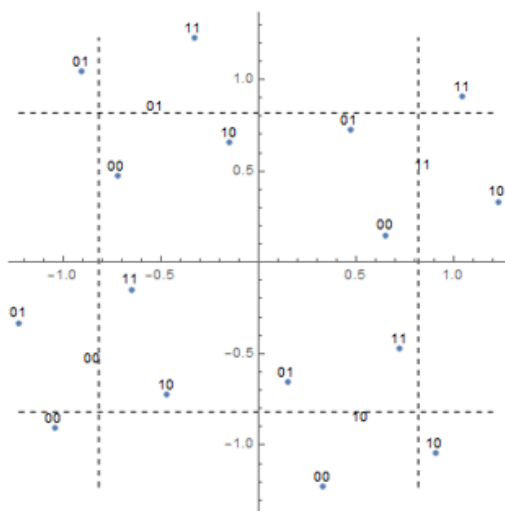
$$(\operatorname{Re}_1 + \operatorname{Im}_1 + \operatorname{Im}_2) - (2l-3)\operatorname{Re}_2 < 0 \ \&$$

$$\operatorname{Re}_1 - \operatorname{Im}_1 - \operatorname{Re}_2 + \operatorname{Im}_2 > 0 \ \&$$

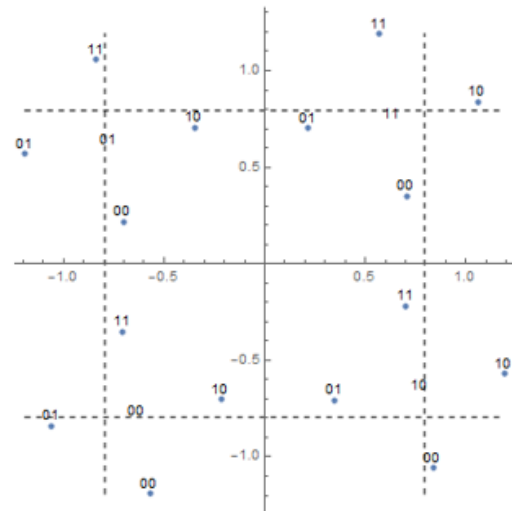
$$\operatorname{Re}_1 + \operatorname{Im}_1 - \operatorname{Re}_2 - \operatorname{Im}_2 > 0 \ \&$$

$$\operatorname{Re}_1 - \operatorname{Im}_1 - \operatorname{Re}_2 - \operatorname{Im}_2 < 0$$

Case 2j



(2j - 1)



(2j - 2)

Case (2j-1)

1110 is on the border, and 1111 is not. 1101 and 1100 will lie in region C if:

$$\operatorname{Re}[1100] < q_{th} \ \& \ \operatorname{Im}[1100] > 0 \ \& \ \operatorname{Im}[1101] < q_{th}$$

$$\operatorname{Re}_1 - \operatorname{Im}_1 - \operatorname{Re}_2 + \operatorname{Im}_2 < \left(1 - \frac{1}{l-1}\right) (\operatorname{Re}_1 - \operatorname{Im}_1 + \operatorname{Re}_2 + \operatorname{Im}_2) \ \&$$

$$\operatorname{Re}_1 + \operatorname{Im}_1 - \operatorname{Re}_2 - \operatorname{Im}_2 > 0 \ \&$$

$$\operatorname{Re}_1 + \operatorname{Im}_1 + \operatorname{Re}_2 - \operatorname{Im}_2 < \left(1 - \frac{1}{l-1}\right) (\operatorname{Re}_1 - \operatorname{Im}_1 + \operatorname{Re}_2 + \operatorname{Im}_2);$$

$$(l-1)(\operatorname{Re}_1 - \operatorname{Im}_1 - \operatorname{Re}_2 + \operatorname{Im}_2) < (l-2)(\operatorname{Re}_1 - \operatorname{Im}_1 + \operatorname{Re}_2 + \operatorname{Im}_2) \ \&$$

$$\operatorname{Re}_1 + \operatorname{Im}_1 - \operatorname{Re}_2 - \operatorname{Im}_2 > 0 \ \&$$

$$(l-1)(\operatorname{Re}_1 + \operatorname{Im}_1 + \operatorname{Re}_2 - \operatorname{Im}_2) < (l-2)(\operatorname{Re}_1 - \operatorname{Im}_1 + \operatorname{Re}_2 + \operatorname{Im}_2);$$

$$(\operatorname{Re}_1 - \operatorname{Im}_1 + \operatorname{Im}_2) - (2l-3)\operatorname{Re}_2 < 0 \ \&$$

$$\operatorname{Re}_1 + \operatorname{Im}_1 - \operatorname{Re}_2 - \operatorname{Im}_2 > 0 \ \&$$

$$(\operatorname{Re}_1 + \operatorname{Re}_2) + (2l-3)(\operatorname{Im}_1 - \operatorname{Im}_2) < 0$$

Case (2j-2):

1111 is on the border, and 1110 is not. 1101 and 1100 will lie in region C if:

$$\text{Re}[1101] > 0 \& \text{Im}[1101] < q_{th} \& \text{Re}[1100] < q_{th} \& \text{Re}[1110] > q_{th}$$

$$\text{Re}_1 - \text{Im}_1 - \text{Re}_2 - \text{Im}_2 > 0 \&$$

$$\text{Re}_1 + \text{Im}_1 + \text{Re}_2 - \text{Im}_2 < \left(1 - \frac{1}{l-1}\right) (\text{Re}_1 + \text{Im}_1 + \text{Re}_2 + \text{Im}_2) \&$$

$$\text{Re}_1 - \text{Im}_1 - \text{Re}_2 + \text{Im}_2 < \left(1 - \frac{1}{l-1}\right) (\text{Re}_1 + \text{Im}_1 + \text{Re}_2 + \text{Im}_2) \&$$

$$\text{Re}_1 - \text{Im}_1 + \text{Re}_2 + \text{Im}_2 > \left(1 - \frac{1}{l-1}\right) (\text{Re}_1 + \text{Im}_1 + \text{Re}_2 + \text{Im}_2);$$

$$\text{Re}_1 - \text{Im}_1 - \text{Re}_2 - \text{Im}_2 > 0 \&$$

$$(l-1)(\text{Re}_1 + \text{Im}_1 + \text{Re}_2 - \text{Im}_2) < (l-2)(\text{Re}_1 + \text{Im}_1 + \text{Re}_2 + \text{Im}_2) \&$$

$$(l-1)(\text{Re}_1 - \text{Im}_1 - \text{Re}_2 + \text{Im}_2) < (l-2)(\text{Re}_1 + \text{Im}_1 + \text{Re}_2 + \text{Im}_2) \&$$

$$(l-1)(\text{Re}_1 - \text{Im}_1 + \text{Re}_2 + \text{Im}_2) > (l-2)(\text{Re}_1 + \text{Im}_1 + \text{Re}_2 + \text{Im}_2);$$

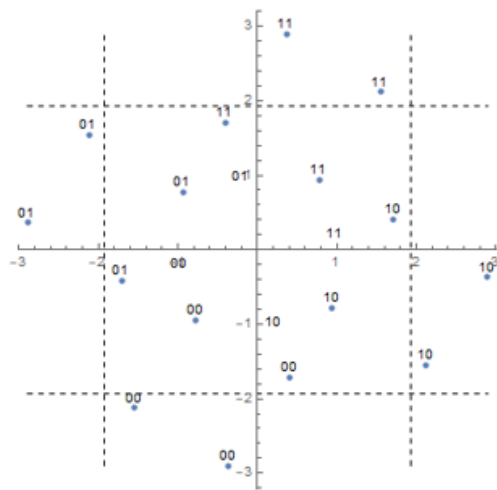
$$\text{Re}_1 - \text{Im}_1 - \text{Re}_2 - \text{Im}_2 > 0 \&$$

$$(\text{Re}_1 + \text{Im}_1 + \text{Re}_2) - (2l-3)\text{Im}_2 < 0 \&$$

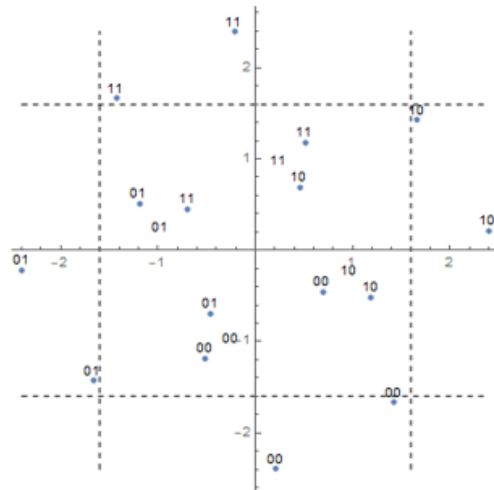
$$(\text{Re}_1 + \text{Im}_2) + (2l-3)(-\text{Im}_1 - \text{Re}_2) < 0 \&$$

$$(\text{Re}_1 + \text{Re}_2 + \text{Im}_2) - (2l-3)\text{Im}_1 > 0$$

**Case 2k**



**(2k - 1)**



**(2k - 2)**

Case (2k-1):

1110 is on the border, and 1111 is not. 1011 and 0110 will lie in region C if:

$$\operatorname{Re}[1011] > 0 \& \operatorname{Re}[1011] < q_{th} \& \operatorname{Im}[1011] > 0 \& \operatorname{Im}[0110] < q_{th}$$

$$\operatorname{Re}_1 + \operatorname{Im}_1 + \operatorname{Re}_2 - \operatorname{Im}_2 > 0 \&$$

$$\operatorname{Re}_1 + \operatorname{Im}_1 + \operatorname{Re}_2 - \operatorname{Im}_2 < \left(1 - \frac{1}{l-1}\right) (\operatorname{Re}_1 - \operatorname{Im}_1 + \operatorname{Re}_2 + \operatorname{Im}_2) \&$$

$$-\operatorname{Re}_1 + \operatorname{Im}_1 + \operatorname{Re}_2 + \operatorname{Im}_2 > 0 \&$$

$$\operatorname{Re}_1 - \operatorname{Im}_1 - \operatorname{Re}_2 + \operatorname{Im}_2 < \left(1 - \frac{1}{l-1}\right) (\operatorname{Re}_1 - \operatorname{Im}_1 + \operatorname{Re}_2 + \operatorname{Im}_2);$$

$$\operatorname{Re}_1 + \operatorname{Im}_1 + \operatorname{Re}_2 - \operatorname{Im}_2 > 0 \&$$

$$(l-1)(\operatorname{Re}_1 + \operatorname{Im}_1 + \operatorname{Re}_2 - \operatorname{Im}_2) < (l-2)(\operatorname{Re}_1 - \operatorname{Im}_1 + \operatorname{Re}_2 + \operatorname{Im}_2) \&$$

$$-\operatorname{Re}_1 + \operatorname{Im}_1 + \operatorname{Re}_2 + \operatorname{Im}_2 > 0 \&$$

$$(l-1)(\operatorname{Re}_1 - \operatorname{Im}_1 - \operatorname{Re}_2 + \operatorname{Im}_2) < (l-2)(\operatorname{Re}_1 - \operatorname{Im}_1 + \operatorname{Re}_2 + \operatorname{Im}_2);$$

$$\operatorname{Re}_1 + \operatorname{Im}_1 + \operatorname{Re}_2 - \operatorname{Im}_2 > 0 \&$$

$$(\operatorname{Re}_1 + \operatorname{Re}_2) + (2l-3)(\operatorname{Im}_1 - \operatorname{Im}_2) < 0 \&$$

$$-\operatorname{Re}_1 + \operatorname{Im}_1 + \operatorname{Re}_2 + \operatorname{Im}_2 > 0 \&$$

$$(\operatorname{Re}_1 - \operatorname{Im}_1 + \operatorname{Im}_2) + (2l-3)(-\operatorname{Re}_2) < 0$$

Case (2k-2):

1111 is on the border, and 1110 is not. 1011 and 0110 will lie in region C if:

$$\operatorname{Re}[0110] > 0 \& \operatorname{Im}[0110] < q_{th} \& \operatorname{Im}[0110] > 0 \& \operatorname{Re}[1011] < q_{th}$$

$$-\operatorname{Re}_1 - \operatorname{Im}_1 + \operatorname{Re}_2 + \operatorname{Im}_2 > 0 \&$$

$$\operatorname{Re}_1 - \operatorname{Im}_1 - \operatorname{Re}_2 + \operatorname{Im}_2 < \left(1 - \frac{1}{l-1}\right) (\operatorname{Re}_1 + \operatorname{Im}_1 + \operatorname{Re}_2 + \operatorname{Im}_2) \&$$

$$\operatorname{Re}_1 - \operatorname{Im}_1 - \operatorname{Re}_2 + \operatorname{Im}_2 > 0 \&$$

$$\operatorname{Re}_1 + \operatorname{Im}_1 + \operatorname{Re}_2 - \operatorname{Im}_2 < \left(1 - \frac{1}{l-1}\right) (\operatorname{Re}_1 + \operatorname{Im}_1 + \operatorname{Re}_2 + \operatorname{Im}_2);$$

$$-\operatorname{Re}_1 - \operatorname{Im}_1 + \operatorname{Re}_2 + \operatorname{Im}_2 > 0 \&$$

$$(l-1)(\operatorname{Re}_1 - \operatorname{Im}_1 - \operatorname{Re}_2 + \operatorname{Im}_2) < (l-2)(\operatorname{Re}_1 + \operatorname{Im}_1 + \operatorname{Re}_2 + \operatorname{Im}_2) \&$$

$$\operatorname{Re}_1 - \operatorname{Im}_1 - \operatorname{Re}_2 + \operatorname{Im}_2 > 0 \&$$

$$(l-1)(\operatorname{Re}_1 + \operatorname{Im}_1 + \operatorname{Re}_2 - \operatorname{Im}_2) < (l-2)(\operatorname{Re}_1 + \operatorname{Im}_1 + \operatorname{Re}_2 + \operatorname{Im}_2);$$

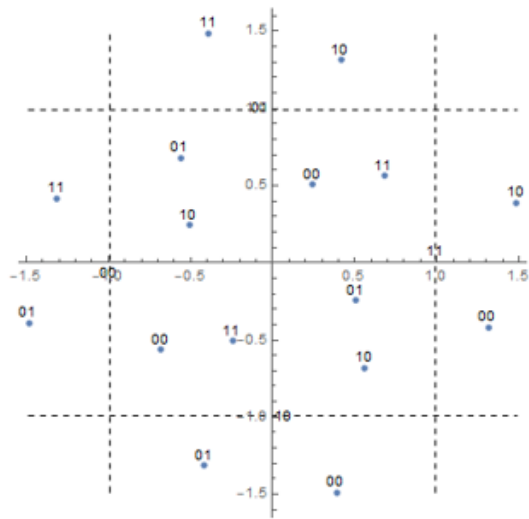
$$-\operatorname{Re}_1 - \operatorname{Im}_1 + \operatorname{Re}_2 + \operatorname{Im}_2 > 0 \&$$

$$(\operatorname{Re}_1 + \operatorname{Im}_2) - (2l-3)(\operatorname{Im}_1 + \operatorname{Re}_2) < 0 \&$$

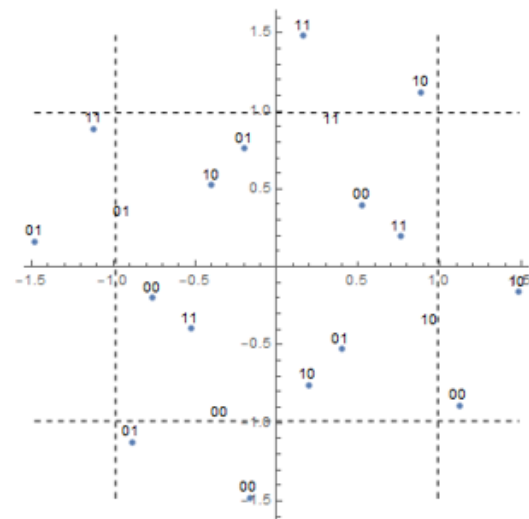
$$\operatorname{Re}_1 - \operatorname{Im}_1 - \operatorname{Re}_2 + \operatorname{Im}_2 > 0 \&$$

$$(\operatorname{Re}_1 + \operatorname{Im}_1 + \operatorname{Re}_2) + (2l-3)(-\operatorname{Im}_2) < 0$$

## Case 2l



(2l - 1)



(2l - 2)

Case (2l-1):

1110 is on the border, and 1111 is not. 1111 and 0100 will lie in region C if:

$$\operatorname{Re}[1111] < q_{th} \ \& \ \operatorname{Re}[1111] > 0 \ \& \ \operatorname{Im}[1111] < q_{th} \ \& \ \operatorname{Im}[1111] > 0 \ \& \ \operatorname{Re}[0100] > 0 \ \& \ \operatorname{Re}[0100] < q_{th} \ \& \ \operatorname{Im}[0100] > 0$$

$$\operatorname{Re}_1 - \operatorname{Im}_1 + \operatorname{Re}_2 - \operatorname{Im}_2 < \left(1 - \frac{1}{l-1}\right) (\operatorname{Re}_1 - \operatorname{Im}_1 + \operatorname{Re}_2 + \operatorname{Im}_2) \ \&$$

$$\operatorname{Re}_1 - \operatorname{Im}_1 + \operatorname{Re}_2 - \operatorname{Im}_2 > 0 \ \&$$

$$\operatorname{Re}_1 + \operatorname{Im}_1 + \operatorname{Re}_2 + \operatorname{Im}_2 < \left(1 - \frac{1}{l-1}\right) (\operatorname{Re}_1 - \operatorname{Im}_1 + \operatorname{Re}_2 + \operatorname{Im}_2) \ \&$$

$$\operatorname{Re}_1 + \operatorname{Im}_1 + \operatorname{Re}_2 + \operatorname{Im}_2 > 0 \ \&$$

$$-\operatorname{Re}_1 - \operatorname{Im}_1 - \operatorname{Re}_2 + \operatorname{Im}_2 > 0 \ \&$$

$$-\operatorname{Re}_1 - \operatorname{Im}_1 - \operatorname{Re}_2 + \operatorname{Im}_2 < \left(1 - \frac{1}{l-1}\right) (\operatorname{Re}_1 - \operatorname{Im}_1 + \operatorname{Re}_2 + \operatorname{Im}_2) \ \&$$

$$\operatorname{Re}_1 - \operatorname{Im}_1 - \operatorname{Re}_2 - \operatorname{Im}_2 > 0;$$

$$(l-1)(\operatorname{Re}_1 - \operatorname{Im}_1 + \operatorname{Re}_2 - \operatorname{Im}_2) < (l-2)(\operatorname{Re}_1 - \operatorname{Im}_1 + \operatorname{Re}_2 + \operatorname{Im}_2) \ \&$$

$$\operatorname{Re}_1 - \operatorname{Im}_1 + \operatorname{Re}_2 - \operatorname{Im}_2 > 0 \ \&$$

$$(l-1)(\operatorname{Re}_1 + \operatorname{Im}_1 + \operatorname{Re}_2 + \operatorname{Im}_2) < (l-2)(\operatorname{Re}_1 - \operatorname{Im}_1 + \operatorname{Re}_2 + \operatorname{Im}_2) \ \&$$

$$\operatorname{Re}_1 + \operatorname{Im}_1 + \operatorname{Re}_2 + \operatorname{Im}_2 > 0 \ \&$$

$$-\operatorname{Re}_1 - \operatorname{Im}_1 - \operatorname{Re}_2 + \operatorname{Im}_2 > 0 \ \&$$

$$(l-1)(-\operatorname{Re}_1 - \operatorname{Im}_1 - \operatorname{Re}_2 + \operatorname{Im}_2) < (l-2)(\operatorname{Re}_1 - \operatorname{Im}_1 + \operatorname{Re}_2 + \operatorname{Im}_2) \ \&$$

$$\operatorname{Re}_1 - \operatorname{Im}_1 - \operatorname{Re}_2 - \operatorname{Im}_2 > 0;$$

$$(\operatorname{Re}_1 - \operatorname{Im}_1 + \operatorname{Re}_2) - (2l-3)\operatorname{Im}_2 < 0 \ \&$$

$$\operatorname{Re}_1 - \operatorname{Im}_1 + \operatorname{Re}_2 - \operatorname{Im}_2 > 0 \ \&$$

$$(\operatorname{Re}_1 + \operatorname{Re}_2 + \operatorname{Im}_2) + (2l-3)\operatorname{Im}_1 < 0 \ \&$$

$$\operatorname{Re}_1 + \operatorname{Im}_1 + \operatorname{Re}_2 + \operatorname{Im}_2 > 0 \ \&$$

$$-\operatorname{Re}_1 - \operatorname{Im}_1 - \operatorname{Re}_2 + \operatorname{Im}_2 > 0 \ \&$$

$$(-\operatorname{Im}_1 + \operatorname{Im}_2) + (2l-3)(-\operatorname{Re}_1 - \operatorname{Re}_2) < 0 \ \&$$

$$\operatorname{Re}_1 - \operatorname{Im}_1 - \operatorname{Re}_2 - \operatorname{Im}_2 > 0;$$

Case (2l-2):

1111 is on the border, and 1110 is not. 1100 and 1011 will lie in region C if:

$$\text{Im}[1100] > 0 \ \& \ \text{Re}[1100] > 0 \ \& \ \text{Re}[1100] < q_{th} \ \& \ \text{Re}[1011] > 0 \ \& \ \text{Re}[1011] < q_{th} \ \& \ \text{Im}[1011] > 0 \ \& \ \text{Im}[1011] < q_{th}$$

$$\text{Re}_1 + \text{Im}_1 - \text{Re}_2 - \text{Im}_2 > 0 \ \&$$

$$\text{Re}_1 - \text{Im}_1 - \text{Re}_2 + \text{Im}_2 > 0 \ \&$$

$$\text{Re}_1 - \text{Im}_1 - \text{Re}_2 + \text{Im}_2 < \left(1 - \frac{1}{l-1}\right) (\text{Re}_1 + \text{Im}_1 + \text{Re}_2 + \text{Im}_2) \ \&$$

$$\text{Re}_1 + \text{Im}_1 + \text{Re}_2 - \text{Im}_2 > 0 \ \&$$

$$\text{Re}_1 + \text{Im}_1 + \text{Re}_2 - \text{Im}_2 < \left(1 - \frac{1}{l-1}\right) (\text{Re}_1 + \text{Im}_1 + \text{Re}_2 + \text{Im}_2) \ \&$$

$$-\text{Re}_1 + \text{Im}_1 + \text{Re}_2 + \text{Im}_2 > 0 \ \&$$

$$-\text{Re}_1 + \text{Im}_1 + \text{Re}_2 + \text{Im}_2 < \left(1 - \frac{1}{l-1}\right) (\text{Re}_1 + \text{Im}_1 + \text{Re}_2 + \text{Im}_2);$$

$$\text{Re}_1 + \text{Im}_1 - \text{Re}_2 - \text{Im}_2 > 0 \ \&$$

$$\text{Re}_1 - \text{Im}_1 - \text{Re}_2 + \text{Im}_2 > 0 \ \&$$

$$(l-1)(\text{Re}_1 - \text{Im}_1 - \text{Re}_2 + \text{Im}_2) < (l-2)(\text{Re}_1 + \text{Im}_1 + \text{Re}_2 + \text{Im}_2) \ \&$$

$$\text{Re}_1 + \text{Im}_1 + \text{Re}_2 - \text{Im}_2 > 0 \ \&$$

$$(l-1)(\text{Re}_1 + \text{Im}_1 + \text{Re}_2 - \text{Im}_2) < (l-2)(\text{Re}_1 + \text{Im}_1 + \text{Re}_2 + \text{Im}_2) \ \&$$

$$-\text{Re}_1 + \text{Im}_1 + \text{Re}_2 + \text{Im}_2 > 0 \ \&$$

$$(l-1)(-\text{Re}_1 + \text{Im}_1 + \text{Re}_2 + \text{Im}_2) < (l-2)(\text{Re}_1 + \text{Im}_1 + \text{Re}_2 + \text{Im}_2);$$

$$\text{Re}_1 + \text{Im}_1 - \text{Re}_2 - \text{Im}_2 > 0 \ \&$$

$$\text{Re}_1 - \text{Im}_1 - \text{Re}_2 + \text{Im}_2 > 0 \ \&$$

$$(\text{Re}_1 + \text{Im}_2) + (2l-3)(-\text{Im}_1 - \text{Re}_2) < 0 \ \&$$

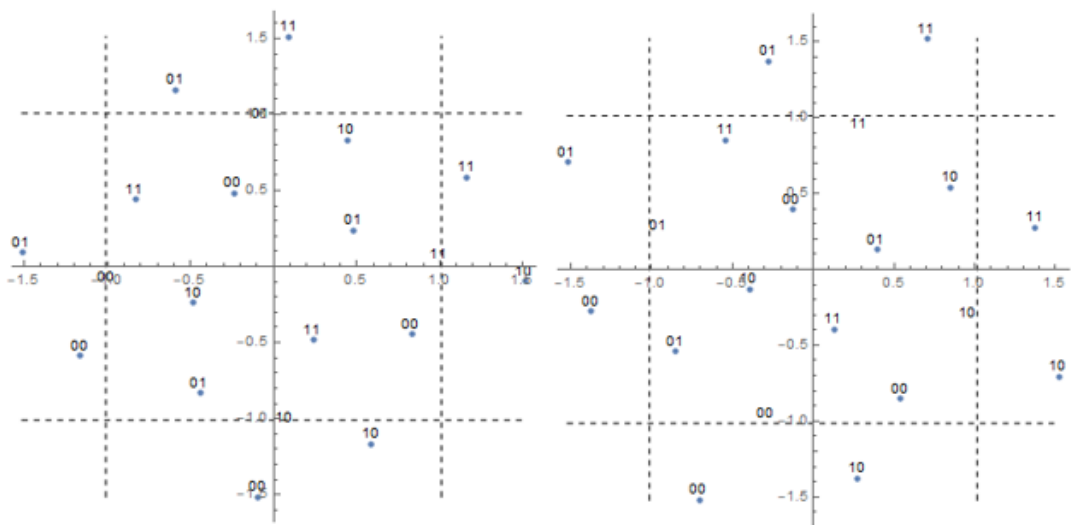
$$\text{Re}_1 + \text{Im}_1 + \text{Re}_2 - \text{Im}_2 > 0 \ \&$$

$$(\text{Re}_1 + \text{Im}_1 + \text{Re}_2) + (2l-3)(-\text{Im}_2) < 0 \ \&$$

$$-\text{Re}_1 + \text{Im}_1 + \text{Re}_2 + \text{Im}_2 > 0 \ \&$$

$$(\text{Im}_1 + \text{Re}_2 + \text{Im}_2) + (2l-3)(-\text{Re}_1) < 0$$

## Case 2m



(2m - 1)

(2m - 2)

Case (2m-1):

1110 is on the border, and 1111 is not. 1101 and 0110 will lie in region C if:

$$\operatorname{Re}[1101] > 0 \& \operatorname{Im}[1101] > 0 \& \operatorname{Im}[1101] < q_{th} \& \operatorname{Re}[0110] > 0 \& \operatorname{Re}[0110] < q_{th} \& \operatorname{Im}[0110] < q_{th}$$

$$\operatorname{Re}_1 - \operatorname{Im}_1 - \operatorname{Re}_2 - \operatorname{Im}_2 > 0 \&$$

$$\operatorname{Re}_1 + \operatorname{Im}_1 + \operatorname{Re}_2 - \operatorname{Im}_2 > 0 \&$$

$$\operatorname{Re}_1 + \operatorname{Im}_1 + \operatorname{Re}_2 - \operatorname{Im}_2 < \left(1 - \frac{1}{l-1}\right) (\operatorname{Re}_1 - \operatorname{Im}_1 + \operatorname{Re}_2 + \operatorname{Im}_2) \&$$

$$-\operatorname{Re}_1 - \operatorname{Im}_1 + \operatorname{Re}_2 + \operatorname{Im}_2 > 0 \&$$

$$-\operatorname{Re}_1 - \operatorname{Im}_1 + \operatorname{Re}_2 + \operatorname{Im}_2 < \left(1 - \frac{1}{l-1}\right) (\operatorname{Re}_1 - \operatorname{Im}_1 + \operatorname{Re}_2 + \operatorname{Im}_2) \&$$

$$\operatorname{Re}_1 - \operatorname{Im}_1 - \operatorname{Re}_2 + \operatorname{Im}_2 < \left(1 - \frac{1}{l-1}\right) (\operatorname{Re}_1 - \operatorname{Im}_1 + \operatorname{Re}_2 + \operatorname{Im}_2);$$

$$\operatorname{Re}_1 - \operatorname{Im}_1 - \operatorname{Re}_2 - \operatorname{Im}_2 > 0 \&$$

$$\operatorname{Re}_1 + \operatorname{Im}_1 + \operatorname{Re}_2 - \operatorname{Im}_2 > 0 \&$$

$$(l-1)(\operatorname{Re}_1 + \operatorname{Im}_1 + \operatorname{Re}_2 - \operatorname{Im}_2) < (l-2)(\operatorname{Re}_1 - \operatorname{Im}_1 + \operatorname{Re}_2 + \operatorname{Im}_2) \&$$

$$-\operatorname{Re}_1 - \operatorname{Im}_1 + \operatorname{Re}_2 + \operatorname{Im}_2 > 0 \&$$

$$(l-1)(-\operatorname{Re}_1 - \operatorname{Im}_1 + \operatorname{Re}_2 + \operatorname{Im}_2) < (l-2)(\operatorname{Re}_1 - \operatorname{Im}_1 + \operatorname{Re}_2 + \operatorname{Im}_2) \&$$

$$(l-1)(\operatorname{Re}_1 - \operatorname{Im}_1 - \operatorname{Re}_2 + \operatorname{Im}_2) < (l-2)(\operatorname{Re}_1 - \operatorname{Im}_1 + \operatorname{Re}_2 + \operatorname{Im}_2);$$

$$\operatorname{Re}_1 - \operatorname{Im}_1 - \operatorname{Re}_2 - \operatorname{Im}_2 > 0 \&$$

$$\operatorname{Re}_1 + \operatorname{Im}_1 + \operatorname{Re}_2 - \operatorname{Im}_2 > 0 \&$$

$$(\operatorname{Re}_1 + \operatorname{Re}_2) + (2l-3)(\operatorname{Im}_1 - \operatorname{Im}_2) < 0 \&$$

$$-\operatorname{Re}_1 - \operatorname{Im}_1 + \operatorname{Re}_2 + \operatorname{Im}_2 > 0 \&$$

$$(-\operatorname{Im}_1 + \operatorname{Re}_2 + \operatorname{Im}_2) + (2l-3)(-\operatorname{Re}_1) < 0 \&$$

$$(\operatorname{Re}_1 - \operatorname{Im}_1 + \operatorname{Im}_2) + (2l-3)(-\operatorname{Re}_2) < 0$$

Case (2m-2):

1111 is on the border, and 1110 is not. 1110 and 1001 will lie in region C if:

$$\operatorname{Re}[1001] > 0 \& \operatorname{Im}[1001] > 0 \& \operatorname{Im}[1001] < q_{th} \& \operatorname{Re}[1110] > 0 \& \operatorname{Re}[1110] < q_{th} \& \operatorname{Im}[1110] < q_{th}$$

$$\operatorname{Re}_1 + \operatorname{Im}_1 - \operatorname{Re}_2 - \operatorname{Im}_2 > 0 \&$$

$$-\operatorname{Re}_1 + \operatorname{Im}_1 + \operatorname{Re}_2 - \operatorname{Im}_2 > 0 \&$$

$$-\operatorname{Re}_1 + \operatorname{Im}_1 + \operatorname{Re}_2 - \operatorname{Im}_2 < \left(1 - \frac{1}{l-1}\right) (\operatorname{Re}_1 + \operatorname{Im}_1 + \operatorname{Re}_2 + \operatorname{Im}_2) \&$$

$$\operatorname{Re}_1 - \operatorname{Im}_1 + \operatorname{Re}_2 + \operatorname{Im}_2 > 0 \&$$

$$\operatorname{Re}_1 - \operatorname{Im}_1 + \operatorname{Re}_2 + \operatorname{Im}_2 < \left(1 - \frac{1}{l-1}\right) (\operatorname{Re}_1 + \operatorname{Im}_1 + \operatorname{Re}_2 + \operatorname{Im}_2) \&$$

$$\operatorname{Re}_1 + \operatorname{Im}_1 - \operatorname{Re}_2 + \operatorname{Im}_2 < \left(1 - \frac{1}{l-1}\right) (\operatorname{Re}_1 + \operatorname{Im}_1 + \operatorname{Re}_2 + \operatorname{Im}_2);$$

$$\operatorname{Re}_1 + \operatorname{Im}_1 - \operatorname{Re}_2 - \operatorname{Im}_2 > 0 \&$$

$$-\operatorname{Re}_1 + \operatorname{Im}_1 + \operatorname{Re}_2 - \operatorname{Im}_2 > 0 \&$$

$$(l-1)(-\operatorname{Re}_1 + \operatorname{Im}_1 + \operatorname{Re}_2 - \operatorname{Im}_2) < (l-2)(\operatorname{Re}_1 + \operatorname{Im}_1 + \operatorname{Re}_2 + \operatorname{Im}_2) \&$$

$$\operatorname{Re}_1 - \operatorname{Im}_1 + \operatorname{Re}_2 + \operatorname{Im}_2 > 0 \&$$

$$(l-1)(\operatorname{Re}_1 - \operatorname{Im}_1 + \operatorname{Re}_2 + \operatorname{Im}_2) < (l-2)(\operatorname{Re}_1 + \operatorname{Im}_1 + \operatorname{Re}_2 + \operatorname{Im}_2) \&$$

$$(l-1)(\operatorname{Re}_1 + \operatorname{Im}_1 - \operatorname{Re}_2 + \operatorname{Im}_2) < (l-2)(\operatorname{Re}_1 + \operatorname{Im}_1 + \operatorname{Re}_2 + \operatorname{Im}_2);$$

$$\operatorname{Re}_1 + \operatorname{Im}_1 - \operatorname{Re}_2 - \operatorname{Im}_2 > 0 \&$$

$$-\operatorname{Re}_1 + \operatorname{Im}_1 + \operatorname{Re}_2 - \operatorname{Im}_2 > 0 \&$$

$$(\operatorname{Im}_1 + \operatorname{Re}_2) + (2l-3)(-\operatorname{Re}_1 - \operatorname{Im}_2) < 0 \&$$

$$\operatorname{Re}_1 - \operatorname{Im}_1 + \operatorname{Re}_2 + \operatorname{Im}_2 > 0 \&$$

$$(\operatorname{Re}_1 + \operatorname{Re}_2 + \operatorname{Im}_2) + (2l-3)(-\operatorname{Im}_1) < 0 \&$$

$$(\operatorname{Re}_1 + \operatorname{Im}_1 + \operatorname{Im}_2) + (2l-3)(-\operatorname{Re}_2) < 0$$

## Definitions of Acronyms

ARA	Accumulate-Repeat-Accumulate
ADC	Analogue to Digital Converter
AP	Access Point
AWGN	Additive White Gaussian Noise
BBU	Baseband (processing) Unit
BER	Bit Error Ratio
BPSK	Binary Phase Shift Keying
BS	Base Station
CRC	Cyclic Redundancy Check
C-RAN	Cloud Radio Access Network
CND	Check Node Decoder
CNE	Check Node Encoder
CSI	Channel State Information
CPRI	Common Public Radio Interface
CWDM	Coarse Wavelength Division Multiplexing
DWDM	Dense Wavelength Division Multiplexing
DAC	Digital to Analogue Converter
ECC	Error Correction Capacity
EGC	Equal Gain Combining
FFT	Fast Fourier Transform
FEC	Forward Error Correction
FSC	Frequency Selective Channel
FDM	Frequency Division Multiplex
GF	Galois Field
IFFT	Inverse Fast Fourier Transform
ISI	Inter-symbol Interference

---

IBI	Inter-block Interference
LLR	Log-likelihood Ratio
LSB	Least Significant Bit
LoS	Line-of-Sight
mm-wave	Millimetre-wave
MMSE	Minimum Mean Square Error
MRC	Maximum Ratio Combining
MIMO	Multiple-Input-Multiple-Output
ML	Maximum Likelihood
MISO	Multiple-Input-Single-Output
MSB	Most Significant Bit
OBSAI	Open Base Station Architecture Initiative
OFDM	Orthogonal Frequency Division Multiplexing
QPSK	Quadrature Phase Shift Keying
QAM	Quadrature Amplitude Modulation
RMS	Root Mean Square
RRU	Remote Radio Unit
RF	Radio Frequency
RSC	Reed-Solomon Code
RRH	Remote Radio Head
SNR	Signal to Noise Ratio
SIMO	Single-Input-Multiple-Output
SW	Slepian-Wolf
SSB	Second Significant Bit
VND	Variable Node Decoder
VNE	Variable Node Encoder
ZF	Zero-Forcing

## List of Symbols

$P(x)$	Probability of Event $x$
$P(x,y)$	Joint probability mass function of discrete variables $x$ and $y$
$E_b/N_0$	Bit energy to noise density ratio
$\sigma$	Noise standard deviation
$N_0$	Noise power spectral density
$E(x)$	Expectation of variable $x$
$\int_x^y$	Integration from $X$ to $Y$
$\sum_{x=0}^Y a_x$	Summation of adding $a_x$ from $x=0$ to $x=Y$
$\prod_{x=0}^Y a_x$	Product of multiplying $a_x$ from $x=0$ to $x=Y$
$exp$	The exponential function
$log$	The logarithmic function
$\  \ $	The Euclidean distance
$   $	Absolute value
$( )^H$	Complex conjugate
$( )^{-1}$	Inverse function
$H(X)$	Entropy of variable $X$
$H(X,Y)$	Joint entropy of variable $X$ and $Y$
$H(X/Y)$	Conditional entropy of variable $X$ and $Y$
$I(X;Y)$	Mutual information of variable between $X$ and $Y$
$I(X;Y/Z)$	Conditional mutual information of variables $X$ and $Y$ given variable $Z$
$Re[.]$	Real part of element
$Im[.]$	Imaginary part of element

*min*      Minimum value

*max*      Maximum value

## Bibliography

- [1] C.-L. I et al., "Toward green and soft: A 5G perspective", *IEEE Communications Magazine.*, vol. 52, no. 2, pp. 66-73, Feb 2014.
- [2] M. Peng , C. Wang , V. Lau , and H. V. Poor , “ Fronthaul-constrained cloud radio access networks: insights and challenges ,” *IEEE Wireless Communications .*, vol. 22 , no. 2 , pp. 152 – 160 , 2015.
- [3] A. Checko, H. L. Christiansen, Y. Yan, L. Scolari, G. Kardaras, M. S. Berger, and L. Dittmann, “Cloud RAN for mobile networks – A technology overview,” *IEEE Communications. Surveys, Tutorials*, vol. 17, no.1, pp. 405-426, First quarter 2015.
- [4] J. Wu, Z. Zhang, Y. Hong, and Y. Wen, ”Cloud Radio Access Network (C-RAN): a primer,” *IEEE Network.*, vol. 29, no. 1, pp. 35–41, Jan 2015.
- [5] “White paper of next generation fronthaul interface,” China Mobile Research Institute, Tech. Rep. V1.0, Jun 2015.
- [6] K. Murphy, “Centralized ran and fronthaul,” Ericsson, Tech. Rep., May 2015.
- [7] J. G. Proakis, Digital Communications, New York, McGraw-Hill, 3rd Edition, 1995
- [8] C. Liu *et al.*, “A novel multi-service small-cell cloud radio access network for mobile fronthaul and computing based on radio-over-fiber technologies,” *IEEE Journal of Lightwave Technology.*, vol. 31, no. 17, pp. 2869-2875, Sep 2013.
- [9] A. Scarfo, “The evolution of data center networking technologies,” in *Data Compression, Communications and Processing (CCP), 2011 First International Conference on IEEE*, pp. 172 – 176, 2011.
- [10] D. Pompili, A. Hajisami, H. Viswanathan, "Dynamic provisioning and allocation in Cloud Radio Access Networks (C-RANs)", *Ad Hoc Networks*, vol. 30, pp. 128-143, 2015.
- [11] CPRI, “Common Public Radio Interface (CPRI), interface specification,” V6.0, Available: [www.cpri.info](http://www.cpri.info), 2018.
- [12] D. Falconer, S. Ariyavisitakul, A. Benyamin-Seeyar, and B. Eidson, ”Frequency domain equalization for single-carrier broadband wireless systems,” *IEEE Communications Magazine.*, vol.40, no. 4, pp. 58–66, Apr 2002.
- [13] V. Dawar, R. Sharma, “Reduction in bit error rate from various equalization techniques for MIMO technology,” *International Journal of Soft Computing and Engineering.*, ISSN:2231-2307, Volume-2, Issue-4, Sep 2012..
- [14] A. Goldsmith, Wireless Communications, Cambridge Univ. Press,2004.

- 
- [15] W. C. Jakes, *Diversity Techniques*. Wiley-IEEE Press, pp. 389-544, 1974
- [16] B. Sklar, *Digital communications*. Prentice Hall NJ, vol. 2, 2001.
- [17] A. Paulraj, R. Nabar, and D. Gore, Introduction to space-time wireless communications. Cambridge university press, 2003.
- [18] S. O. Rice, "Statistical properties of a sine wave plus random noise," *Bell System Technical Journal*, vol. 27, pp. 109-157, Jan 1948.
- [19] A. Abdi, "On the estimation of the  $K$  parameter for the Rice fading distribution," *IEEE Communications Letters.*, vol. 5, no. 3, pp. 92-94, Mar 2001.
- [20] Patrick Marsch and Gerhard Fettweis, "On uplink network MIMO under a constrained backhaul and imperfect channel knowledge," *IEEE International Conference on Communications*, Germany, 2009.
- [21] C. Wang, K. S. Au, R. D. Murch, W. H. Mow, R. S. Cheng, V. Lau, "On the performance of the MIMO zero-forcing receiver in the presence of channel estimation error," *IEEE Transactions on Wireless Communications.*, vol. 6, no. 3, pp. 805-810, Mar 2007.
- [22] H.-Y. Fan, MIMO Detection Schemes for Wireless Communications, Hong Kong University of Science and Technology, 2002.
- [23] Yong Soo Cho, Jaekwon Kim, Won Young Yang, Chung-Gu Kang, MIMO-OFDM Wireless Communication with MATLAB, John Wiley & Sons (Asia), Singapore, 2010.
- [24] M. Joham. W. Utschick. and J. A. Nossek. "Linear transmit processing in MIMO communications systems," *IEEE Transactions on Signal Processing*, vol.53, no.8, 2005.
- [25] Allen Gersho and Robert M Gray. *Vector Quantization and Signal Compression*. Springer, 1992.
- [26] Y. Wang, Lab Manual for Multimedia Lab, Experiment on Speech and Audio Compression. Sec. 1-2.1.
- [27] N. C. Beaulieu, "Introduction to 'linear diversity combining techniques'," *Proc. IEEE*, Vol. 91, No. 2, pp. 328-330, Feb 2003.
- [28] D. G. Brennan, "Linear diversity combining techniques," *Proc. IRE*, Vol. 47, pp. 1075-1102, Jun 1959.
- [29] S.P. Jadhav and V.S. Hendre, "Performance of maximum ratio combining (MRC) MIMO systems for Rayleigh fading channel," *International Journal of Scientific and Research Publications*, Vol.3, Issue.2 Feb 2013

- [30] J. Ahn and H.S. Lee, "Frequency domain equalization of OFDM signal over frequency non selective Rayleigh fading channels," *Electronic Letters*, Vol. 29, No. 16, pp. 1476-1477, 1993.
- [31] L.J. Cimini, "Analysis and simulation of digital mobile channel using orthogonal frequency division multiplexing," *IEEE Transactions on communications*. Vol. 33, No. 7, pp 665-675, Jul 1985.
- [32] J. Cimini and N.R. Sollenberger, "OFDM with diversity and coding for advanced cellular internet services," *IEEE conference proceedings VTC*, 1998.
- [33] K. F. Nieman and B. L. Evans. "Time-domain compression of complex baseband LTE signals for cloud radio access networks," *IEEE Global Conference on Signal and Information Processing., (GlobalSIP)*, pp. 1198-1201, Austin, USA, Dec 2013.
- [34] W. Lee, O. Simeone, J. Kang, and S. Shamai, "Multivariate fronthaul quantization for downlink C-RAN," *arXiv:1510.08301*.
- [34] A. Vosoughi, M. Wu, and J. R. Cavallaro, "Baseband signal compression in wireless base stations," *IEEE Global Conference on Signal and Information Processing., (GLOBECOM)*, pp. 4505-4511, Anaheim, USA, Dec 2012.
- [35] T. M. Cover and J. A. Thomas, *Elements of Information Theory* (Wiley Series in Telecom-munications and Signal Processing). Wiley-Interscience, 2006.
- [36] B. Murray, I. Collings, "AGC and quantization effects in a zero-forcing MIMO wireless system," *Proc. IEEE 63rd Vehicular Technology Conference.*, vol. 4, pp. 1802-1806, May 2006.
- [37] A. Mezghani, M.-S. Khoufi, J. A. Nossek, "A modified MMSE receiver for quantized MIMO systems," *ITG/IEEE WSA*, Vienna, Austria, pp. 1-5, 2007.
- [38] M. Ivrlac, J. Nossek, "Challenges in coding for quantized MIMO systems," *IEEE International Symposium on Information Theory.*, pp. 2114-2118, Jul 2006.
- [39] A. Mezghani, M. Rouatbi, J. Nossek, "An iterative receiver for quantized MIMO systems," *Proc. 16th IEEE Mediterranean Electrotechnic Conference., (MELECON)*, pp. 1049-1052, Mar 2012.
- [40] S. Wang, Y. Li, J. Wang, "Multiuser detection in massive spatial modulation MIMO with low-resolution ADCs," *IEEE Transaction on Wireless Communications.*, vol. 14, no. 4, pp. 2156-2168, Apr 2015.
- [41] M. Oltean and M. Nafornita, "The cyclic prefix length influence on OFDM transmission BER," tom 48(62), Fascicola 2, 2003.

- [42] M. Peng *et al.*, "Heterogeneous cloud radio access networks: a new perspective for enhancing spectral and energy efficiencies," *IEEE Wireless Communications.*, vol. 21, no. 6, pp. 126–35, Dec 2014.
- [43] C. Liu *et al.*, "A novel multi-service small-cell cloud radio access network for mobile fronthaul and computing based on radio-over-fiber technologies," *IEEE Journal of Lightwave Technology.*, vol. 31, no. 17, pp. 2869–75. Sep 2013.
- [44] S. Park *et al.*, "Joint decompression and decoding for cloud radio access networks," *IEEE Signal Processing Letters.*, vol. 20, no. 5, pp. 503–06, May 2013.
- [45] D. Slepian and J. Wolf, "Noiseless coding of correlated information sources," *IEEE Transactions on Information Theory*, vol. 19, no. 4, pp. 471 – 480, Jul 1973.
- [46] N. Xie and A. Burr, "Distributed cooperative spatial multiplexing with Slepian Wolf code," in *2013 IEEE 77th Vehicular Technology Conference (VTC Spring)*, pp. 15, Jun 2013.
- [47] N. Xie and A. Burr, "Cooperative spatial multiplexing with distributed amplify-and forward relays," in *2012 International Symposium on Wireless Communication Systems (ISWCS)*, pp. 616-620, Aug 2012.
- [48] N. Xie and A. Burr, "Implementation of Slepian Wolf theorem in a distributed cooperative spatial multiplexing system," *20<sup>th</sup> European Wireless Conference.*, pp.1-5, 2014
- [49] T. Javornik, G. Kandus, F. Vejrazka, "Modulation schemes for wireless access," *Radio engineering*, Vol. 9, No. 4, Dec 2000.
- [50] D. Dutt Bohra, A. Bora, "Bit error rate analysis in simulation of digital Communication Systems with different Modulation Schemes," *International Journal of Innovative Science.*, vol. 1 Issue 3, May 2014.
- [51] N. V. Panicker, A. K. Suresh, "BER performance evaluation of different digital modulation schemes for biomedical signal transceivers under AWGN and fading channel conditions," *International Journal of Engineering and Advanced Technology (IJEAT)*, Vol. 3 Issue 5, Jun 2014.
- [52] V. Chau, "Fading channel characterization and modelling," Doctoral dissertation, California State University, Northridge. 2012.
- [53] E. Taissir, "Effet of AWGN and fading (Rayleigh and Rician) channels on BER performance of Free Space Optics (FSO) communication systems," *International Journal of Research in Wireless Systems (IJRWS).*, Vol. 2 Issue 2, Jun 2013.

- [54] A.S. Babu, K.S. Rao, "Evaluation of BER for AWGN, Rayleigh and Rician fading channels under various modulation schemes," *International Journal of Computer Applications.*, Vol. 26 No. 9, Jul 2011.
- [55] B.L. Ahlem, M.B. Dadi and C.B. Rhaimi "Evaluation of BER of digital modulation schemes for AWGN and wireless fading channels," *Information Technol and Computer Applications Congress (WCITCA)*, Present at Jun 2015.
- [56] W. W. Peterson, D. T. Brown, "Cyclic codes for error detection," *Proc. IRE*, vol. 49, no. 1, pp. 228-235, Jan 1961.
- [57] T. Mandel, J. Mache, "Selected CRC polynomials can correct errors and thus reduce retransmission," *Proc. WITS (DCOSS)*, pp. 1-6, Jun 2009.
- [58] R. W. Hamming, "Error detecting and error correcting codes," *Bell Syst. Tech. J.*, vol. 29, no. 2, pp. 147-160, Apr 1950.
- [59] S. Lin, D. J. Costello, *Error Control Coding*, 2004, Prentice-Hall.
- [60] C.K.P. Clarke. Reed-Solomon error correction, BBC R&D White Paper, WHP 031, Jul 2002.
- [61] M. Kaur and V. Sharma, "Study of forward error correction using Reed—Solomon codes," *International Journal of Electronics Engineering.*, vol. 2, pp. 331 – 333, 2010.
- [62] S. B. Wicker, *Error Control Systems for Digital Communication and Storage*, 1995, Prentice-Hall.
- [63] R. T. Chien, "Cyclic decoding procedure for the Bose–Chaudhuri–Hocquenghem codes," *IEEE Transactions on Information Theory.*, vol. 10, no. 4, pp. 357-363, Oct 1964.
- [64] "Reed-Solomon (RS) Coding Overview," VOCAL Technologies, Ltd., Rev. 2.28n, 2010.
- [65] E. R. Berlekamp, R. E. Peile and S. P. Pope. "The application of error control to communications," *IEEE Communications Magazine.*, vol. 25, no. 4, pp. 44-57, Apr 1987.
- [66] J. Garcia-Frias, "Compression of correlated binary sources using turbo codes," *IEEE Communications Letters.*, vol. 5, no. 10, pp. 417 –419, Oct 2001.
- [67] J. Garcia-Frias and Y. Zhao, "Near-Shannon/Slepian-Wolf performance for unknown correlated sources over AWGN channels," *IEEE Transactions on Communications*, vol. 53, no. 4, pp. 555 – 559, Apr 2005.
- [68] V. Tervo, T. Matsumoto, and P.-S. Lu, "Distributed joint source-channel coding for correlated sources using non-systematic repeat-accumulate based codes," *Wireless*

*Personal Communications.*, pp. 1–15, 2012. [Online]. Available: <http://dx.doi.org/10.1007/s11277-012-0579-5>

[69] S. ten Brink and G. Kramer, “Design of repeat-accumulate codes for iterative detection and decoding,” *IEEE Transactions on Signal Processing.*, vol. 51, no. 11, pp. 2764 – 2772, Nov 2003.

[70] J. Lodge, R. Young, P. Hoeher, and J. Hagenauer, “Separable MAP ‘filters& rdquo’ for the decoding of product and concatenated codes,” in *IEEE International Conference on Communications., 1993. ICC '93 Geneva. Technical Program, Conference Record.*, vol. 3, pp. 1740–1745 vol.3, May 1993.

[71] G. D. Forney, "On decoding BCH codes," *IEEE Transactions on Information Theory.*, vol. 1T-11, pp. 549-557, Oct 1965.

[72] L. Hanzo, T. Liew, and B. Yeap, *Turbo Coding, Turbo Equalisation and Space-Time Coding for Transmission over Fading Channels.* Wiley, 2002.

[73] S. ten Brink, “Code doping for triggering iterative decoding convergence,” in *2001 IEEE International Symposium on Information Theory., 2001. Proceedings.*, 2001, p. 235.

[74] H. Wymeersch, *Iterative Receiver Design.* UPH, Shaftesbury Road, Cambridge, CB2 8BS, United Kingdom: Cambridge University Press, Sep 2007.

[75] G. Lindell, “Some exact union bound results for maximum likelihood detection in MIMO systems,” in *International Symposium on Information Theory.. ISIT 2005. Proceedings.*, pp. 2223 –2227, Sep 2005.

[76] J. Hagenauer, E. Offer, and L. Papke, “Iterative decoding of binary block and convolutional codes,” *IEEE Transactions on Information Theory.*, vol. 42, no. 2, pp. 429 –445, Mar 1996.

[77] C. Shannon, “A mathematical theory of communication,” *Bell System Technical Journal*, vol. 27, pp. 379–423, 623–656, Oct 1948. [Online]. Available: <http://cm.belllabs.com/cm/ms/what/shannonday/shannon1948.pdf>

[78] C. Berrou, A. Glavieux, and P. Thitimajshima, “Near Shannon limit error-correcting coding and decoding: Turbo-codes,” in *IEEE International Conference on Communications., 1993. ICC '93 Geneva. Technical Program, Conference Record.*, vol. 2, pp. 1064–1070 vol.2, May 1993.

[79] Z.H. He, C.J. Hu, T. Tao and C. Ma, “A compression scheme for LTE baseband signal in C-RAN,” *9<sup>th</sup> International Conference on CHINACOM*, 2014.

- [80] S. Park *et al.*, "Robust and efficient distributed compression for cloud radio access networks," *IEEE Transaction on Vehicular Technology.*, vol. 62, no. 2, pp. 692-703, Feb 2013.
- [81] H J Son, S M Shin "Fronthaul size: calculation of maximum distance between RRH and BBU," 1st April 2014. Available:  
[http://www.netmanias.com/en/?m=view&id=blog\\_mbl&no=6276](http://www.netmanias.com/en/?m=view&id=blog_mbl&no=6276)
- [82] J. Li *et al.*, "Resource allocation optimization for delay-sensitive traffic in fronthaul constrained cloud radio access networks," *Proc. IEEE Systems Journal.*, pp. 1-12, Sep 2017.
- [83] Y. Shi, J. Zhang, and K. Letaief, "Group sparse beamforming for green cloud-RAN," *IEEE Transactions on Wireless Communications.*, vol. 13, no. 5, pp. 2809-2823, May 2014.
- [84] Y. Zhou, W. Yu, "Optimized beamforming and backhaul compression for uplink MIMO cloud radio access networks," *Proc. IEEE GLOBECOM Workshops*, pp. 1487-1492, Dec 2014.
- [85] S. H. Lim, Y.-H. Kim, A. El Gamal, S.-Y. Chung, "Noisy network coding," *IEEE Transactions on Information Theory.*, vol. 57, no. 5, pp. 3132-3152, May 2011.
- [86] A. Wiesel, Y. C. Eldar, and S. Shamai (Shitz), "Zero-forcing precoding and generalized inverses," *IEEE Transactions on Signal Processing.*, vol. 56, no. 9, pp. 4409-4418, Sep 2008.
- [87] N. Xie, "Distributed cooperative spatial multiplexing system," Ph.D. dissertation, University of York, Department of Electronics, Aug 2014. [Online] Available:  
<http://theses.whiterose.ac.uk/7650/1/thesis.pdf>.
- [88] A. Wyner, J. Ziv, "The rate-distortion function for source coding with side information at the decoder," *IEEE Transactions on Information Theory.*, vol. 22, no. 1, pp. 1-10, Jan 1976.
- [89] E. Graves and T.F. Wong "Information integrity between correlated sources through Wyner-Ziv coding," *IEEE Information Theory Workshop*, pp. 332-336, 2015.
- [90] Fujitsu, The benefits of cloud-ran architecture in mobile network expansion," White Paper, Fujitsu, 2015.
- [91] Z. Liu, S. Cheng, A. D. Liveris, and Z. Xiong, "Slepian-wolf coded nested lattice quantization for wyner-ziv coding: High-rate performance analysis and code design," *IEEE Transactions on Information Theory.*, vol. 52, no. 10, pp. 4358-4379, Oct 2006.
- [92] M.H. Kalos and P.A. Whitlock, Monte Carlo Methods, Second Edition, 2008, ISBN:978-3-527-40760-6.

- [93] C.-L. I, J. Huang, R. Duan, C. Cui, X. Jiang, L. Li, "Recent progress on C-RAN centralization and cloudification," *IEEE Access*, vol. 2, pp. 1030-1039, Sep 2014.